Final Technical Report

SERDP Project MM-1272

Enhanced Electromagnetic Tagging for Embedded Tracking of Munitions and Ordnance During Future Remediation Efforts

Revision 2

Principal Investigator: Keith A. Shubert, Ph.D.

To

Strategic Environmental Research and Development Program

901 North Stuart Street
Suite 303
Arlington, VA 22203-1853

From

Battelle
The Business of Innovation

Battelle Columbus Operations

505 King Avenue

Columbus, Ohio 43201-2693

June 2007

K.A. Shubert, R.J. Davis, T.J. Barnum, B.D. Balaban, R.L. Amdor, B.J. Sikorski,
T.J. Peters, and J.W. Griffin

This report is a work prepared for the United States Government by Battelle. In no event shall either the United States Government or Battelle have any responsibility or liability for any consequences of any use, misuse, inability to use, or reliance on the information contained herein, nor does either warrant or otherwise represent in any way the accuracy, adequacy, efficacy, or applicability of the contents hereof.

Approved for public release; distribution is unlimited

REPORT DOCUMENTATION PAGE

Form Approved
OMB No. 0704-0188

The public reporting burden for this collection of information is estimated to average 1 hour per response, including the time for reviewing instructions, searching existing data sources, gathering and maintaining the data needed, and completing and reviewing the collection of information. Send comments regarding this burden estimate or any other aspect of this collection of information, including suggestions for reducing the burden, to the Department of Defense, Executive Services and Communications Directorate (0704-0188). Respondents should be aware that notwithstanding any other provision of law, no person shall be subject to any penalty for failing to comply with a collection of information if it does not display a currently valid OMB control number.

PLEASE DO NOT RETURN YOUR FORM TO THE ABOVE ORGANIZATION.

1. REPORT DATE *(DD-MM-YYYY)*	2. REPORT TYPE	3. DATES COVERED *(From - To)*
30-06-2007	Final Technical Report	23-09-2002 - 30-06-2007

4. TITLE AND SUBTITLE

Enhanced Electromagnetic Tagging for Embedded Tracking of Munitions and Ordnance During Future Remediation Efforts

5a. CONTRACT NUMBER

DACA72-02-C-0020

5b. GRANT NUMBER

5c. PROGRAM ELEMENT NUMBER

6. AUTHOR(S)

K.A. Shubert, R.J. Davis, T.J. Barnum, B.D. Balaban, R.L. Amdor, B.J. Sikorski, T.J. Peters, and J.W. Griffin

5d. PROJECT NUMBER

MM-1272

5e. TASK NUMBER

5f. WORK UNIT NUMBER

7. PERFORMING ORGANIZATION NAME(S) AND ADDRESS(ES)

Battelle Columbus Operations, 505 King Ave., Columbus, OH 43201

8. PERFORMING ORGANIZATION REPORT NUMBER

9. SPONSORING/MONITORING AGENCY NAME(S) AND ADDRESS(ES)

Strategic Environmental Research and Development Program,
901 North Stuart Street
Suite 303
Arlington, VA 22203-1853

10. SPONSOR/MONITOR'S ACRONYM(S)

11. SPONSOR/MONITOR'S REPORT NUMBER(S)

12. DISTRIBUTION/AVAILABILITY STATEMENT

Approved for public release; distribution is unlimited

13. SUPPLEMENTARY NOTES

14. ABSTRACT

The program's objective was to investigate means of tagging ordnance items before they are fired or launched and thereby allow a more efficient means for locating unexploded ordnance (UXO) while maintaining very low false alarm rates. Five candidate munitions were selected as being representative of meeting the criteria. Physical mounting options for these five candidate munitions are documented in this report. After investigating radio frequency identification (RFID) tags, Battelle concluded that the Texas Instruments' Tiris 125-kHz magnetic field-sensitive tags offer the highest probability of success for detecting munitions buried three feet or less below the surface. Battelle concludes that using Tiris RFID tags on munitions before they are fired would pay dividends to the U.S. Government. Battelle believe that our testing at the Aberdeen Test Center in 2005 and 2006 demonstrated that properly embedded tags on UXO items can be detected to the needed depth of three feet. Fully developed above-ground interrogators could scan munition ranges at reasonable rates, with a one meter-wide swath and an estimated speed of 2 to 3 mph.

15. SUBJECT TERMS

Unexploded ordnance, UXO, detection, RFID, EM modeling

16. SECURITY CLASSIFICATION OF:			17. LIMITATION OF ABSTRACT	18. NUMBER OF PAGES	19a. NAME OF RESPONSIBLE PERSON
a. REPORT	b. ABSTRACT	c. THIS PAGE			Keith A. Shubert, Ph.D.
U	U	U	SAR	206	19b. TELEPHONE NUMBER *(Include area code)* 614.424.4916

This report was prepared under contract to the Department of Defense Strategic Environmental Research and Development Program (SERDP). The publication of this report does not indicate endorsement by the Department of Defense, nor should the contents be construed as reflecting the official policy or position of the Department of Defense. Reference herein to any specific commercial product, process, or service by trade name, trademark, manufacturer, or otherwise, does not necessarily constitute or imply its endorsement, recommendation, or favoring by the Department of Defense.

CONTENTS

Page

TABLES

FIGURES

ACRONYMS

Acronym	Definition
2-D	Two-dimensional
3-D	Three-dimensional
ABS	Acrylonitrile Butadiene Styrene
ADAM	Area Denial Anti-Personnel Mine
AMPTIAC	Advanced Materials Processing Technology
ATC	Aberdeen Test Center
CEB	Combined Effects Bomb
DMC	Dough Moulded Compound
EFP	Explosively Formed Penetrator
EM	Electromagnetics
FEM	Finite Element Method
FSK	Frequency Shift Keyed
GPS	Global Positioning System
GSP	Ground Safety Pin
HE	High Explosive
HERO	Hazards of Electromagnetic Radiation to Ordnance
IC	Integrated Circuit
kHz	kilohertz
MHz	megahertz
PNNL	Pacific Northwest National Laboratory
PVC	Polyvinyl Chloride
Q	Quality Factor
RF	Radio Frequency
RFID	Radio Frequency Identification
rms	Root-mean squared
SERDP	Strategic Environmental Research and Development Program
UHF	Ultra-High Frequency
UXO	Unexploded Ordnance
W	Watts

Executive Summary

This report summarizes work on SERDP Project MM-1272, "Enhanced Electromagnetic Tagging for Embedded Tracking of Munitions and Ordnance During Future Remediation Efforts." Battelle was the prime contractor working with Navy, Air Force, and Army partners. Battelle scientists at Pacific Northwest National Laboratory also contributed to this effort. The program's objective was to investigate means of tagging ordnance items before they are fired or launched and thereby allow a significantly more efficient means for locating unexploded ordnance (UXO) while maintaining very low false alarm rates.

Battelle investigated candidate munitions to ensure that only realistic tagging approaches were considered. Selection criteria included future munitions, high use-rate munitions, high dud-rate munitions, munitions of reasonable sizes, munitions with penetration depths less than three feet, and munitions used in training. Five candidate munitions were selected as being representative of meeting the criteria. Physical mounting options for these five candidate munitions are documented in this report. After investigating radio frequency identification (RFID) tags, Battelle concluded that the Texas Instruments' Tiris™ 125-kHz magnetic field-sensitive tags offer the highest probability of success for detecting munitions buried three feet or less below the surface. Figure 1 shows the chosen tags. These tags are passive; they do not require batteries. Instead, the tags harvest energy from the above-ground detection equipment and transmit a digital signal that indicates their presence. The lack of a battery implies that the tagged ordnance item could sit in storage for years and still be functional.

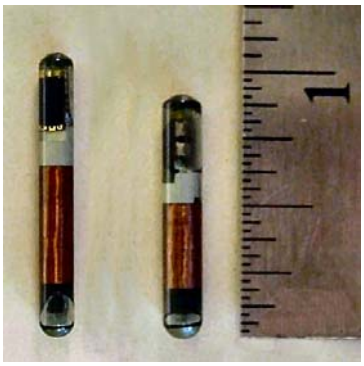

Figure 1. The Tiris RFID tags selected to aid detection of buried UXO

Battelle's initial project work included laboratory experimentation. This report summarizes detection range- and tag survivability-experimental work on these passive, low-frequency RFID tags. Detection ranges of five feet or more were achieved in air (no soil) configurations. Presence of soil was shown to exhibit little effect on detection range of the tags. The presence of the metal munition casing had a significantly larger effect than soil.

The design of the above-ground interrogator was critically important. Battelle's design goals were to employ equipment capable of detecting a buried UXO item up to three feet deep with a searching swath width of about one meter. Electromagnetic modeling work and investigations of current RFID readers indicated that the most challenging aspect was inducing a sufficiently large magnetic field on the buried tag to provide it power to energize its electronics, including its transmitter. The final design of the interrogator is shown in Figure 2. This photograph, with the interrogator's top removed to display its components, shows the one-meter diameter transmit coil, the three independent receive coils, and the electronics module. The big transmit coil turns a large magnetic field on and off many times per second. If a tag is nearby, the magnetic field is coupled into its solenoidal-wound coil and its electronics are

powered. The tag waits for the large field to turn off and then transmits its digital signal. The receive coils listen for the tag's low-level digital signal during the off time of the transmit coil.

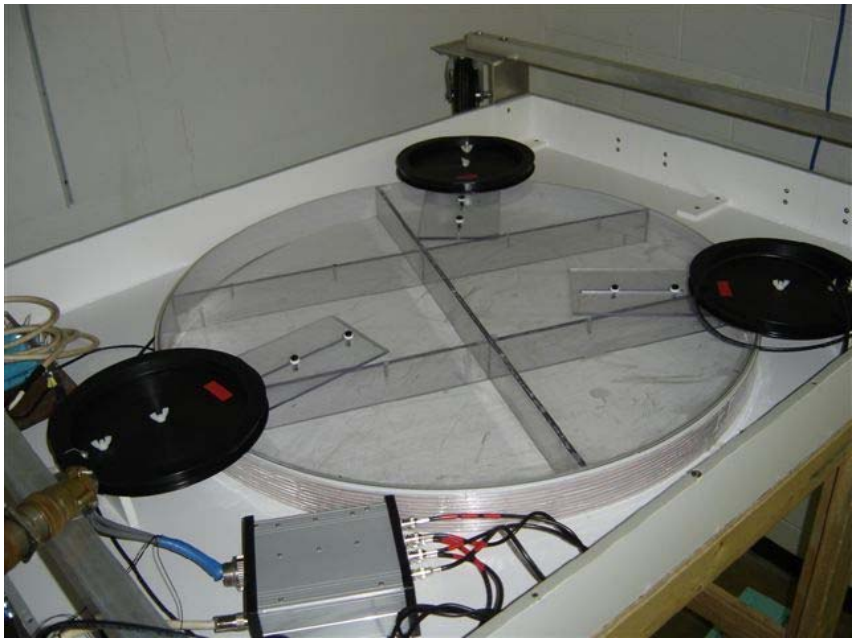

Figure 2. View of the above-ground detection equipment showing the one-meter diameter transmit coil and the three independent detection coils

Battelle performed electromagnetic modeling of the tags and munitions to understand the effects of the munition's metal shell on detection depths. This modeling also aided understanding the designs and configurations required to transmit energy from the above-ground interrogator to the tag and from the tag back to the above-ground receiver. Project modeling efforts demonstrated detection depths to three feet are achievable with the equipment demonstrated during this project. The effects of the above-ground interrogating coil being offset from being directly above the munition were investigated to maximize swath widths of search scans and to minimize costs. Figure 3 shows calculated magnetic field levels on a buried cylinder. Early results indicated one-meter wide swaths would be possible with one-meter diameter search coils. Finite element modeling was employed to calculate electric field levels that would exist near ordnance items and fuzes that might be located immediately below the transmit coil, as high electric field levels might energize the fuze electronics. The calculated electric field was at least a factor of ten below published safety thresholds at 125 kHz.

At its ordnance evaluation facility, Battelle evaluated the capability of the Tiris tags to withstand large accelerations by firing tags embedded in shotgun loads. Tags were seen to survive launch accelerations greater than 40,000 g's (projectiles were captured in Styrofoam) and velocities greater than 800 feet per second during these evaluations. No definitive data were found but informal discussions with ordnance experts indicated the highest acceleration/deceleration levels experienced by U.S. munitions were in the low 20,000 g's (anecdotal information did not indicate if this value was acceleration or deceleration). Only one randomly-chosen tag was tested in this manner. Further testing and analysis would be needed to ensure tag functionality rates acceptable to the Government.

Battelle performed in-ground testing at the Aberdeen Test Center in 2005 and 2006. Both sets of testing confirmed the required one-meter detection depth but neither test exhibited the desired 100 percent detection rate. In both years, Government personnel buried nine tagged surrogates and three non-tagged surrogates. In 2005, all the surrogates were detected and reported to Aberdeen Test Center except one,

but Battelle's position estimates were not precise. The one surrogate that was not reported is evident in the data; Battelle's analysis of the data was in error. In 2006, all the surrogates except one were detected and reported. Again, position estimates were not accurate. The tag on the single surrogate that was not detected in 2006 did not appear to be functioning properly. It was buried only one foot deep and it does not appear in any of the received data sets. Aberdeen Test Center personnel uncovered the surrogate after the test and found it to be working intermittently.

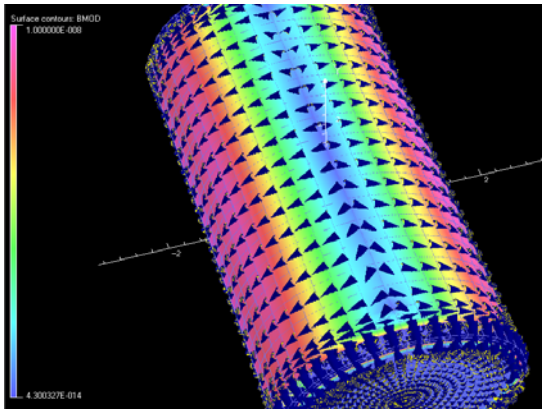

Figure 3. Depiction of the theoretical magnetic field levels near the surface of a cylindrically-shaped munition surrogate

During this project, researchers at Pacific Northwest National Laboratory (PNNL) investigated the potential for applying higher-frequency tags (UHF frequencies near 900 MHz) to the problem of surface munition items such as bomblets and grenades. SERDP's guidelines included the desire for longer stand-off detection ranges, five to ten feet, and better position resolution than that available with 125-kHz tags. The results of PNNL's efforts included in this report indicate UHF RFID tags could be useful in this surface ordnance problem. The antennas of the commercial-off-the-shelf UHF tags tested during this effort are similar in size to the munitions, however, which might limit military acceptance.

Battelle concludes that using Tiris RFID tags on munitions before they are fired would pay dividends to the U.S. Government. We believe that our testing at the Aberdeen Test Center in 2005 and 2006 demonstrated that properly embedded tags on UXO items can be detected to the needed depth of three feet. Fully developed above-ground interrogators could scan munition ranges at reasonable rates, with a one-meter-wide swath and an estimated speed of two to three miles per hour. This type of search would provide a very high probability of UXO detection. Ground clutter and munition scrap would not influence the detection probability or the false alarm rate. False positives would require a tag to survive a munitions explosion. False negatives would require tag operation failure that could be caused by fastening a non-functioning tag to a munition or damage to the tag during handling, launch, or impact. False negatives would be reduced by tag testing at the factory after the tags are fastened to the munition and use of multiple tags on each munition.

It is possible that the high false alarm rate of current UXO search methodologies drives the cost of remediation. Battelle believes further testing and a detailed analysis would show the tagged-munition methodology to yield huge overall savings in the future by reducing the false alarm rate. This savings will be realized even when the costs incurred in mounting commercial-off-the-shelf RFID tags on munitions are considered.

Battelle recommends that the Government consider the following steps toward realizing this significant future cost savings: Identify the designers of future munitions to allow tags to be integrated from their

inception, provide the resources to refine the interrogation module receive system, and provide interfaces to potential users, range commanders, and controllers of current candidate munitions to discuss and encourage the mounting of tags on existing ordnance items, at least at testing and research ranges.

Battelle believes this project has demonstrated that the Tiris RFID technology can aid the Government in significantly reducing the cost of remediating and maintaining training and testing ranges in the future. The technology requires additional incremental development steps and significant military buy-in before actual deployment, but this project has shown that commercial-off-the-shelf RFID technology can be leveraged to achieve less expensive, safer, and lower pollution-level ordnance ranges.

1 Performing Organizations

This project was conducted for the Strategic Environmental Research and Development Program (SERDP) by Battelle Columbus Operations. Battelle's partners include the Department of Energy's Pacific Northwest National Laboratory, which is managed by Battelle, and ordnance experts at the Air Force's 46th Test Wing at Eglin Air Force Base, Florida, the Army's TACOM/ARDEC organization in Adelphi, Maryland, and the Naval Explosive Ordnance Technology Division in Indian Head, Maryland.

The project COTR was Ms. Melissa Miller at NAVSEA, Indian Head. Technical and managerial contributors include Dr. Anne Andrews, Mr. Charles Pellerin, Dr. Jeffrey Marqusee, and Mr. Bradley Smith in the SERDP program office. Administrative support to SERDP was provided by HydroGeoLogic, Inc.

Individuals involved at Battelle included Dr. Keith Shubert as the Project Manager and Principal Investigator, Mr. Russell Amdor as the primary munitions expert, and Mr. Tom Barnum, Mr. Bryan Balaban, and Mr. Grant Hampel as electrical engineers. Mr. Richard Davis provided the finite element modeling expertise. Mr. Brian Sikorsky contributed the mechanical mounting analysis. Dr. Vince Puglielli assisted with Quality System assurance and served as a consultant on electrical and ordnance issues. Mr. John Sledge from Eglin Air Force Base provided ordnance information and samples. Mr. James Campbell provided ordnance information from the Army and Mr. Robert Daily provided the Navy perspective. Mr. Jeffrey Griffin and Mr. Tim Peters at Pacific Northwest National Laboratory contributed most of the high frequency RF tag data and perspective.

2 Project Background

The detection of unexploded ordnance (UXO) in military firing ranges has proved to be very difficult. Because the requirement for remediation continues, the Government must consider to approaches. To enable the DoD to conduct cost effective training missions in the future with increased safety for personnel and property, and without negative environmental impact, significant advances in detection and identification of UXO must be pursued, implemented, and complemented with rigorous and modified operational protocol. To this end, Battelle investigated the potential for placing radio frequency (RF) tags or lower frequency electromagnetic (EM) tags on future ordnance items to aid in locating UXO in the ground. The overall objective of this program was to advance current tag capability to survive the operating conditions associated with munitions, provide information on the munitions location, and minimize the false alarm rate. The ability to discriminate between UXO and clutter items continues to be crucial in reducing the cost of UXO remediation.

The tags considered during this project would be secured to the candidate ordnance item and would be capable of surviving the delivery system. The tag must also survive ground impact and terrain penetration, of nonfunctioning (i.e., unexploded) ordnance items. The buried tag must respond to and then signal the UXO Tag Interrogation Module when the detection system is brought nearby. Our approach for this study was to determine reasonable operating objectives for current RF tag technology or other innovative tagging devices and evaluate the tag technology against known constraints or established and prioritized operational criteria.

Battelle pursued two concepts for passive tags (no batteries) on the ordnance item. Battelle had been pursuing one concept for an active tag (requires batteries) as a risk reduction activity but this effort was halted early in the project. The Government requires an inexpensive tag that can be interrogated through three feet of soil using an above-ground, mobile interrogator. The two primary issues of concern are the ability to detect a buried tag located on steel or iron ordnance items and the survivability of the tag, which includes the need for the tag to stay attached to the munition.

The focus of the project team was in five distinct but related technical areas.

- The behavior of magnetic fields in the ordnance search configuration using finite element computer analysis
- Alternatives for fastening the EM tags to the five chosen munition candidates
- The behavior of EM tags, RF tags, and passive UHF tags in laboratory settings and controlled field settings
- The ability of the EM tags to withstand severe shock loading was explored in a munitions lab
- The capability of the above-ground interrogator to detect the surrogate-mounted tags in blind tests at the Aberdeen Test Center

Several minor tasks were also pursued. These tasks included the investigation of the quality factor specification in Texas Instruments' Tiris™ tags, and the use of the finite-element modeling results to predict the safety of generating large magnetic fields in the presence of munition and ordnance items.

3 Project Objective

The program objective was to tag ordnance items before they are delivered, which will allow a significantly more efficient means for locating UXO and discriminating UXO from clutter. Battelle was to advance current RF tag capability to survive the operating conditions associated with munitions, provide information on the munitions location and perhaps identity, and be compatible with operational deployment.

The tag investigated by Battelle will be secured to the candidate ordnance item, potentially using means described in this report, and will be capable of surviving the delivery system. The tag will also survive ground impact and penetration in the case of the ordnance item not exploding. The buried tag will signal the UXO tag interrogation module when the detection system is brought nearby.

4 Technical Approach

Battelle Columbus led and managed the UXO tagging effort. Battelle scientists in Columbus and at PNNL investigated candidate EM and RF tag/interrogator systems. These efforts included adapting to anticipated operational requirements and the knowledge base of the Energetic Systems and Security Technology Department in Columbus. Army, Air Force, and Navy personnel consulted with Battelle when operational or ordnance issues arose.

Two significant technical challenges were addressed during this project. First, the electronics and coils secured to the UXO item, the EM UXO tag, must survive the shock and temperature environment of the weapon delivery system and the impact and penetration of the ground. Second, the EM UXO tag must provide sufficient signal to the EM UXO Interrogation System for the Interrogation System to detect it in the ground with the tag in close proximity to the munition, generally a massive metal object. The Interrogation System must also indicate the location of the ordnance item. Minimization of false alarms is essential.

The coils and electronics on the tag will be located in a milled groove or other void in the exterior of the UXO item. Several approaches were considered. Modeling of electromagnetic fields was used to optimize the location and design of the tag.

It is important to note that Battelle focused on passive systems. One active system was investigated. Active systems, which require a battery or other energy source on the ordnance tag, are less practical because of unknown delays in ordnance shelf life and unknown time that the device will be in the ground before remediation activities occur. Scientists at PNNL conducted an experimental investigation of the active system as a Risk Reduction activity and because of the importance of unexploded surface munitions. Battelle and the Government agreed to halt this activity in 2004.

Two main modules are required to establish the required tag system – the tags and the Interrogation Module. The UXO tags will be fastened to or integrated into the projectile or bomb. The EM UXO Interrogation Module will be moved along the ground to excite the passive tags and to detect their replying signal.

Both laboratory and field-testing were key factors in design verification. The first step was to develop a test plan, which would provide a platform to evaluate basic tag/interrogator design concepts and to evaluate tag/interrogator prototypes. The test plans for testing at West Jefferson and at Aberdeen Test Center were generated in 2005. A second Aberdeen Test Center plan was developed in 2006.

4.1 Buried Munition RFID Tag Technology

For the case of buried munitions, Battelle focused on RFID tags that operate in the 125-kHz[1] range because of the low attenuation characteristics of these signals in most ground media. Modeling during this study indicated higher frequencies could offer lower attenuation values but commercial tags were not found that operate between 125 kHz and 400 MHz, which is too high a frequency for reasonable ground penetration. Tiris tags from Texas Instruments were of primary interest because of their characteristic of not replying until the interrogating signal has turned off. The modeling and experimental efforts, which

[1] The Tiris tags used during this study operated in a frequency-shift keying modulation format; the two frequencies used were 123.2 kHz and 134.2 kHz. Although the center frequency is 128.7 kHz, general discussions in this report refer to frequencies near “125 kHz” in order to simplify the text.

are discussed subsequently in this report, made known that the ground medium and the presence of the metallic munition modify the electrical characteristics of the Tiris tags. It is possible that future efforts involving Tiris designers might result in a custom tag that is more advantageous for the buried munition detection application but such research was outside the scope of this study.

4.2 FALSE ALARMS

Battelle believes the false alarm rate for this technology is very low because a false alarm will not exist unless a Tiris 125-kHz RFID tag that is not attached to a munition is in the presence of the detection system. Battelle considers three possibilities exist that will cause a false alarm:

1. A munition explodes and the RFID tag is not destroyed.

2. An RFID tag is separated from its munition during flight or entry into the soil.

3. Stray Tiris 125-kHz RFID tags are somehow present in or on the ground.

No attempt was made to investigate the probabilities of these four conditions occurring. Common sense may indicate that possibility 2. is the most likely. This concern emphasizes the need to securely attach the tag to the munition. This report presents potential approaches to fastening tags to munitions but this project did not include investigations of the likelihood of the separation of the tag from the munition.

4.3 FALSE NEGATIVES

It is possible that variations in the two frequencies generated by the tag could vary over some small spectral range. Such a possibility was not investigated as part of this project. If a sophisticated receiver system was built in the future, the filters and detection algorithms must be designed to allow for possible frequency value variations to ensure that tag frequency drift does not cause tagged ordnance items to be missed.

4.4 TASK DESCRIPTIONS FROM THE PROPOSAL/CONTRACT

4.4.1 Task 1. Establish Operational Parameters

The initial portion of the task was completed in 2003. The deliverable product was a set of five candidate ordnance items that Battelle provided to the Government. The five recommended items were chosen based on evaluations by Battelle's experts, discussions with and recommendations of our military partners, and discussions with SERDP and Institute for Defense Analysis experts.

4.4.2 Task 2. UXO EM Tag Design

The Government required a tag that could be interrogated through three feet of soil using an above ground mobile interrogator. The four primary issues of concern were the ability to detect a tag in very close proximity to a large metallic object, the ability to detect a buried tag, the ability to discriminate between a tagged ordnance item and range clutter, and tag survivability. A design was generated including key factors such as (1) RF frequency selection, (2) tag and interrogator antenna design, and (3) tag size, location on the ordnance item, and packaging. Detectability is driven primarily by RF frequency and antenna design along with supporting tag and interrogator modulation electronics. Electromagnetic

modeling software assisted in optimizing the tag design in terms of frequency, configuration, size, shape, and on-ordnance location. Starting in 2004, ordnance items that remain on or very near the surface were considered separately. Battelle explored the potential for passive UHF tags to be used on these surface-class munitions. Initial feasibility concepts were evaluated in the laboratory or local ground testing for proof-of-concept. Next, prototypes (tag and interrogator) were developed and lab tested on simulated munitions samples. Several iterations followed to optimize the design, after which the prototypes were submitted to controlled field-testing. Our approach included the conceptualization, design, and performance testing of several tag/interrogator candidate systems.

4.4.3 Task 3. Testing

A test plan was developed that provided a platform for evaluating basic tag/interrogator design concepts and tag/interrogator prototypes. The test plan required the use of static and dynamic test munitions samples and environmental chambers. Static test samples were used to establish detection performance while dynamic samples were used to mimic launch and impact. One active tag system based on existing RF ID technology was tested in the ground to quantify detection depths versus operational parameters.

4.4.4 Task 4. Data Analysis and Recommendations

We conducted analysis of the test data during the entire course of the project to allow the Government to make Go/No-Go decisions. Hardware subjected to the testing protocol was evaluated for ease of system integration. This systematic approach led to the optimization and characterization of promising techniques for embedded RF tags. Battelle's final recommendations are included in this report.

4.4.5 Task 5. Reporting

The Battelle-led team submitted quarterly reports, Annual Reports, and this Final Technical Report. The Final Technical Report documents the information obtained and collectively summarized by the advisors and team members. The team also participated in reviews as required by SERDP.

5 Project Accomplishments

5.1 INTRODUCTION

This section summarizes the project's accomplishments. One effort addressed laboratory experimentation. It included some initial experiments and findings that would help keep later design and testing work in perspective. Work was also done to prepare an appropriate laboratory at Battelle that would allow somewhat realistic experiments while incorporating required safety considerations. Another effort involved modeling of the magnetic fields needed to get energy from the above-ground interrogator to the tag and from the tag back to the above-ground receiver. At the start of the project, it was assumed that propagation of energy through lossy ground media was the primary issue. Experimentation and direction from SERDP management changed this focus to concerns about placing EM and RF tags near large metal ordnance items. The model used is simulated above-ground coils, lossy ground, and metal items near the tags.

In addition to the change in focus (from concerns about ground loss to issues involving fields near large metal objects) discussions with SERDP managers and others resulted in increased concern and focus on the dangers of surface and very-near surface munitions. This concern resulted in an increased emphasis on the potential for using higher frequency RF tags to help locate surface UXO. PNNL had been investigating the potential for using RF tags as a risk reduction activity. The investigation of these RF tags is considered more of a complementary activity.

Another item communicated from the Government to the team was the relative importance of the portion of the munition containing the fuze. Some ordnance items comprise a nosecone-type module containing fuze electronics and a larger module containing most of the explosive material. In fact, the module containing the fuze may be more dangerous than the larger module because the energetic material associated with the fuze is less stable than the main load of explosive material. As a result, tags must be embedded in the nosecone of munitions that have the potential to be broken up upon impact. Additional tags may also be included on the main body.

At no charge to the project, an information specialist at the Advanced Materials and Processes Technology Information Analysis Center (AMPTIAC) performed a search of their DTIC database and the Internet for information on future munitions using polymer rather than metal housings. These non-metal enclosures would be ideal for the Tiris tags being investigated. AMPTIAC was not able to locate any useful resources.

5.2 MECHANICAL MOUNTING OF THE LOW-FREQUENCY TAGS ON THE CANDIDATE MUNITIONS

This section summarizes the research and recommendations for applying a tracking device to five different munitions, namely the BLU-97, MK-52 practice bomb, M720, M229, and 155 mm projectile. A previous study, conducted in 2003, resulted in these munitions being chosen as representative samples for the scope of this project. Because these munitions vary considerably in physical shape and size, no universal attachment method seemed feasible; however, specialized techniques are proposed for each of these munitions. This initial research into the mounting feasibility and potential approaches was completely a paper study. No physical testing was performed during the timeframe of this investigation.

5.2.1 Mechanical Mounting Requirements

The following general requirements were identified as being of concern, even though no firm quantitative values are available at this time:

- Munitions
  - Goal of tagging
    - Locating explosive, casing, etc.
  - What munitions are being tagged
  - Firing details per type
    - G loading and rotation
  - Modifying munitions
    - Inertia changes, aerodynamics
    - Maximum depth of casing intrusion (per type)
    - Areas of limit (example: where the bomb holder is located)
  - Part separation issues (what needs to be tagged)
  - Quantity anticipated
    - Near term/long term
  - Degrade munitions during tag installation
    - Chemical reactivity due to machining
  - HAZMAT issues
- Environment of Use
  - Properties of munitions landing site
    - Temperature/Humidity/Pressure/Acidity
  - Terrain of military ranges
    - Sand/Rocky/Lake/Tundra/Desert
  - Distance to detect when buried in ground
    - Effect terrain has on distance
    - Nominal/tolerance
  - Operating conditions throughout operating cycle (including flight conditions)
- Tag/Attachment Characteristics
  - Size (s)
  - Location desired
    - Possibly custom fit each type of munitions
  - Operating requirements
    - Withstand firing/impact g's
  - Life expectancy (including storage conditions)
    - Tag
    - Attachment
  - Critical spacing if inside munitions casing
    - Tolerance on location to outside of casing
    - Tolerance to surrounding metal
  - How different attachment methods affect performance of tags or munitions
- Cost and benefit
  - Cost of recovery vs. cost of adding tags

- Envisioned use: scenario for munitions with tags

5.2.2 Mechanical Mounting Assumptions

The following general assumptions were made in the mounting study:

- Sensor tracking device attached to the munitions
    - False alarms must be minimized
    - Texas Instruments TI-RFID Tiris transponder [http://www.ti.com/tiris/docs/products/transponders/transponders.shtml]
    - Two sizes, shown in Figure 4.
        - Larger unit dimensions: cylindrical, $^{5}/_{32}$-inch diameter with $1\ ^{7}/_{32}$-inch length
        - Smaller unit dimensions: cylindrical, $^{5}/_{32}$-inch diameter with $^{29}/_{32}$-inch length
- Electromagnetic sensor characteristics
    - Cylindrical tag geometry allows for better entry of magnetic field
    - Metallic munition repels the tag's magnetic field
    - Separation between metallic surface and tag is critical
        - Designated to be 0.17-inch separation, nominal
    - Optimal tag location is near the ends, not the center of the munitions
    - Permeable groove filler helps push magnetic field into tag
    - Soil conductivity has little effect on magnetic field strength
    - Sensor cannot be placed inside of a metal casing
- Destruction of the tag (rendering the tag inoperable to prevent false alarms)
    - Explosion of a successfully detonated munition will destroy the tag sensor device
    - Fail safe may be designed into the system
- Munition Selection Criteria
    - Failure rate at firing range
    - Commonality of use

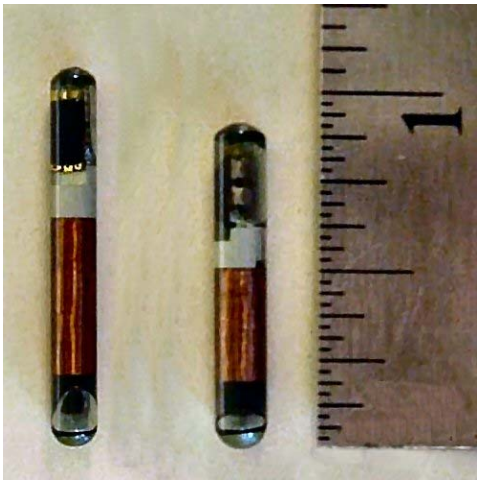

Figure 4. Two sizes of the Tiris solenoidal tags

5.2.3 Proposed Mounting Schemes for the Candidate Munitions

This section presents details on possible mounting approaches to the munitions selected as candidates during the 2003 effort on this project.

BLU-97: General Description

The BLU-97 Combined Effects Bomb (CEB) is a submunition commonly loaded into a CBU-87 and is effective against armor, personnel, and material. A total of 202 BLU-97 submunitions are loaded in CBU-87, which offers a footprint of approximately 200 m by 400 m. The bright yellow casing of the BLU-97 is cylindrical in shape, approximately 20 cm long and 6 cm in diameter. It contains a shaped charge, scored steel casing and zirconium ring for anti-armor, fragmentation, and incendiary capability. The case is made of scored steel designed to break into approximately 300 preformed ingrain fragments for defeating light armor and personnel.

These bomblets are dispensed over a relatively large area and a small percentage of them typically fail to detonate, so there is an unexploded-ordnance hazard associated with this weapon. These submunitions are not mines, and are not timed to go off as anti-personnel devices; however, if they are disturbed or disassembled, they may explode. The BLU-97 has a ten-year storage life, have a 0.95 Mach Environment Drop at 300 feet to 40,000 feet, and an operating pressure of 14 pounds per square inch.

Figure 5. BLU-97 views

BLU-97 housed inside of the CBU-87

BLU-97: Tagging recommendation Option 1, Disk

Tag locating concerns:

- The casing is thin and scored for fragmentation; therefore, to maintain designed performance, do not remove material from the casing or add a rigid band around the diameter.
- BLU-97s are packed into larger munitions, so any protrusions from diameter of the case may interfere with the packing ratio.
- A parachute deploys from the top surface (surface with the thin metal fins), so attachment to this surface is not recommended.

Tag locating proposal:

- Manufacture thin plastic (PVC, ABS) circular disk (1¼-inch diameter by $^{5}/_{16}$-inch thick), to house the RFID tag and the required 0.17-inch offset from the steel casing
- Rivet to bottom surface of casing

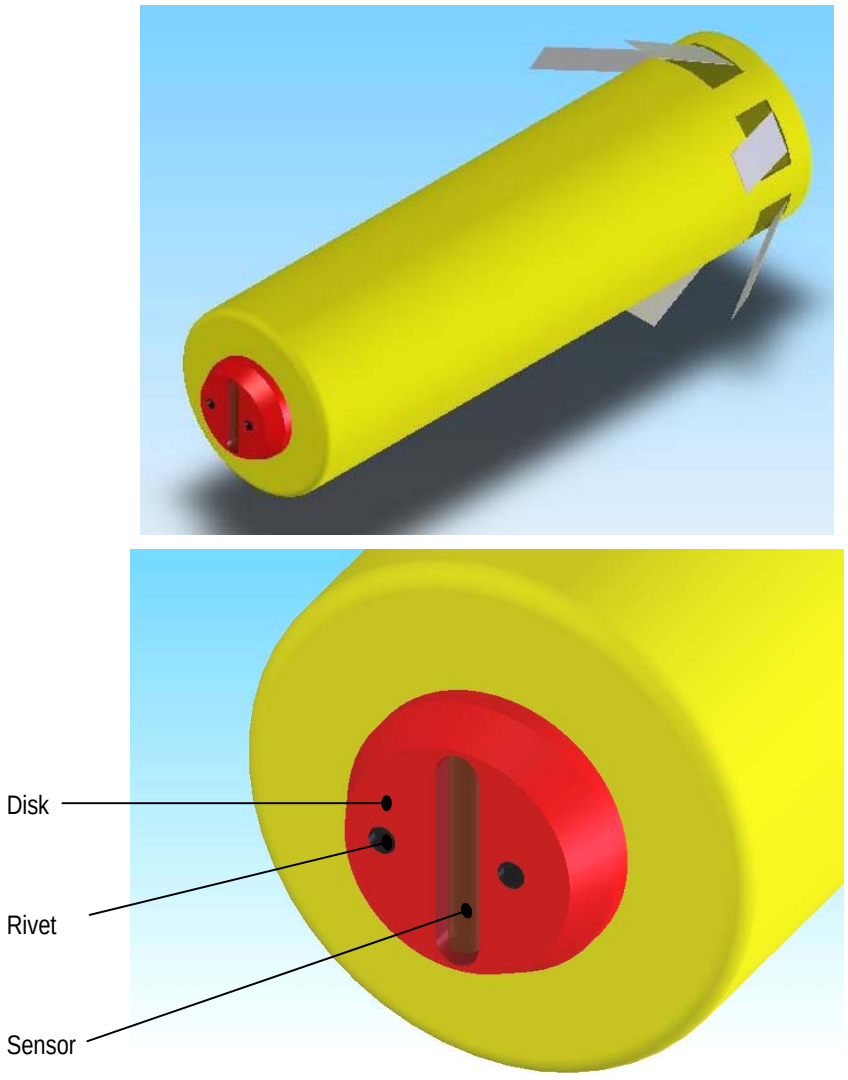

Figure 6. Mounting *Option 1* for BLU-97

BLU-97: Tagging recommendation Option 2, Plug

Tag locating proposal:

- Cut a 1¼-inch diameter hole in the bottom surface of the casing
- Manufacture a rubber plug to fit inside the casing as shown in Figure 7
    - With a hard surface finish on the top side, so inner casing spring can seat
    - With a 0.155-inch sleeve on the radial edge (to slide in the RFID tag)
    - The plug will be easier to install if it has the tapered shape shown in Figure 6
- From the inside of the casing, press the plug through the 1¼-inch diameter hole
- Slide the tag into the cylindrical sleeve and press in the cap

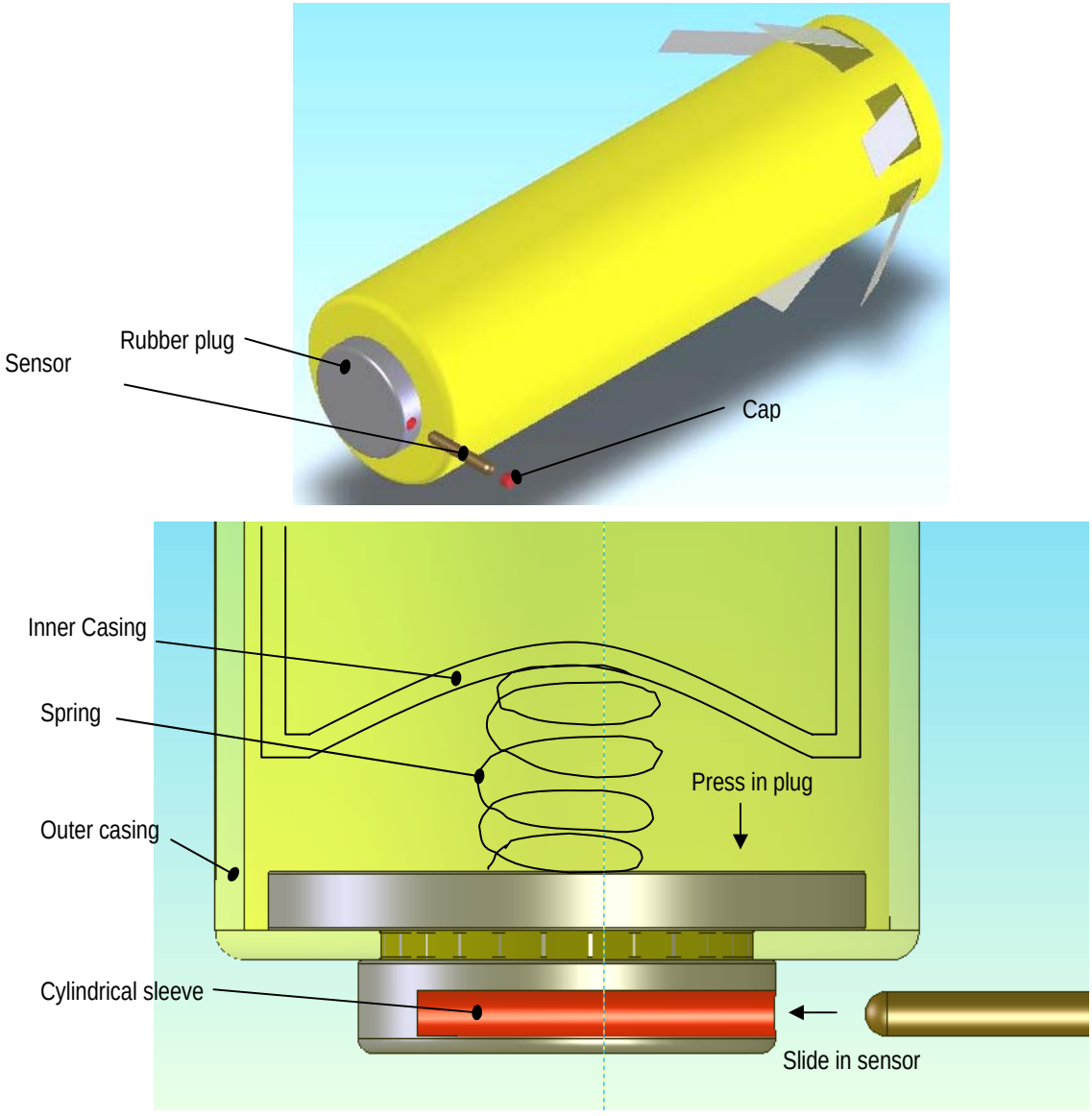

Figure 7. Mounting *Option 2* for BLU-97

BLU-97: Tagging recommendation Option 3, Molded-in RFID tag plug

Tag locating proposal:

- Same general concept as O*ption 2* (except the tag is molded during manufacturing)
- Cut a 1¼-inch diameter hole in the bottom surface of the casing
- Manufacture a rubber plug to fit inside the casing
    - The plug will be easier to install if it has the tapered shape shown in Figure 6
- Mold the tag into the plug using an injection molding process
- From the inside of the casing, press the plug through the 1¼-inch diameter hole

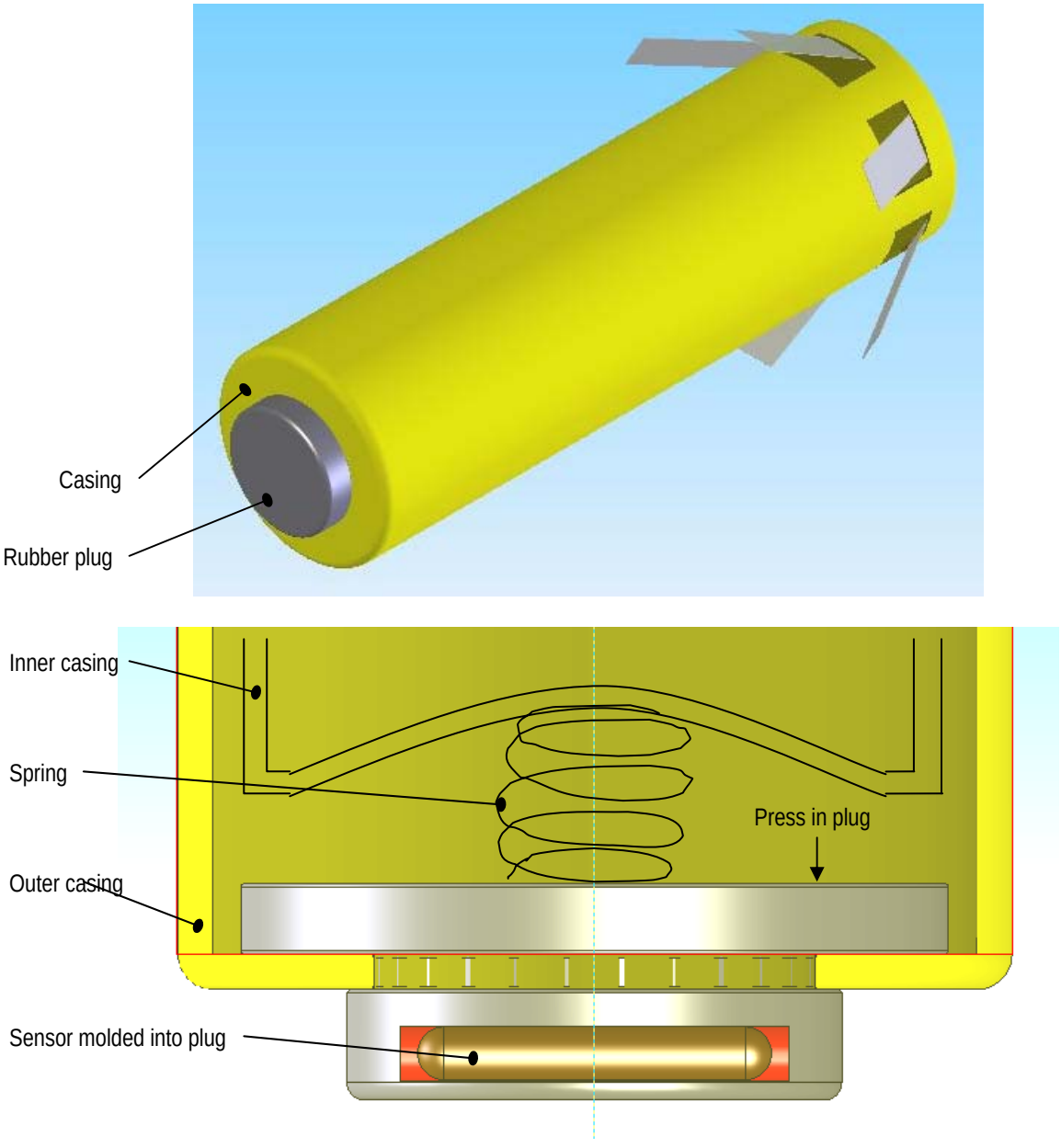

Figure 8. Mounting *Option 3* for BLU-97

MK-52 Practice Bomb: General Description

The 3-kg MK-52 bomb is used for practicing delivery techniques adopted for the 500-lb MK-82 bomb. This practice bomb can be carried and released from the TER-9 rack or from a SUU-20. When used on the TER-9, the practice bomb is fitted with its safety/suspension lug in the raised position (12 o'clock) and suspended from the jaws on the rack by the safety/suspension lug, with a ground safety pin (GSP). When used on the SUU-20, the bomb is fitted inverted, with the safety/suspension lug at the 6-o'clock position and gripped by the caliper type suspension system. The MK-52 is designed to emit smoke and a flash signal through the open end of the body upon impact. This spotting charge is prevented from being initiated after preparation and while attached to a bomb rack by the raised safety/suspension lug. The safety/suspension lug is restrained in its raised position by the GSP.

The MK-52 consists of three main assemblies: a body, a nose assembly, and a cartridge assembly. The bomb body comprises a cylindrical Dough Moulded Compound (DMC) plastic tube with four external integrally molded stabilizing fins at the rear. The wall thickness of the body is thicker at the rear section than the forward section, and there is a step that restrains rearward movement of the cartridge assembly. The GSP passes through a hole in the wall of the cartridge assembly and locates into the cartridge assembly when the safety/suspension lug is the raised position; the GSP will not fit when the safety/suspension lug is lowered.

Figure 9. MK-52 Practice bomb

MK-52 Practice Bomb: Tagging recommendation, Option 1 place RFID tag inside

Tag locating proposal:

- Locate the RFID tag internally.
- Because the casing of the MK-52 is plastic, the casing will not interfere with the function of the magnetic field-based transponder.
- Because the spotting charge emitted from this bomb is mild, the tag's proximity to the charge could help ensure sensor destruction upon successful detonation.

- The tag could be placed between the nose and body assemblies or between the body and the cartridge assemblies.

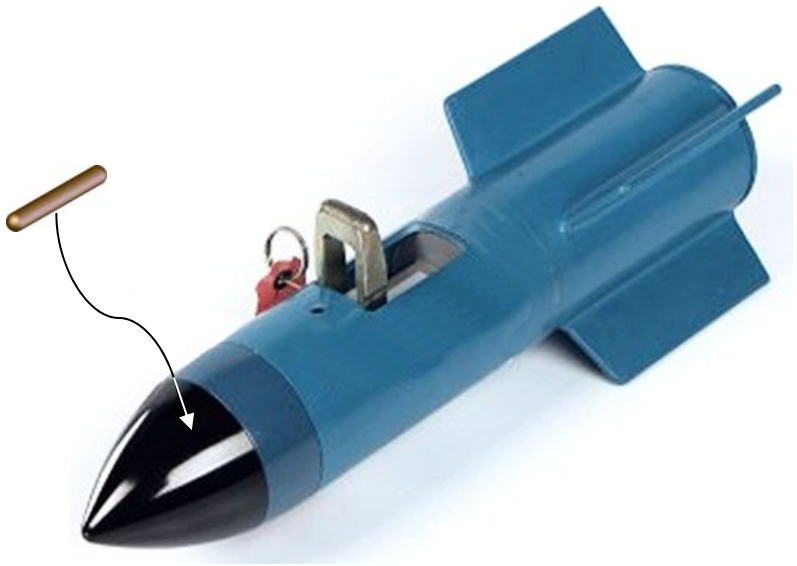

Figure 10. *Option 1* for mounting tag in nose of MK-52

MK-52 Practice Bomb: Tagging recommendation, Option 2 on the tube

Tag locating proposal:

- Place a total of four RFID tags, equally spaced on the rear portion of the tube, equally spaced between the fins
- Practice bomb consists of a composite molded tube, with a 0.30-in wall thickness
- Remove a 0.30-inch wide by 0.15-inch deep groove
- Set the tag in position with epoxy
- The removed material will be completely filled by the tag and epoxy to from a smooth surface that minimizes aerodynamic drag
- Adhesive tape maybe applied over the tag for additional retention

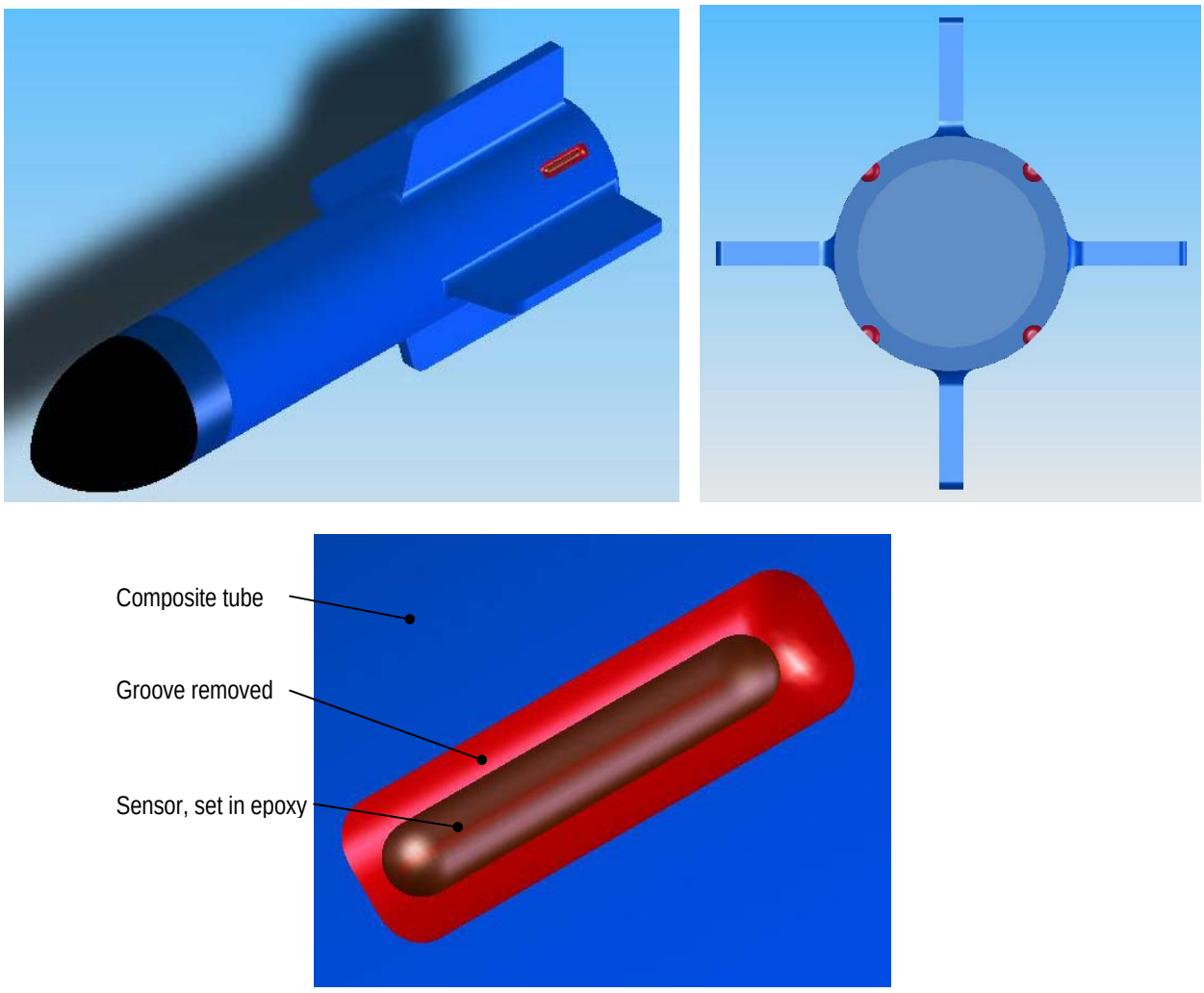

Figure 11. *Option 2* mounting tags in MK-52 main body near tail

MK-52 Practice Bomb: Tagging recommendation, Option 3 on the fins

Tag locating proposal:

- Place a total of four tags, equally spaced on the outer surface of the fins, located ½ inch from the rear surface
- Remove material 0.30 inch deep
- Set the tag in position with epoxy
- The removed material will be completely filled by the tag and epoxy to from a smooth surface to not impede existing aerodynamics
- Adhesive tape maybe applied over the tag for additional retention

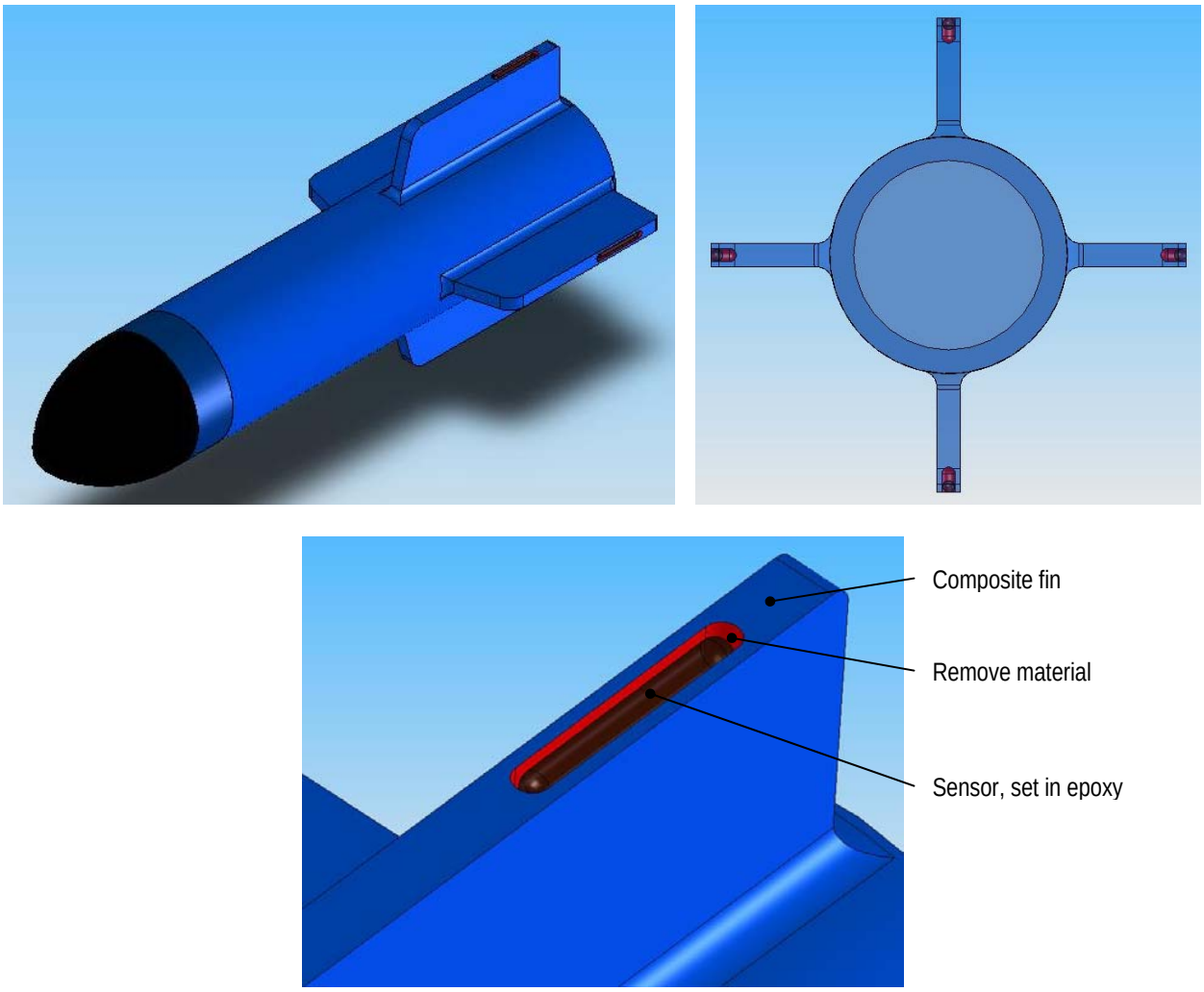

Figure 12. Mounting tag in MK-52 fins, *Option 3*

M720: 60mm High Explosive Cartridges: General Description

The M720 High Explosive Cartridges are designed for use with the M224 60mm Mortar System and are used against personnel, bunker, and light materiel targets. The high-fragmentation steel projectile is loaded with Composition B explosive. The M720 is equipped with the M734 Multi-Option Fuze that can be set to function in the proximity, near surface burst, impact, or delay mode. The mortar is a high-angle-of-fire weapon, smooth-bore, and weighs 1.68 kg (3.7 pounds). It is muzzle-loaded and can be drop-fired or trigger-fired.

The M720 consists of the following major components:

- Projectile Body Assembly
- M204 Propelling Charge
- M702 Ignition Cartridge
- M27 Fin Assembly
- M935 Point Detonating Fuze or M734 Multi-Option Fuze

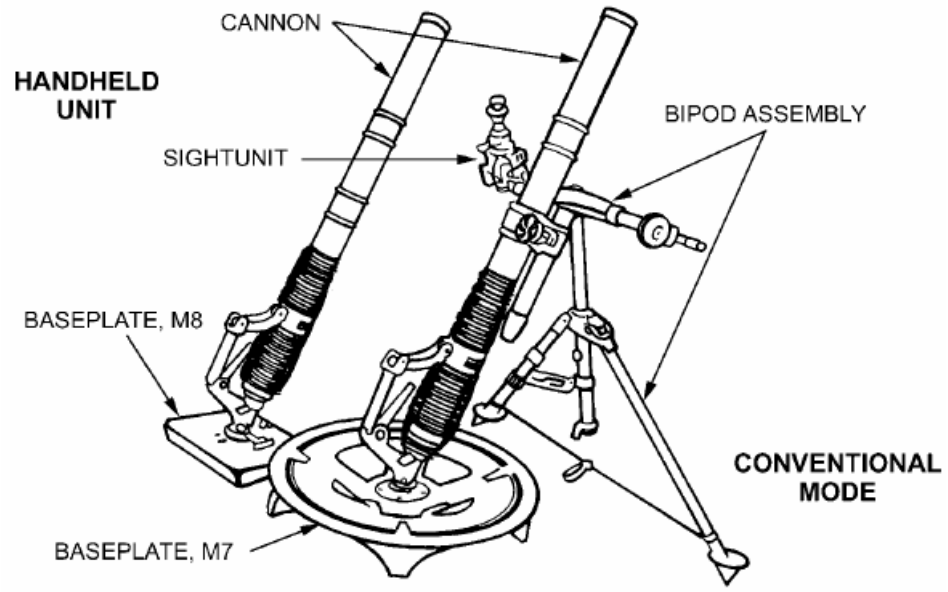

Figure 13. 60mm cartridges

M720: 60mm Cartridges: Tagging recommendation, Option 1 Modify the fuze

Locating proposal:

- The M720 has various multi-option fuzes that are threaded interchangeable parts
- Design and build a new fuze that houses four equally spaced tags
- The modified fuze will have a plastic (ABS) band around the section that previously had stand off ribs. This band will provide a smooth transition from the tip to the body of the M720. Within the structure, 0.17-inch spacing is provided to the metal casing, for magnetic energy to enter the tag. Grooves seat the tag in epoxy resin, giving a flush fit.
- A band of tape can be affixed as a secondary mechanism to ensure tag attachment

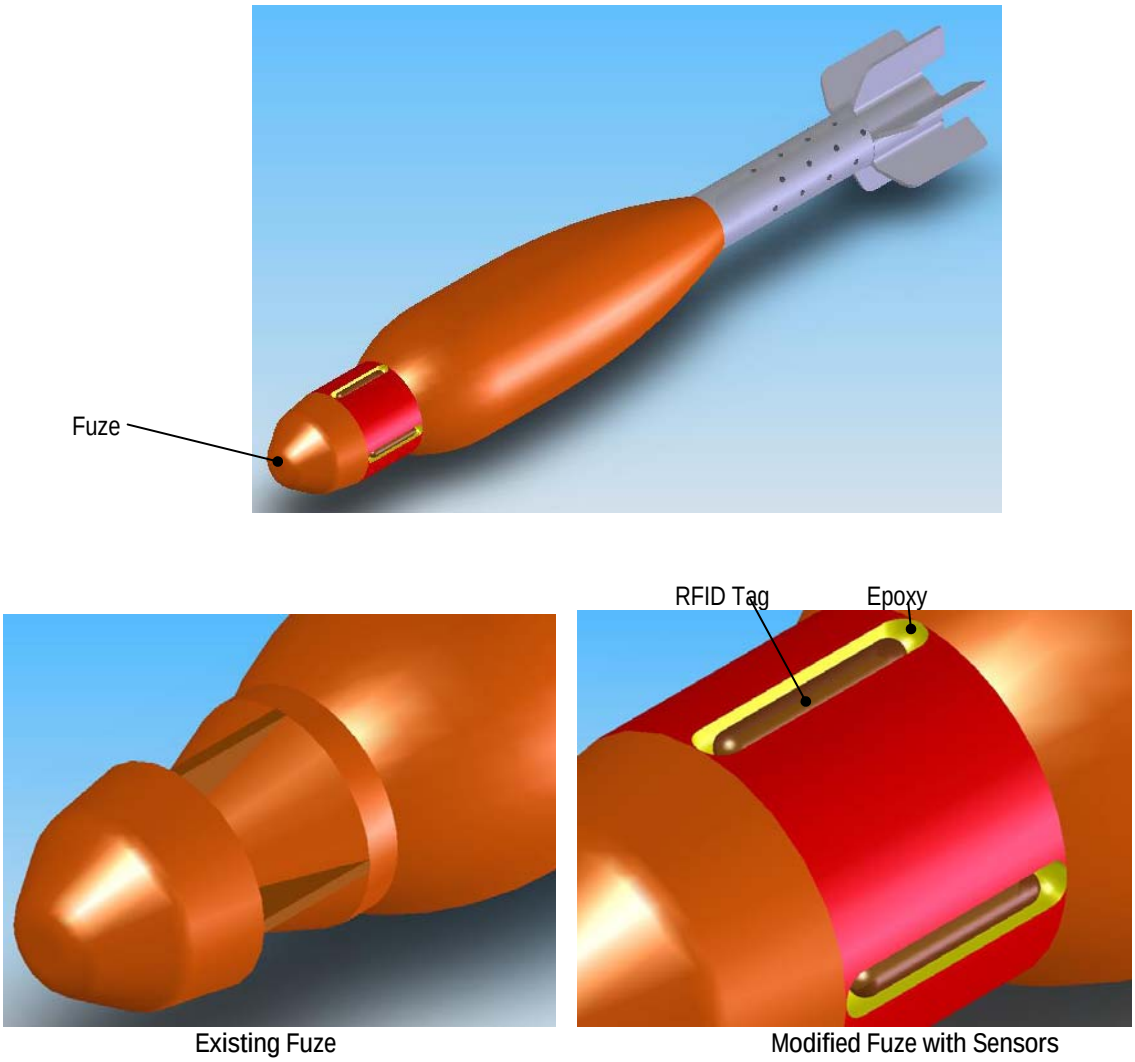

Figure 14. 60mm cartridge *Option 1*

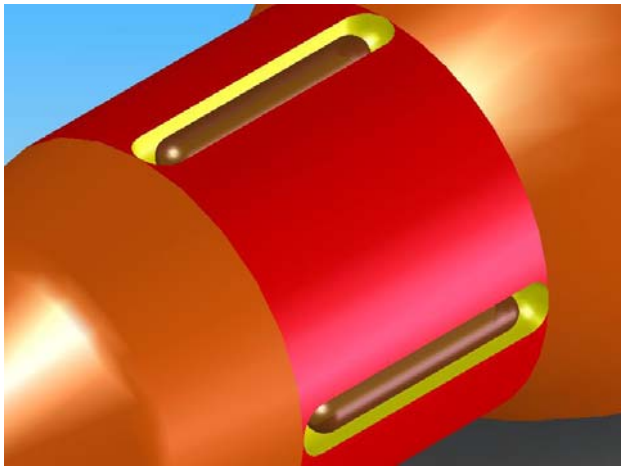

Figure 15. 60mm cartridge *Option 1*

M720: 60mm Cartridges: Tagging recommendation, Option 2 Ring attachment

Tag locating proposal:

- The front portion of the M720 will not experience intense heat during launching
- Remove a band of material 0.30 inches by 1.25 inches in size, just behind the fuze section
- Manufacture a plastic band to fit in the previously removed section, with four tags molded in and equally spaced
- Wrap the plastic band around the area of removed material and attach
- This example uses snap tabs, molded within the structure, and two #10 screws to secure the band; however, other mechanical methods are possible to fasten the unit to the munition

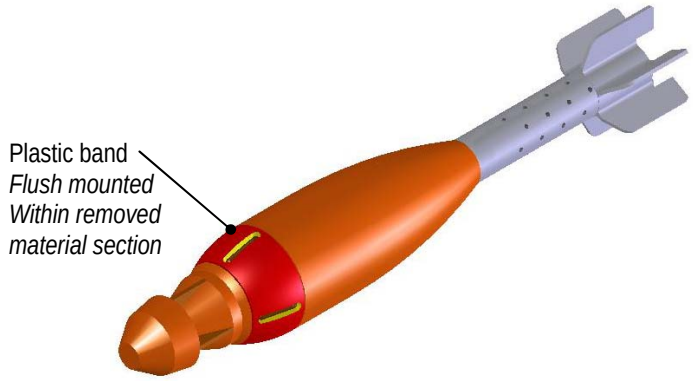

Figure 16. 60mm cartridge *Option 2*

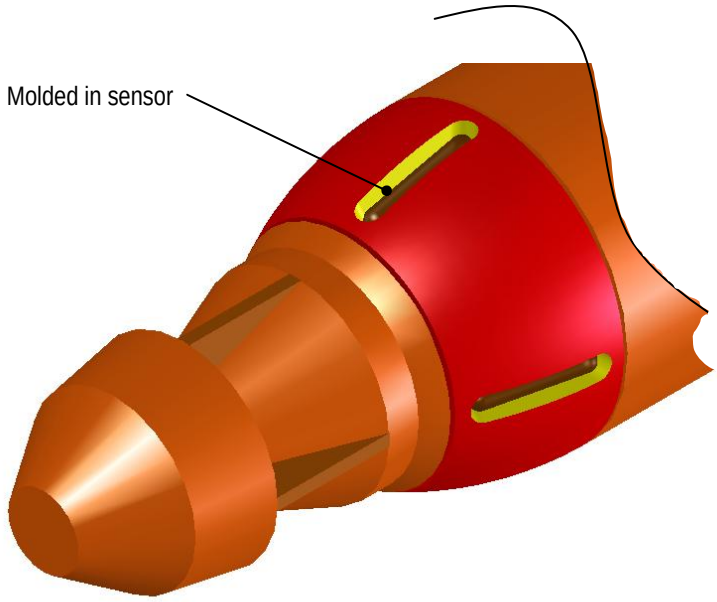

Figure 17. M720: 60mm cartridge mounting *Option 2*

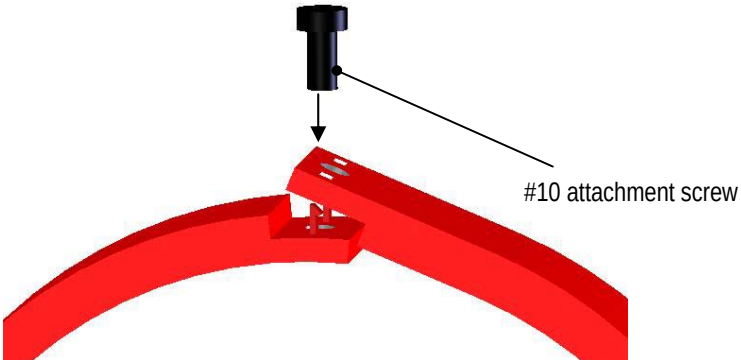

Figure 18. M720 attachment ring concept

M229 HE Warhead: General Description

The M229 HE Warhead is an elongated version of the M151 warhead and is commonly referred to as the "17 Pounder." It was designed and developed to increase the lethality and destructiveness of the 10-pound high explosive warhead. Upon detonation, the M229 fragments into thousands of small, high-velocity fragments. The diameter is 2.75 inches (70 mm), the length is 26.0 inches, and the total weight of the loaded, unfuzed warhead is 16.1 pounds (17 pounds with the fuze). The temperature limits for storage and firing the M229 are -65° F to +150° F.

Figure 19. M229 HE warhead

Figure 20. M229 launch option

M229 HE Warhead: Tagging Recommendation

Locating proposal:

- The M229 warhead uses the same M423 fuze as the M151 warhead (not part of this study), so tags placed in the fuze will allow both munitions to be tagged.
- Fuze modification:
  - Four equally spaced grooves, 0.32 inches deep, 1.25 inches long, and 0.20 inches wide
  - Set tags in epoxy
  - Wrap tape around diameter for secondary retention mechanism

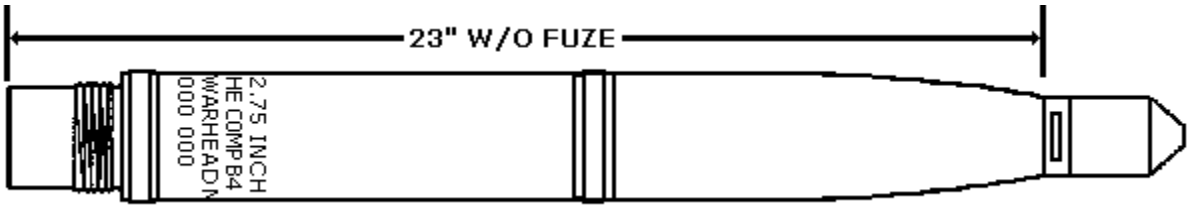

Figure 21. M229 HE warhead

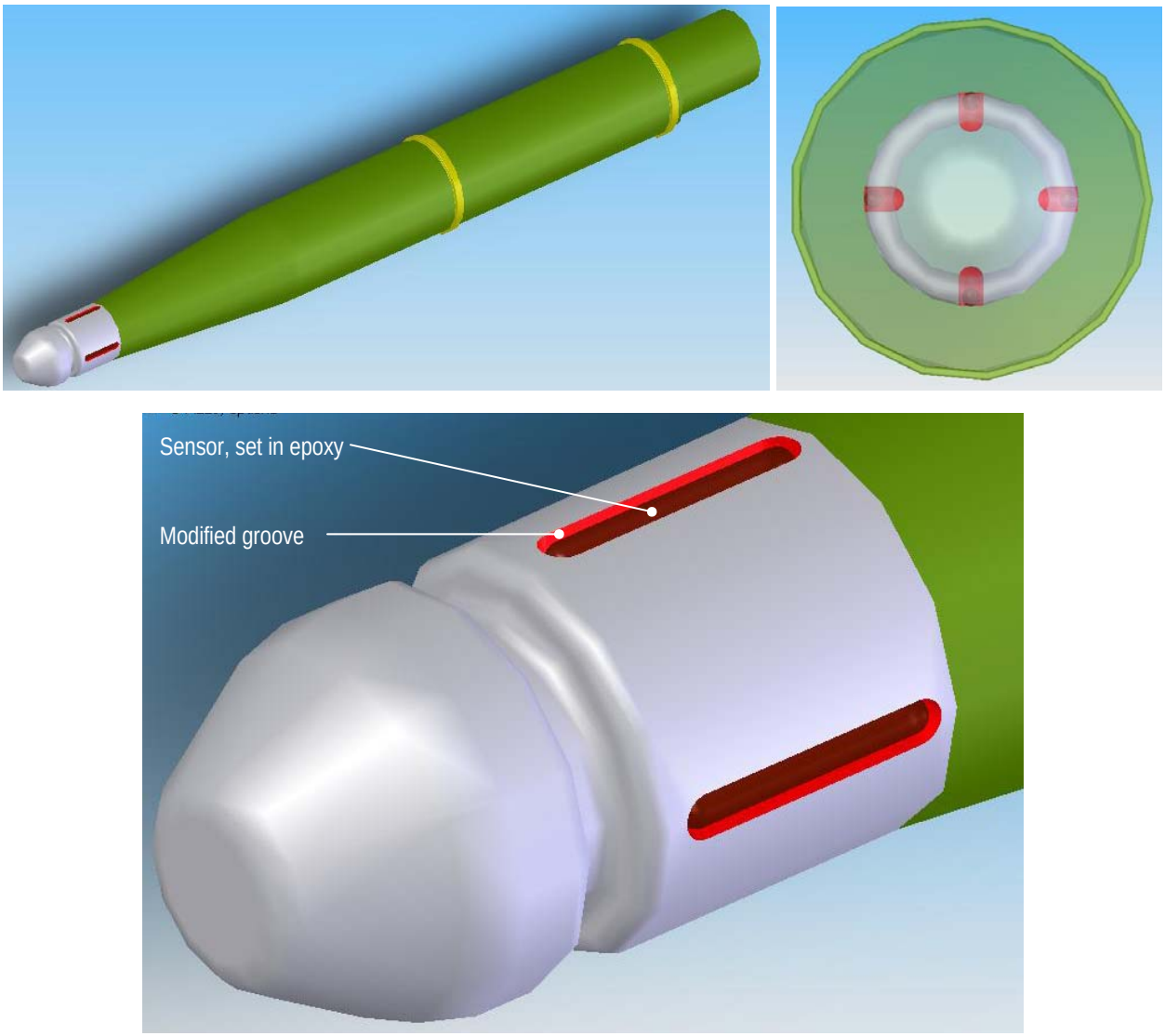

Figure 22. M229 mounting option

155mm Projectile: General Description

The 155mm Projectiles offer a broad range of options for the battlefield. They can be used as bursting projectiles, cargo carrying projectiles, and smart/guided projectiles. These warheads are also described as High Explosive (HE), Smoke, or Illuminating projectiles. They are commonly launched from the 155mm Howitzer or can be cannon launched.

The body design of the projectile depends on the intended payload. Components may include a high-fragmenting steel body (aluminum on some types), welded rotating band, payload, fuse, charges, and some form of base. The weight of the projectiles depends on the payload. Typical weight is 80 to 100 pounds, including payload.

Examples:
Bursting: The Army's standard explosive, M107, consists of a hollow steel shell containing high explosive. A fuze adapter is screwed into the body and brazed in place. The shell is hollow forged of AISI 1045.

Cargo Carrying: The M731 delivers Area Denial Anti-personnel Mine (ADAM) mines. The mines are expelled from the projectile (approximately 600 meters) over the designated target.

Smart/Guided: Cannon-launched guided projectiles, such as the M712 Copperhead, is a 155-mm, separate-loading, laser-guided, HE projectile. It is heavier (137.6 pounds) and longer (54 inches) than the standard 155mm projectile. The M712 projectile consists of three main sections: a guidance section (forward), warhead section (center), and control section (rear). Smart projectiles, such as the M898 SADARM, combines microwave, infrared, and signal processing technologies to sense and destroy armored vehicles.

Bursting **Cargo carrying** **Smart**

Figure 23. 155mm projectile in three configurations

155mm Projectile, M1XX Bursting: Tagging Recommendation

Tag locating proposal:

The 155mm projectile has many variations and uses; however, modifying a common component, such as the fuze, to house a tag could provide a general solution. Otherwise, specific 155mm projectiles need to be identified for custom attachment.

The M1XX bursting series are similar in shape and deployment. The body consists of a hollow AISI 1045 steel shell that is conventionally streamlined with a boat tail base to provide aerodynamic efficiency, and filled with a high explosive agent. The wall has a larger thickness in the rear portion; however, the rear section is exposed to high heat during launching. Therefore, the front portion may offer a location away from the heat.

- Remove a band of material from the front portion of the body, 0.3 inches deep by 1.25 inches wide
- Manufacture a plastic band with four molded in tags, equally spaced
- Wrap the plastic band around the area of removed material and attach with two screws
- This example uses snap tabs, molded within the structure, and two screws to secure the band; however, other mechanical methods are possible to fasten the unit to the munition

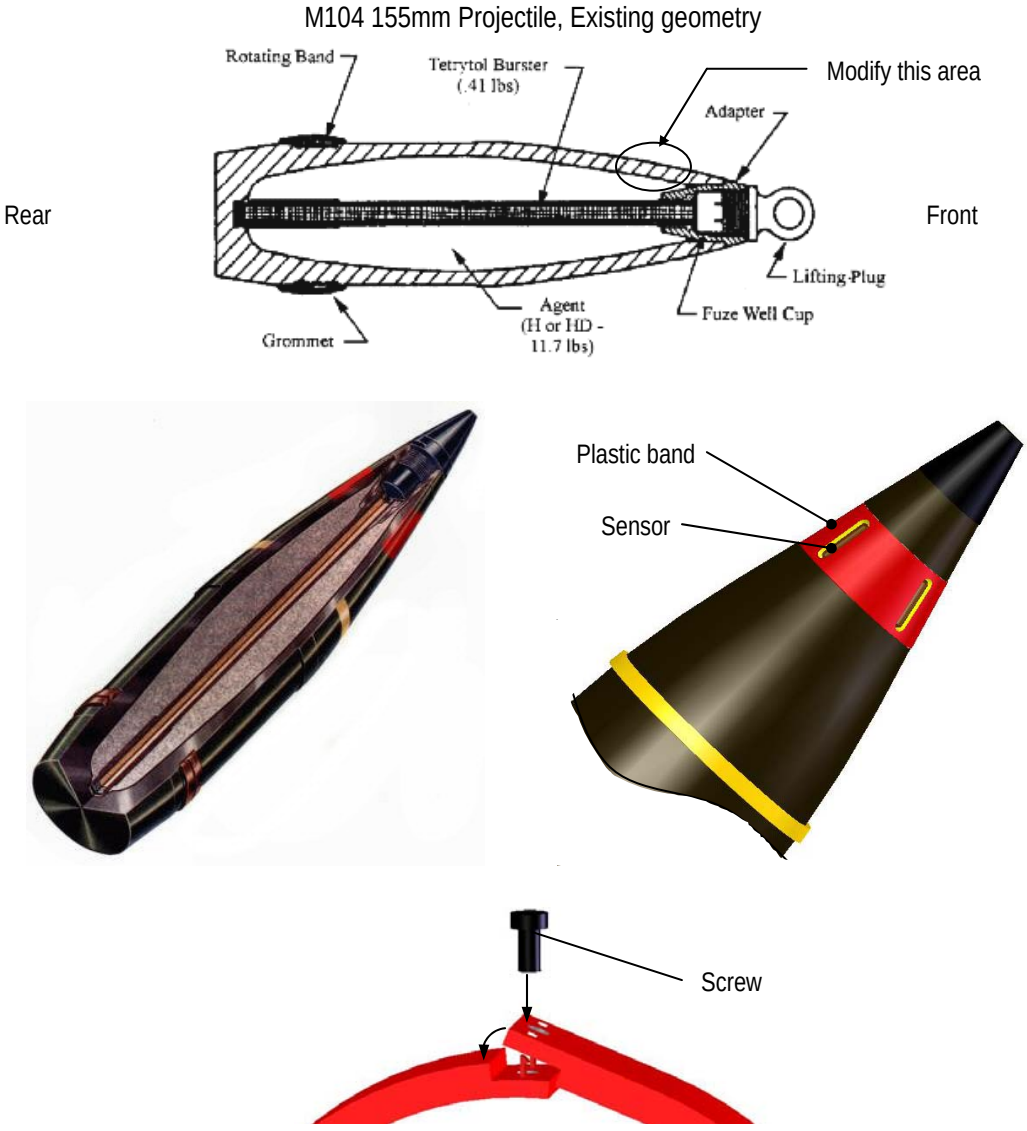

Figure 24. 155mm projectile, M1XX bursting: tagging recommendation

155mm Projectile, Cargo Carrying: Tagging Recommendation

This submunition-carrying munition was not considered in this study.

5.2.4 Munition Mounting Characteristics

Table 1 provides a summary comparison of the munitions and potential approaches to mounting.

Table 1. The five munition candidate's characteristics and potential mounting approaches

Munitions	Dimensions	Type	Casing	Launch	Detonate	Weight	Attachment	Concern
BLU-97	Cylindrical: Diameter 6 cm (2.4inches) Length 20 cm (7.8 inches)	submunition 150-200 per bomb air dropped from (CBU-87)	scored steel casing breaks into 300 fragments, zirconium ring for incendiary effect	dropped at 300-400feet, parachute slows and stabilizes for impact at the proper angle	two fuses 1.detonate on impact 2.detonate if unexploded bomb disturb on the field		Add disk structure to bottom surface	Destroy tag with a successful detonation, Packing ratio in CBU-87
MK-52	Length 14 inches	practice bomb	Dough Moulded Compound (DMC) plastic tube	may be carried and released from TER-9 rack or a SUU-20		3 kg (6.6 pounds)	Put tags 1. Inside unit 2. In fins 3. On tube	Destroy tag with a successful detonation
M720	Length 14 inches	Mortar Range: 70 to 3,490 meters 20 rounds per min.	steel	muzzle-loaded, smooth-bore, high-angle-of-fire weapon	drop-fired or trigger-fired	18 pounds	Modify fuze	Verify functionality of modified fuze
M229	Diameter 2.75 inches Length 26 inches	bursting radius 10 m, high velocity fragments can exceed 50 m	base section is constructed of steel or cast iron	unguided air-launched 2.75-inch diameter rockets	drop-fire	17 pounds	Modify fuze	Verify functionality of modified fuze
155mm Projectile	Diameter 155mm (6.1 inches) Length ~50 inches	Bursting Cargo carrying Smart / Guided	steel	Howitzer or cannon	Impact or over target	80 to 100 pounds	Remove material and attach a band	Heat from launch Structure wall thickness

5.2.5 Concerns about Mounting of Munitions

This section of the report contains findings based on initial research into attaching a transponder to various types of munitions; however, no physical testing was completed during the investigation. Therefore, effort must continue to verify all recommendations before implementing the modifications.

The list below highlights critical concerns that require attention and verification:

- Environmental
  - Manufacturing modifications to attach the tag
    - Worker safety
    - Bio friendliness
  - RFID tag and attachment method
    - Degradation in storage over time
    - Emissions in the field after use

- Munitions performance
  - Substantial physical testing to verify
    - Effectiveness of tag attachment method
    - Firing, targeting, and explosion performances are unaltered
    - Sensing device has high probability of locating unexploded ordnances
    - RFID tag is non-functioned on successfully detonated munitions

- Timeframe
  - Initial launch of tagging operation
  - Actual field testing
  - Incorporation of technology to other munitions, retrofitting

- Quantity level
  - Envisioned use for munitions with tags

- Other RFID tag geometries available?
  - Simplify assembly
  - Lower cost

- Typical munitions storage
  - 10 year target storage life
  - 20-30 year storage often experienced

5.3 MODELING

This section provides a summary of the modeling effort and the primary results. Details are provided in Section 7, Appendix A, beginning on page 109.

5.3.1 Modeling Introduction

Following Battelle's presentation at the April 2003 In Process Review, several discussions took place between Government and Battelle personnel regarding the focus and emphasis of this project. The meeting at SERDP included experts from the UXO and UXO sensor communities. There was general agreement that the EM and radio frequency tags Battelle is investigating will encounter difficulties when placed on or near steel/iron ordnance items because of the influence of the metal on the electromagnetic field. It was the consensus that the technical issue Battelle was confronting with its highest priority at that time, propagation of 125-kHz electromagnetic energy in soil, was not the most challenging issue. While Battelle experimental work on the proximity issue indicated promising findings during initial investigations, it became clear to all that this tag-near-metal aspect of the program should be made the highest priority. Since that time, Battelle has been applying Vector Fields finite element analysis software to model magnetic fields associated with tags located very near massive metal objects.

Initially, Battelle employed two-dimensional (2-D) models[2] to determine indicators of behavior versus changes in key parameters. Once a general understanding was achieved using the 2-D models, we employed actual munition drawings to model the situation in three dimensions (3-D). The 3-D models were then optimized and calibrated to the actual equipment used during experimentation and testing. The 2-D models were exercised quickly and inexpensively to indicate trends in parameters. The 3-D models were used in 2004. Modeling was performed in two separate and distinct modes. First, the field coupled into the tag from the large above-ground interrogating coil was calculated. Second, the field at the above-ground receiver coil transmitted by the munition-mounted tag was calculated. These two fields are somewhat independent of each other because the relationship between the amplitude of the field received by the munition-mounted tag and the amplitude of the field transmitted by the tag are not linearly related.

5.3.2 Situations Modeled and Conclusions

The solenoidal tag shown in Figure 4 was considered in all modeling activities. Situations that were modeled and analyzed include:

- Effects of size and shape of the "groove" in the munition where the tag was mounted. **Conclusion:** Groove shape was shown to have minimal influence on the field coupled into the tag coil. The length of the groove was found to be more important for the solenoidal tag in that about one-quarter inch of clearance was needed between the tag's coil (both ends) and the end of the groove. The effect of the composition of the material containing the tag was also investigated. Magnetic material between the tag and the metal can aid in coupling the interrogation signal into the tag.

- The solenoid tag and the pancake tag were both modeled near the munition. **Conclusion:** The solenoid tag showed clear advantages in this situation. The boundary conditions of the magnetic field at the surface of the metal caused this advantage.

- We made initial estimates of the electric and magnetic fields in the vicinity of the tag due to the above-ground interrogation coil. We also estimated the voltage level available at the above-ground receive coil due to the tag's transmission. **Conclusion:** Both of these levels appeared to be acceptable at greater than a three-foot separation. We calculated electric field values due to the high-energy above-ground interrogation coil and found them below the field limits of known Government safety levels, even for munition items very near the transmitting coil.

[2] Rectangular (infinite in one dimension) or axi-symmetric.

- We calculated the maximum electric field level immediately below the large (one-meter diameter) transmit coil to investigate potential safety issues. **Conclusion:** The results are provided in Section 5.5. Results showed the field on the bottom of the cylindrical or cone-shaped object is about one-half the value of the field on the top. This result is a little surprising and good news; the field below the munition is the same order of magnitude as the field above the munition.

- We examined the relationship between the 2-D and 3-D models. **Conclusion:** The analysis showed the 3-D fields are smaller than their 2-D counterparts but relative predictions match well when corrected by a scaling factor, which is a function of the vertical separation between the tag and the above-ground coil

- We performed a MathCAD analysis of the dipole moment of the solenoidal tag coil. **Conclusion:** This analysis was used to confirm the finite element approach as there was general agreement between the two methods. MathCAD results were also used to fine-tune the finite element parameters.

- We calculated dipole moments and fields for two tag positions on cylindrical munitions (near the center and near the edge) and two orientations (axial and circumferential) for each position. **Conclusion:** These calculations aided in determining the number of tags required on a given ordnance item and the best positions for the tags, given that the orientation of the munition in the ground will be arbitrary and unknown.

- We investigated the magnitude of the magnetic field levels on the surface of a cylindrical munition as a function of munition depth, munition orientation, tag position, tag orientation, and offset of the above-ground interrogation coil (distance between the center of the coil and the position directly above the buried munition). **Conclusion:** This field level relates to the field available to a munition-mounted coil. Figure 25 shows the magnetic field level on two munitions (vertical and horizontal) as a function of depth for a realistic signal from the one-meter diameter interrogating coil. For the assumed threshold of 8.5 μT on the transponder coil, this plot shows is possible to excite the transponder to a depth of about 40 inches. The offset of the interrogating coil correlates to a coil moving above the ground surface with the possibility that the coil does not pass directly above the munition. The munition surface field levels for the offset interrogating coil will provide an understanding of how wide the search swath widths can be. If, for example, the magnetic field levels near the surface of the munition remained high enough to excite the tag when the coil center is one interrogating coil radius away from the munition, the swath width can then be one full diameter of the interrogating coil. Figure 26 shows a result for possible offsets of the center of the interrogating coil from the position directly above a vertical munition. This plot shows the offset has to be 15 inches or less, which implies the offset must be less than the radius of the interrogating coil. The final result of this analytical investigation concluded that for a three-foot deep munition, the coil offset must be one coil radius or less, which implies the swath width can be as wide as the one-meter coil for successful excitation of the tags on a three-foot deep munition.

- We also explored an alternative munition shape that included a cone-like profile common to many munitions. **Conclusion:** The cone-shaped bodies have larger fields at the smaller end but similar flux distributions, which implies a preference for placing the tags at the smaller cone-shaped end.

- We used our 3-D modeling software to investigate the effects of the tag being situated in a "plug" cut into the side of a thin-shell munition. **Conclusion:** This need for considering a plug is

dictated by the need to offset the tag from the conducting surface by a certain amount, which in some cases will be greater than the thickness of the munition's metal shell. Preliminary two-dimensional modeling activity shows the plug helps in getting energy to the tag but hurts a little bit in getting tag-generated energy back to the surface of the ground. (The field transmitted by the tag is independent of the tag's received field, except for the fact that the received field powers the tag. For this reason, reciprocity does not apply to these two independent fields.)

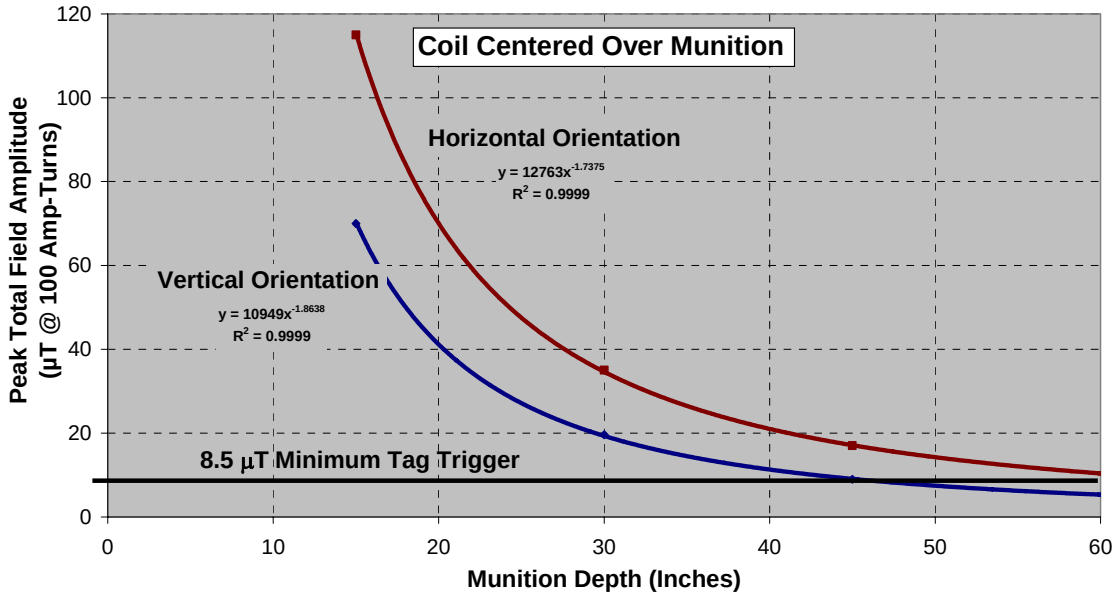

Figure 25. Magnetic field on the surface of a munition versus depth in the ground for realistic interrogating signal strength (vertical and horizontal munitions)

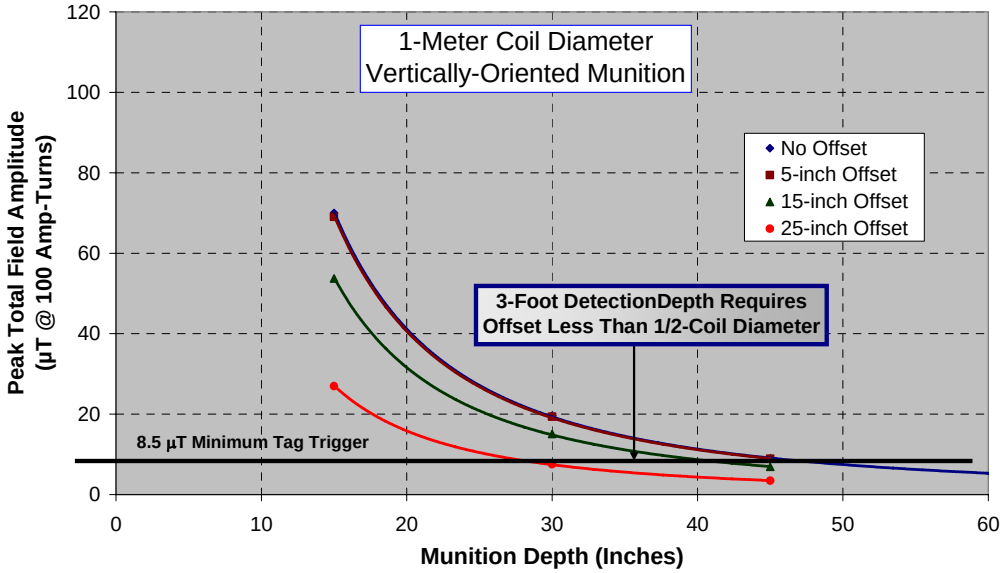

Figure 26. Magnetic field on the surface of a munition versus depth in the ground for realistic interrogating signal strength, a vertically-oriented munition, and coil center offsets of zero, 5 inches, 15 inches, and 25 inches.

The finite element software was used to generate graphical displays of the magnetic fields generated by the above-ground coil on the munition and fields generated by the tag located on the munition. A few of those renderings are presented here to provide a general feel for the type of information obtained. Figure 27 provides results for the field on a cylinder that is directly below the center of the interrogating coil. The upper figures provide drawings of the two configurations and the lower figures depict the fields. The colors provide information on the field amplitudes and the arrows point in the vector direction of the magnetic field at indicated points.

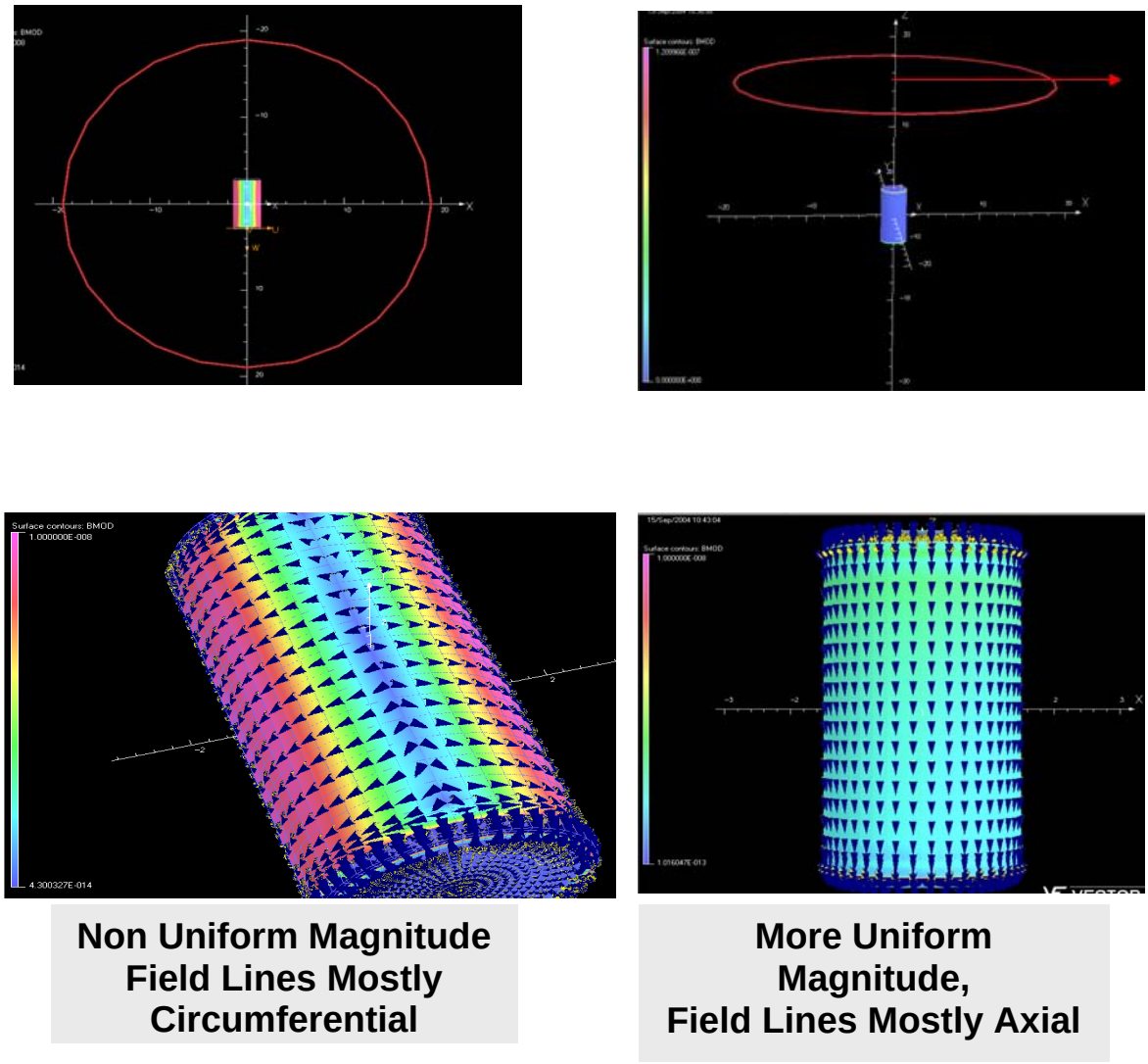

Figure 27. This figure shows the finite element analysis outputs. Both examples show the magnetic field intensity and vector direction for the interrogating coil directly above a horizontally-oriented (left) and a vertically-oriented (right) munition. The units are Tesla per Amp-Turn and the range of colors is between 4.3×10^{-14} (blue) and 1×10^{-8} (magenta)

Figure 28 shows a comparison between the magnetic field amplitudes on the top and bottom of the horizontal cylinder. As stated, the field on the bottom of the cylinder is smaller than the field on the top but the amplitude is the same order of magnitude.

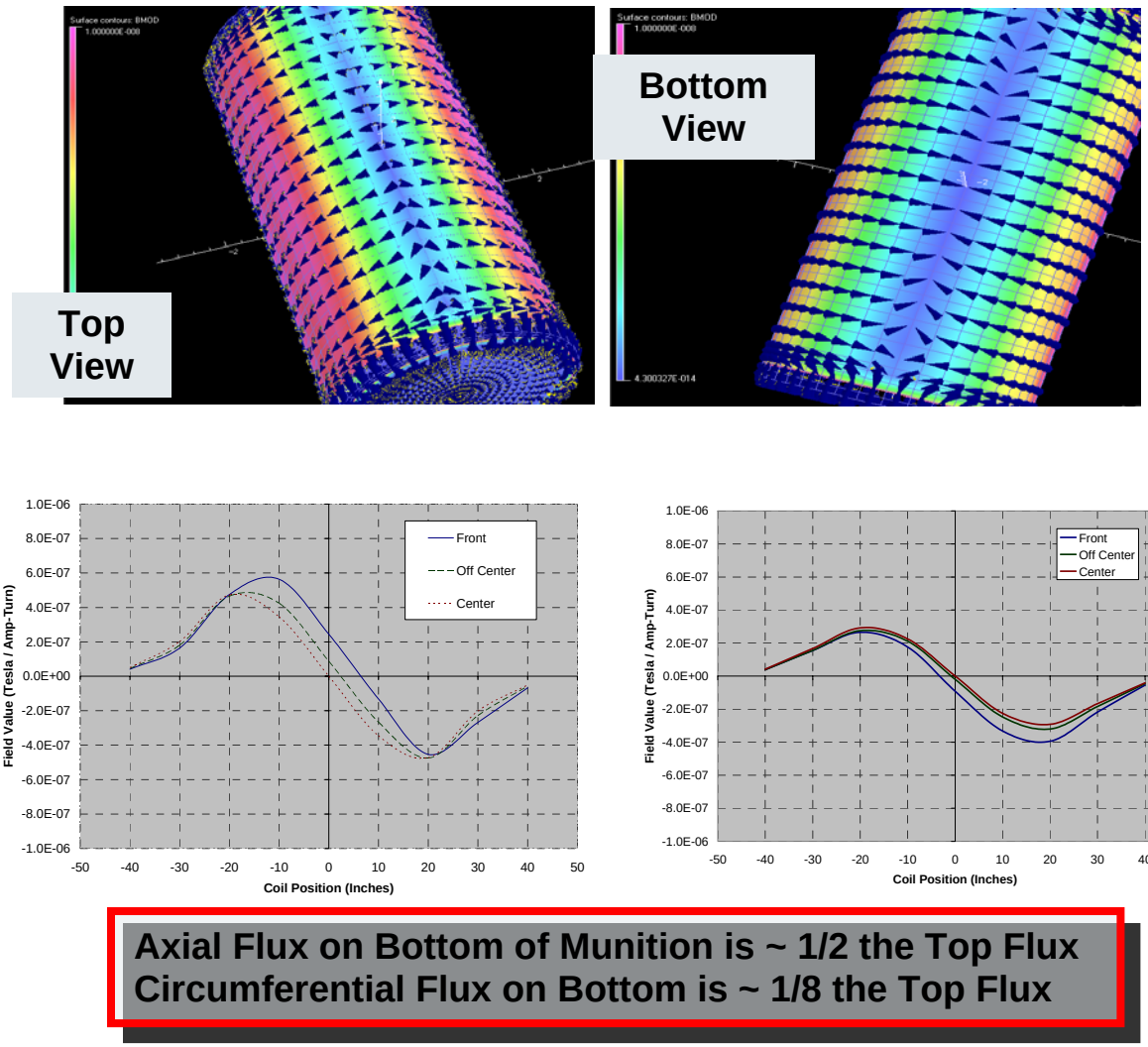

Figure 28. Comparison of magnetic flux lines and values on top (left figures) and bottom (right figures) of horizontal cylinder directly below center of transmitting coil. The bottom graphs show the magnitude of the transmitted flux near the transceiver as a function of transmitting coil position relative to the center of the munition for transceivers located near the munition edge (front), center of munition (center) and in-between (off-center)

5.3.3 Tag Placement On the Munition

Calculations were also performed that provided insight into the placement of the tag on the munition. In general, it was seen that the preferable position was placing the tag near the ends of the ordnance body rather than in the center. Figure 29 shows the field levels as the interrogating coil is scanned past the buried ordnance item. The left curve corresponds to the search coil moving parallel to the axis of the horizontal munition and the right curve corresponds to the coil moving perpendicular to the munition's cylindrical axis. The horizontal variable is distance between the center of the interrogating coil and the center of the munition. Field amplitude at the tag is shown for three tag positions: at the end of munition body (labeled front), at the center of munition body (center), and just off the center of the munition's body (off-center). The curve at the right shows that the center position is unacceptable because it is possible that the center of the coil could pass directly over a munition and not excite its tag and therefore not sense

its presence. In reality, the probability of this occurring is extremely low because no munition will have the perfect rotational symmetry of this simulated vertical target and be excited at its exact center.

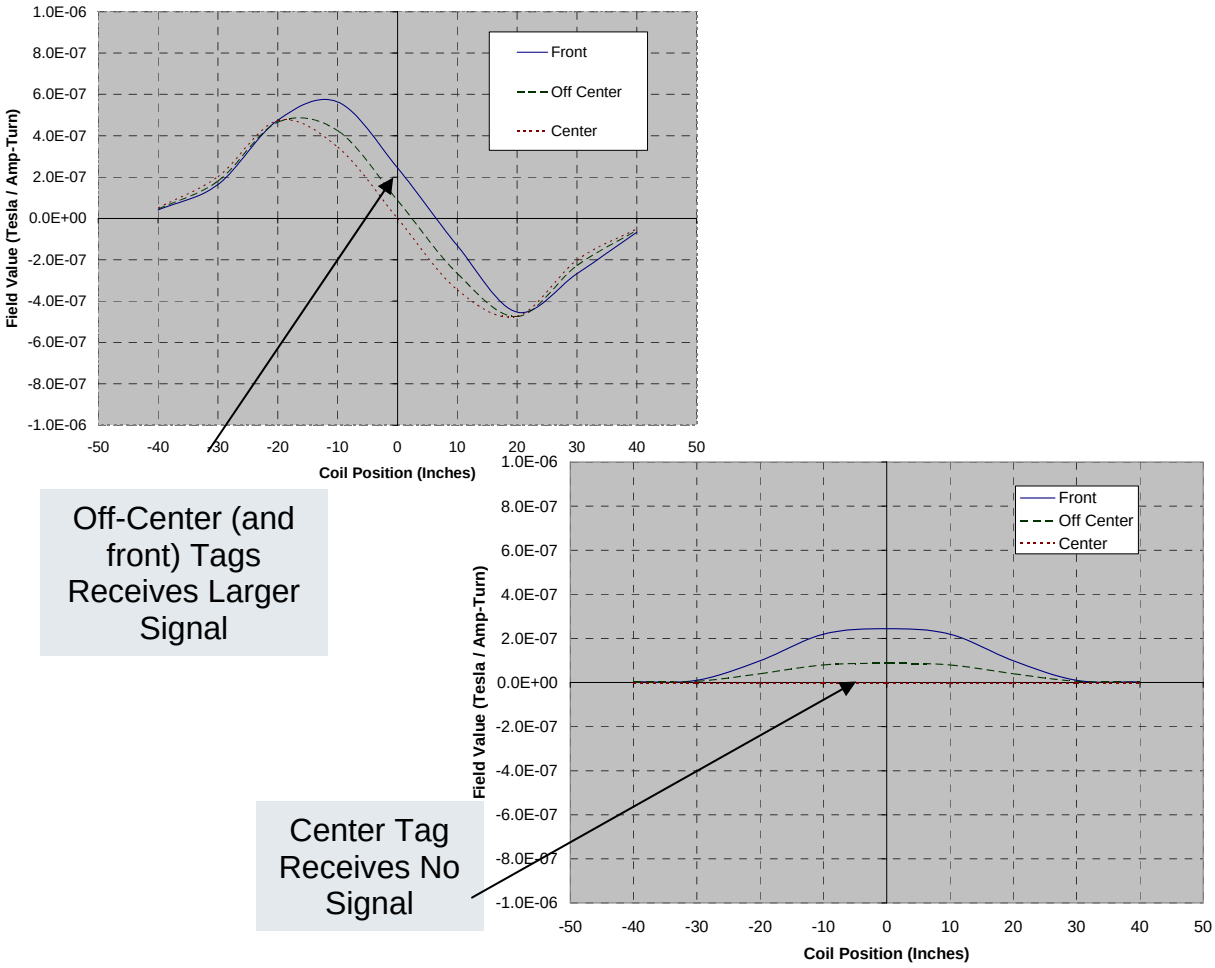

Figure 29. Responses calculated as the interrogating coil moved past the munition, in the simulation of a UXO search procedure. The left curve corresponds to the search coil moving parallel to the axis of the horizontal munition and the right curve corresponds to the coil moving perpendicular to the munition's cylindrical axis.

The fields output by the tag were also calculated using Texas Instruments' specification for the 32-mm long tag as 80.5 to 102.5 Amps/m. Figure 30 shows the peak amplitude calculated in a plane 15 inches above a horizontal tag located at the center of the cylinder's side. The upper-left presentation in Figure 27 is a histogram three-dimensional-type plot. The lower right chart shows the same data presented as a contour plot, the presentation mode used in most of Battelle's analysis.

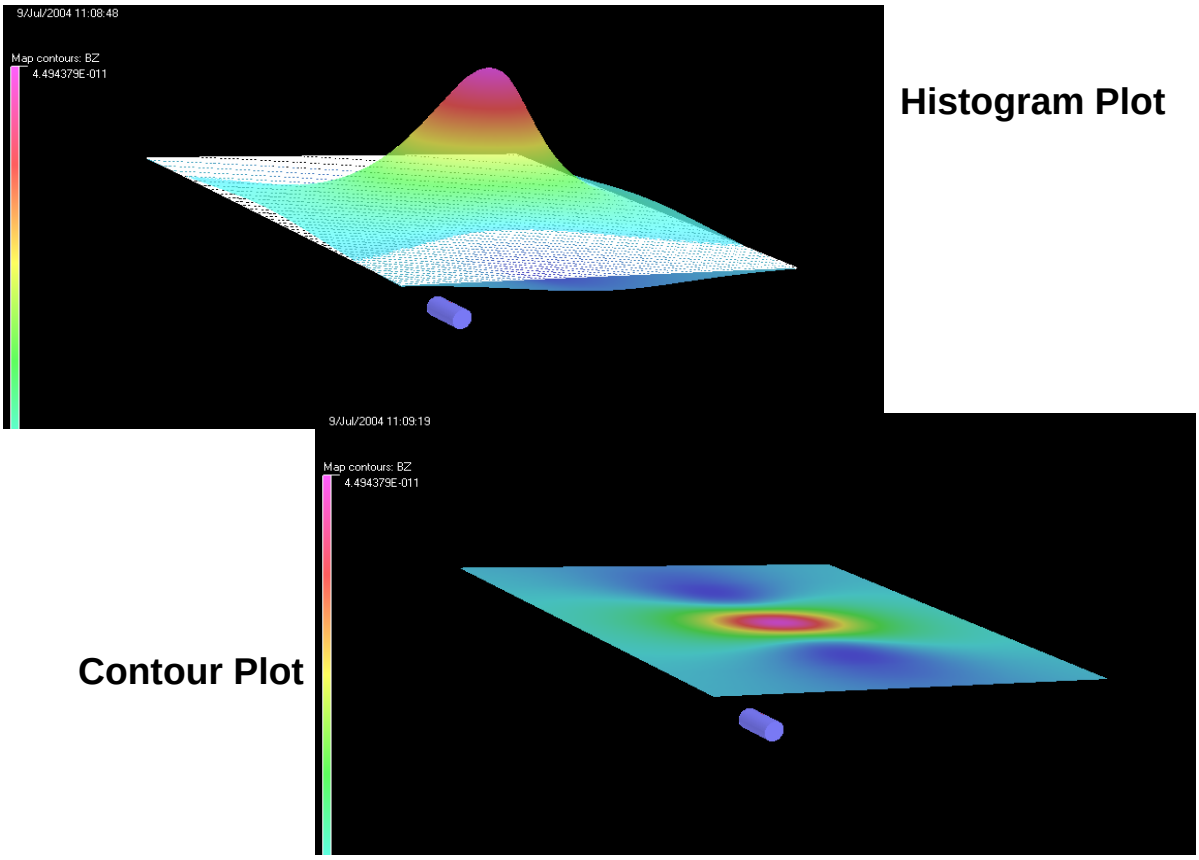

Figure 30. Peak amplitudes at location 15 inches above tag with munition oriented parallel to surface is about 50 pT per Amp-Turn

The information in these plots can be used to calculate the signal that will be generated in an above-ground pickup coil of a given orientation (for maximum signal, the pickup coil must be orthogonal to the direction of the flux lines). Figure 31 shows how the voltage in the above-ground pickup coil can be calculated as the coil moves past the buried munition.

5.3.4 Modeling Summary

This effort has added insight that would have been very difficult, time-consuming, and expensive to achieve using experimentation.

The following findings are included as a summary of that work:

- The metallic munition repels the magnetic field produced by the tag, increasing the magnitude of the signal received by the receiver coil.
- The separation between the surface and the tag is important (0.25 inch gap increases the field by a factor of 2.5 over a 0.1-inch separation).
- The tag location on the munition is important. For example, on the long side of the munition, it is advantageous to locate the tag near the ends rather than near the center.
- When the tag is embedded in a "groove," a wider and deeper groove is better; however the shape of the groove is of much lesser importance.

- Permeable filler in the groove helps (μ cores, μ_r of 500, in epoxy) to get energy into the tag. The filler has little effect on the signal from the tag back to the surface. (The field to the tag powers the tag's integrated circuit but the field produced by the tag is not related to the incident field in any linear, reciprocal way.)

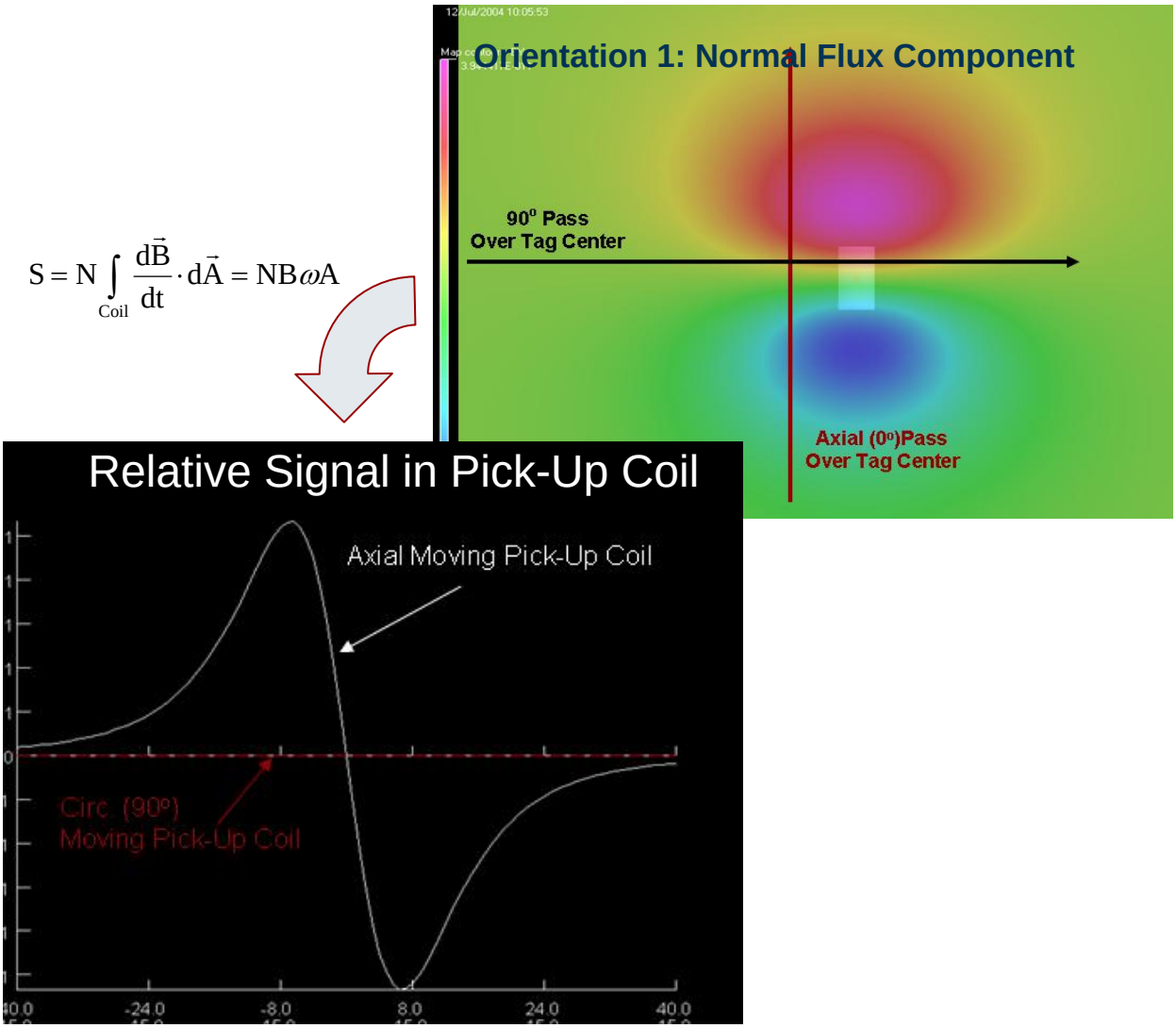

Figure 31. Sample calculation of the voltage in a pickup coil as the coil is moved past the tagged target. The false-color units of the upper-right plot are Tesla per Amp-Turn. The vertical units in the bottom plot are relative to voltage levels. Absolute values are not available because the transmitted field is in Tesla per Amp-Turn. The horizontal values in the lower plot are inches with the zero inch value being the above-ground coil directly over the center of the ordnance item

- Lower conductivity in the metal ordnance object results in lower eddy current amplitudes and therefore lower loss. Two common metals were investigated. They were Aluminum (3.7×10^7 S/m) and Iron (0.7×10^7 S/m). Twenty percent variations about their common values

were examined. Relative magnetic permeability values ranged from 1 (for Aluminum) to between 100 and 1000 (for the Iron and plug material).

- Soil conductivity has little effect on magnetic field strength.

Modeling provided insight into behavior of the fields for distinct angular positions of the ordnance item (vertical to horizontal) as the above-ground coils are moved in a large ground-area survey. The effect of multiple ordnance items near the interrogating coils can also be determined.

5.4 EXPERIMENTAL EFFORTS

5.4.1 EM Tags Buried Up to Three Feet Deep

Battelle made the decision to use Texas Instruments' Tiris tags because they are passive (no batteries) and they do not reply until after the transmitter has turned off. Competing low-frequency systems reply only during the reader's interrogation, which complicates several aspects of the detection system's electronics design.

During the initial years of the project, we characterized the solenoidal tag and the one-meter diameter transmit coil in the laboratory using the structure shown in Figure 32. The Tiris tags respond with a frequency-shift-keyed (FSK) signal near 129 kHz (center frequency is about 128.7 kHz; the 3 db points are at about 123.2 and 134.2 kHz). Initial experiments were performed to measure the voltage level at the tag coil without a munition item. Ranges greater than six feet were observed; it appeared that adequate energy would be available to the tag. These experiments were repeated with the tag near a munition. Similar results were seen as long as the tag was not too near the ordnance item. Later experiments observed the field generated by the tag at the above-ground receiving coil. Even at separations greater than six feet, signal-to-noise ratios greater than 5 dB were observed when averaging was performed. Figure 33 shows a spectrum analyzer view of the FSK signal with a 7-dB signal-to-noise ratio.

Significant differences exist between the tag's receive dynamic range and its resulting transmitted dynamic range. While not characterized in detail, the Tiris tags were designed to respond to low-level interrogating field level values but not be damaged by much higher interrogating field levels. This receive dynamic range may be 40 or 50 dB. The dynamic range of the tag's reply is much smaller. It generates a magnetic field reply that always lies between 3 and 5 dB levels. The receive circuitry protects its front end from very high voltage levels but the tag-generated reply signal is much lower in that case. This protection is a result of a voltage regulator in the RFID tag that is present so one cannot easily over-energize it at short range and destroy it from high voltage.

As the data presented in this report are in the frequency-domain format of Figure 33, some detailed explanation of this plot in the context of digital FSK modulation may be helpful. The data set in Figure 33 was taken with a digital oscilloscope that measures voltage waveforms as a function of time. The digital portion of the integrated circuit (IC) in the Tiris tag outputs a digital data stream of 64 bits that include synchronization information, and information written to its memory, which in the case of a tagged munition might be its type, serial number, date of manufacture, etc. The information bits are encoded but remain a short digital waveform. This digital waveform then drives modulation circuitry that, in simple terms, transmits a tone near 123 kHz to represent a logical "one" and a tone near 134 kHz to represent a logical "zero." When the oscilloscope trace is viewed in traditional time-domain mode, the signal is nearly impossible to decipher. However, modern oscilloscopes can transform a time-domain data set and plot it in the frequency domain. Figure 33 shows a representative frequency-domain plot of the tag output. The horizontal axis is frequency between 100 kHz and 150 kHz (5 kHz per major division). The vertical axis is amplitude plotted in dB. This uncalibrated vertical axis has no absolute reference point but

ratios between amplitude levels are meaningful. For example, at 123 kHz, the labeled point is about 7 dB higher than the noise floor at this frequency. This type of frequency-domain spectrum analyzer plot is useful for detecting the presence of a digital FSK signal but it is not useful for determining the information content of the digital signal. The ultimate detection system will demodulate the FSK signal and determine the underlying information content. Such detail is not necessary in this proof-of-concept type program. In a future effort, processing could be added to the detection circuitry that would perform the Fourier transform to convert the data to the frequency domain and allow signal processing that would aid in identifying low-level signals in the presence of noise, a task that cannot be accomplished on the digital oscilloscope. Timing of the two binary frequencies is shown in Figure 34. Qualitative information on the tag's reply is provided in Figure 34.

The time delay between the transmitter turning off and the tag's reply was difficult to measure. The delay may be deterministic, based on a signal threshold or other parameter, but it appeared to be random in nature when examined on an oscilloscope. This delay was not important because the tag always begins its reply with 16 "pre-bits" before its 8 start bits. The receiver does not always sense all the pre-bits but the 8 start bits provide adequate synchronization information.

Figure 32. Laboratory setup for characterizing the one-meter transmit coil and the Tiris tags

Figure 36 shows the Tiris tag mounted on the BLU-97 munition. The tag was mounted 0.17 inches from the steel body using a 0.11-inch thick ferrite spacer and a 0.06-inch thick circuit board spacer. The circuit board spacer allowed probes to be attached for monitoring voltage levels.

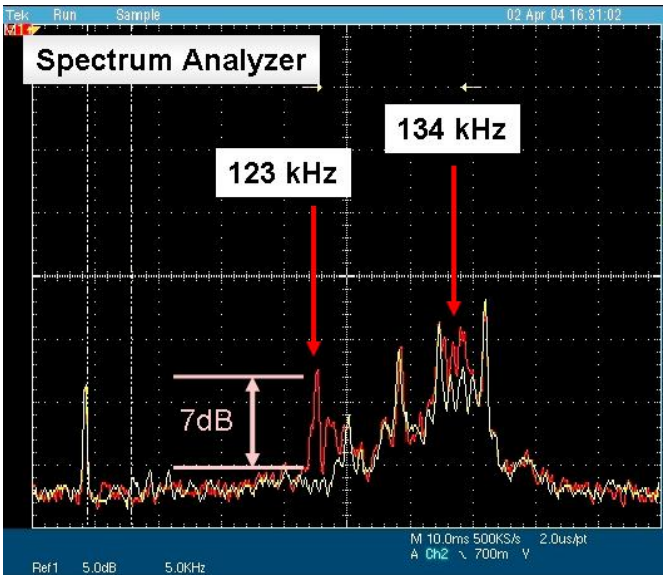

Figure 33. Spectrum analyzer view of the Tiris tags that use frequency shift keying between about 123 kHz and 134 kHz. This data set was obtained with 32-mm solenoidal tag 0.29 inches from BLU-97 surface with the tag response averaged over 50 samples.

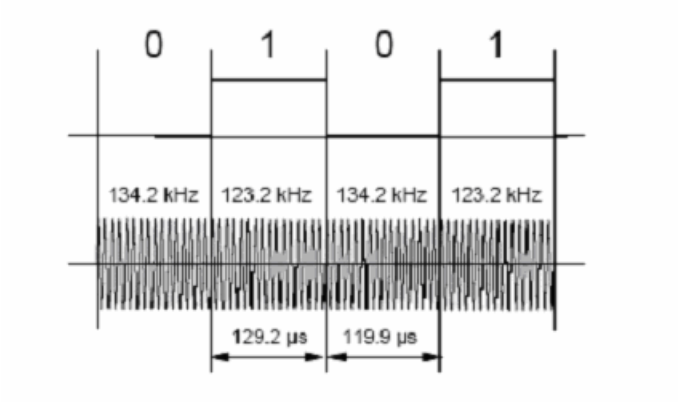

Figure 34. Details of the tag's reply signal showing the timing of the two FSK frequencies

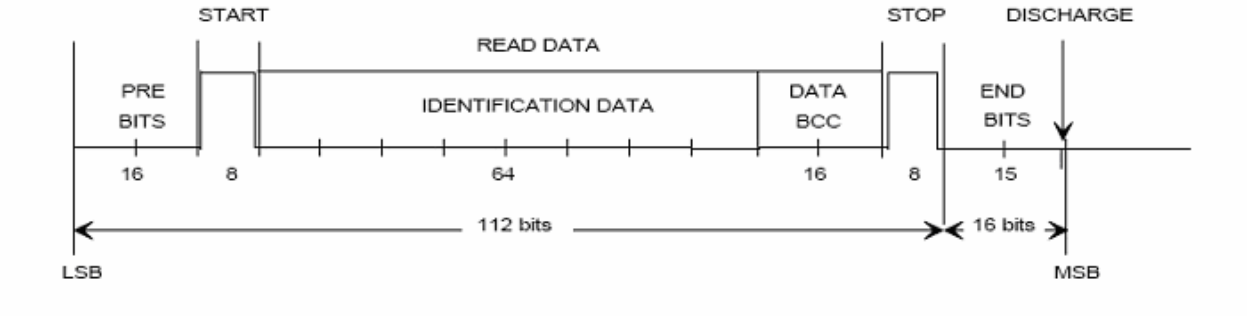

Figure 35. Texas Instruments' depiction of the tag's reply message

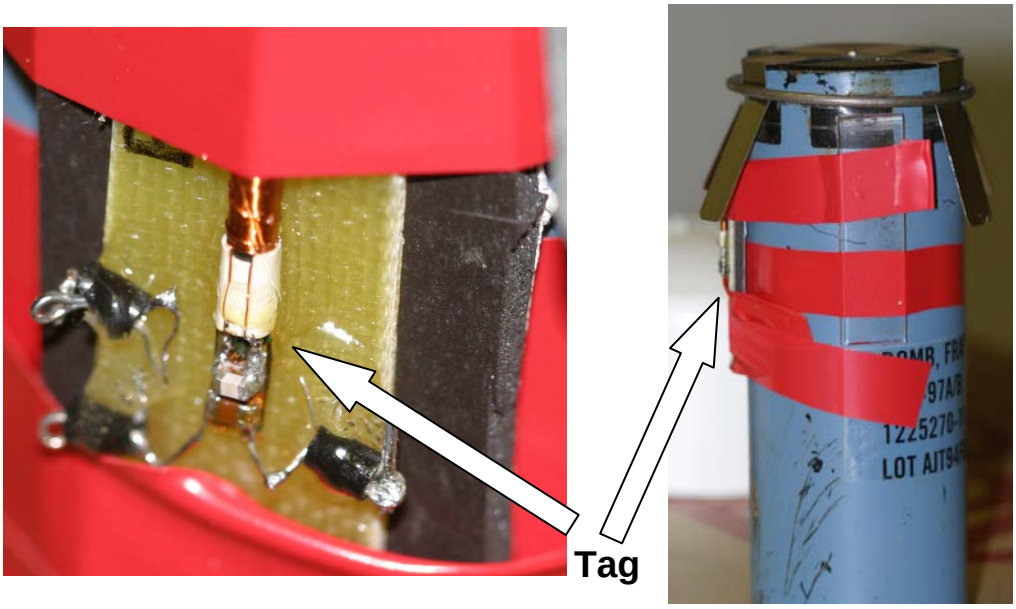

Figure 36. Tiris solenoidal tag mounted on a BLU-97

Our 2005 field testing at West Jefferson with the laboratory tag interrogation system revealed the lab system's lack of capability to function in a sufficiently robust manner to allow its further use outdoors. Therefore, much of our 2005 activities involved the design and implementation of a more robust system. This section of the report describes the design activities, the challenges, Battelle's means of meeting the challenges, and the results of testing the new system at the Aberdeen Test Center (ATC) located at Aberdeen Proving Ground, Maryland.

5.4.2 Interrogation System Development Activities

There were several important needs that had to be addressed before the system could be returned to the field environment. The required changes included:

- Implementing three receive coils in the above-ground interrogation system. The transmitting coil is one meter in diameter but the receive coils are much smaller and must be on the periphery of the transmit coil. The use of multiple receive coils increased the probability of receiving the reply from a munition-mounted tag.

- The system must be able to move without shutting down. The lab system used in the initial West Jefferson tests could not be safely moved along the ground without being powered down. Several design modifications were needed to make the system more robust.

- Tuning of receive coils. If the receive coils were wound with too many turns, proper tuning was not achievable because of the capacitance in the coaxial cable connected between the coil and the receive circuitry. If the receive coils had too few a turns, the receive signal distance was reduced. The solution to this problem was to use as many turns as possible (about 82 turns in the final design) and use a different coaxial cable with a smaller capacitance value per foot.

- Making the cart containing the coils more functional in the field. We opted to use pneumatic tires and allowed all four wheels to rotate independently to improve maneuverability at ATC. These tires also allow the cart to handle uneven ground.

- Modifying the system to be battery powered. Due to the high power and energy levels required for the transmit coil, converting the system to be battery powered became a challenge. Not only did the system need to run on batteries but it also needed to have built-in current limit capabilities to protect the circuitry. It was also desired to use batteries that could be purchased at stores in most parts of the country. We decided to go with deep-cycle batteries from Optima, which can be purchased in many different types of stores. We then designed a power module that is controlled by the microprocessor that determines the amount of voltage that the system has available and controls the current accordingly.

- Automating the tuning of the transmit coil. It was shown during preliminary tests at West Jefferson that, as the coil was moved across the ground surface, the coil's peak resonance frequency would shift and cause the signal from the tag to be reduced. The new design included implemented an auto-tuning feature. The microprocessor now tunes the system automatically to the peak of the resonance frequency thereby maximizing the response from the tag as the cart is moved. Changes to the receive coil characteristics as a function of ground position were not explored but could be in a future effort.

- Reducing the noise/interference from the electronics. The electronics introduce significant noise/interference when the circuit boards are not laid out properly and parts are not picked appropriately. In the new design, special care was taken to lay out the boards to minimize undesired interference from other parts of the electronics package. Shields were added around the receiver parts to help reduce noise. Also, certain DC/DC converters were found to induce undesired signal spikes in the frequency band of concern, so new converters were chosen to reduce the spikes in the band of interest.

- Included in the noise reduction challenge was the ability to turn the transmit coil and associated circuitry off in time to turn the receive coils on and sense the tag's signal. The power converter that drove the transmit coil created large amounts of unwanted noise signal, and if the transmit coil was on when the receive coils were activated, the receive circuitry could have been damaged. A process of shutting down the unnecessary electronics during the tag reply receiving period was developed and implemented in the microprocessor code.

- A new receiver board was designed to incorporate the multiple receive channels and minimize undesired signals from other parts of the electronics package.

- A new drive circuit was designed to reduce size and improve electrical efficiency.

- A new control board was designed that integrated a power module to regulate the voltage from the batteries to the drive circuit. This architecture provides the user with control over the voltage driving the coil, which provides a current limit. This arrangement also helped make the system more mobile by eliminating one piece of lab equipment.

- The interrogation system (transmit coil, receive coils, capacitors, receive/transmit circuitry) were placed in a custom enclosure. The cart was made from a PVC material to reduce weight and still have sufficient strength to withstand field testing. The cart was sealed with RTV around the seams and a foam gasket around the top seam to provide limited weather proofing. The casters were placed on metal supports that also helped reinforce the cart structure (the increased metal in

the surrounding area of the coils did not seem to impact performance). The coils were placed in a way that they would not be covered by any of the metal. Caster lifts were also provided to increase the height of the coils for traversing rough terrain. A safety light, with an audible alarm, was added to indicate when the system was fully powered. These devices were intended to alert people to stand clear of the powered interrogation system.

- The batteries were integrated into a separate box with casters. The box included a set of chargers for the batteries and a 24 VDC to 120 VAC inverter to power equipment from the battery box. This box also included a user display to provide information to the user (i.e. battery voltage, coil voltage, and electronics temperature). A commercial-off-the-shelf enclosure was purchased to function as the power/control unit.

5.4.3 High-Frequency RF Tags - Surface and Near-surface Tags

Battelle investigated RF tags that operate at 450 and 900 MHz. Battelle and the Government decided not to investigate the harmonic-generation tagging concept included in Battelle's original proposal. This decision was made because of the success of the Tiris experiments and because of perceived difficulties we would have when fielding harmonic systems.

Battelle was directed to discuss available commercial-off-the-shelf ultra-high frequency (UHF) passive tags and their potential for application to munitions tagging. Battelle prepared a White Paper and submitted it to SERDP in early July 2004. Battelle's initial investigations were conducted based on Internet resources and discussions with several vendors. Limited modeling of the electric field was also performed. The information included reflects findings as of June 2004, with the caveat that technology is changing rapidly in this technology area. Battelle's conclusions reported to the Government were the following:

> Based on the limited information explored during this brief study, Battelle believes this technology may be applicable to the surface and near-surface UXO problem. The ranges advertised and claimed by vendors and the industry in general appear to be adequate when the transponder is on the surface. The amount of digital information that can be written to the tag, around 100 bits, appears adequate at first glance. The costs of transponders and readers are very reasonable. Limiting factors concerning wet soil and vegetation must be considered. Battelle cannot recommend that significant resources be committed to this new technology without a more in-depth laboratory and modeling investigation. Some of the issues that must be explored include:
>
> - The effects on detection range of leaves, live grass, and small amounts of dirt being on the tag
> - The effect of dipole size on the detection range
> - The effect of placing these transponders on metallic items and the modifications required on each candidate munition
> - The increase in range possible with larger interrogating powers and more sensitive receivers
> - The impact of the electric field not being parallel to the tag's dipole

- The maximum safe electric field levels near surface and near-surface munitions

Evidence of the maturity of this technology includes the existing standards and the multiple vendors that cooperated on setting the standards, and the large number of vendors manufacturing transducers, readers, and associated products. Cost is not a significant concern in the UXO tag application because most of the transponders and readers were developed for tracking very inexpensive items that forced the vendors to pursue only very low-cost technologies.

Battelle and SERDP agreed to discontinue the work on the 450 MHz active tags and instead focus on tags operating near 900 MHz, which are referred to as UHF tags.

5.4.3.1 Evaluation of the AWID UHF Tags

Tests were conducted with the Applied Wireless Identification (AWID) Model LR-911 passive tag reader system to determine the suitability of this system for detection of near surface munitions. Two types of tags were evaluated: the APT-1014 and the APL-1216. Photographs of these two tag types appear in Figure 37.

Two sets of tests were conducted. One set was performed in the laboratory to determine the detection range as a function of distance and azimuth angle from the reader centerline. These tested were accomplished with the tags hand held in air, as well as with the tags mounted on a copper pipe (12-inch length by 3.5-inch outside diameter). The copper pipe is a surrogate for a steel munitions casing anticipated in the UXO application (the non-ferrous nature of the copper is not an issue at UHF, where electrical conductivity is the important parameter). It was found that the APL-1216 was not detected by the LR-911 reader when mounted on the copper pipe. Hence, for the second set of outdoor tests, only the APT-1014 was evaluated. The tag was attached to the copper pipe and placed in a hole in the ground. Various amounts of soil and leaves (dry and wet) were used to cover the tag/pipe. The maximum detection distance was measured with these various coverings. In addition, the effect of tag orientation on detection range was evaluated.

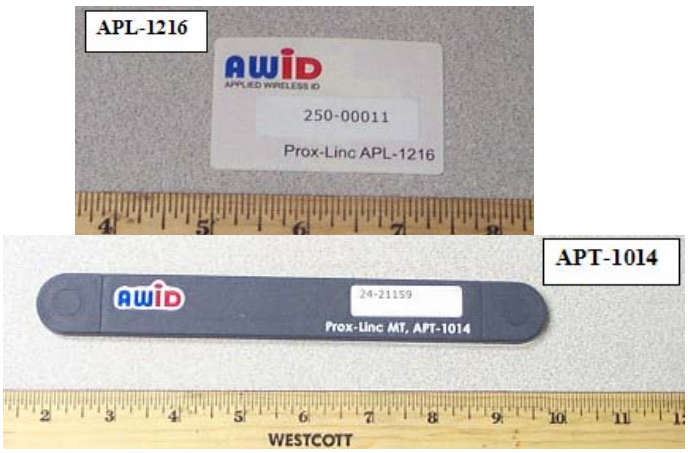

Figure 37. The two AWID passive tags evaluated in this study

5.4.3.1.1 AWID Tag Laboratory Testing

The lab test set-up is shown in Figure 38. A protractor was attached to the top of the LR-911 reader, which was mounted atop a tripod. Maximum tag read distances were measured as a function of azimuth angle (with respect to the reader centerline). The tag was held perpendicular to the string attached to the reader.

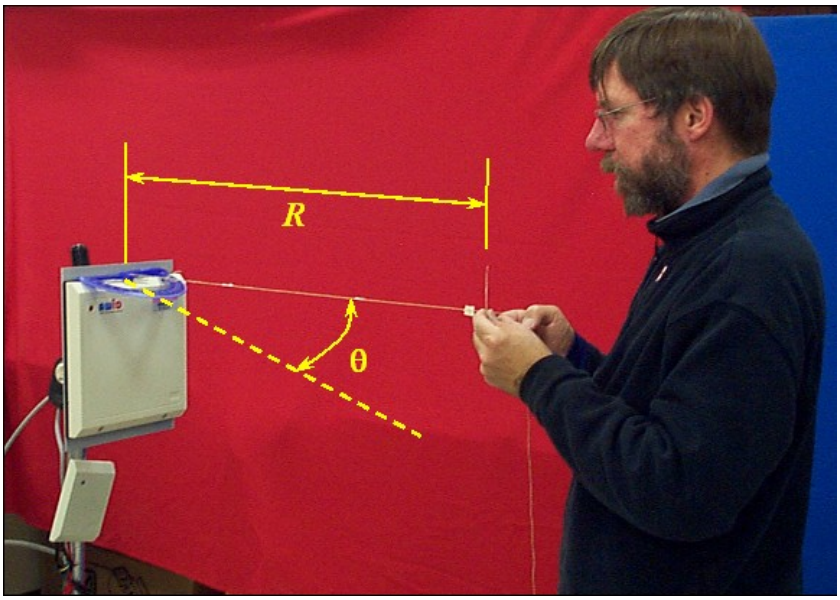

Figure 38. Laboratory geometry for AWID UHF tag evaluation

The range as a function of distance and angle for the APT-1014 tag is shown in Figure 39. There appears to be no difference in the maximum detection range whether this tag is attached to the copper tubing or not.

A similar test was conducted on the APL-1216 tag. The range from this tag was substantially less than the APT-1014 (1.9 feet versus 9.25 feet) perpendicular distance, pattern width 1.4 feet versus 8 feet). In addition, no signal could be obtained when this tag was attached to the copper pipe. The laboratory tests are also summarized in Figure 39. In these plots, maximum read range is plotted as a function of azimuth angle from the LR-911 reader centerline. Red (square) markers indicate maximum read range for handheld tags in air. Green (triangular) markers indicate maximum read range for the tag attached to the copper pipe. An ellipse was found to fit the data sets to a degree. It could be considered the main lobe in the analogy of an antenna pattern.

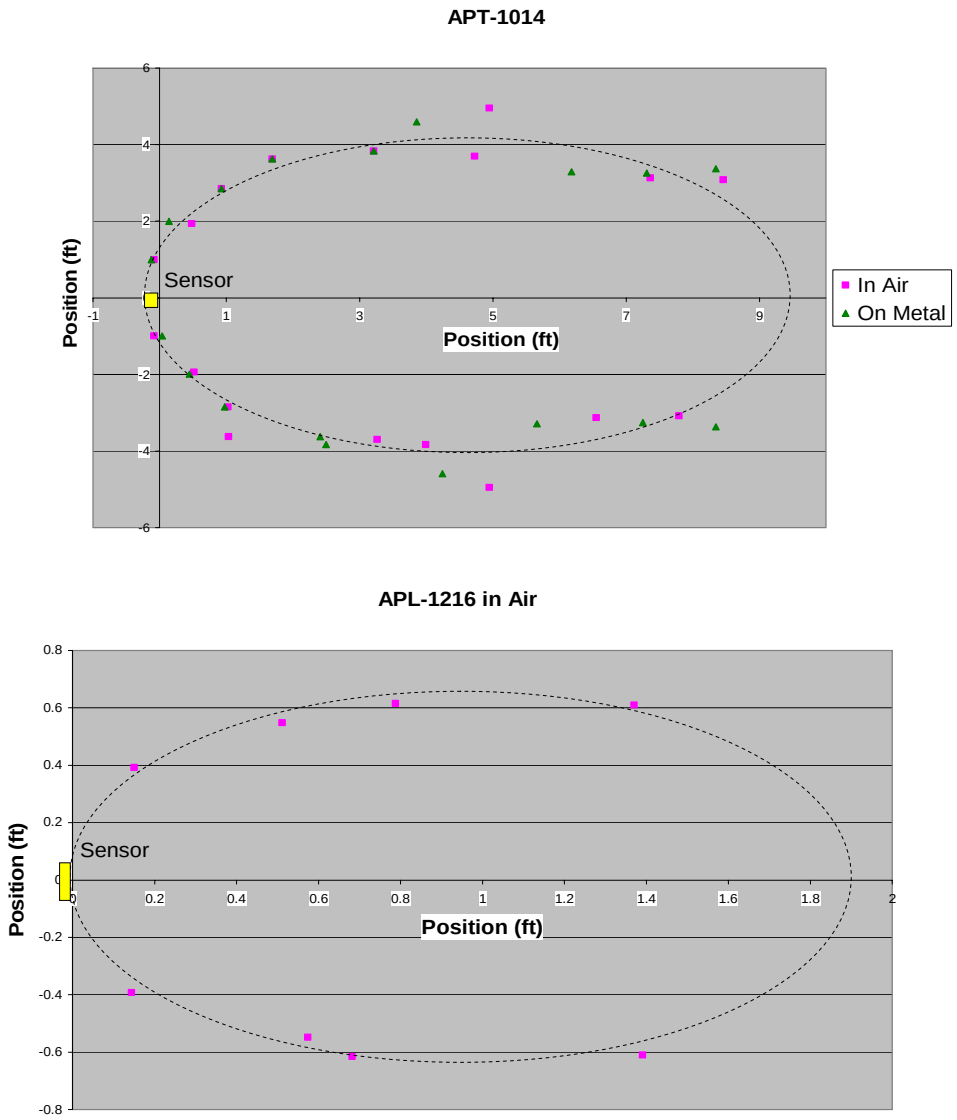

Figure 39. Laboratory measurements of AWID UHF tag range versus azimuth angle

5.4.3.1.2 AWID Tag Outdoor Testing

For the outdoor tests, a six inch deep hole was dug in sandy, moist soil. The APT-1014 tag was attached to the copper pipe and was placed in the hole, as shown in Figure 40.

Figure 40. AWID UHF tag and pipe geometry for outdoor measurements

Seven inches of dry leaves were placed on top of the tag/pipe. Perpendicular to the tag, the signal was detected 9.25 feet above, similar to the laboratory test. With the tag oriented vertically (i.e., on top of the pipe) and the LR-911 reader 42 inches above the ground (stomach level), a tag read was still obtainable at a 42 inch lateral displacement from the tag vertical centerline. This range is similar to that obtained in the laboratory measurements.

Maximum detection ranges were also measured as a function of pipe rotation angle to simulate the range of tag orientations anticipated for a buried munition. Measurement geometry is shown in Figure 41. Experimental data appear in Figure 42.

The leaves were then replaced with moist sandy soil. The tag was only detectable when the LR-911 reader was positioned directly overhead. It was also found that it was necessary to keep the long dimension of the reader parallel to the length of the tag; otherwise the vertical detection distance would decrease by 50 percent or more. The detection distance as a function of soil depth is shown in Figure 43. The increase in detection distance between 2.75 and 4 inch soil thicknesses was repeatable. It was probably caused by mounding the soil to achieve greater depths (Figure 44), whereas the first 2.75 inches of soil overburden is below ground.

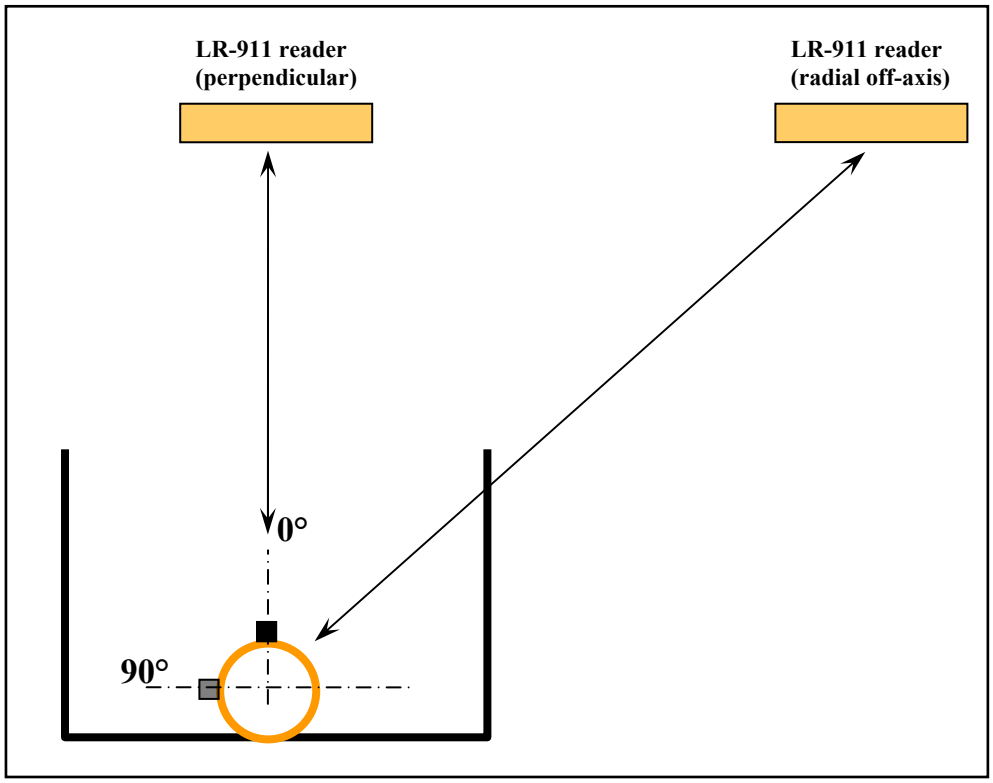

Figure 41. Measurement geometry for determination of maximum AWID tag range in soil. The pipe is rotated over a 90 degree range for these measurements. In the 90 degree orientation, the copper pipe shields the tag from the reader.

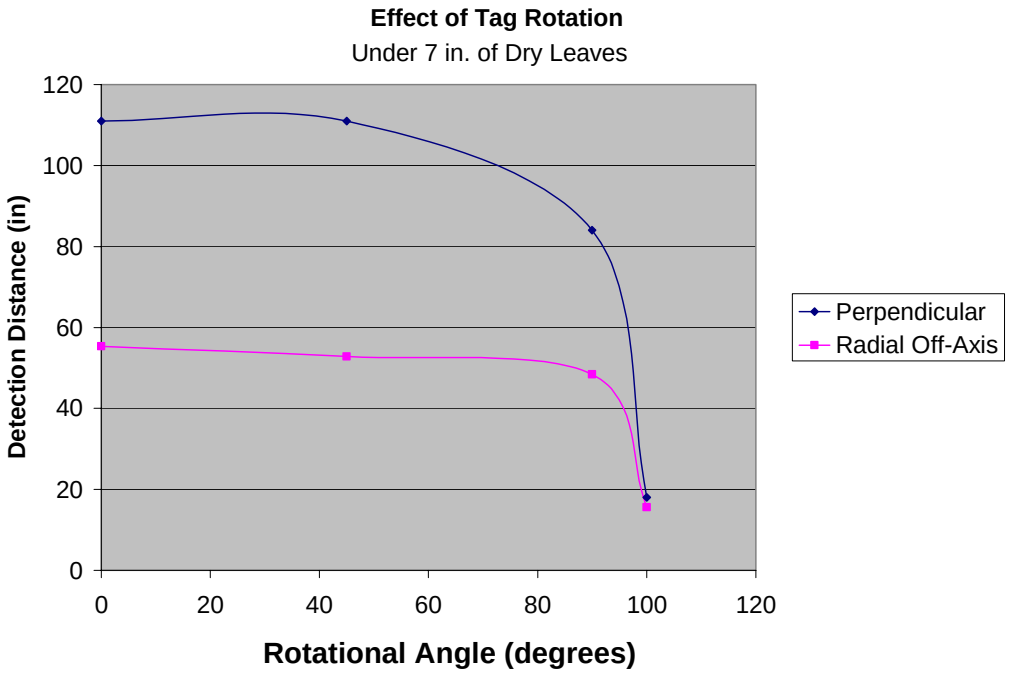

Figure 42. AWID tag detection range as a function of orientation on copper pipe

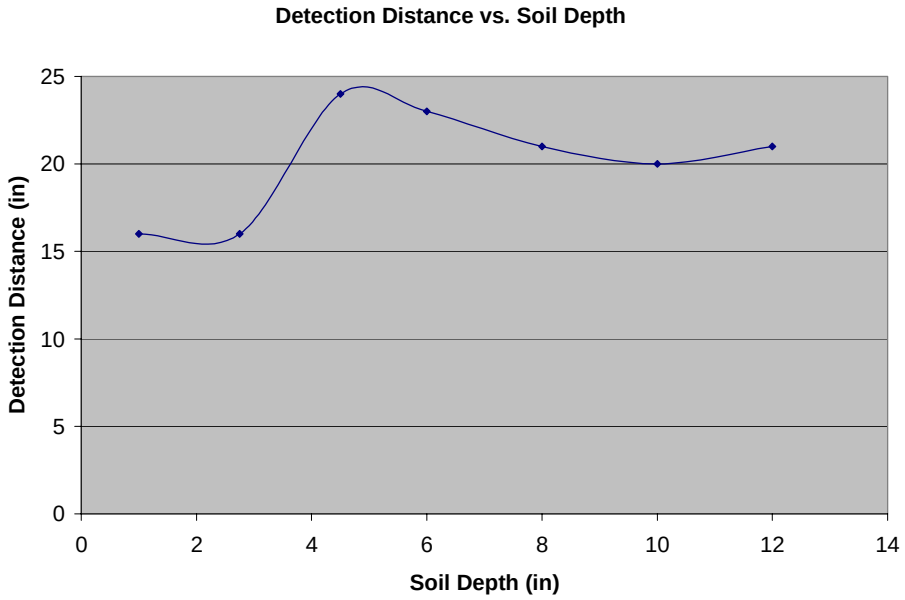

Figure 43. AWID tag detection range (directly above tag) as a function of soil overburden depth.

Figure 44. Mounding of soil to achieve greater overburden thickness.

Leveling the ground and placing two inches of dry leaves over the soil did not change the detection distance. However, if the leaves became wet, the detection distance decreased from 14 to 11 inches. Removing the leaves and making the soil wet further decreased the detection distance from 14 inches to 9 inches. Removing the soil and placing wet leaves around the tag and copper tube decreased the detection distance from 111 inches to 31 inches.

5.4.3.1.3 AWID UHF Tag Conclusions

These tests can be used to estimate detection ranges for buried munitions using passive UHF tags. The detection distance is dependent on overburden density (soil or leaves), thickness, and moisture content. For example, if the munitions were buried in dry leaves, the detection distance would be the same as in air. But if the leaves are wet, the detection distance decreases to about 25 percent of the distance with dry leaves. Similarly, if the soil is very wet, the detection distance decreases to about 64 percent of the distance in moist soil. The detection distance is also strongly dependent degree of shielding due to adjacent metal. The second tag investigated in this study, APL-1216, is probably not suitable for

detection of buried munitions. This passive tag was unreadable when it was mounted on a conducting (copper) tube.

5.4.3.2 Trolley Scan Ecotag Small/Medium RF Tag

5.4.3.2.1 Trolley Scan Introduction

Tests were conducted on the Trolley Scan RF tag tracker to determine the suitability of this system for detection of near-surface munitions. The tag for this reader is shown in Figure 45. The system is manufactured in South Africa and, as shown from the tests, has a large detection distance in air.

Two set of tests were conducted. One set was performed in the laboratory to determine the detection range as a function of distance and azimuth angle from the reader centerline. The other sets of tests were conducted by mounting the tag on a copper pipe (12-inch length with 3.5-inch outside diameter), placing the assembly in a hole in the ground, and covering it with various overburdens of leaves and dry and wet soil. As discussed in this report, although the tag has tremendous range when held in air, the range decreased to nearly zero when dirt or leaves are placed above a tag mounted on a conducting surface.

Figure 45. Trolley Scan UHF tags; naked tag (above); tag in plastic laminate (below)

5.4.3.2.2 Trolley Scan Laboratory Tests

The test setup is shown in Figure 46. The tag was held in air, and the maximum detection distance was determined over a range of azimuth angles. The output power of the Trolley Scan transmitter was set at 3 Watts (W) for these tests. Its maximum power is 3.8 W, but the instructions indicated the system could overheat when the power was set above 3.5 W. The FCC requires, for the general population, the exposure limit for a device operating at 900 MHz is 0.6 mW/cm^2. The Matrics system lists its output power as 1 W. The AWID system documentation did not discuss its output power.

The results of the laboratory tests, shown in Figure 47, indicate that there was a substantial difference in the detection distance whether the RF tag was orientated with its long side horizontal or vertical. As with the other commercial systems, the tag could not be detected when placed in intimate contact with a copper pipe. However, unlike the APL-1216 AWID tag, placing a thin insulating material between the tag and the copper pipe did enable detection.

Figure 46. Laboratory setup of range and azimuth measurements with the Trolley Scan RF tag system

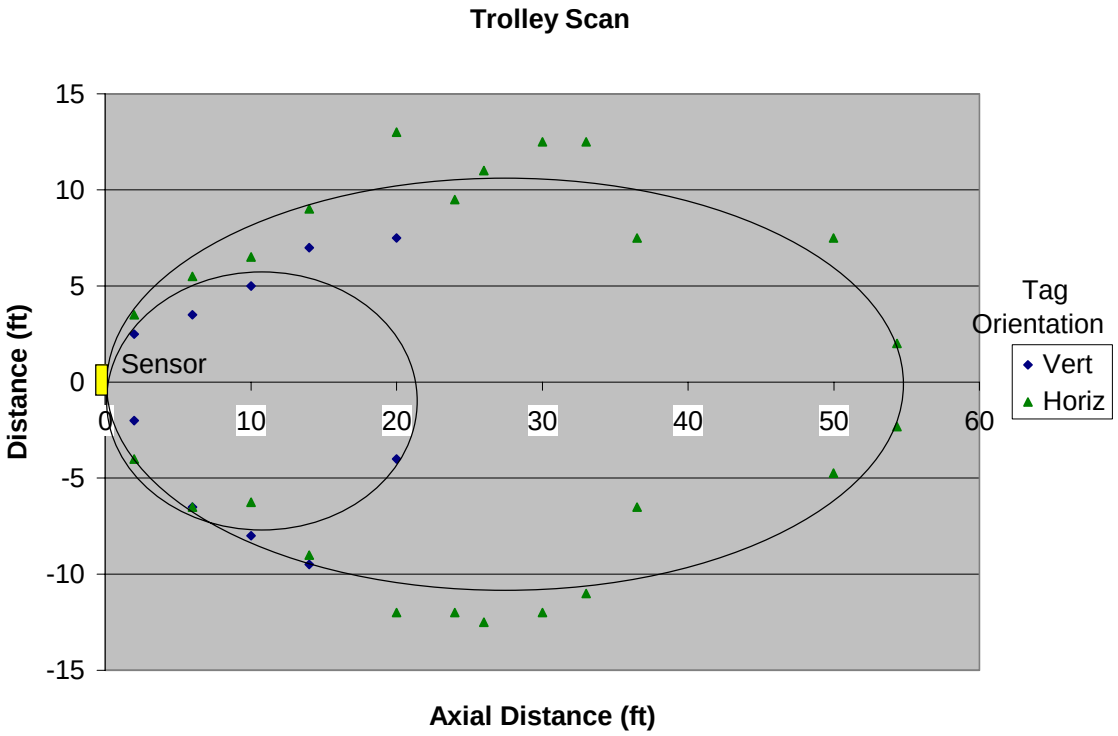

Figure 47. Laboratory measurement of tag range and azimuth angle with the Trolley Scan tags

We were able to get the Trolley Scan tag to work under the soil. With a Styrofoam® backing, we were able to read the RF tag when placed on a copper pipe, but the signal decreased quickly when we put overburden on top of the tag. Further investigations indicated that this degradation was caused by the paper that surrounds the RF tag circuit touching the chip in the tag. A plastic enclosure was built around

the tag, as shown in Figure 48. This modification resulted in the tag becoming 0.13 inches thick, compared to 0.07 inches thick over the chip area for the tag as supplied by the manufacturer.

In the laboratory, we tested the configuration with a 0.23-inches thick, low-density foam spacer between the RF tag and the copper pipe. The results are shown in Figure 49. There was a substantial difference in the detection pattern whether the antennas were parallel or perpendicular to the length of the copper pipe.

Outdoors, the detection distance was measured with the plastic-encapsulated tag in three inches of soil as a function of soil moisture content. When the interrogating antenna was configured to be parallel to the pipe, the detection distance was greater than 30 inches for moisture content between 5 and 13 percent.

Discussions with Dr. Tom Van Doren, from the University of Missouri-Rolla, a leading expert on electromagnetic susceptibility of circuit board layouts, indicated that we might be able to get these tags to work on a copper pipe if we could readjust the antenna length. This configuration was tested with the Trolley Scan and the AWID APL-1216 tags. We were most successful with the Trolley Scan RF tag. We could mount the tag directly onto the copper pipe with a shorting wire properly placed in the circuit. The placement of the shorting wire is very delicate, and although we can get a signal with this arrangement, it is necessary to be physically close to the antenna in order to get it to work. It appears that the impedance of the munition body is part of the receiving circuit and that this concept was not useful.

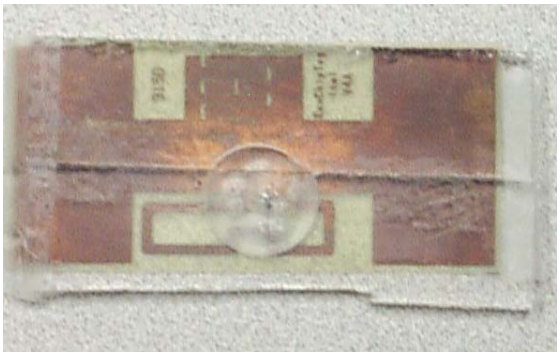

Figure 48. Trolley Scan tag within plastic enclosure

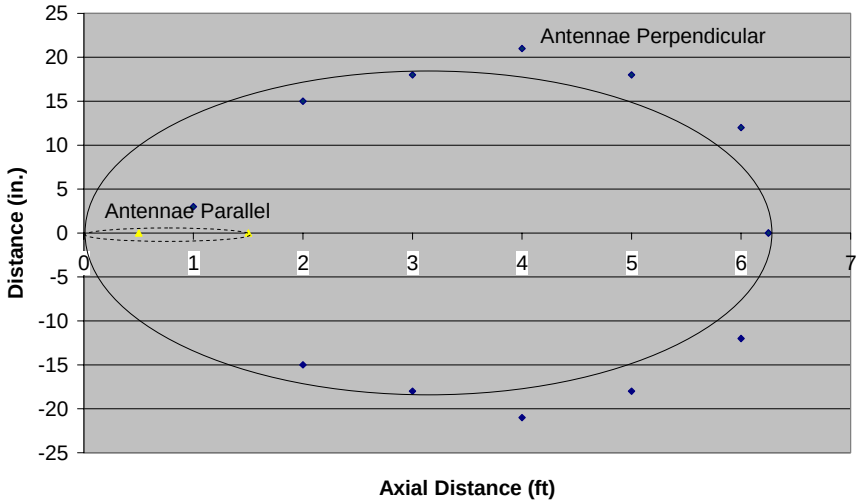

Figure 49. Detection results for the modified Trolley Scan RF Tag System (copper pipe in air)

5.4.3.2.3 Trolley Scan Outdoor Tests

The Trolley Scan RF tag was mounted on a copper pipe with a 0.1-inch thick Styrofoam® spacer between the RF tag and the copper pipe. A picture of the test setup is shown in Figure 50.

Figure 50. Outdoor tests with the Trolley Scan system

With no leaves or soil overburden, the tag could be detected about 35 inches away, similar to the lab tests. However, even with a shallow overburden, the signal decreases quickly, as shown in Figure 51. The soil moisture was 4 percent by weight for this test. As can be seen from Figure 51, the signal decreases dramatically with just a shallow covering. Any covering, even a piece of masking tape used to mount the tag to the copper pipe, affected the detection distance. The tag mounted on the copper pipe was undetectable under dry leaves.

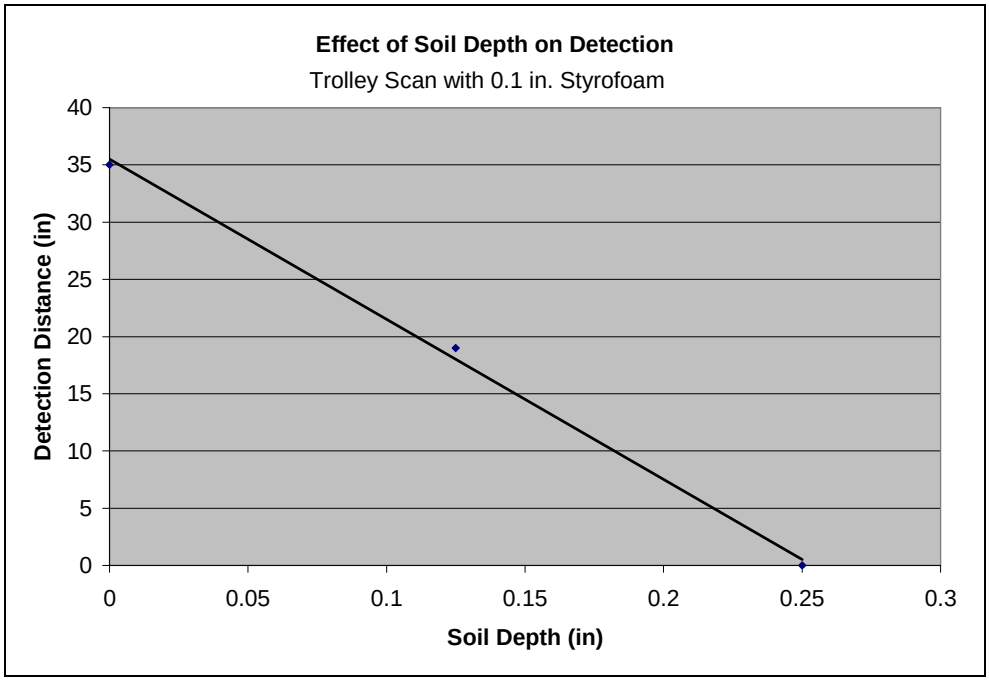

Figure 51. Effect of soil depth on detection distance for the Trolley Scan RF tag

5.4.3.2.4 Trolley Scan System Conclusion

Although the system can detect tags at long distances when the tags are in air, the detection distance becomes minimal when the tag is placed on a munition and overburden, such as soil or leaves, are placed over the tag. It is apparently a signal that is easily attenuated by material between the tag and reader. By placing a hard plastic cover and spacers over the tag circuit, it is possible to detect this tag under several inches of soil, even when the soil is saturated with water. The thickness of the modified assembly used for these tests was 0.13 inch. With appropriate engineering, it may be possible to decrease this thickness to about 0.07 inch, about the maximum thickness of the tag in the plastic pouch as delivered by the manufacturer. However, a backing material between the tag and the munition is also required, which adds another 0.1 to 0.2 inch to the RF tag assembly.

5.4.3.3 Matrics AR-400 Tag Tracker

5.4.3.3.1 Matrics Introduction

Tests were conducted on the Matrics Model AR-400 tag tracker to determine the suitability of this system for detection of near surface munitions. The tag for this reader is shown in Figure 52. This system is designed to be used to track tags on crates and boxes and, unlike the other commercial tag reader systems evaluated in this study, requires a computer to start and stop the tracking system. It was with great difficulty, compared with the other tag readers evaluated in this study, that we were able to get the software operational.

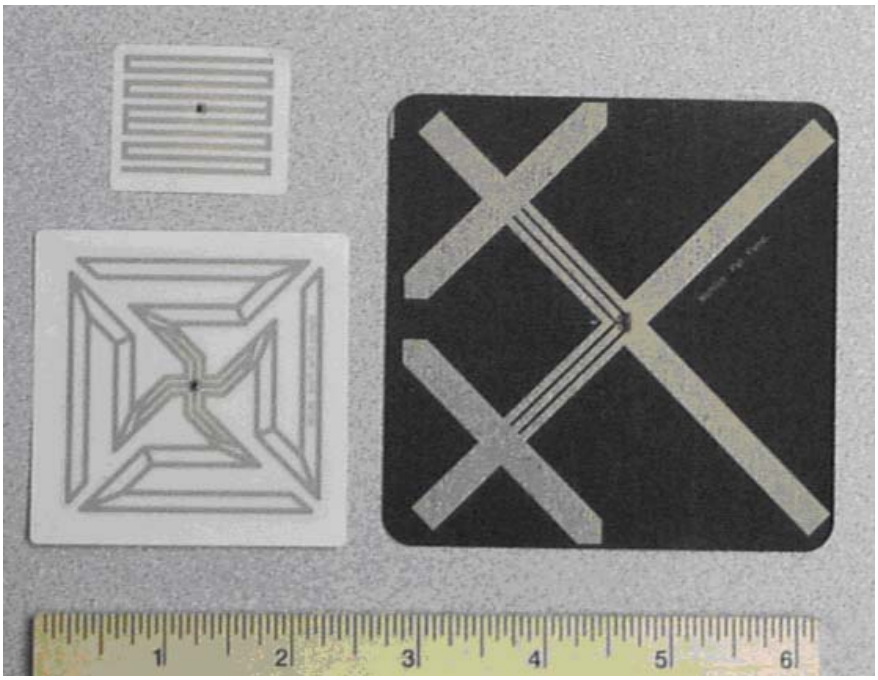

Figure 52. Matrics AR-400 tag configurations

Two sets of tests were conducted. One set was performed in the laboratory to determine the detection range as a function of distance and azimuth from the reader centerline. The other sets of tests were conducted by mounting the tag on a copper pipe (12-inch length with a 3.5-inch outside diameter) and placing the assembly in a hole in the ground and covering it with various amounts of leaves and dry and wet soil. The maximum detection distance was measured with these coverings. In addition, the effect of tag orientation on detection range was evaluated.

5.4.3.3.2 Matrics Laboratory Tests

The test setup is shown in Figure 53. The tag was held in air, and the maximum detection distance and azimuth angle (with respect to the reader centerline) were measured.

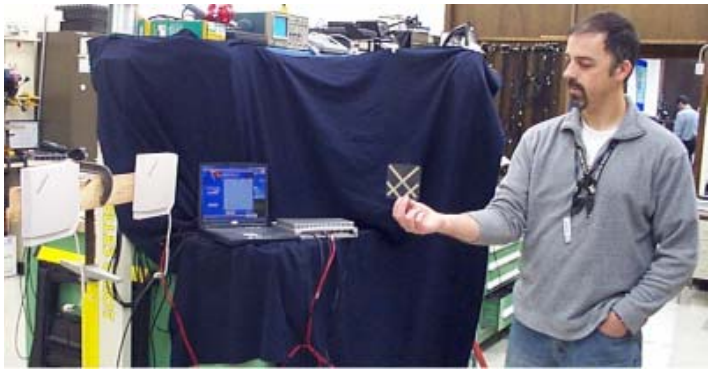

Figure 53. Laboratory setup of range and azimuth measurements with the Matrics tag

Results of the laboratory tests are summarized in Figure 54 below. The detection was asymmetric, being more sensitive on the right side than the left. This is a function of the placement of the transmitting and receiving antennas. For these tests, the transmit/receive antennas were separated by 21 inches. There is no indication in the manual as to the optimum separation, so it was made roughly the same as suggested for the Trolley Scan system. Unlike the Trolley Scan system, Matrics card orientation is not critical.

As with the AWID and Trolley Scan RF tag systems, the tag could not be detected when placed on the copper pipe. Placing a 0.08-inch thick Styrofoam® spacer between the tag and the copper pipe results in the detection of the tag when it is 3 feet from the antennas. Under the same conditions, the minimum thickness of the low density foam backing is 0.188 inches when the wax paper that comes with the tag remains on the tag. If it is removed, or the foam thickness decreases to 0.125 inches, the signal could not be detected three feet away.

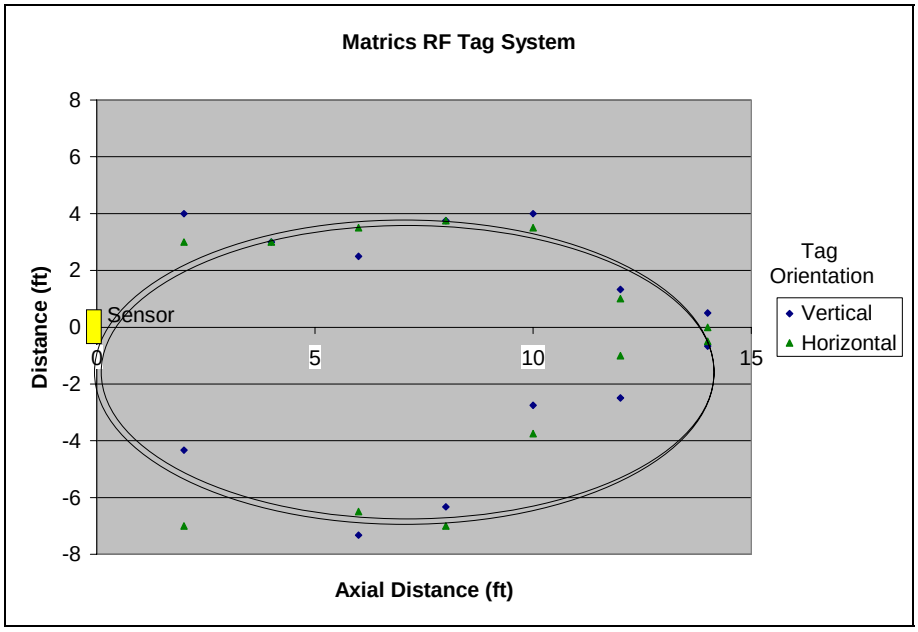

Figure 54. Laboratory measurement of tag range and azimuth angle of Matrics tags

5.4.3.3.3 Matrics Outdoor Tests

The Matrics tag with a 0.188-inch thick low-density foam placed between the tag and the copper pipe was placed in a six-inch deep hole, as shown in Figure 55. With 1.75 inches of dry leaves above the tag, a signal was detectable when the antennas are 63 inches above the copper tube and their axes are parallel to the length of the tube, and 53 inches if the antennas axes are perpendicular to the tube length. Holding the antennas at waist level, a signal could be detected 21 inches off-axis from the tag when the axis of the antennas were perpendicular to the length of the copper tube, and at 17 inches when the antenna's axes were parallel to the long axis of the copper tube.

Antennas Parallel to Munition Length

Antennas Perpendicular to the Munition Length

Figure 55. Outdoor test with Matrics system

Tag at 0 degrees

Tag at 45 degrees

Figure 56. Tag rotation geometry

The above tests were done with the tag facing straight up (zero degrees). Rotating the tag under the leaves (as shown in Figure 56), the relationship between the rotation angle and maximum detection distance directly above the tag is shown in Figure 57.

Rotating the tag back to zero degrees, the effect of soil depth on detection distance directly above the tag mounted on the copper pipe is shown in Figure 58. The soil moisture was 3.4 percent by weight. No signal was detected when the soil moisture was increased to 8.5 percent by weight.

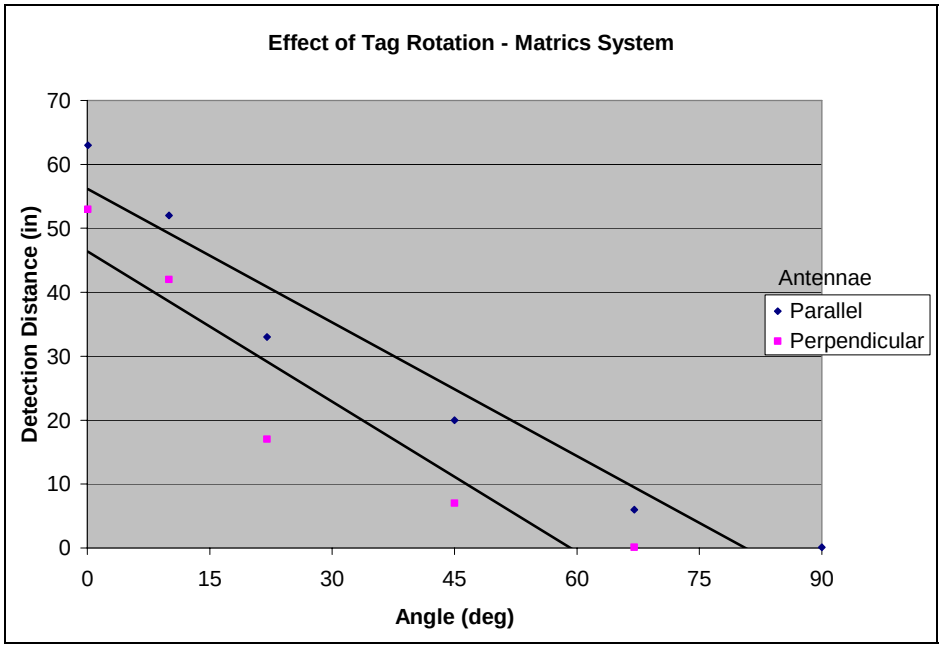

Figure 57. Matrics tag detection range as a function of orientation of copper pipe

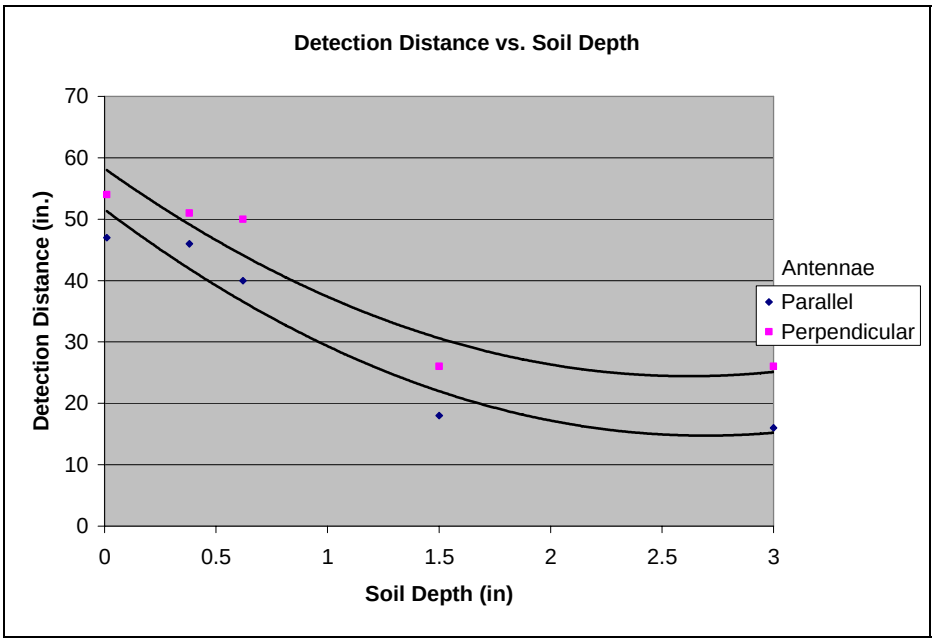

Figure 58. Matrics tag detection range as a function of soil depth

5.4.3.3.4 Matrics System Conclusions

The Matrics system was the most difficult to get operating because it requires a computer to start the tag reading process. Unlike the other systems, the reader does not have a beeper, which would facilitate tag location. The four-inch by four-inch tag can be used for this application, but it is large. The other Matrics tags tested in this study either did not work on the copper pipe or when soil was placed over them. Only the four-inch by four-inch Matrix tag may be acceptable for this application. It is possible that the Emerson & Cuming isolation material could be tuned for this tag, but this configuration was not tested in this study. Although orientation of the antennas to the tag is not critical with this system when the tag is in air, there was some difference noted when the tag is mounted on the copper pipe and buried in the ground.

5.4.3.4 Evaluation of UHF Tag Spacing Materials

Evaluation of both the AWID and the Trolley Scan passive RF tag systems indicated a need for a dielectric barrier between the planar (card type) tags and the metal targets. Hence, an evaluation of potential "spacer" materials was initiated. Several types of insulating materials were tested, and pictured in Figure 59. The materials examined included rubber, Styrofoam®, Teflon®, polypropylene, various loaded dielectric materials, and low/high density foam. Testing was also conducted on commercial RF absorbing materials, such as the MAC 6400 material from MWT Materials, Passaic, New Jersey and various samples from RF Products, San Marcos, California. The testing was done with and without the tag circuit enclosed in its plastic and/or paper envelope. The test setup is shown in Figure 60, and a summary of the results is given in Table 2.

Styrofoam® appears to be the best backing material, and the relation between detection distance and thickness of the Styrofoam® is shown in Figure 61. The minimum effective backing thickness was found to be 0.08 inches.

The next best material was Teflon®. The results are shown in Figure 62. A minimum of 0.12-inch thickness of Teflon® is required to detect a signal three feet from the antennas, compared with 0.08 inches of Styrofoam®.

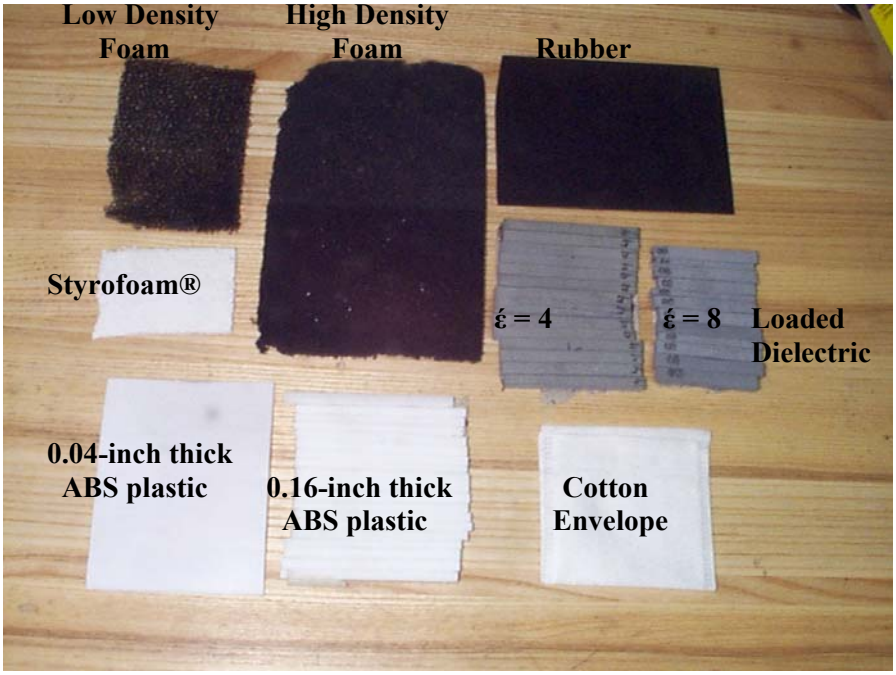

Figure 59. Insulating materials examined

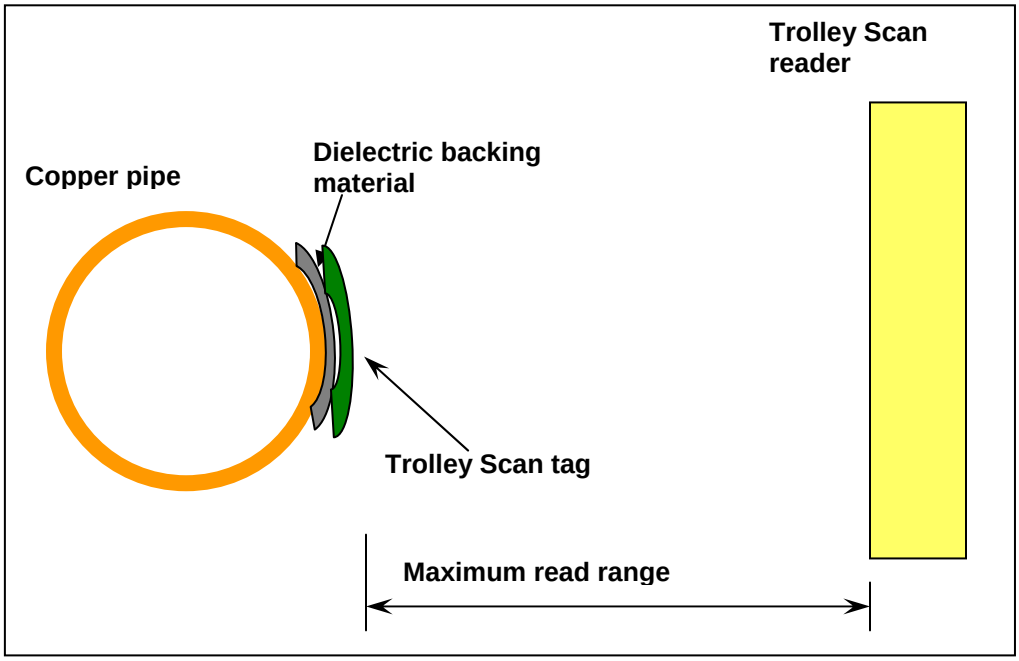

Figure 60. Measurement geometry for tests with backing materials

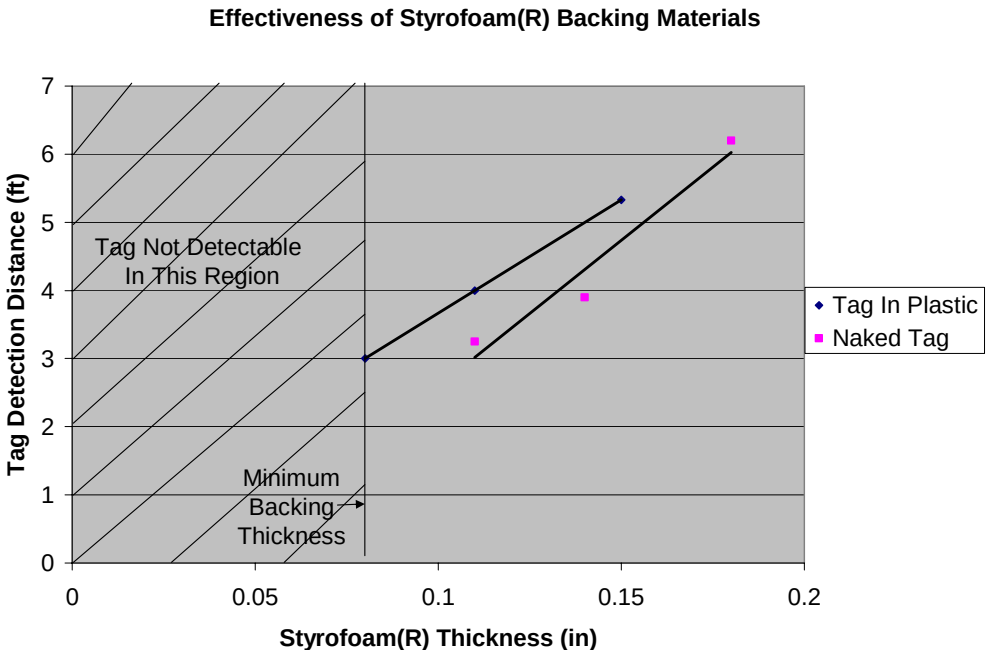

Figure 61. Detection distance as a function of Styrofoam® backing thickness when Trolley Scan RF tag is placed on a conductor

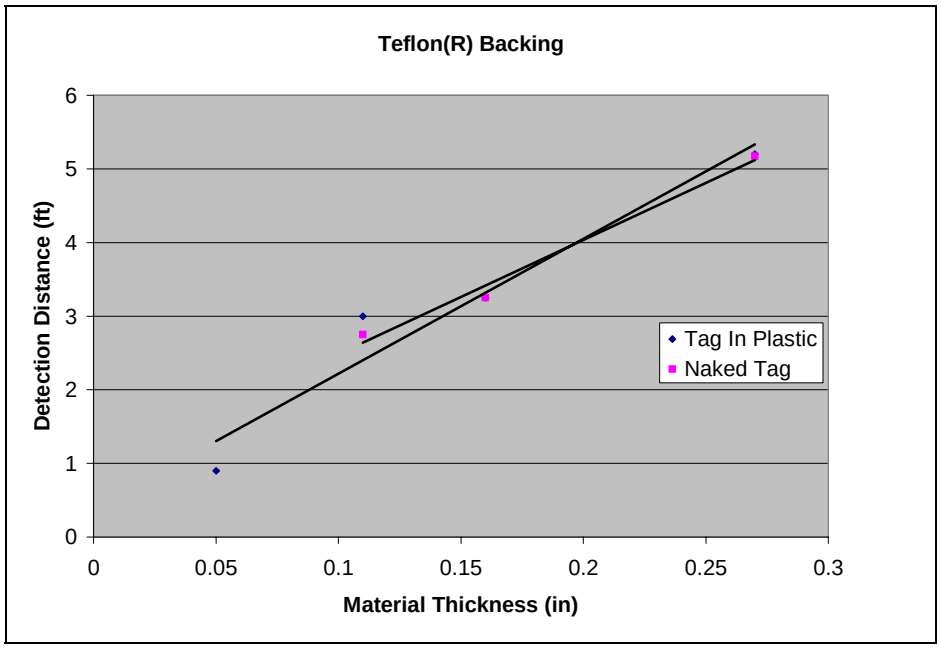

Figure 62. Detection distance as a function of Teflon backing thickness when Trolley Scan RF tag is placed on a conductor

Table 2. Effectiveness of dielectric backing materials for increasing tag read range

Material	Thickness (inches)	Effectiveness (feet)
Styrofoam®	0.08	3
Teflon®	0.15	3
Loaded dielectric (ε_r = 4)	0.215	3
Loaded dielectric (ε_r = 8)	0.217	No Signal Detected
Low density foam	0.25	3
High density foam	0.216	No Signal Detected
Rubber	0.066	No Signal Detected
Cotton envelope	0.016	No Signal Detected
Polypropylene plastic	0.178	No Signal Detected
ABS plastic	0.040, 0.057, 0.165	No Signal Detected
Acrylic plastic	0.05	No Signal Detected
PVC plastic	0.016	No Signal Detected
Carbon paper	0.001	No Signal Detected
Commercial RF Backing Materials:		
MAC6400	0.125	No Signal Detected
2016	0.138	No Signal Detected
2234	0.030	No Signal Detected
2238	0.053	No Signal Detected
2240	0.068	No Signal Detected
4001	0.500	6
5114	0.237	No Signal Detected
5115	0.118	No Signal Detected

Commercial RF Backing Material Definitions:

Material	Mfg	Description
MAC6400	1	composite, consisting of resistive material spacers and ground-plane, encased in a nylon fabric with moisture barrier
2016	2	magnetically loaded natural rubber surface wave absorber
2234	2	magnetically loaded silicone base surface wave absorber
2238	2	magnetically loaded silicone base surface wave absorber
2240	2	magnetically loaded silicone base surface wave absorber
4001	2	urethane based foam with open-cell structure
5114	2	open cell urethane foam dipped in a resistive solution
5115	2	open cell urethane foam dipped in a resistive solution

Manufacturer:

1. MWT Materials, Passaic, New Jersey, www.mwt-materials.com
2. RF Products, San Marcos, California, www.lairdtech.com

Low density foam also proved useful as a backing material. The results are shown in Figure 63.

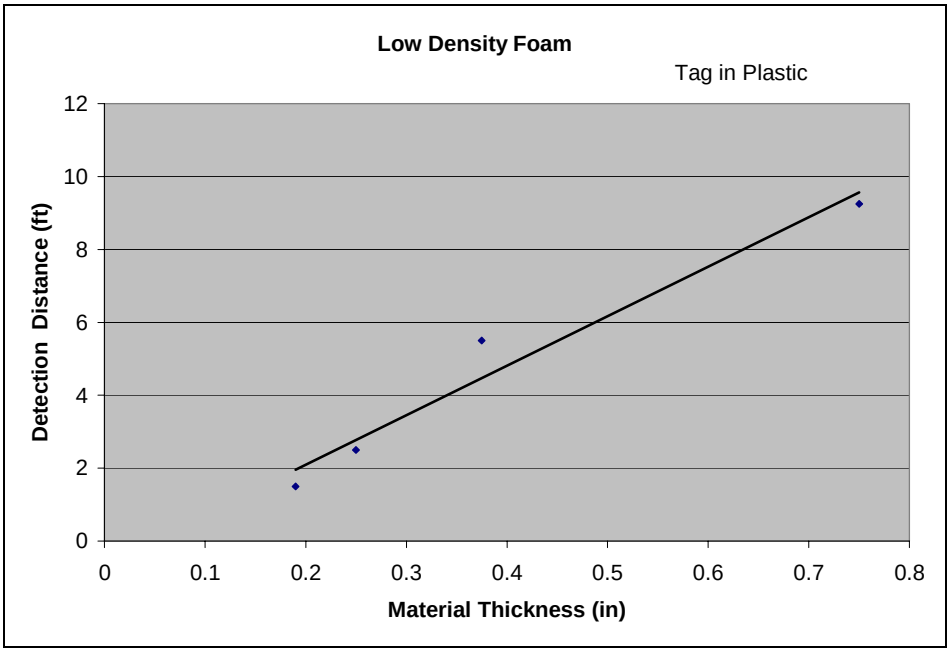

Figure 63. Detection distance as a function of the thickness of low-density foam when Trolley Scan RF tag is placed on a conductor

Using the loaded dielectric material ($\varepsilon_r = 4$), a signal could be detected three feet away with a material thickness of 0.215 inch when the tag is encased in the plastic pouch envelope. A signal could not be

detected when the tag was outside the plastic envelope. For higher dielectric constants ($\varepsilon_r = 8$), no signal could be detected, whether or not the tag was enclosed in its plastic envelope.

No signal could be detected using the high-density black foam, even when the material thickness was as great as 0.21 inches. This was true whether the tag was inside or outside its plastic envelope. Similarly, no signal was detected with 0.059-inch thick polypropylene plastic as the insulating material between the RF tag and the copper pipe. No signal was seen with MuMetal as a backing material, a metal material exhibiting a high magnetic permeability. This was true whether the MuMetal was in a sheet or wire form.

Rubber backing did not work. Even if the rubber backing is not attached to the copper pipe, a signal could not be detected when the RF tag card, in its plastic envelope, was placed against the rubber. Surprisingly, a signal was detected up to 6.4 feet away when the tag was outside the plastic envelope and against the rubber as long as the rubber was not against the copper pipe.

The commercial insulating materials exhibited similar characteristics. No signal was detected when the copper pipe was placed near the tag with the insulating material with exception to the material that was equivalent to the foam with large voids, as discussed above. Several of the material extinguished the signal reflected from the tag when they were placed near the tag, even without the copper pipe. This finding is similar to the results with the rubber backing discussed above.

As discussed previously in this report, the APT-1014 AWID tag was detectable even when mounted on the copper pipe. One of these tags was disassembled, as shown in Figure 64. The circuit is enclosed in a thick plastic case, 0.05 inch thick in the front and 0.11 inch thick in the back. Double sided copper tape, available commercially from 3M, is used to attach the plastic case to the conducting metal. Placing this copper tape on the back of the Styrofoam® spacer did not increase the detection distance. However, the APT-1014 AWID tag will not work on the copper pipe unless this copper tape is between the tag and the pipe. Also, the plastic enclosure needs to be completely closed in order to detect a signal when the APT-1014 is placed on a copper pipe. Taking this tag out of its plastic case, it was found that a signal could be detected from the tag as long as there is at least 0.25 inches of foam between the tag and the copper pipe. Enclosing the Trolley Scan and Matrics tags in a sealed plastic box and/or putting the copper tape behind them did not increase the detection ranges.

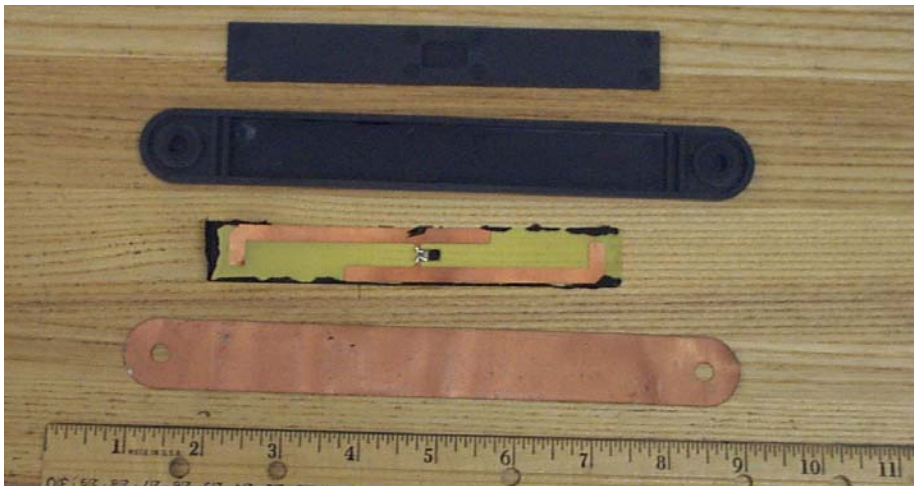

Figure 64. Disassembled APT-1014 AWID tag

A literature survey indicated that Emerson & Cuming (EC) Microwave Products, Inc has a backing material that can be put behind a RF tag that allows it to be used on metal. The material has to be tailored to the tag, and has to use an EPC class 0 or class 1, or an ISO 18000-6 read protocol. The APL-1216 RF

tag from AWID uses this protocol, the Trolley Scan RF tag does not. Two APL-1216 RF tags were sent to EC to determine if they could use their product on these devices. As reported previously, we were not able to get the APL-1216 tag to read on a copper pipe with the insulating backing materials that we investigated previously. EC supplied some sample material, shown in Figure 65, that, when attached to the back of the tag, does allow the AWID RF tag to be read when placed on the copper pipe. The material is about 0.1 inch thick. A nondisclosure agreement had to be signed in order to receive and test this material, because EC has a patent pending on it; further details cannot be provided at this time

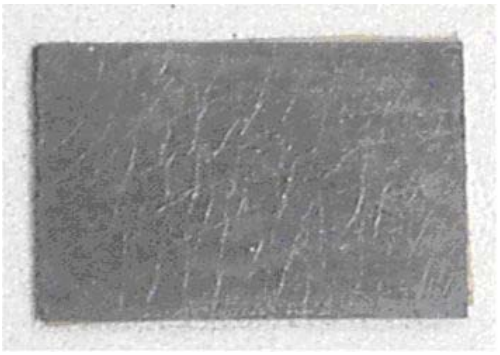

Figure 65. Emerson & Cuming backing material

We then tested this material, first in the laboratory then outdoors. The indoor test results are shown in Figure 66, and we actually had a slight increase in the detection distance with the tag mounted on a copper pipe with this backing material between the RF tag and the pipe then we had with the APL-1216 RF tag in air. But the tag had to be mounted so its length is parallel to the length of the copper pipe. When it was placed perpendicular to the length of the copper pipe, no signal was detected. Similar encouraging results were obtained in outdoor measurements.

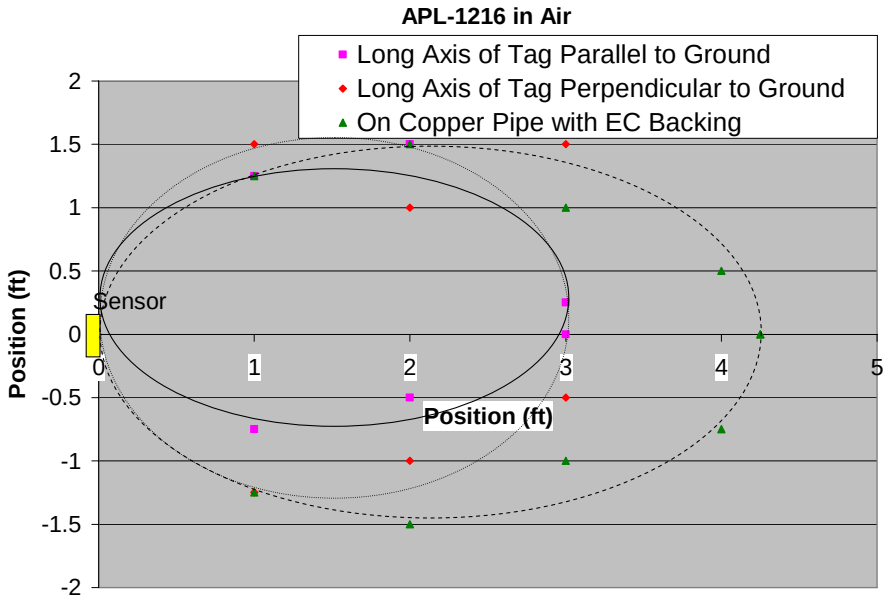

Figure 66. Detection distance of APL-1216 in air with the EC material backing

A suggestion was made that a high-permeability magnetic shielding material placed behind the RF tag might result in better detection characteristics of the RF tag on the copper pipe. A kit was ordered

containing a variety of different thicknesses and permeability materials, as well a high-permeability wire that was used to try to break up the flux lines. None of these materials aided performance. As soon as the high-permeability material came close to the RF tags, the signal could not be detected. These materials are used to shield low-frequency electronic fields, but these tags are operating at 900 MHz. The material appears to be ineffective in shielding for this application.

5.4.3.5 UHF Tag Performance Summary

Several commercial RF tags were investigated in this study. Table 3 summarizes the characteristics of these tags and the results of this study.

Because different backing materials were used for the different tests, the chart in Figure 67 indicates the equivalent thickness of Styrofoam® for a given thickness of low-density foam, based on the tests discussed in this report. As one can see, all of the tests were performed with an equivalent of about 0.1-inch thick Styrofoam® backing material.

The results of these tests indicate it is possible to detect a high frequency RF tag on a simulated munition (copper pipe). It is necessary to put a backing material, of a minimum 0.1 inch thickness, between the munition and the tag. A signal can be detected when this mounted tag is placed under the soil.

Table 3. UHF Tag performance summary

	Size (inches) (L x W x H)	Detection Distance In Air (feet)	On Copper Pipe Under 2 inches of Soil (feet)	Backing Material Thickness
AWID				
APT-1014	**8 x 1 x 0.18**	**8.5**	**1.25**	**None Needed**
APL-1216	**2.5 x 1.6 x 0.02**	**4.0**	**2.5**	**Emerson & Cumming, 0.1 inch**
Trolley Scan	**3.25 x 1.5 x 0.04 (had to be modified to 0.12 inch)**	**6.25(a)**	**2.2 (b)**	**a) Styrofoam®, 0.1 inch** **b) Low Density Foam, 0.23 inch**
Matrics				
Single Dipole	**1.1 x 1.1 x 0.02**	**No Signal on Copper Pipe**	**No Signal on Copper Pipe**	**N/A**
Dual Dipole	**2.5 x 2.5 x 0.02**	**3.0**	**No Signal in Soil**	**Styrofoam®, 0.1 inch**
Dual Dipole	**3.6 x 3.6 x 0.02**	**5.4**	**4.6**	**Low Density Foam, 0.18 inch**

For the RF tags tested in this study, the AWID APL-1216 is the smallest practical tag. It is possible that the Matrics single-dipole tag, which is smaller in size, might be usable, but a suitable backing material was not identified. The Emerson & Cumming isolator material could be tuned for this tag, but further characterization is needed to confirm this possibility. Testing indicated that a modified Trolley Scan RF tag also could be used for this application.

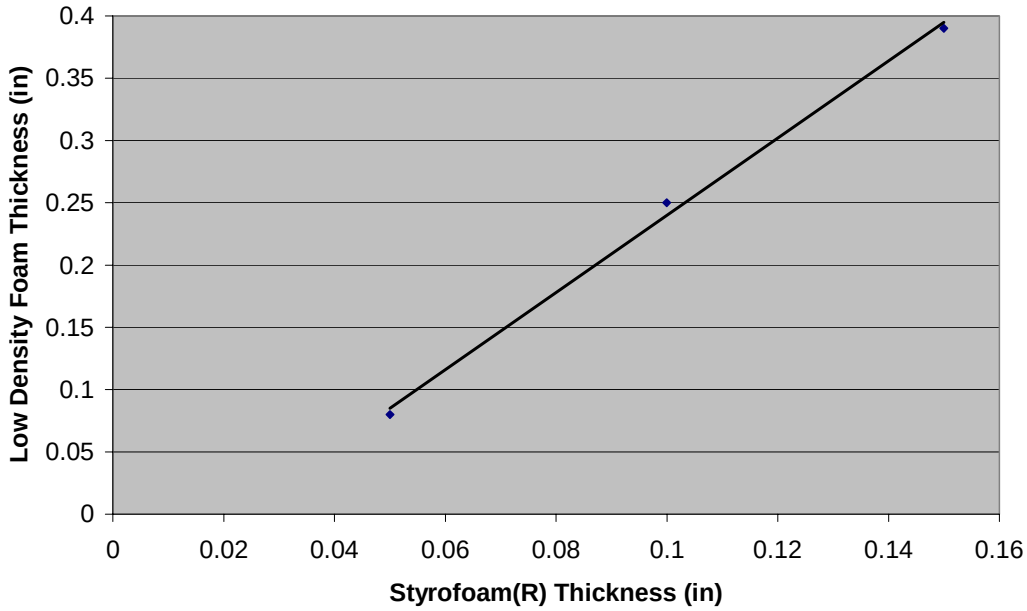

Figure 67. Equivalent thickness of Styrofoam® for a given thickness of low-density foam

It may also be possible to tune the RF tags to negate the effects of placing them on metal objects. Further understanding of the tag circuitry would be needed, information not easily obtained from manufacturers.

5.4.4 Tag Survivability Characterization

Battelle performed tag launch acceleration and velocity characterization testing to explore tag survivability potential. These tests were conducted at Battelle's West Jefferson, Ohio munitions testing facilities. A "soft catch" was employed using a combination of Styrofoam and duct tape to reduce deceleration forces. Tiris tags were removed from their glass containers, potted, and placed inside polypropylene cylinders that were inserted as shotgun shell loads. Tag survival was determined using a Tiris reader to monitor the tag's response with the proper digital signal. Initial results were encouraging despite some testing problems (expired gunpowder and glitches in acceleration measurement devices). A single tag was fired 11 times; it survived the first 10 events. The final firing at 67,000 g's allowed the polypropylene slug to strike a steel plate, which did incapacitate the tag. The tag did survive documented accelerations up to 43,000 g's and a maximum velocity of 809 feet per second. Anecdotal information provided to Battelle indicated maximum accelerations of military guns is about 20,000 g's. Table 4 shows the results of this initial testing. Photos of the shotgun and Styrofoam soft catching setup are shown in Figure 68.

Table 4. Results of inital launch characterizations at Battelle's munitions facility

Single Shotgun Load Fired Into Styrofoam				
Shot Number	In-Bore Acceleration (g's)	Deceleration (Stopping) (g's)	Velocity (feet/s)	Tag Response
1	10,000	500	340	Good
2	27,000	2,250	277	Good
3	33,000	N/A	681	Good
4	12,750	220	375	Good
5	26,900	N/A	575	Good
6	10,800	1,600	381	Good
7	15,850	900	438	Good
8	43,100	N/A	809	Good
9	N/A	N/A	882	Good
10	N/A	N/A	475	Good
11	67,500	N/A*	1,158	Bad

* Load struck metal plate behind Styrofoam

Figure 68. Setup of the firing tests at West Jefferson showing the shotgun, the shotgun shell containing the tag, and the Styrofoam fixture for the soft catch of the test slug

5.5 TESTING AT ABERDEEN PROVING GROUND

Battelle tested the tagged-ordnance system in 2005 and 2006 at the Aberdeen Test Center located at Aberdeen Proving Ground. The same munition surrogates were used during both tests; nine tagged surrogates were buried with three untagged surrogates nearby to simulate the presence of buried clutter. The above-ground detection system was used in both tests, with minor improvements present in 2006.

5.5.1 2005 Testing of EM Tags at Aberdeen Test Center

Much of the EM tag effort in 2005 was focused on preparing the hardware for testing at ATC. This section describes these tests and the results of the tests.

5.5.1.1 2005 Test Plan

The Test Plan Summary sent to Aberdeen Test Center in September 2005 and is included in the 2005 Annual Report. The basic plan was for ATC to bury nine tagged ordnance surrogates at different depths and orientations. In addition, non-tagged surrogates were buried near three of the tagged surrogates to simulate the effects of nearby clutter objects. The nine targets were buried in a fairly small area because there was no need to test search rate at this point in the development cycle. ATC buried the objects in a four-meter by four-meter area. The locations and depths of these objects are provided in Table 5 and are shown graphically in Figure 69.

Table 5. Burial characteristics of the surrogates at Aberdeen Test Center

Tagged Surrogate	Depth (feet)	Dip (degrees)	Untagged Surrogate	Other Conditions
1	1	0		Tag on top
2	2	0		Tag on top
3	3	0	1	Tagged surrogate parallel to the surface with the tag down. Untagged surrogate 6 inches above and parallel to the tagged surrogate.
4	1	45		Tag up toward ground surface.
5	2	45	2	The untagged item is 1-foot to the side, parallel, and at the same depth as the tagged surrogate.
6	3	45		Tag up toward ground surface.
7	1	90		Tag up toward ground surface.
8	2	90	3	The untagged item is 1-foot to the side, parallel, and at the same depth as the tagged surrogate.2
9	3	90		Tag up toward ground surface.

Note: Item depth is measured to the center of the minor axis for horizontal targets and the midpoint of the major axis for the inclined and vertical targets.

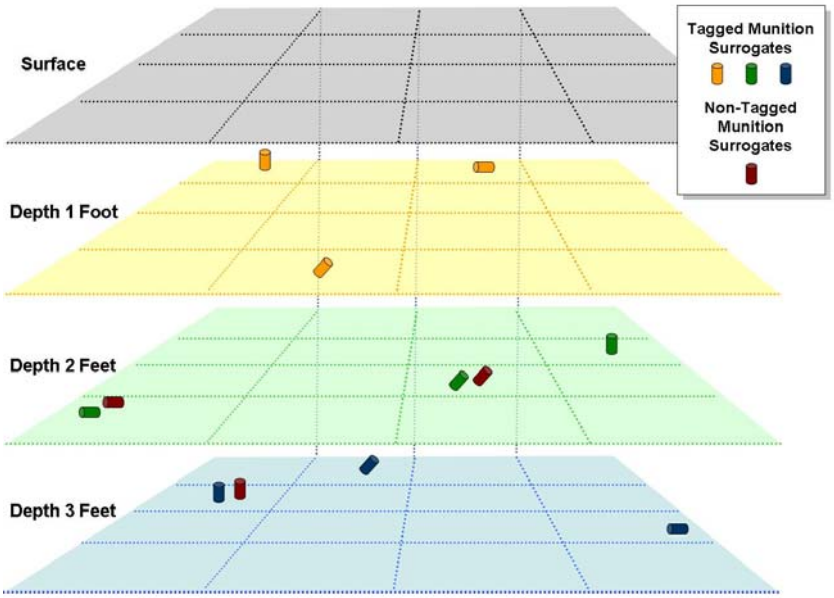

Figure 69. Multiple-depth view of the tagged ordnance items buried at Aberdeen Test Center in 2005

Battelle prepared 12 munition surrogates that would be employed during the Aberdeen testing. The surrogates were solid steel cylinders that were two inches in diameter and 12 inches long. The nine surrogates had tags embedded in grooves cut in them. A photo of one of the tagged cylinders is shown in Figure 70. The tag had 0.17 inches of ferrite material between it and the surrogate munition.

Figure 70. Munition surrogate later buried at Aberdeen Test Center. The tag is evident below the red tape.

5.5.1.2 2005 Testing at Aberdeen Test Center

Battelle personnel traveled to Aberdeen Proving Ground and performed the search for the buried targets the week of November 2005. Testing took place only on November 1. Battelle performed analysis of the data on November 2 and reported its predicted positions that day. ATC provided the location and depth information of the buried objects after Battelle placed flags in the soil predicting the positions.

Battelle used the detection system shown in Figure 71. The transmit coil is one meter in diameter and the receive coils are 12 inches in diameter.

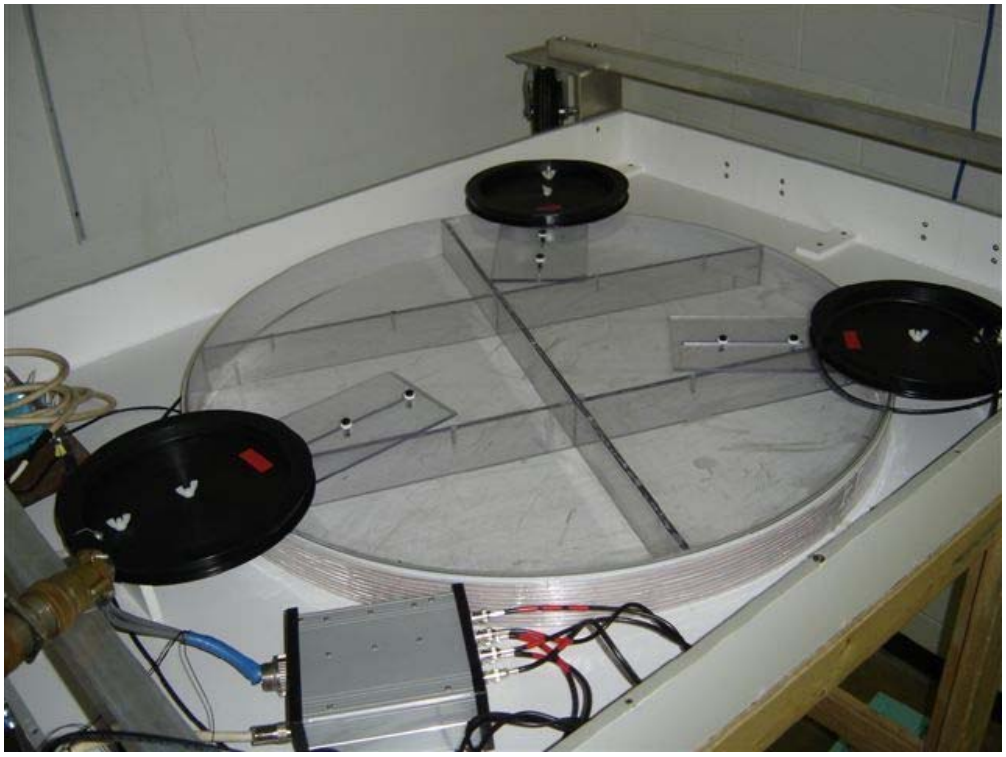

Figure 71. The interior of the coil module showing the one-meter diameter transmit coil and the three separate receive coils

The photograph in Figure 72 shows both modules. The coil module is on the left and the electronics module is on the right. The silver electronics module contains batteries and an inverter that powers the digital oscilloscope on top of the box. The signals from the three receive coils were plotted on the oscilloscope after the scope performed Fourier transforms on the signals. The Tiris tags respond with a frequency-shift keyed signal, with energy shifting between about 123 kHz and 134 kHz. The FSK signal, if interpreted properly, provides the digital data stream reply of the tag. The frequency-domain information on the plot provided evidence of the tag's modulation shifting energy between 123.2 kHz and 134.2 kHz. All of the screen plots of the data taken at ATC are provided in Appendix B of the 2005 Annual Report.

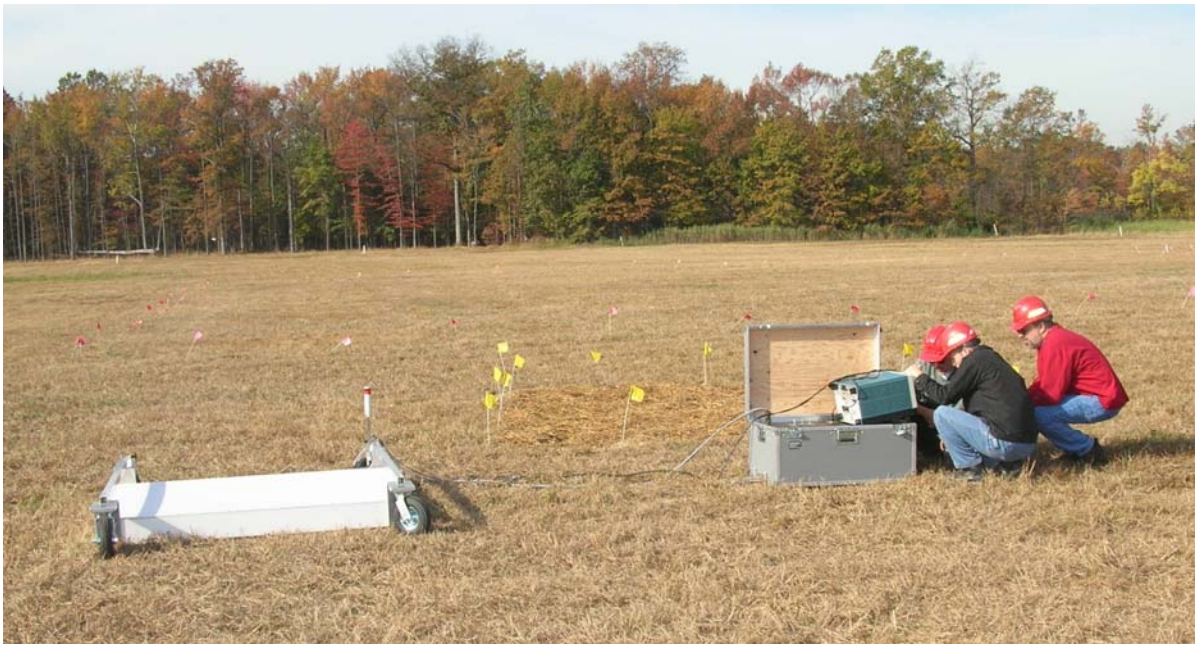

Figure 72. Coil module and electronics module being used at Aberdeen Test Center in 2005

Figure 73. Marking predicted surrogate locations at Aberdeen Test Center in 2005

The locations of the surrogates (tagged and non-tagged), Battelle's predicted positions, and data acquisition points are shown in the plot of Figure 74. The square markers indicate the positions of the tagged surrogates, the three triangles indicate where non-tagged surrogates were placed, the large circles represent Battelle's predicted positions of the tagged surrogates, and the diamonds indicate the position of the center of the transmit coil when data sets were recorded. The depth of each tagged surrogate is indicated with text, presenting the same information provided in Figure 69 and Table 5.

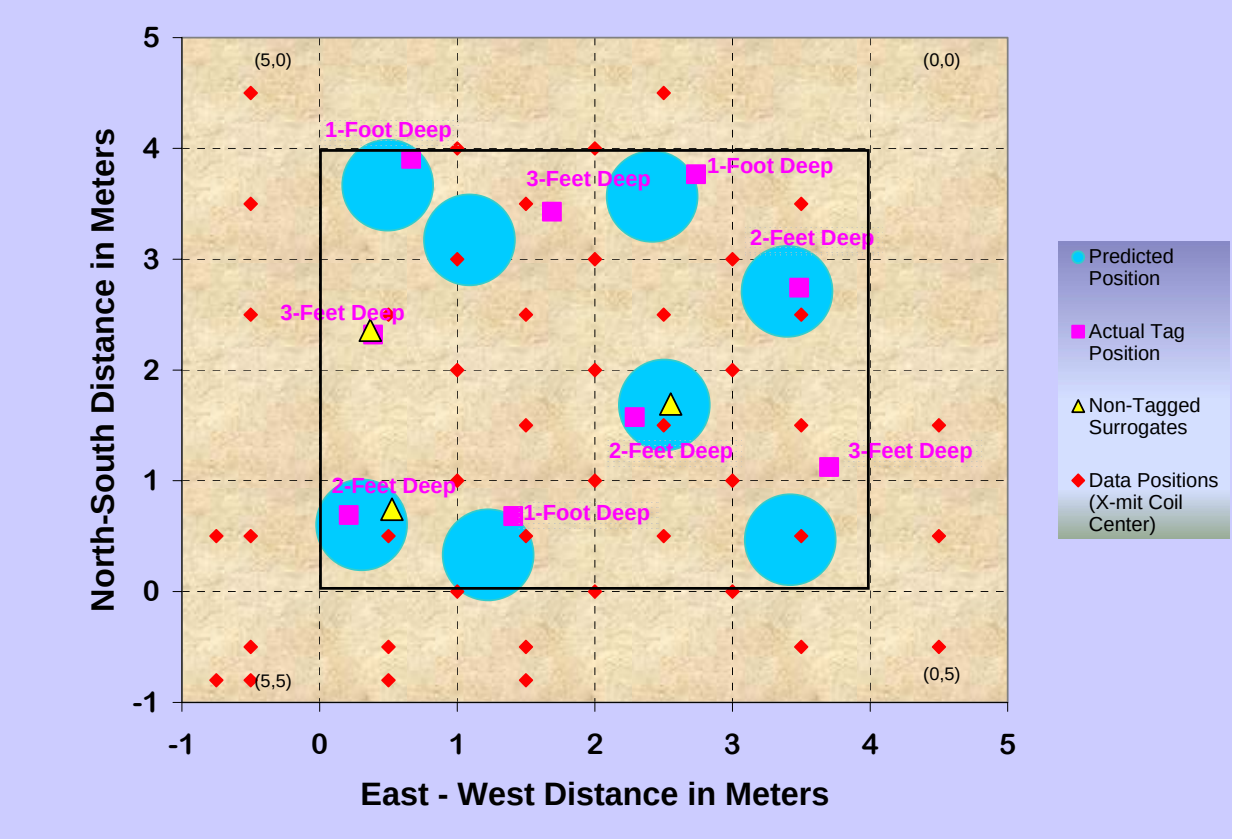

Figure 74. Plan view of the 2005 test grid at Aberdeen Test Center showing the actual tagged munition positions, Battelle's predicted positions, and the positions where Battelle acquired data

Battelle's predicted positions are indicated with large-diameter circles because of the large "footprint" of the coil module. The circle represents the uncertainty in the predicted position of the buried tag, an uncertainty similar to resolution cell size in an image. At this time, we do not know what our resolution cell size is but it is probably a function of the depth of the munition. A shallow munition might be detectable when the center of the coil module is one meter from the position of the buried tag but a three-foot-deep tag might only be detectable when the center of the coil is within 10 inches of the tag. Modeling studies would help determine these parameters.

Our data sets were frequency-domain images on the oscilloscope screen. One example plot is provided in Figure 75. The horizontal axis represents frequency and the vertical axis indicates signal strength in dB. The left vertical yellow cursor is positioned at 123 kHz and the right vertical cursor is positioned at 134 kHz. Very little signal is evident at the positions of the cursors. Figure 76 shows the same plot when the coil module is positioned over a tagged surrogate. The signal strength is significantly higher at the two cursors. The tag is replying to the interrogating signal by modulating between 123.2 kHz and 134.2 kHz.

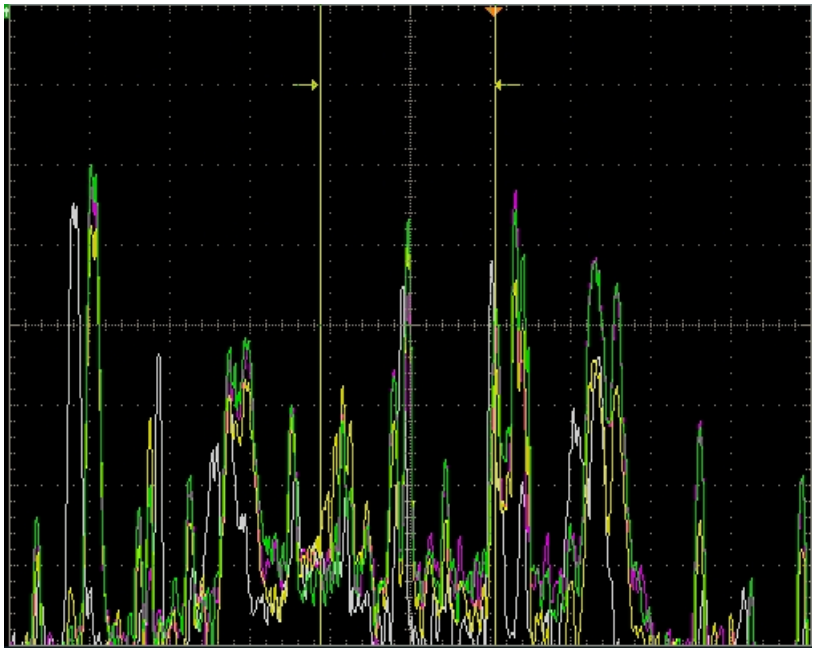

Figure 75. Example data plot with no tagged surrogate present. The plot provides frequency as the horizontal axis and signal strength in dB along the vertical axis. The yellow vertical cursors are at 123 kHz and 134 kHz

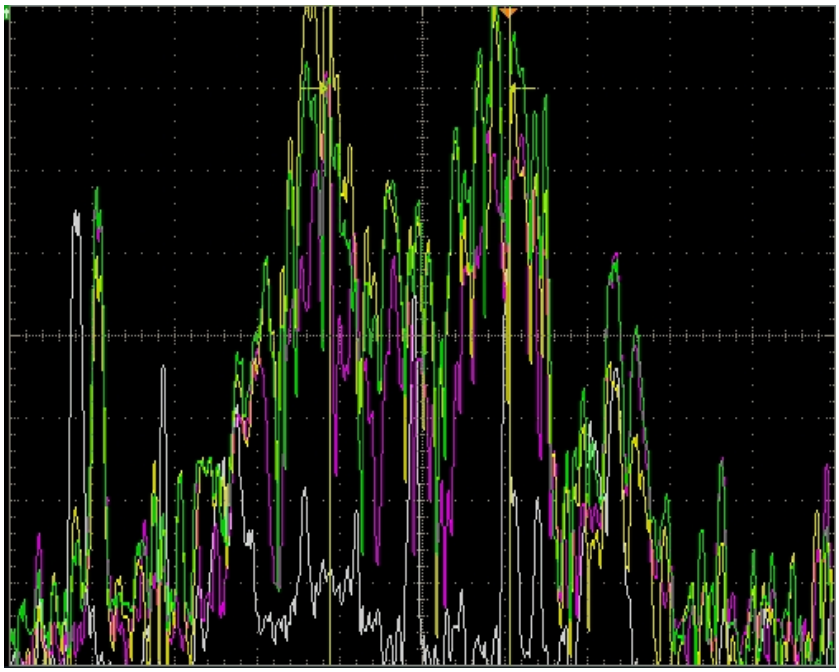

Figure 76. Example data plot with coil module positioned above a tagged surrogate. The signal strength is much higher at the two cursor positions

5.5.1.3 2005 ATC Testing Results

Battelle's analysis and decision-making processes for the 2005 ATC tests were not optimal. We also had not anticipated multiple buried objects being sensed simultaneously, which occurred because the surrogates were buried in a fairly small area. (The sensing of multiple tags is a realistic situation, but it had not been anticipated nor investigated in the lab.) The multiple simultaneous detections and the fact that we had not used a coil module with three receive coils previously led to confusion and difficulty making decisions. In order to examine the data and make detection decisions, the frequency-domain oscilloscope plots were laid out on a large conference room table in an arrangement corresponding to the test grid. The paper plots were then visually examined and predicted positions were recorded. These positions were then marked with pink flags, as shown in the photograph of Figure 73. After Battelle left ATC, Government personnel surveyed the flags and reported the actual positions of Battelle's predicted target locations.

Battelle predicted the positions of eight buried tagged surrogates. As stated previously, nine tagged surrogates were sent to ATC but the actual number buried was unknown to Battelle. Figure 74 shows we were reasonably successful in predicting the positions of the eight targets we flagged.

One tagged surrogate was missed completely. The missed surrogate, which was buried three feet below the surface, is shown in Figure 74 at position (0.5, 2.5). It is described as Tagged Surrogate number 3 in Table 5 with the description "Tagged surrogate parallel to the surface with the *tag down*[3]. The untagged surrogate was six inches above and parallel to the tagged surrogate." The Figure shows that a data set was taken directly over the missed surrogate. After Battelle provided its predictions and ATC supplied the actual positions, we examined the data set taken at (0.5, 2.5) to see if the tag's signal existed in the data set. In fact, the tag's signal was very strong in the frequency-domain plot, which is shown in Figure 76. One has to ask the question as to why it was not reported to ATC when it was clearly evident in the data set. Battelle concludes that our analysis and decision-making processes were flawed. We thought the signal was coming from the tag we predicted at position (1.2, 3.2).

While it is disappointing that we did not predict this tagged surrogate, it is encouraging that the tag's signal is very strong in the data. Even though the tagged-surrogate was buried at the maximum depth (three feet), with the tag below the surrogate, and with an untagged surrogate six inches above the tagged surrogate, the tag's signal is clearly seen. Battelle feels that improved data presentation, analysis, and interpretation will allow similar tags to be correctly predicted in future assessment exercises.

The complete 2005 data set taken at ATC is included in Appendix B of the 2005 Annual Report.

Battelle received ATC's official report on December 14, 2005. ATC's plot of the buried tagged surrogates, the buried untagged surrogates, and Battelle's predicted positions (labeled as "Interpreted" on the plot) is provided in Figure 77. The ATC plot grid coordinates are provided in terms of planar UTM[4] coordinates. Their truncated UTM values are provided in Table 6.

[3] The phrase "tag down" implies the tag's position on the surrogate is underneath the item, as far from the surface and the coil module as possible and in the untagged surrogate's shadow.

[4] Universal Transverse Mercator projection and grid system commonly used for designating rectangular coordinates on large-scale maps of the non-planar earth. These coordinates are commonly used by Global Positioning System applications.

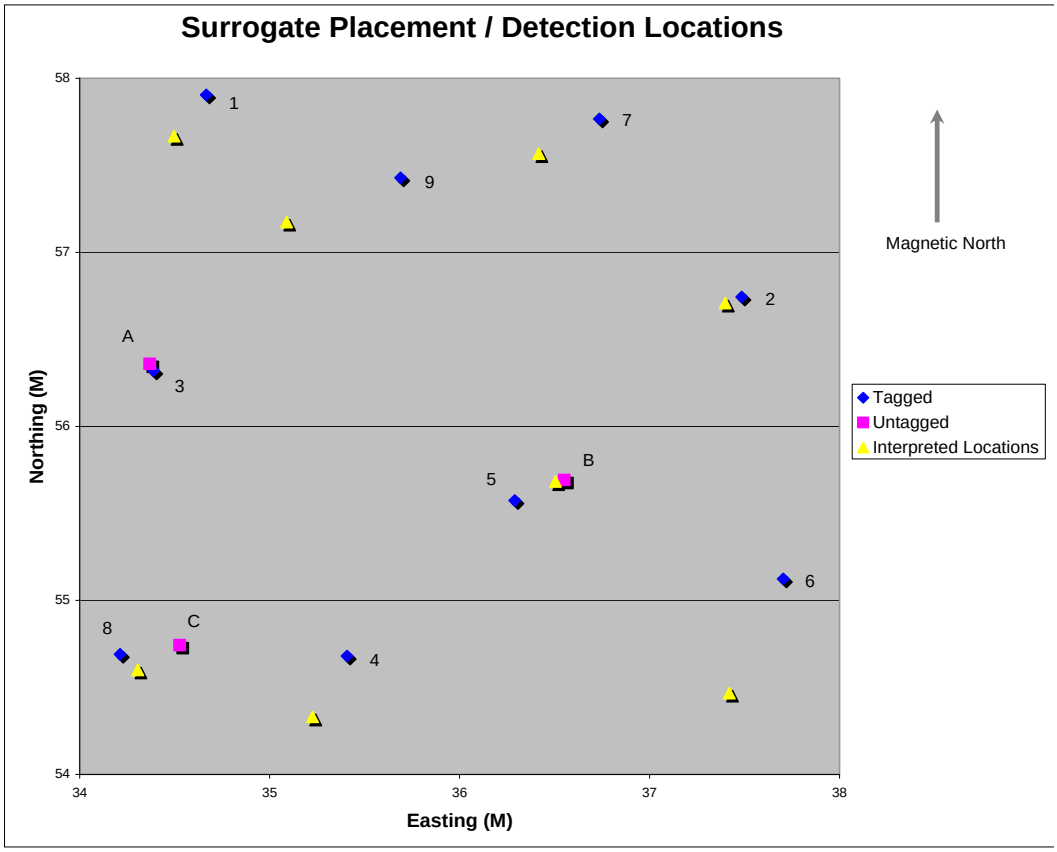

Figure 77. Aberdeen Test Center's plot of the 2005 data shown in Figure 74

Table 6. Aberdeen Test Center's 2005 UTM coordinates of surrogate placement and Battelle's predicted locations

Placement					Detection		
Number	Easting	Northing	Depth (feet)	Dip (degrees)	Pin Number	Easting	Northing
1	34.666	57.905	1.0	0	1	34.496	57.667
2	37.485	56.743	2.0	0	2	35.089	57.174
3	34.389	56.319	3.0	0		Not Detected	
4	35.407	54.681	1.0	45	3	36.417	57.567
5	36.290	55.574	2.0	45	4	37.398	56.709
6	37.704	55.123	3.0	45	5	36.505	55.683
7	36.736	57.767	1.0	90	6	34.306	54.601
8	34.212	54.690	2.0	90	7	35.226	54.331
9	35.689	57.428	3.0	90	8	37.420	54.467
A	34.369	56.359	2.5	0			
B	36.551	55.692	2.0	45			
C	34.526	54.743	2.0	90			

Notes: Color coding pairs tagged and untagged surrogate combinations.
Pin (flag) numbers were manually associated with the closest surrogate.

5.5.2 2006 Testing of EM Tags at Aberdeen Test Center

This section provides information on the testing that took place at ATC in November 2006.

5.5.2.1 2006 Test Plan

The Test Plan Summary sent to Aberdeen Test Center in September 2006 is included as Appendix B, beginning on page 104. The basic plan was for ATC to bury nine tagged ordnance surrogates at different depths and orientations. In addition, non-tagged surrogates were buried near three of the tagged surrogates to simulate the effects of nearby clutter objects. The nine targets were buried in a test lane one meter wide and 25 meters long. The locations of these objects are provided in Table 7 and are shown graphically in Figure 78.

Table 7. Burial characteristics of the surrogates at Aberdeen Test Center in 2006. The left-most columns represent object burial points in UTM coordinates. The columns labeled "X′" and "Y′" represents a truncation of the UTM and a coordinate system rotation to place the X′ and Y′ axes along north and south directions. The Battelle estimates are re-stated in terms of the rotated coordinate system. The column labeled Surrogate represents the numbers assigned by ATC and the depth of each surrogate is identified. Surrogate 4 was detected by Battelle twice, as was surrogate number 3. Battelle did not detect Surrogate 1; Battelle believes the tag on this surrogate was not functioning during this testing.

North	East	North	East	Surrogate	Depth	Description	Battelle Estimates	
X	Y	X'	Y'		(feet)		X'	Y'
4369575.201	402838.899	19.6453492	0.025127897			surrogate 4 tip		
4369575.036	402838.902	19.48177459	0.003279612			surrogate 4 tail	18.150	0.000
4369575.112	402838.905	**19.55645907**	**0.982324952**	**4**	1	surrogate 4 cntr	21.450	-0.622
4369578.062	402839.132	22.43877021	0.685740562			surrogate 6 tip		
4369577.953	402839.19	22.32228732	0.726688535			surrogate 6 tail		
4369578.002	402839.167	**22.37418898**	**0.288680829**	**6**	3	surrogate 6 cntr	23.100	0.622
4369572.675	402839.47	17.06220555	0.20975155			surrogate 5 tip		
4369572.504	402839.497	16.88908985	0.210727977			surrogate 5 tail		
4369572.599	402839.474	**16.98646835**	**0.797723498**	**5**	2	surrogate 5 cntr	15.675	-0.622
4369572.607	402839.278	17.02385359	0.009708737			slug b tip		
4369572.447	402839.326	16.85845461	0.033100608			slug b tail		
4369572.535	402839.288	16.95116856	0.008767007			slug b cntr		
4369570.065	402840.12	**14.38413652**	**0.540155937**	**9**	3	surrogate 9 vert		
4369567.534	402840.555	11.81650263	0.509262511			surrogate 3 tip		
4369567.372	402840.586	11.65168301	0.515546946			surrogate 3 tail	12.375	0.000
4369567.452	402840.568	**11.73348016**	**0.490217228**	**3**	3	surrogate 3 cntr	11.550	0.000
4369567.532	402840.557	11.8142246	0.510938987			slug a tip		
4369567.36	402840.588	11.63951871	0.515719533			slug a tail		
4369567.448	402840.571	11.72907449	0.512147097			slug a cntr		
4369562.848	402841.559	**7.03280645**	**0.202878367**	**7**	1	surrogate 7 vert	7.425	0.622
4369560.316	402841.141	**4.592465644**	**0.99690907**	**8**	2	surrogate 8 vert	4.125	-0.622
4369560.348	402841.39	4.586654875	0.254071477			slug c vert		
4369558.583	402842.41	2.688331703	0.997034556			surrogate 2 tip		
4369558.411	402842.398	2.52009254	0.959304145			surrogate 2 tail		
4369558.498	402842.403	**2.605351137**	**0.022668887**	**2**	2	surrogate 2 cntr	2.475	0.622
4369556.584	402842.336	0.72319527	0.623248788			surrogate 1 tip		
4369556.416	402842.374	0.55139117	0.635551278			surrogate 1 tail		
4369556.502	402842.357	**0.638969697**	**0.368321935**	**1**	1	surrogate 1 cntr		

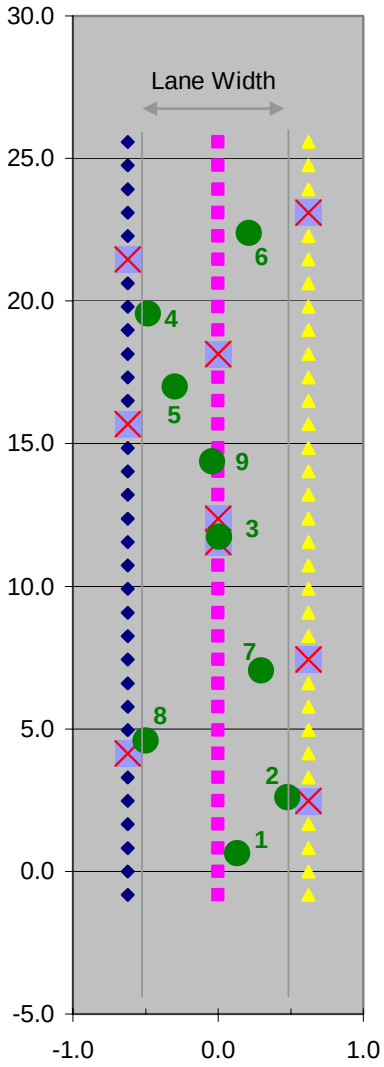

Figure 78. Plan view of the tagged ordnance items buried at Aberdeen Test Center in 2006. The test lane was one meter wide and 25 meters long; the lane width and length scales in the figure are not identical. The blue diamonds, magenta squares, and yellow triangles represent data acquisition locations. The blue squares with red crosses indicate Battelle's estimate of surrogate locations and the numbered round green circles indicate the actual surrogate positions.

5.5.2.2 2006 Testing at Aberdeen Test Center

The 12 munition surrogates used at ATC in 2005 were used again in 2006. The surrogates were solid steel cylinders that were two inches in diameter and 12 inches long. The nine surrogates had embedded tags in grooves cut in them for placement of the Tiris tags. A photo of one of the tagged cylinders was shown in Figure 70. The tag had 0.17 inches of ferrite material between it and the surrogate munition.

Figure 79 shows both modules in use at ATC. The coil module is on the left and the electronics module is on the right. The silver electronics module contains batteries and an inverter that powers the digital oscilloscope on top of the box. The signals from the three receive coils were plotted on the oscilloscope after the scope performed Fourier transforms on the signals. The Tiris tags respond with a frequency-shift keyed (FSK) signal, with energy shifting between 123.2 kHz and 134.2 kHz. The FSK signal, if

interpreted properly, provides the digital data stream reply of the tag. The frequency-domain information on the plot provided evidence of the tag's modulation shifting energy between 123.2 kHz and 134.2 kHz. All of the screen plots of the data taken at ATC in 2006 are provided in Appendix C of this report.

Figure 79. Coil module and electronics module being used at Aberdeen Test Center in 2006

5.5.2.3 2006 ATC Testing Results

Figure 80 represents the same data as in Figure 78 with the long lane being divided into five segments. This depiction allows the test lane width and length to be drawn to the same scale.

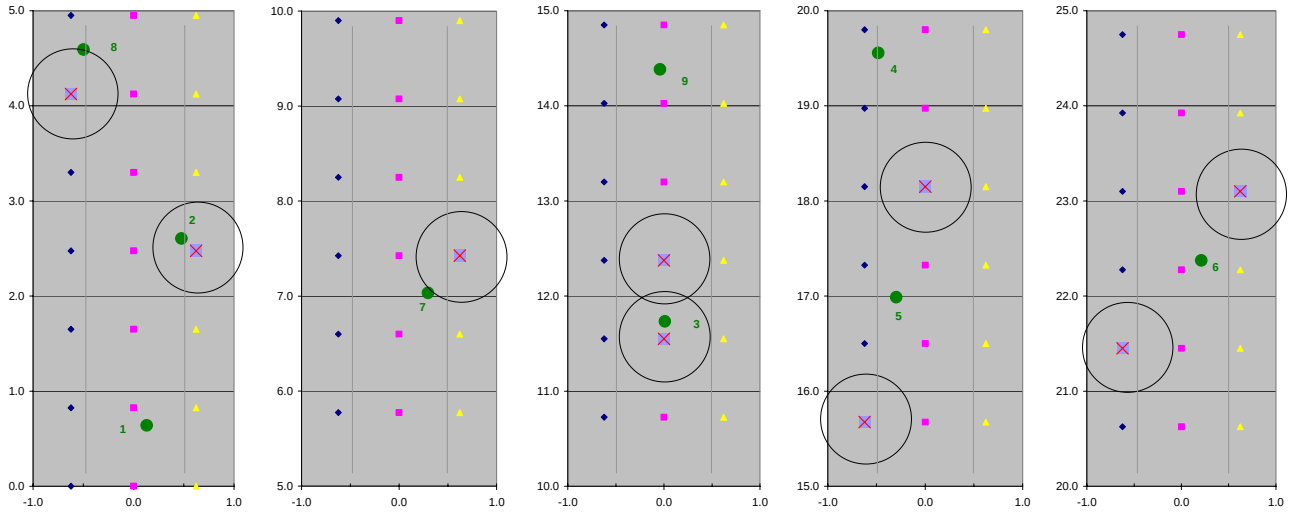

Figure 80. Plan view of the 2006 test lane divided into five equal segments. The data acquisition positions are shown as blue diamonds, red squares, or yellow triangles. ATC emplacements are shown as numbered green circles and Battelle's estimates are shown with red X symbols inside 1-m diameter circles that symbolize the size of the resolution area of Battelle's estimates

Battelle's predicted positions are indicated with large-diameter circles in Figure 80 because of the large "footprint" of the coil module. The circle represents the uncertainty in the predicted position of the buried tag, an uncertainty similar to resolution cell size in an image. We have not evaluated what our resolution

cell size is but it is probably a function of the depth of the munition. A shallow munition might be detectable when the center of the coil module is one meter from the position of the buried tag but a three-foot-deep tag might only be detectable when the center of the coil is within 10 inches of a point directly above the tag.

Our data sets are in the form of frequency-domain images on the oscilloscope screen. One example plot is provided in Figure 81. The horizontal axis represents frequency and the vertical axis indicates signal strength in dB. The left vertical red cursor is positioned at about 124 kHz and the right vertical cursor is positioned at about 134.5 kHz. Very little signal is evident at the positions of the cursors. The drawing on the right shows the position of the interrogation module in the test lane when the data was acquired. The green waveform represents the response of the green receive coil and the brown and magenta waveforms represent the signals from the brown and magenta coils, respectively. Figure 82 shows the same plot when the coil module is positioned near a tagged surrogate. The signal strength is significantly higher at the two cursors. The tag is replying to the interrogating signal by modulating between 123.2 kHz and 134.2 kHz.

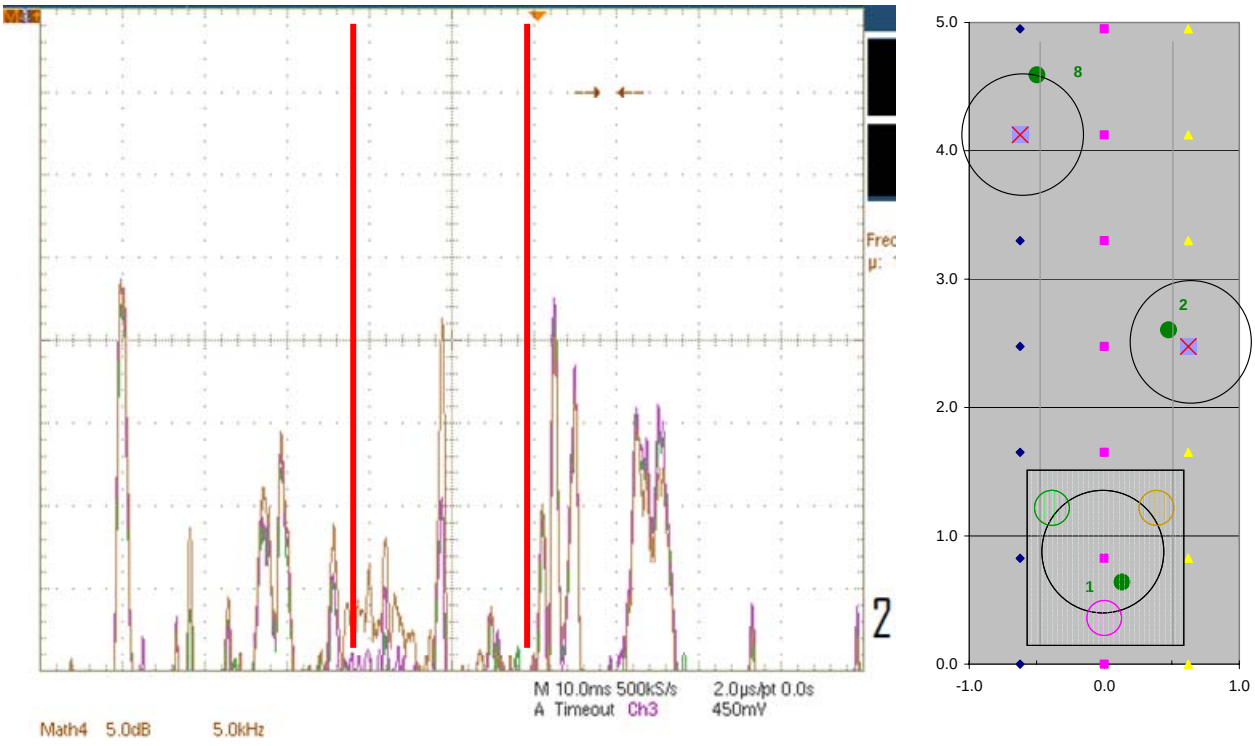

Figure 81. Example data plot with no tagged surrogate present. The plot provides frequency as the horizontal axis and signal strength in dB along the vertical axis. The drawing on the right shows the position of the interrogation module in the test lane when the data was acquired.

The data plots provided in Appendix C are presented in this same format.

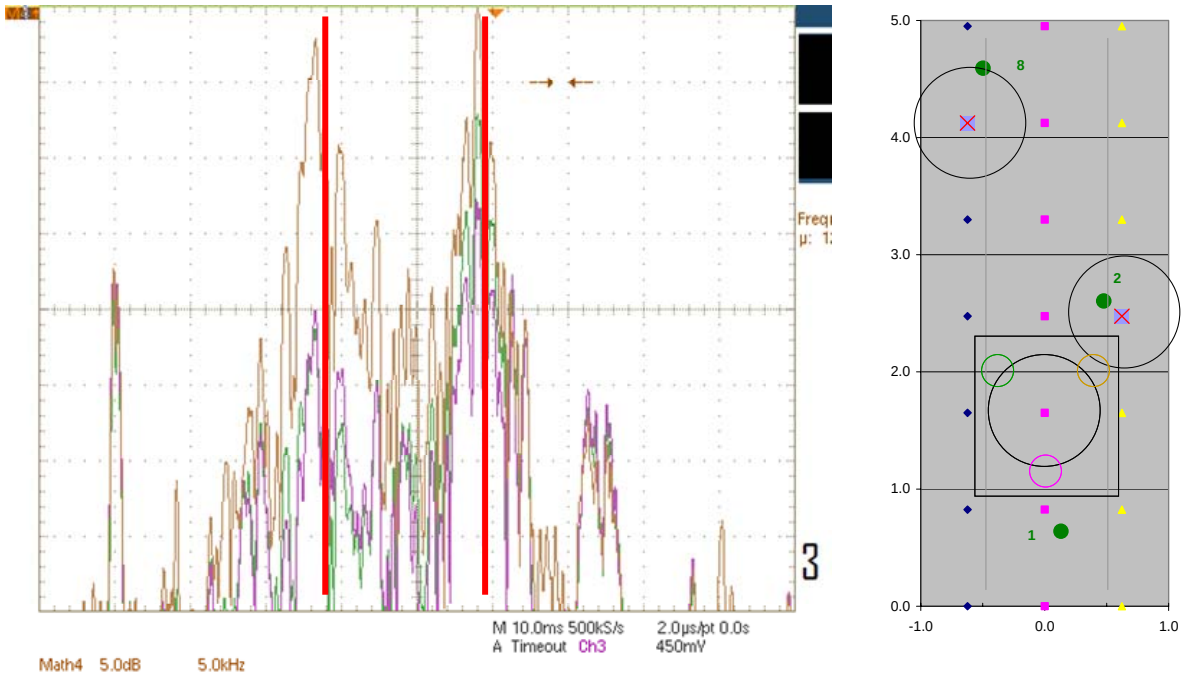

Figure 82. Example data plot with coil module positioned above a tagged surrogate. The signal strength is much higher at the two cursor positions indicated by the vertical red lines. The signal is strongest in the brown receive coil, which is near surrogate 2

Nine tagged surrogates were buried by ATC in 2006 and Battelle identified the location of what we believed were nine surrogates (one surrogate was missed and one surrogate was indicated twice). Examination of the data in Figure 80 shows general agreement between actual and estimated locations between meters 2 and 12 (surrogates 2, 8, 7, and 3).

Of primary interest is surrogate 1, located near meter 1 and in the center of the test lane. The detection interrogation equipment did not detect this tagged surrogate at all. The oscilloscope output from point (2, C), with a view position in the test lane, is provided in Figure 83. The transmit coil is directly over the green dot that represents the tagged surrogate. The magenta receive coil is very near the tagged surrogate. The data taken at position (2, R) is shown in Figure 84. No signal from surrogate 1 can be identified. It can be seen that the transmit coil is still nearly over the buried surrogate and the green and magenta receive coils are near the buried surrogate.

Battelle's analysis concluded that tagged surrogate 1 was not functioning. We cannot prove that this surrogate was inactive but we did ask ATC to carefully unearth the surrogate and use a Battelle-provided sensor system to determine the tag's functionality. Mr. Gary Rowe of ATC used the detector and showed that the tag was functioning only intermittently as he dug down to the tag, exposed it, and removed it on 14 December 2006. The full text of his e-mail message to Battelle was:

> "I converted the interrogator device you sent me to operate on battery power and [went] out to the test lane. I did not get a response from the RF tag until enough dirt was removed to get the antenna with 6-inches of the surrogate. The response was not constant. After a few seconds the tag stopped responding. We completely uncovered it, interrogated the tag a second time while the surrogate was still in the ground, and again got an intermittent response. Testing the tag with the surrogate removed from the ground still produced intermittent replies.

I confirmed that the interrogator device, on battery power, was working properly (before and after my trip to the field) by using the spare RF tags you had provided at the beginning of the program.[5]"

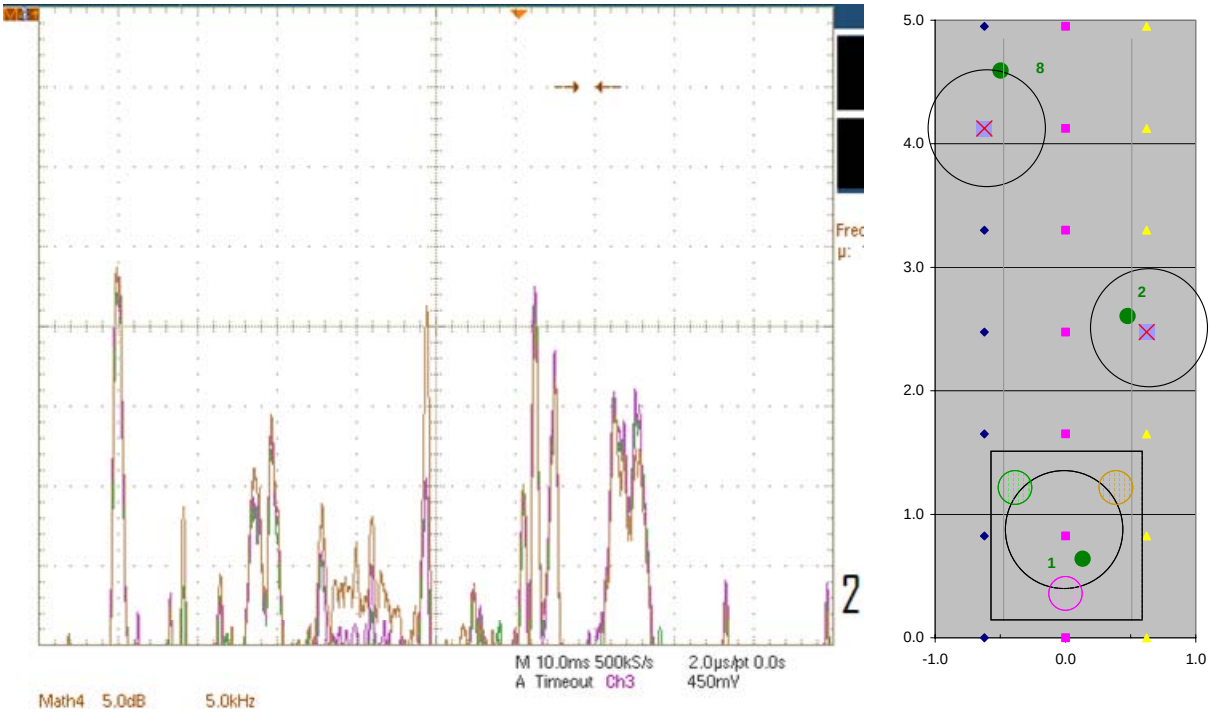

Figure 83. The plot shows data taken at point (2, C), which was directly over surrogate 1. The relevant portion of the test lane is shown on the right, with the position of the interrogation module, including its transmit coil and three receive coils

The plots of Figure 83 and Figure 84 that represent data taken above surrogate 1 (buried one foot beneath the surface) can be contrasted to the waveforms seen in Figure 85, which corresponds to surrogate 3, which is 3 feet deep. The signal from the deeper surrogate 3 is seen to be very strong.

As stated previously, Battelle believes these plots show that surrogate 1 was not functioning the day data was taken at the ATC test lane.

Past the 12 meter mark in the test lane, examination of Figure 80 reveals that Battelle detected the buried surrogates but was not accurate in indicating the positions of the surrogates. While we believe our position-indicating system was poor, the plot confirms the confusing situation we encountered during our 2005 testing at ATC. We worked to develop a DSP-based receiver and analysis system during 2006 but were unable to complete fabrication and testing with available resources. This type of automated system will be necessary to refine performance but the data provided in Appendix C demonstrate that these munitions-mounted radio frequency identification (RFID) tags will aid the Government in locating buried unexploded ordnance.

[5] E-mail message from Gary Rowe of Aberdeen Test Center to Keith Shubert of Battelle, 14 Dec 2006.

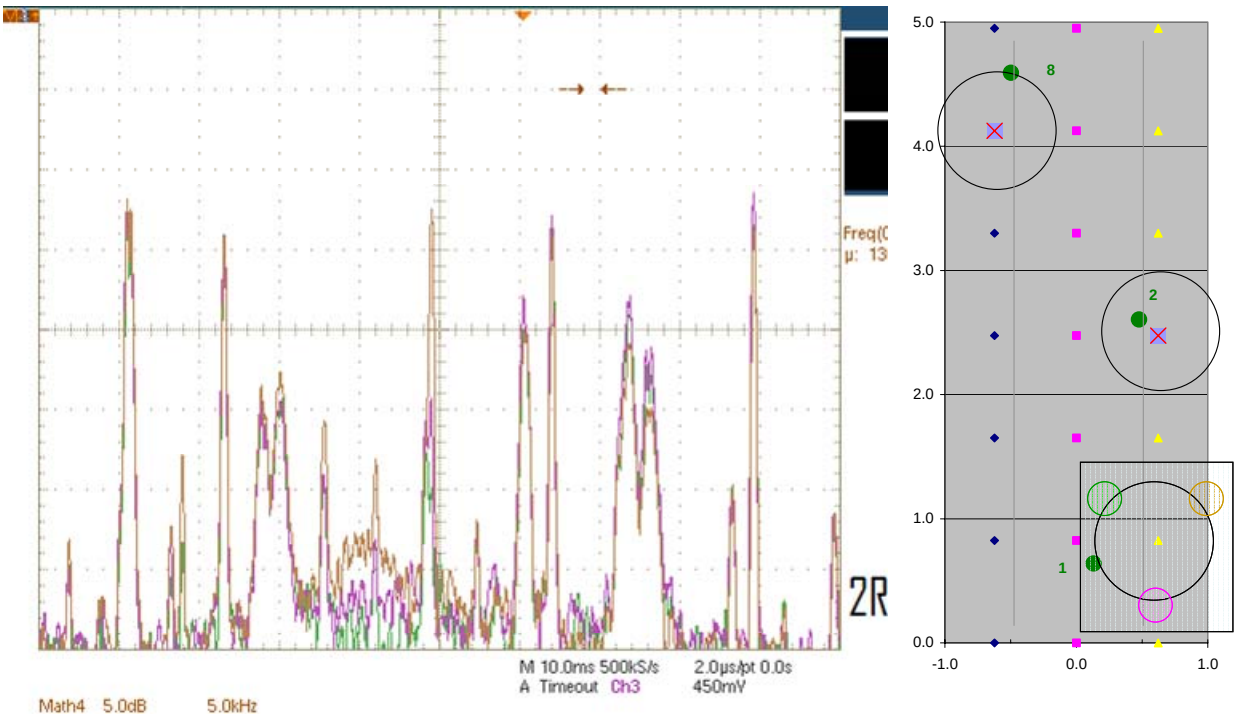

Figure 84. Data taken at position (2, R)

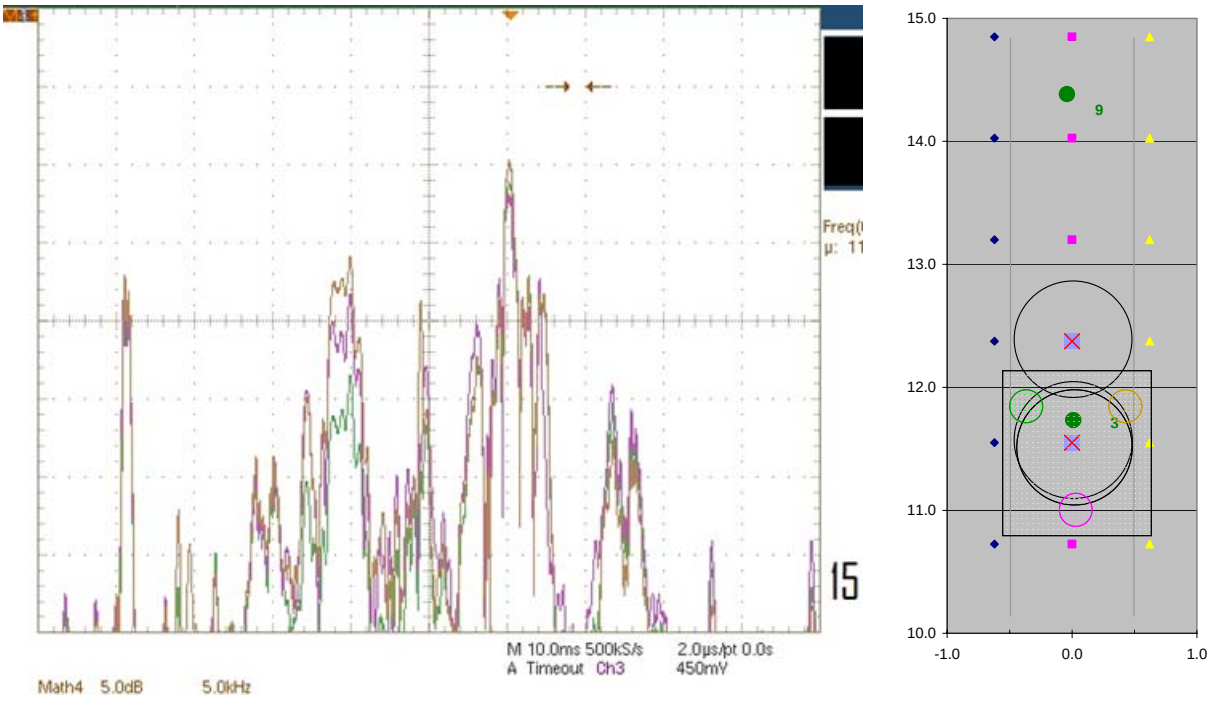

Figure 85. Data taken at point (15, C), above surrogate 3, which is buried 3 feet beneath the surface

5.6 TRANSPONDER QUALITY FACTOR STUDY

The Tiris transponders specify a minimum Quality factor[6] (*Q*) for them to respond to an interrogating signal. This specification results in a need to apply some minimum magnetic field and have the transponder in a material configuration (generally related to nearby metal structures) that maintains its *Q* above a value of about 60. Our laboratory studies showed the metal of the munition casing had a significant impact on the *Q* of the transponder so we performed a study to understand the effects of mounting the Tiris tags.

In free space, the *Q* of the transponder coils was found to be about 94. The test setup shown in Figure 86 was created to simulate the transponder embedded in a munition's steel body. The pieces of the 1018 carbon steel were moved to provide alternative groove sizes to the tests. Two wall sizes were used, 12.7 and 6.35 mm, in the studies. We also simulated 90° and 45° wall angles. The coil's inductance and resistance were measured with input signal of 100 kHz at 100 mV with the RF capacitor removed.

Figure 86. Test configuration including the Tiris transponder and four pieces of carbon steel used to simulate the tag embedded in a munition. The walls are at 90° in this photograph.

Six different ferrite thicknesses manufactured by API Delevan were used to mitigate the effects of the steel being in close proximity to the transponder's coil. One sample result is shown in Figure 87, which provides a feel for the variation that can occur with wall height, wall angle, and area of the groove. The study result shows two potential groove configurations;

- 36 mm by 15 mm, 90° walls, 2.3-mm thick ferrite on walls and 4.6 mm-thick ferrite on bottom; Q=66.3, Volume =0.5133 cubic inches

- 36 mm by 10 mm, 90° walls, 2.3-mm thick ferrite on walls, 4.6-mm thick ferrite on bottom plus additional layer of FR4 circuit board: Q = 63.68, Volume=0.365 cubic inches

[6] *Q* can be defined in several ways but two ways stand out in this application. As stated below, it is the ratio of the inductance to the resistance of the receiving coil of the tag. It can also be defined as the ratio of the resonance frequency to the bandwidth, which is a measure of the relative narrowness of the resonance curve. These definitions are discussed in *Electrical Engineering Circuits, Second Edition*, H.H. Skilling, John Wiley and Sons, Inc., New York, 1957, p. 228.

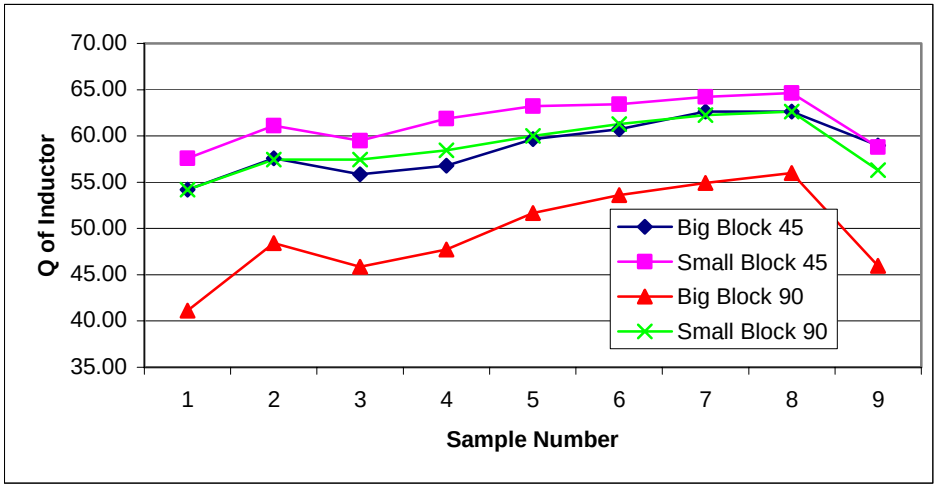

Figure 87. Sample result of varying block size and wall angle. The sample number refers to lengths and widths of the void around the steel walls

Some of the conclusions of this study include

- 45° walls raise *Q*, but may be difficult to manufacture and increase needed volume
- At least 4.6 mm-thick layers of Ferrite are needed to meet goals with 90° walls
- Extra layers of air gap using FR4 circuit board increase *Q*, but not as much as additional ferrite

These measured results are consistent with the modeling results but were important because they confirmed those findings in a more quantitative fashion using real materials.

5.7 Power Level and Frequency Allocation Issues

During 2003, Battelle had brief conversations with Navy officials (NSWC at Dahlgren Division) about Hazards of EM Radiation to Ordnance (HERO) issues and frequency allocation issues. Some advice and three documents were provided.

Current HERO levels were passed to us in a 2002 report[7]. The curves in this report specify the maximum safe level at 100 kHz to be between 10 and 40 V/m (rms), depending on the sensitivity of the munition. The current design of the Battelle one-meter diameter coil has been predicted to be about 0.5 V/m immediately below the coil, which lies well below the HERO safety level. The HERO level and values at 100 kHz are shown in Figure 88.

In 2003, the Navy cautioned us to be concerned with frequency allocation issues. They sent us a report that details U.S. Government allocations (we did not receive the title page of the report and therefore cannot cite it). At this point in our work, we will maintain awareness of this issue and calculate electric field values near the above-ground transmitting coil in our modeling work. We believe our radiated

[7] Michael Purello, "New Maximum Allowable Environments (MAE) For HERO Unsafe Ordnance and HERO Susceptible Ordnance," Dahlgren Division, Naval Surface Warfare Center, Systems Electromagnetic Effects Branch (J52), June 2002.

levels will be very low. Eventually, we will confront this frequency allocation issue at each testing site and work with the Government to get it resolved.

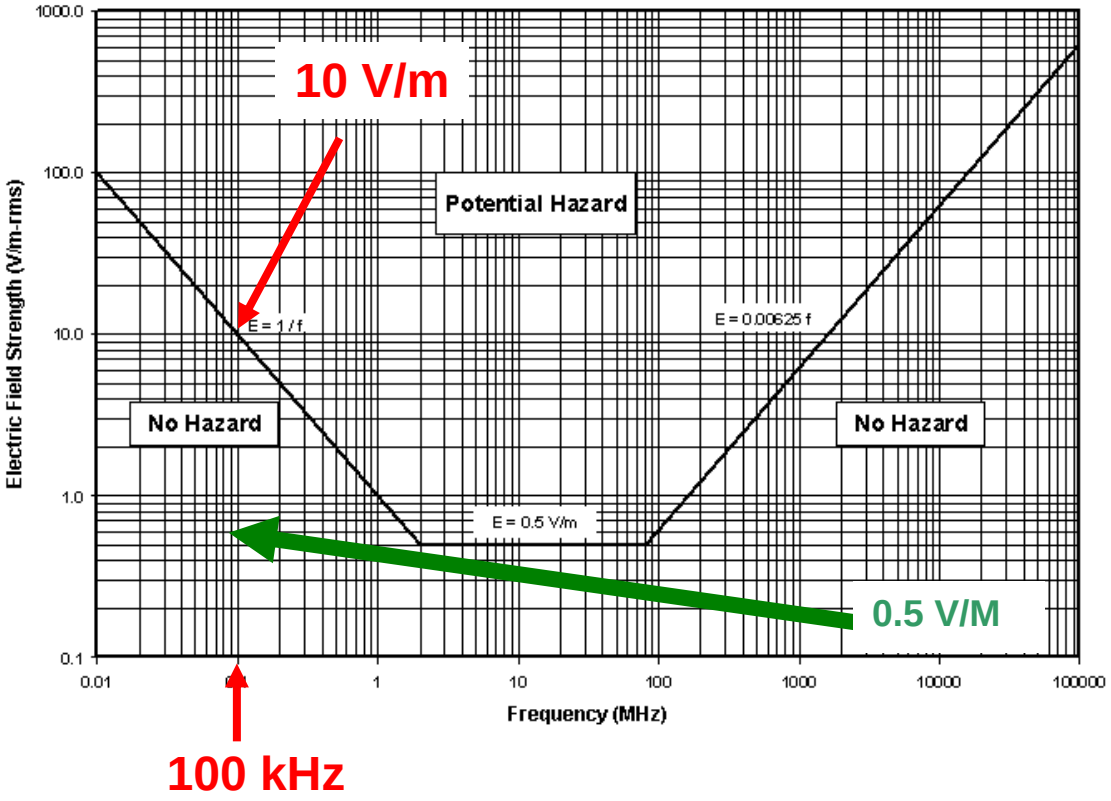

Figure 88. HERO safety levels and the theoretical value of the Battelle one-meter diameter interrogating coil

5.8 PUBLICATIONS

One peer-reviewed paper was published during the course of this project. The bibliographic citation of the paper is the following:

> "Buried Ordnance Detection: Electromagnetic Modeling of Munition-Mounted Radio Frequency Identification Tags," R.J. Davis, K.A. Shubert, T.J. Barnum, and B.D. Balaban, *IEEE Transactions on Magnetics*, Vol. 42, No. 7, pp. 1883-1891, July 2006.

One presentation was made to a U.S. Government organization and two posters were displayed at the Annual Partners in Environmental Technology Technical Symposium and Workshop:

> "SERDP Munitions Tagging Project," presented at the 26th Meeting of the Range Environmental Group - Range Commanders Council, Atlanta, Georgia, June 8, 2004.
>
> "Enhanced Electromagnetic Tagging for Embedded Tracking of Munitions and Ordnance During Future Remediation Efforts," Program Guide, Partners in Environmental Technology Technical Symposium and Workshop, Washington, DC, December 2004, 2005.

6 Conclusions and Recommendations

Tagging munitions with low-frequency, passive EM tags before they are fired, in order to simplify and reduce costs of detecting buried UXO while minimizing false alarms, is multi-faceted, complex, and challenging. Battelle's work confronted many of the issues involved in developing this technology and consistently demonstrated the potential for this type of RFID system to aid the Government in solving a challenging and expensive environmental problem.

6.1 CONCLUSIONS

Battelle concludes that the use of the prescribed RFID tags on munitions before they are fired would pay major dividends to the U.S. Government. We believe that our testing at the Aberdeen Test Center in 2005 and 2006 demonstrated that properly-embedded tags on UXO items can be detected to the needed depth of three feet. Fully-developed above-ground interrogators could scan munition ranges at reasonable rates, with a one-meter-wide swath and an estimated speed of two to three miles per hour. This type of search would provide a very high probability of detection. We made no attempt to estimate the false alarm rate but a false alarm would occur only when a munition exploded but did not damage the RFID tag, or when a tag separated from its munition. Ground clutter and munition scrap would not influence the detection probability or the false alarm rate. The major factor in the cost of remediation may be the high false alarm rate of current UXO search methodologies. Battelle believes a detailed analysis would show the tagged-munition methodology to yield huge overall savings in the future, even though cost would be incurred mounting commercial-off-the-shelf RFID tags on munitions.

The Tiris EM tags that operate near 125 kHz enjoy an advantage because this low-frequency energy is not significantly attenuated by soil. The disadvantage of using this low frequency is the long wavelength of the energy and the resulting lack of resolution as to the location of the buried UXO item. Battelle's modeling showed that this low ground attenuation situation might improve at higher frequencies, with the potential for slightly better detection system resolution. Unfortunately, the next highest frequency commercial-off-the-shelf RF tags operate in the 400 MHz region, where ground attenuation would be too high. An RFID tag system for buried UXO detection will probably have a position resolution of one to two meters, but this value has not been investigated in detail.

The interrogation system requires improvement but the effectiveness of the basic technology and methodology has been demonstrated.

With regard to transitioning the technology to the armed services, significant efforts are needed to coordinate with the various military offices that design and control munitions, particularly designers of new munitions. Such an effort can be conducted more effectively now that limited success has been demonstrated.

In summary, Battelle offers the following conclusions as a result of this effort:

- Tiris EM tags manufactured by Texas Instruments that operate near 125 kHz are the best choice for this application. They operate at a frequency that sees little loss through most types of soil. Their reliance on the magnetic field, rather than the electric field, further justifies their use. They are small and can be mounted on the five candidate munitions using reasonable approaches. They require about 0.17-inch ferrite spacer between themselves and any metallic portions of the munition. They could be embedded directly into the bodies of polymer-based munition casings.

- Battelle provided a theoretical basis for concluding that generic munitions can be detected to a depth of three feet in soil using the mechanical and electrical equipment developed as part of this project.

- Testing at the Aberdeen Test Center confirmed the results of the modeling effort that the munition-mounted tags can be detected through three feet of soil when properly fastened to the munition.

- Battelle demonstrated the potential for the Tiris tags to survive accelerations over 40,000 g's and velocities of 800 feet per second, which are believed to be adequate for currently-used firing and weapon delivery systems.

- Battelle developed and presented concepts for mounting the Tiris tags on the five candidate munitions considered during this project.

- Battelle provided a theoretical basis for believing that the large electric fields generated by the interrogation system are below HERO safety levels, which implies the detection system will not set off a buried UXO item.

- Battelle demonstrated the potential for using passive UHF tags on surface and near-surface ordnance items with detection ranges of several feet. The required tag antennas are large and will not be appropriate for some submunitions.

- Battelle designed, fabricated, and tested an above-ground detection system comprising powering and receiving electronics, a single one-meter diameter transmitting coil, and three receiving coils.

6.2 RECOMMENDATIONS

Battelle recommends that the Government consider the following steps:

- Identify the designers of future munitions to allow tags to be integrated from their inception.

- Provide the resources to refine the interrogation module receive system to include 12-bit analog-to-digital converters, digital signal processing chips, differential global positioning system modules, and suitable software to aid in better localization of the buried tagged munitions.

- Provide interfaces to

    - Potential users

    - Range commanders

    - Controllers of current candidate munitions to discuss and encourage the mounting of tags on existing ordnance items, at least at testing and research ranges

Battelle believes this project has demonstrated that the Tiris RFID technology can aid the Government in significantly reducing the cost of remediating and maintaining training and testing ranges in the future. The technology needs incremental development steps and significant military buy-in before actual deployment, but this project has shown that commercial-off-the-shelf RFID technology can be leveraged and will eventually lead to a less expensive, safer, and lesser-polluting set of ordnance ranges.

7 Appendix A: Modeling Details

7.1 BACKGROUND

Electromagnetic finite element modeling for this project is done using Vector Fields[8] software. This software has a complete range of two- and three-dimensional electromagnetic design, modeling, analysis, and simulation components. Battelle has successfully been using this software package on a variety of projects for over a decade.

For two-dimensional analyses (Cartesian-X-Y and axisymmetric), the program OPERA-2d is used. For three-dimensional analyses, OPERA-3d program is used. Each program contains various modules that will solve a subset of Maxwell's Equations for a specific problem type.

The following narrative provides a general overview of finite element modeling (FEM) as it pertains to electromagnetics, and more specifically to the Vector Fields Electromagnetic FEM package.

7.1.1 The Finite Element Method

Vector Fields' finite element algorithms are used to obtain solutions to partial differential or integral equations that cannot be solved by analytical methods. These equations describe the spatial and temporal variation of a field either directly in terms of the field variable, for example the magnetic flux density ***B***, but more often using a potential function that is related to the field by a gradient or curl operation. The finite element method is generally applicable to any problem with any type of non-linearity. The method is based on division of the domain of the equation (volume of space in which the equation is satisfied) into small volumes (the finite elements). This division of the volume into smaller volumes is commonly referred to as discretisation. Within each finite element a simple polynomial is used to approximate the solution. These concepts are independent of the number of space dimensions in finite element analysis.

Consider a Poisson type equation describing a potential function ϕ in one dimension:

$$\nabla \cdot \varepsilon \nabla \phi = \rho \tag{1}$$

The potential function, ϕ, might be an electrostatic potential, in which case ρ would be a line charge density. In order to define ϕ, boundary conditions are required; these may be either assigned values of ϕ or its derivative, for example:

$$\frac{\partial \phi}{\partial x} = 0 \tag{2}$$

In all electromagnetic field examples, it is essential that the potential be defined with at least at one point in the domain; otherwise an infinite number of solutions could be generated by adding an arbitrary constant to the solution. To solve equation (1) using a finite element method, the domain is divided into line elements. A typical first order line element would have two nodes numbered, e.g. 1 and 2. Within this element, the potential, ϕ, will be approximated by a linear polynomial:

$$\phi(x) = a + bx \tag{3}$$

The electrostatic potential, ϕ, will be continuous over the domain, although its derivatives may be discontinuous if the electromagnetic properties, e.g. permittivity, change discontinuously. The finite

[8] http://www.vectorfields.com/

element model is capable of representing this behavior, and it is therefore convenient to characterize the polynomial shown in equation (3) by the values of ϕ at the nodes of the element and use the same nodal value to characterize the polynomials in other elements that meet at the node. A further simplification is introduced by rewriting equation (3) in terms of nodal shape functions, N_i, defined such that:

$$\begin{aligned} N_i(x) &= 1; \quad x = x_i \\ N_i(x) &= 0; \quad x = x_j, \quad x \neq j \end{aligned} \tag{4}$$

Here, x_i is the x-coordinate of i^{th} node, etc. The shape functions have the same polynomial form as the ϕ approximation, and equation (3) can be written as:

$$\phi(x) = N_1(x)\,\phi_1 + N_2(x)\,\phi_2 \tag{5}$$

The shape functions N_i are usually expressed in terms of a local coordinate system in the element. This technique can be used to simplify the expressions and furthermore avoids problems of numerical rounding errors. Using the local coordinate system, the shape functions can be written as:

$$\begin{aligned} N_1 &= \frac{1}{2}(1-\xi) \\ N_2 &= \frac{1}{2}(1+\xi) \\ -1 &\le \xi \le 1 \end{aligned} \tag{6}$$

The shape function for a particular node is only defined in the elements that use the node and is zero outside these elements. The approximation to ϕ is described as having local support when nodal shape functions of this type are used. The discrete method of approximating the potential ϕ using characteristic nodal values and associated shape functions that determine the spatial variation of the approximation provides the basis on which several alternative procedures could be used to solve equation (1). Variational methods, least squares, and weighted residual procedures are three of the most frequently used. Weighted residuals have wide application and they are used in the software to develop a numerical solution. An approximate solution is determined by requesting that this function should satisfy:

$$\int W(\nabla \cdot \varepsilon \nabla \phi - \rho)dx = 0 \tag{7}$$

The weighted residual method can be used with either global (defined over the whole domain) approximations to ϕ or the local approximations discussed here. Here, W is a weighting function from which the method gains its name. The Galerkin weighted residual method is the best choice for the types of equation arising in electromagnetism. In this case the basis functions approximating ϕ are also used for the weights. Equation (7) is often referred to as a strong form because of the constraints it places on the functions that can be used in the approximation (the first derivative would clearly have to be continuous over the domain). In general a weak form of equation (7) is used to remove the derivative continuity requirement. This weak form is obtained by integrating equation (7) by parts (in more than one dimension this involves application of Green's theorem). Integrating equation (7) by parts to reduce the order of differentiation applied gives:

$$\int_a^b (\nabla W \cdot \varepsilon \nabla \phi + W\rho) dx - \left[W\varepsilon \frac{\partial \phi}{\partial x} \right]_a^b \tag{8}$$

Here, *a* and *b* are the limits of the domain of the equation. The weak form has several advantages: the functions representing *W* and ϕ do not need derivative continuity and the natural boundary condition on the surface of the domain has emerged. Equation (8) leads directly to a numerical solution method, using the discrete finite elements and shape functions discussed previously. Discretisation of the domain *a-b* into line elements with their associated nodes gives a set of independent weighting functions (the shape functions of the nodes) from which a set of equations can be developed by requiring that equation (8) is satisfied independently for each weight function. The equation for weight function is obtained from:

$$\sum_j \left(\int_a^b (\nabla N_i \cdot \varepsilon \nabla N_j \phi_j + N_i \rho) dx \right) - \left[N_i \varepsilon \frac{\partial \phi}{\partial x} \right]_a^b = 0 \tag{9}$$

for all elements containing node *i*. Taking all the equations for the different weight functions together gives a set of linear equations, which written in a matrix form are:

$$\mathbf{K\Phi} = \mathbf{S} \tag{10}$$

where **K** is a coefficient matrix (often called a stiffness matrix because of the background of finite elements in mechanics), **Φ** is a vector of unknown nodal potential values and **S** the known right hand side vector derived from the prescribed line charge densities or assigned boundary conditions. An individual element of the stiffness matrix consists of terms of the form:

$$K_{kj} = \int_a^b \nabla N_i \cdot \varepsilon \nabla N_j \, dx \tag{11}$$

Note that the local support of the shape functions means that although the integral in equation (11) is taken over the whole domain, only elements containing both nodes *i* and *j* actually contribute. In the equations arising in electromagnetism, the matrix equation (10) is frequently non-linear because the values of the electromagnetic material properties can be dependent on the field intensity. A Newton-Raphson method can be used to solve this type of non-linear equation.

7.1.2 Solution Errors

The local error at a point within a finite element mode is strongly linked to the size of the elements surrounding the point and weakly linked to the average element size over the whole space, although this second source of error becomes more important and less easily estimated in non-linear solutions. The relationship between the local error in the solution and the surrounding elements' size is given by:

$$E(\Phi) = O(h^2) \text{ for linear-shaped functions, and} \tag{12}$$

$$E(\Phi) = O(h^3) \text{ for quadratic-shaped functions.} \tag{13}$$

Here, *E* is the error, *O* means "of the order" and *h* is the linear dimension of the elements. This simple analysis is only true for square elements, but it is reasonable to assume the worst case and use the largest dimension for *h*. Unfortunately, these formulas only give the order of the error; the actual error is dependent on the solution, or more precisely the geometry of the model in the vicinity of the point.

Two methods are used to increase the field precision. First, a nodal weighted averaging improves the field accuracy by an order of *h*. Second, mesh refinement analysis will show where in the model additional finite element discretisation is needed.

7.1.3 Boundary Conditions

Boundary conditions are used in several ways. First, they can provide a way of reducing the size of the finite element representation of symmetrical problems. Second, they are used to approximate the magnetic field at large distances from the problem (far-field boundaries).

Problem symmetry and the symmetry of the fields are implied by the potential boundary conditions applied to the finite element model. The simplest types of boundary condition are:

Simple Boundary Conditions		
Field Symmetry	**Scalar Potential**	**Vector Potential**
$\mathbf{H}_n = 0$ or $\mathbf{B}_n = 0$	$\frac{\partial \phi}{\partial n} = 0$	$\mathbf{A}$ = *constant*
$\mathbf{H}_t = 0$ or $\mathbf{B}_t = 0$	ϕ = *constant*	$\frac{\partial \mathbf{A}}{\partial n} = 0$

The *n* and *t* subscripts refer to the normal and tangential directions to the surface being considered. A potential boundary condition must be specified on at least one node of a finite element mesh. This specification gauges the potential and without it the solution will not be unique.

7.1.4 Steady-State AC Analysis

The set of equations used to solve this project's specific problem is the steady-state AC subset of Maxwell's Equations, also known as the vector Helmholtz equation, with the magnetic vector potential, **A**, as the unknown variable. These equations solve the eddy current problems where the driving currents or voltages are varying sinusoidally in time. This set of equations can analyze skin effect, quasi-non-linear materials, in two-dimensions, both X-Y (infinitely long) and axisymmetric coordinate systems, and three-dimensions. The three-dimensional equation to be solved is

$$\nabla \times \left(\frac{1}{\mu} \nabla \times \mathbf{A} \right) = \mathbf{J}_S + \mathbf{J}_V - \sigma \frac{\partial \mathbf{A}}{\partial t} \tag{14}$$

The current density has been split into the prescribed sources. Here, $\mathbf{J}_s$, is the current density in the source coil's windings, and $\mathbf{J}_v$ is the currents density in the transceiver's windings of external circuits, μ is the magnetic permeability, and σ is the conductivity. In two dimensions, only the *z* (or ϕ) components of **A** exist. Also, since the potential and the currents are varying sinusoidally, they can be expressed as the real parts of complex functions. Equation (14) now becomes

$$-\nabla \cdot \frac{1}{\mu} \nabla A_C = J_C + J_V - i\omega\sigma A_C \tag{15}$$

7.2 BUILDING THE MODEL

The following narrative provides a brief overview of modeling practices used in this project.

7.2.1 Define Geometry

The first part of creating any finite element model is to build the geometric model. Each piece of the model that has a different electromagnetic property, including air, must be modeled individually. Each of these parts is a separate electromagnetic piece of the model. They include the air, soil, munition, munition grooves, transmitting coils, and transceivers. Each electromagnetic piece can be further subdivided into various regions to allow more detail.

In OPERA-2d, the geometry is defined through user input of coordinates. A set of coordinates define an edge of a geometric piece or region of the model. A complete set of coordinates will define an object. All areas of the two-dimensional model must be defined. In OPERA-3d, the two-dimensional model is similarly built and then extruded to define the third dimension. Planning is required to include all three-dimensional regions of interest into the initial two-dimensional model.

For our specific case, the problem is divided into two separate situations: Case 1, coil transmitting a signal to the tag on the munition, and Case 2, the tag transmitting a signal from munition to a receiver. This division allows a more simplified model to be built and examined.

Case 1: Transmitting Signal to EM Tag

For the first case, a standard transmitting coil was modeled. The coil was defined to be 1 meter in diameter and parallel to a flat surface. The winding cross-sectional area is ½ by ½ inch and is considered uniform. The individual turns of coil wire need not be modeled provided the individual wire size is small compared to the coil diameter and the source input is defined in terms of constant current and not voltage. The horizontal location of the coil was a parametric variable. The transmitting coil centered with respect to the munition's center is considered baseline.

Above the coil is air and below the coil is soil. These two regions were given separate identities so that the later could be parametrically analyzed for various soil conditions.

The initial 2-D munition geometry was defined to be rectangular, 6 inches by 3 inches in area. Note, for the axisymmetric case, it is a 6-inch diameter by 3-inch thick disc. This geometry is considered the baseline and used to generate basic information about the electromagnetic system. The geometry was later modified to represent more accurate 2-D munition geometry. In the 3-D situation, the more accurate munition geometry will be used. The coil-to-munition distance was a parametric variable. The baseline was 15 inches. The munition's angular orientation with respect to the transmitting coil was also a parametric parameter. A munition parallel to the surface longwise is considered baseline.

Grooves of various geometries were placed on the surface of the munition. The location of the groove was also varied. The baseline was a rectangular groove centered with the transmitting coil. For these cases, the EM tag was not modeled, since it would have no effect on the electromagnetic fields at its location. In this way, the models were kept generic so that any EM tag's input signal could be studied.

The baseline cases were modeled using both axisymmetric and X-Y symmetries. Although regarded two-dimensional, the axisymmetric model generates true three-dimensional fields. The model is considered two-dimensional only because the results are independent of the axial rotation angle; the model itself is actually three-dimensional. The X-Y models are strictly 2-D and so generate only two-dimensional fields. Of course, cases such as off-centered coils could only be modeled using the X-Y (infinitely long) models, since their geometry is not axisymmetric. A comparison of the baseline cases using axisymmetric and X-Y models was analyzed to provide a conversion factor for mapping the 2-D (X-Y)

results to true 3-D results. Based on previous work in this area, this method is about 85 percent accurate. A new conversion- factor is generated once a 3-D model is solved.

Case 2: Transmitting Signal from EM Tag

For the second case, the same basic 2-D geometry was used. The munition, groove, soil, and air were all chosen from baseline. The transmitting coil was eliminated. A specific EM tag was modeled onto the munition. Its location is a variable. Two types of EM tags were modeled: the pancake coil tag and the solenoid coil tag. Again, the individual turns of wire on these transceivers were not modeled and the coil windings were considered uniform. Baseline was a tag on the top of the munition centered on the munition. Only the baseline pancake coil tag was modeled axi-symmetrically. The geometry of the solenoid tag did not lend itself to this symmetry. Again, the baseline for the pancake coil tag was modeled in both axisymmetric and X-Y symmetries so that a conversion factor could be estimated. Once a 3-D model of the EM tag system is done, a new conversion factor will be generated.

A receiver coil does not need to be modeled. The signal received from the EM tag by a receiver coil depends only on the magnetic flux density linking the coil windings. This value can be calculated independently once the model is solved.

Figure 89 and Figure 90 show the geometry examples for Cases 1 and 2, respectively. Figure 89 shows the basic geometric definition for transmitting a signal from a coil to the EM tag located on a munition, Case 1. Both axisymmetric and X-Y symmetries are shown. An off-centered coil is shown in X-Y symmetry in the bottom figure. Figure 90 shows the basic geometric definition for transmitting a signal from the EM tag located on a munition to a receiving coil at the surface, Case 2. The receiving coil is not modeled. Here, only the X-Y symmetries are shown.

Typically, it takes about two-days to define a baseline two-dimensional model. Once built, variations of this model can be quickly made and stored separately. A typical three-dimensional model can take about a week to build. Variations to the 3-D model generally take about a day.

7.2.2 Define Material Properties

Once the geometry is completed, material properties of the model must be input. The material properties used for our models are given in the table below. Properties are assigned to each individual geometric region or groups of regions that define an object.

Object	Magnetic Permeability (relative)	Conductivity (S/m)
Munition (Iron)	100-linear X52-S non-linear	0.70×10^{7}
Air	1-linear	0.00
Soil	1-linear Other debris (100-linear)	Variable (0.0 to 4.3)
Groove Filler	Variable (1 to 100-linear)	0.00
TR_x Windings (Cu)	1-linear	Variable (0 to 5.9×10^{7})
TR_x Core	Variable (1 to 100- linear)	0.00
T_r-Coil Windings (Cu)	1-linear	N/A

The results for a magnetic non-linear permeability for the munition material were within a few percent of those results that used a linear permeability. Because linear problems solve more quickly, the majority of the analysis used only linear properties. The X52-S refers to a standard B-H curve for that material type.

For the coil windings (both the transmitting coil and transceiver coils), a uniform current density was given so that a constant source current of 1 amp-turn was defined. For the baseline transmitting coil, the current density was 4 Amps per square inch. It varied depending on EM tag geometry. The model calculated electromagnetic fields, and so all signal calculations are linear with the number of amp-turns in a coil. Therefore, the calculated results can be scaled for any constant current flow with the coil.

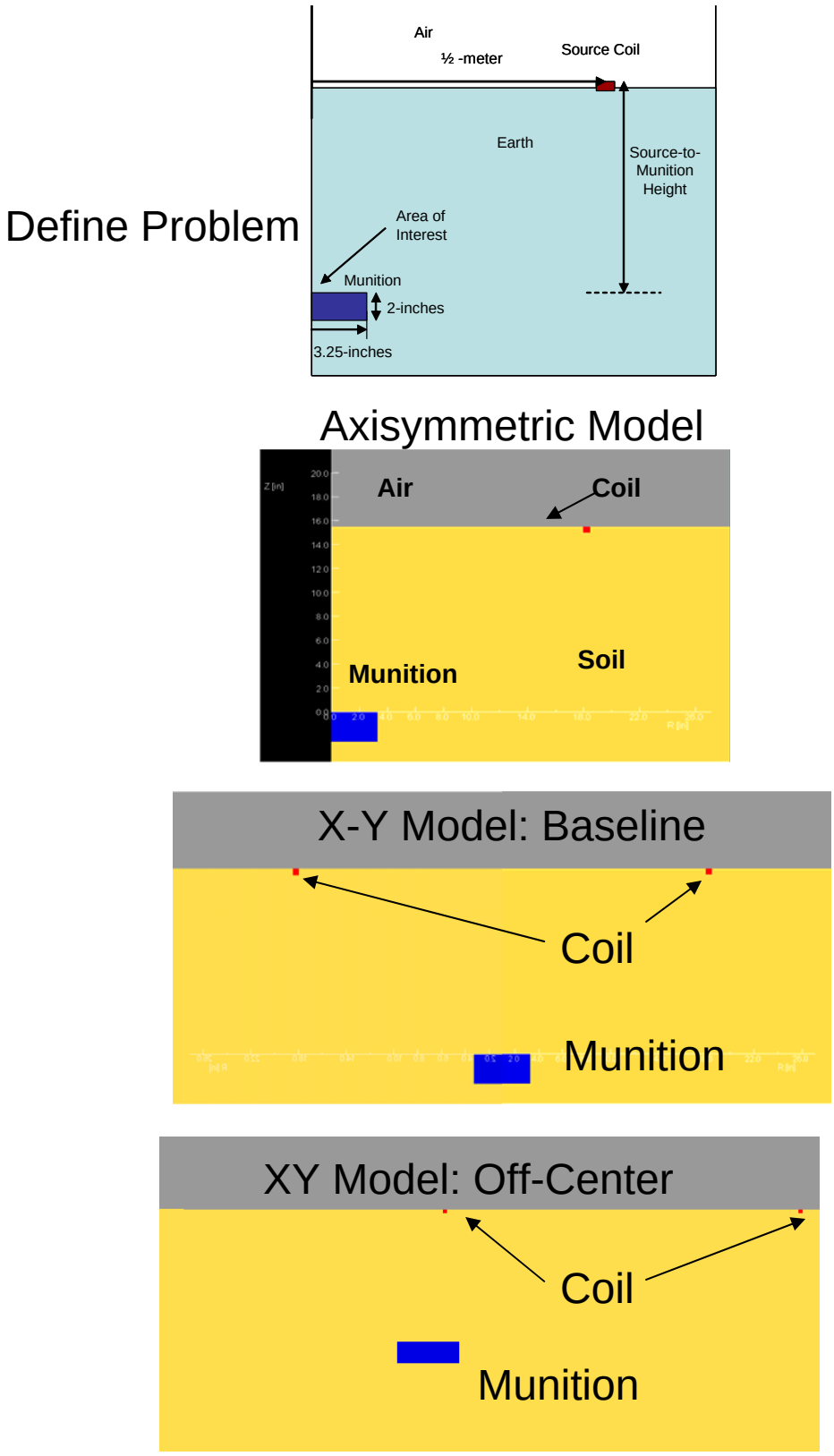

Figure 89. Geometry Examples for the Case of Transmitting Signal to the EM tag

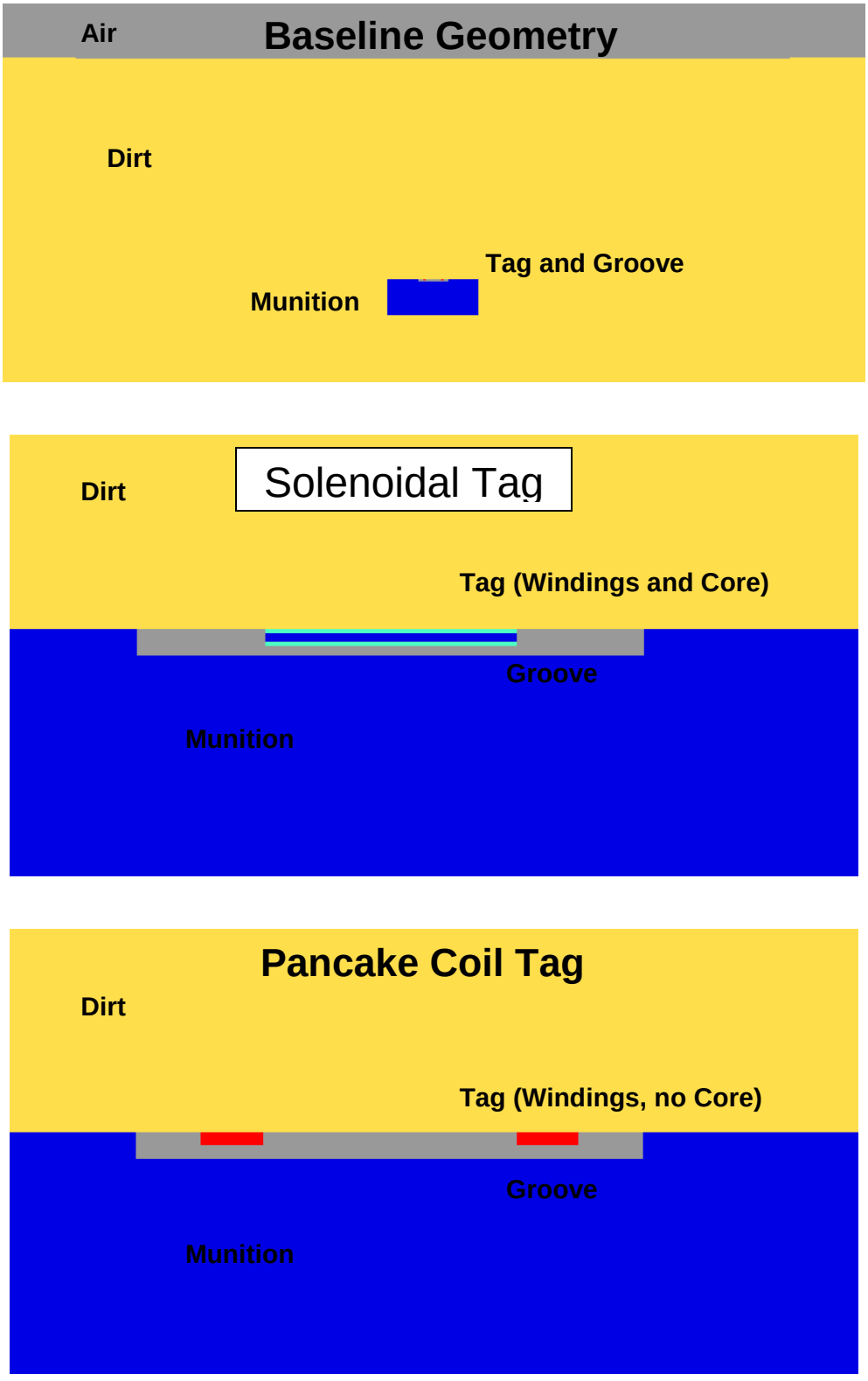

Figure 90. Geometry Examples for the case of transmitting a signal from the EM tag. Both Types of EM tags are shown

7.2.3 Apply Boundary Conditions

Boundary conditions are used to provide a way of reducing the size of the finite element representation of symmetrical problems, and approximate the magnetic field at large distances from the volume of interest (far-field boundaries). There are two types of boundary conditions in Electromagnetics, the Neumann and the Dirichlet. The first defines the potential on a surface; the second defines the normal derivative of the potential on the surface. Either of these conditions is sufficient to lead to a unique solution to the problem. Specifying both on a single boundary cannot lead to a solution. The Vector Fields program will not allow both to be defined simultaneously on a boundary.

For two- and three-dimensional models, the tangential component of the magnetic vector potential is defined to be zero at the edges of the model. The scalar potential is defined to also be zero, if used. This definition implies that the normal component of the magnetic field at infinity is zero, a physically real scenario. Various models made use of symmetry by applying one type or the other as a boundary condition along the surface of symmetry. The boundary conditions are chosen so that the magnetic field is either perpendicular (for symmetric boundaries) or parallel (for anti-symmetric boundaries) along the surface of symmetry. Here, symmetry refers to the source of magnetic energy, which is the current density in the transmitting coils.

7.2.4 Apply Mesh

Once the properties have been input, the model needs to be meshed. Meshing is the procedure whereby the geometric model is broken into the smaller finite elements. The electromagnetic equations, subject to source and boundary conditions, are solved within each of these finite elements. The program will automatically mesh the regions. A finer discretisation in areas of interest can be obtained through user input. Several rules should be followed. First, for conductive material, the element depth size at the surface should be on the order of one-half the skin depth. Skin depth, δ, is defined as

$$\delta = \sqrt{\frac{2}{\omega\sigma\mu}} \tag{16}$$

Larger elements in these regions can lead to higher errors in the solution. For the munition (iron), the element size should be about 3×10^{-5} meters deep for problem frequencies of 200 kHz. Second, mesh refinement techniques can be used to further discretize the model and provide a more accurate solution in certain parts of the model.

Error analysis results can indicate whether or not additional mesh refinement is necessary. For the models in this analysis, an error due to the size of the elements with respect to the model was less than two percent within the regions of interest. On a global scale, the error was kept to less than five percent. This error refers to only the error associated with the size of the element. Error due to geometric or material variations was not included.

Most two-dimensional models required between 100,000 and 200,000 elements. The Vector Fields program will automatically generate a mesh for the problem based on input from the user. The mesh generator typically takes several minutes per mesh. The program also includes a mesh refinement program to help reduce error.

Figure 91 shows good examples of the mesh used for these models. The left figures show the geometry with scale in inches. The top figure set shows the tight mesh near the surface of the munition. The element size here is very small as dictated by the munition's electromagnetic skin depth. The elements just outside the munition are also small to take into account the rapidly changing flux density in this area. The center set of figures shows the mesh near the transmitting coil. Here the elements are somewhat

larger. The bottom set shows the mesh in a groove with an EM tag. Again, the elements must be very small so that rapidly changing flux densities in and near the munition can be calculated correctly. In all cases the mesh densities were sufficient to yield an error less than two percent in the region of interest.

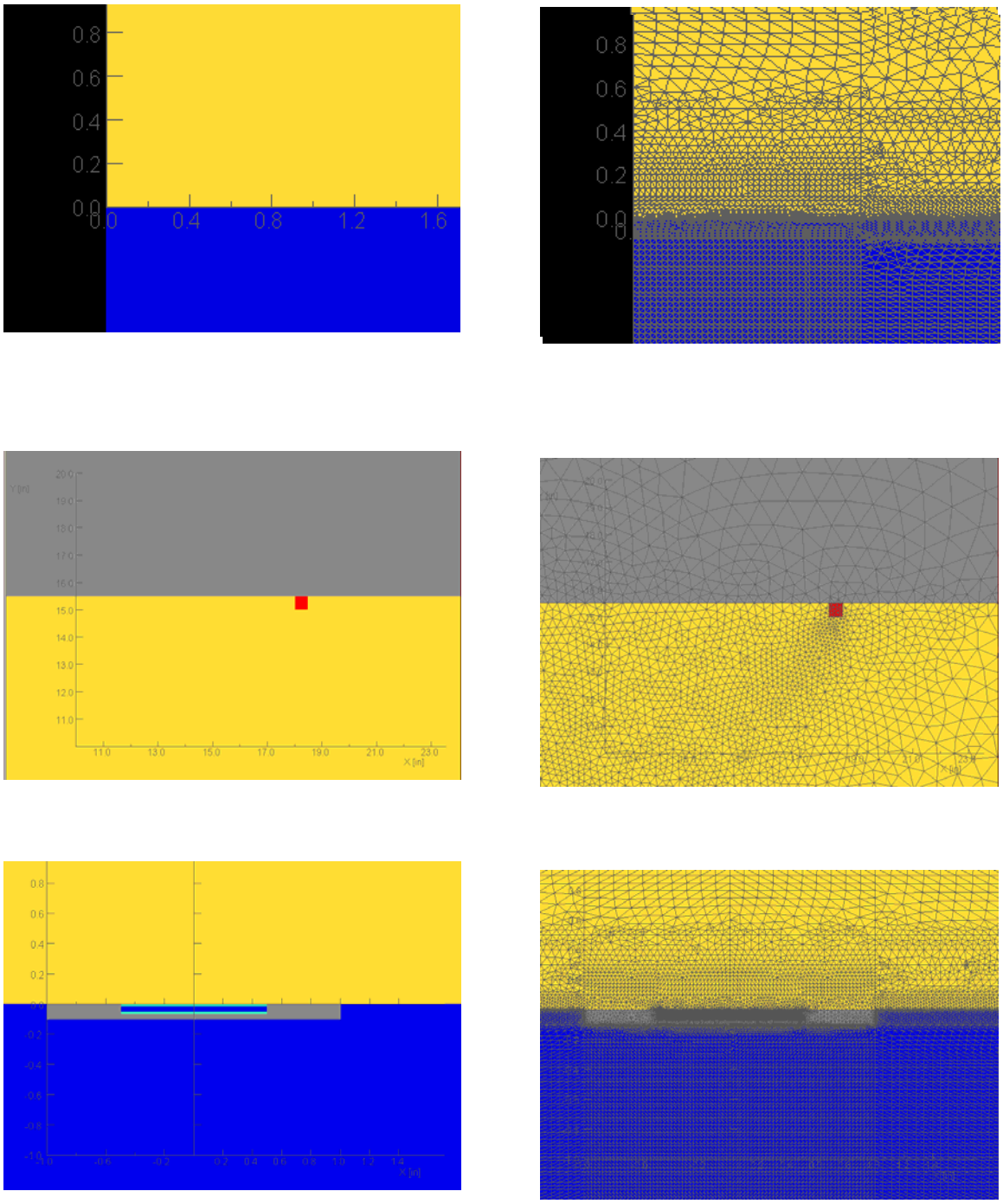

Figure 91. Examples of Mesh near the munition surface (top), the transmitting coil (center), and the munition groove and EM tag (bottom). These meshes yielded errors less than two percent in the regions of interest.

7.2.5 Solve Problem

The basic solution required for our problem type is the steady state AC field. We either have a transmitting coil or a transceiver coil transmitting a magnetic field at some predefined frequency. There is no radiating EM field as with an antenna. Therefore, the general equation solved is Equation (15).

$$-\nabla \cdot \frac{1}{\mu} \nabla A_C = J_C + J_V - i\omega\sigma A_C \tag{17}$$

The finite element technique is used to calculate the magnetic vector potential, *A*, at every element node within the model. For two-dimensional models, the magnetic vector potential is a single component, i.e., a scalar, pointing into the model, and for three-dimensional models, a three-component vector.

Once the magnetic vector potential is known, the magnetic and electric fields and all quantities based on such as measured signals can be calculated. The magnetic field is the curl of the vector potential.

$$\mathbf{B} = \nabla \times \mathbf{A} \tag{18}$$

The electric field is given by:

$$E = -\frac{\partial A}{\partial t} = -i\omega A \tag{19}$$

For two-dimensional problem, the magnetic flux is contained within the plane of the model. The electric field is parallel to the magnetic vector potential. The magnetic and electric fields are orthogonal.

It should be noted that when using axisymmetric models, an axisymmetric modified vector potential is preferable. This potential is defined a *rA*, where *r* is the radial coordinate. This modification allows a more accurate solution near the $r = 0$ axis of symmetry. The equations solved are identical with *A* replaced by *rA*. In solving for the magnetic field, an adjustment is then taken in the axisymmetric curl equation for *B* and differential equation for *E*.

The results can be calculated in any set of units the user wishes. Because of how the source coils were defined, the results will be in *unit* per amp-turn. Therefore, a calculated flux of 1 Tesla is actually 1 Tesla per amp-turn. The result is linear with the number of amp-turns in the source coil.

Normal solving times per two dimensional model case varied between 15 and 30 minutes using a Pentium-based PC with a clock speed of 2.8 GHz and running Windows 2000. RAM of at least 512 Mbytes is required. For three-dimensional models, element number is generally limited to 400,000. Typical solution times are on the order of several hours, although certain more detailed models may take as long as ten hours to solve.

7.2.6 Calculating Signals

The signals received by the EM tags or the receiver coil are a function of the magnetic fields in their respective areas and the receiver's geometric characteristics. The signal received by the EM tag or receiver depends on the magnetic flux linking the coil, *B*, the radian frequency, ω, the area of receiver linked by the flux, *A*, and the number of turns of wire (number of times flux is linked), *N*. If the coil is wrapped around a permeable core, relative permeability of μ, the effective permeability of the core must be taken into account. The effective permeability depends on the relativity permeability and the length-to-diameter ratio of the core. Note, only the flux perpendicular to the coil defined area is included.

$$\mathbf{S} \propto \mathbf{N} \int_{Coil} \frac{d\vec{\mathbf{B}}}{dt} \cdot d\vec{\mathbf{A}} = \mathbf{N}\mu_{eff}\mathbf{B}_0\omega\mathbf{A} \tag{20}$$

Equation (20) provides the induced signal in voltage (volts in SI units) per amp-turns of source coil. Remember, the model calculates flux density per amp-turn of constant current in the source coil. The equation is very good at predicting trends and optimizing the system for detection of signals. It works for both two- and three-dimensional models.

In the absence of any additional external circuitry connected to the receiver, equation (20) may be used to calculate the voltage induces in the windings. The actual signal will depend on the circuitry incorporated with the receiver coil. This additional factor is generally a unitless scalar multiplied by the value for **S**. Also, if a more precise calculation is required when using two-dimensional X-Y symmetry, the conversion factors discussed in the geometry section can be used for the magnetic field. This adjustment is only necessary when the absolute values of the signal are required, otherwise the trend and optimization predictions will be identical regardless.

To generate signals induced in the EM tags as a function of transmitting coil positions, model solutions for each relative coil position must be solved. This result was obtained by remodeling the coil position in 5-inch increments from centered to $\pm$30 inches, a total of 13 models per frequency. For each model, the flux that would link a specific EM tag at a given location on the munition could be calculated from the model's solution.

To generate signals induced in a receiver coil as transmitted by a specific EM tag required only one model per EM tag type, relative location, and munition orientation. A new model was required for each tag and groove geometry including relative location on the munition. This reduction in the number of models required is because the receiver coil need not be modeled. The field values, and so, the signal calculations, could be obtained at any point in the model.

8 Appendix B: 2006 ATC Test Plan

The following Test Plan Summary was sent to Aberdeen Test Center in 2006.

Battelle Buried Tagged Munition Surrogates Test Plan
SERDP Project MM-1272
U.S. Army Aberdeen Test Center

August 24, 2006

This document provides a brief summary of the testing and characterization activities performed at the Aberdeen Test Center (ATC) in 2005 and those to be conducted at ATC in the fall of 2006 on SERDP project MM-1272, *Enhanced Electromagnetic Tagging For Embedded Tracking Of Munitions And Ordnance During Future Remediation Efforts*.

Project Background
The detection of buried unexploded ordnance (UXO) at military firing ranges has proved to be very difficult and expensive. To enable the U.S. Department of Defense to conduct cost-effective training and research missions in the future, with increased safety for personnel and property and without negative environmental impact, significant advances in detection and identification of buried UXO must be pursued and implemented. To this end, Battelle investigated the potential for incorporating electromagnetic tags on future ordnance items as aids to locating buried UXO in the ground with a very high probability of detection and a near-zero false alarm rate. Current focus is on the potential for state-of-the-art passive RFID tags operating near 125 kHz to provide information on the munitions' location, and be compatible with operational and tactical deployment. The tag provides discrimination between UXO and clutter items, which is critical in reducing the cost of UXO remediation.

With these tags, the transmitted energy from the Interrogation Module powers the tag's integrated circuit and the tag replies with a digital signal. The Interrogation Module's receive coil senses the digital signal and reports the existence of the tag and embedded digital data, which might include the munition type, date of manufacture, etc.

Tag Description: The tags being considered will be fastened to the exterior of the candidate ordnance item during the manufacturing process. They must survive the munition's launch, ground impact, and terrain penetration when the item does not explode. The Battelle concept envisions the buried tag responding to and then signaling the UXO Tag Interrogation Module when the detection system is brought above or near the buried UXO item. Two examples of these tags are shown in Figure 1. The left picture shows the Texas Instruments' solenoid tags. These tags comprise a copper coil with 500 turns wrapped around a ferrite core, other circuit elements, and a digitally-based integrated circuit that functions as a receiver, transmitter, and processor with 64 bits of user-written data. A similar tag used for non-contact facility access applications was also investigated. This tag is shown in the right picture of Figure 1. It has the pancake coil design.

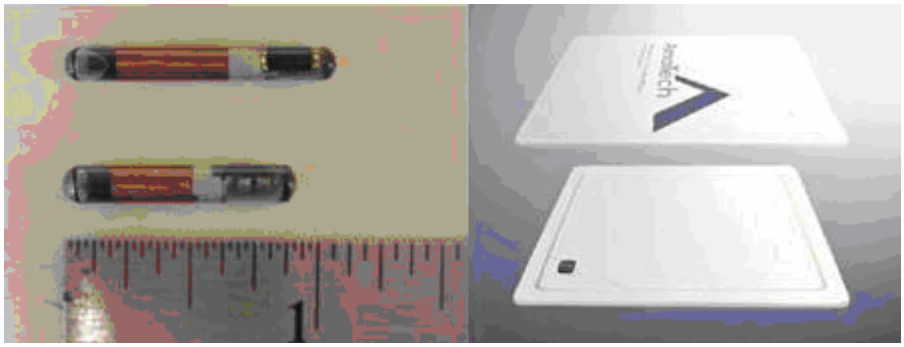

Figure 92. Solenoidal tags on the left and "pancake" tags on the right

2005 Testing at the Aberdeen Test Center

Battelle personnel traveled to Aberdeen Proving Ground and performed the search for the buried targets the week of November 2005. Testing took place only on November 1. Battelle performed analysis of the data on November 2 and reported its predicted positions that day. ATC provided the location and depth information of the buried objects after Battelle placed flags in the soil predicting the positions.

Battelle's analysis and decision-making processes were not optimum. We had not anticipated multiple buried objects being sensed simultaneously, which occurred because the surrogates were buried in a fairly small area. (The sensing of multiple tags is a realistic situation, but it had not been anticipated nor investigated in the lab.) The multiple simultaneous detections and the fact that we had not used a coil module with three receive coils previously led to confusion and difficulty making decisions. Battelle's predicted positions were marked with flags. After Battelle left ATC personnel surveyed the flags and reported the actual positions of Battelle's predicted target locations. A plan view of the test grid is shown in Figure 93. The results are included in Table 8.

Battelle predicted the positions of eight buried tagged surrogates. As stated previously, nine tagged surrogates were sent to ATC but the actual number buried was unknown to Battelle.

One tagged surrogate was missed completely. The missed surrogate, which was buried three feet below the surface, is shown in Figure 74 at position (0.5, 2.5). It is described as Tagged Surrogate number 3 in Table Table 52 with the description "Tagged surrogate parallel to the surface with the *tag down*[9]. The untagged surrogate was six inches above and parallel to the tagged surrogate." The Figure shows a data set was taken directly over the missed surrogate. After Battelle provided its predictions and ATC supplied the actual positions, we examined the data set taken at (0.5, 2.5) to see if the tag's signal existed in the data set. In fact, the tag's signal was very strong. One has to ask the question as to why it was not reported to ATC when it was clearly evident in the data set. Battelle concludes that our analysis and decision-making processes were flawed. We thought the signal was coming from the tag we predicted at position (1.2, 3.2).

[9] The phrase "tag down" implies the tag's position on the surrogate is underneath the item, as far from the surface and the coil module as possible and in the untagged surrogate's shadow.

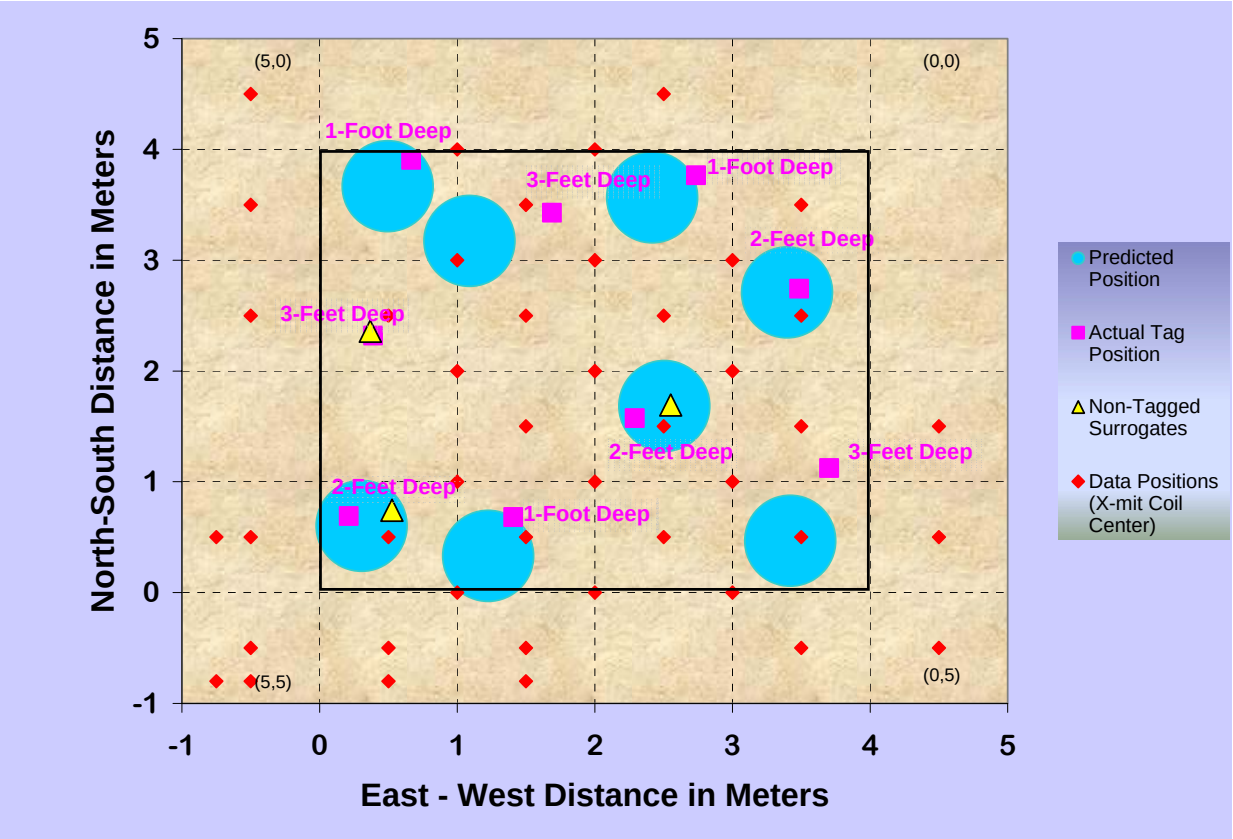

Figure 93. Plan view of the test grid at Aberdeen Test Center showing the actual tagged munition positions, Battelle's predicted positions, and the positions where Battelle acquired data

Table 8. Burial characteristics of the surrogates at Aberdeen Test Center in 2005

Placement					Detection		
Number	Easting	Northing	Depth (feet)	Dip (degrees)	Pin Number	Easting	Northing
1	34.666	57.905	1.0	0	1	34.496	57.667
2	37.485	56.743	2.0	0	2	35.089	57.174
3	34.389	56.319	3.0	0		Not Detected	
4	35.407	54.681	1.0	45	3	36.417	57.567
5	36.290	55.574	2.0	45	4	37.398	56.709
6	37.704	55.123	3.0	45	5	36.505	55.683
7	36.736	57.767	1.0	90	6	34.306	54.601
8	34.212	54.690	2.0	90	7	35.226	54.331
9	35.689	57.428	3.0	90	8	37.420	54.467
A	34.369	56.359	2.5	0			
B	36.551	55.692	2.0	45			
C	34.526	54.743	2.0	90			

Notes: Color coding pairs tagged and untagged surrogate combinations.
Pin (flag) numbers were manually associated with the closest surrogate.

2006 Testing at the Aberdeen Test Center

Aberdeen Test Center has invited Battelle to participate in further evaluations at their testing facilities where independent testing can be achieved and more valuable date can be acquired. To this end, Battelle is submitting this Test Plan.

For the buried tag investigation, Battelle has provided ATC with nine tagged munition surrogates and three untagged munitions surrogates that are to be buried near the munition surrogates.

Blind Detection Tests

Battelle requests that ATC provide one single marked test lane that is three feet wide. Nine tagged surrogates will be buried with nearest-neighbor surrogates being separated by at least two meters. The surrogates will be buried at depths of one, two, or three feet below the surface. At least two surrogates will be in a vertical orientation and two will be in a horizontal orientation. The others will be at angles determined by ATC. Three of the tagged surrogates will have a second surrogate buried near them. The positions and orientations of these surrogates will be determined by ATC but the tagged surrogate and its untagged neighbor will be at least 10 cm apart. Table 2 provides further details.

Table 2. Buried tag details

Buried Tagged Surrogate	Depth (feet)	Dip (degrees)	Untagged Surrogate	Other Conditions
1	1	0		Tag on top
2	2	0		Tag on top
3	3	0	1	Tagged surrogate parallel to the surface with the tag down. Untagged surrogate 6-in above and parallel to the tagged surrogate.
4	1	45		Tag up toward ground surface.
5	2	45	2	The untagged item is 1-foot to the side, parallel, and at the same depth as the tagged surrogate.
6	3	45		Tag up toward ground surface.
7	1	90		Tag up toward ground surface.
8	2	90	3	The untagged item is 1-foot to the side, parallel, and at the same depth as the tagged surrogate.2
9	3	90		Tag up toward ground surface.

Note: Item depth is measured to the center of the minor axis for horizontal targets and the midpoint of the major axis for the inclined and vertical targets.

Buried Tags: Q&A From 2005 Buried Tag Test Plan

ATC Question: Where / how should the depth measurements be taken? To tag, to surrogate midpoint, of particular concern is the angled items. Battelle answer: during the modeling effort, the depth was referenced to the center point of the surrogate so we would like to keep that definition.

ATC Question: Tag orientation in relation to the ground plain? Parallel, perpendicular, nearest or farthest i.e., tag up or down. Battelle answer: to minimize variables for items parallel to the ground surface have all tags on top - except - we would like our "worst case" item to be the following: surrogate parallel to the surface with the tag on the bottom of the surrogate at a depth of 3 feet, with an untagged surrogate directly above and parallel to the tagged surrogate 6 inches above the tagged surrogate.

ATC Question: Does it matter what compass heading the major axis of the item is orientated on?
ATC Recommendation: All should be consistently aligned to minimize variables. Battelle answer: the compass heading is not really a variable to us but it makes sense to have them all aligned north/south or east/west, or whatever direction you choose.

ATC Question: Depth and angle of untagged items?
ATC Recommendation: The untagged item should be parallel to, equidistant from, and at the same depth the tagged surrogate. Battelle answer: I described the worst case above that will employ one of the three untagged items, which matches your first two recommendations. The other two untagged surrogates should be placed as you describe in your recommendation. These two items should be 12 inches from the tagged surrogate.

ATC Question: On the angled items, is the tag at the deep or near-surface end? Battelle answer: place the tags at the deep end.

9 Appendix C: 2006 ATC Test Results

Data Plots from Aberdeen Test Center

This Appendix contains all the data plots taken at ATC in 2006. Figure 94 shows the data in a single plot with the data acquisition point in blue, magenta, and yellow. ATC's emplacement positions are numbered green circules and Battelle's estimated positions shown as red crosses. Figure 74 is repeated as Figure 95 to aid in identifying the location of the data sets in the test grid in the data plots shown in Figure 97 through Figure 191.

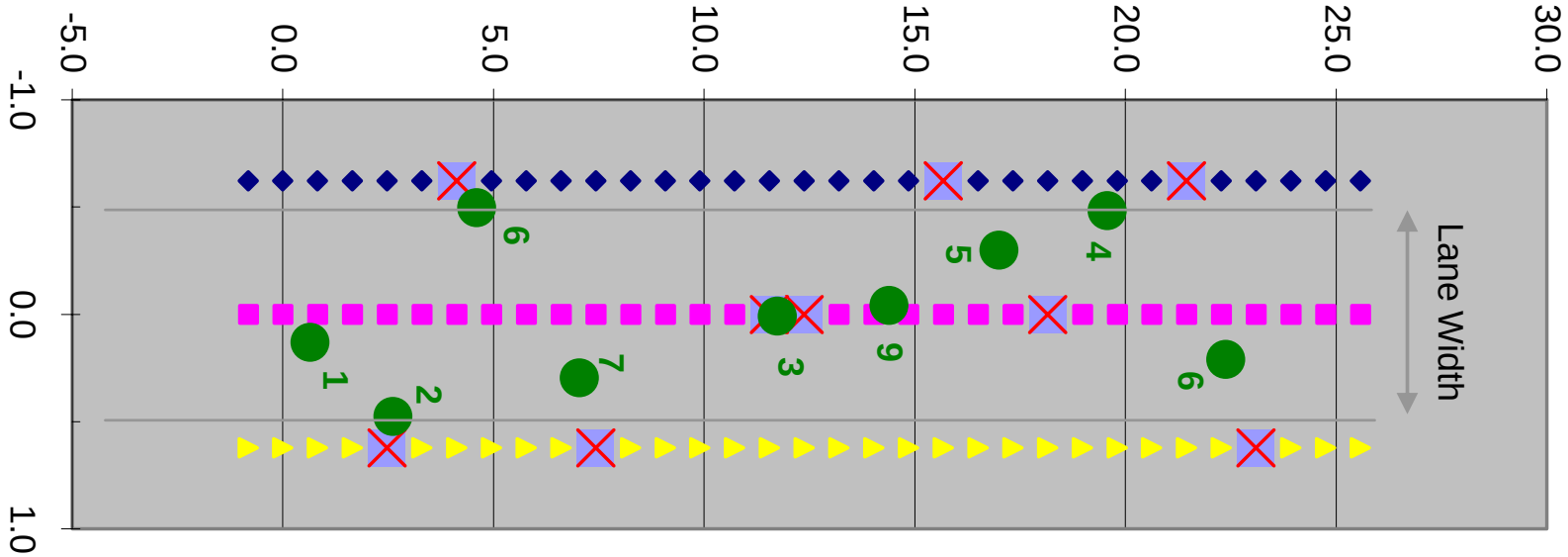

Figure 94. Plot of the test grid, emplacements by ATC (green numbered circles), and Battelle's estimated positions (red X symbols)

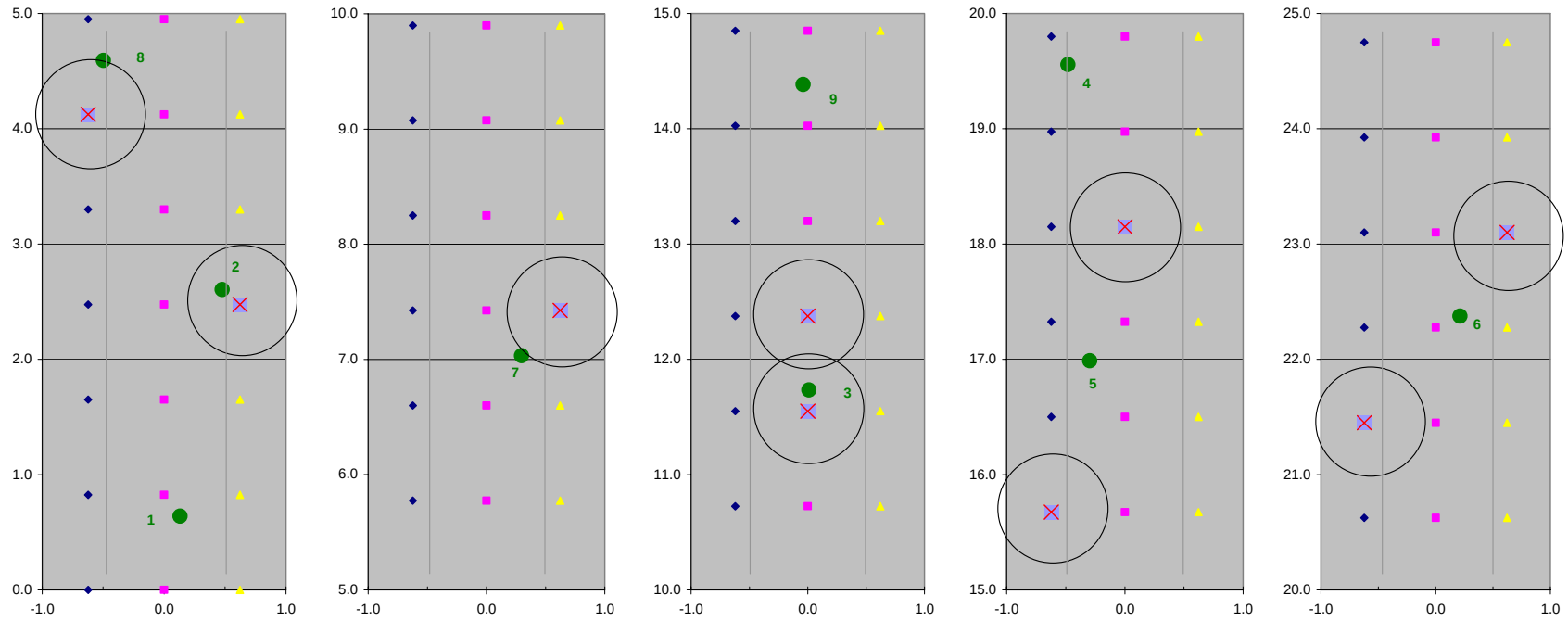

Figure 95. Plan view of the grid at ATC. The data acquisition positions are shown as blue diamonds, red squares, or yellow triangles. ATC emplacements are shown as numbered green circles and Battelle's estimates are shown with red X symbols inside 1-m diameter circles that symbolize the size of the resolution area of Battelle's estimates.

The following pages contain all the data sets taken at ATC in the form of screen captures from the oscilloscope. It is challenging to view all the data and make geometric sense of it. For this reason, each data set is shown at the top of the page and the grid of Figure 95 is provided below the data. A representation of the location of the coil module (depicted in Figure 96) is provided on the grid diagram to aid understanding of location information

A color computer display or high-quality color printout of these figures is necessary because the screen captures used color to identify the distinct waveforms from each of the three receive coils.

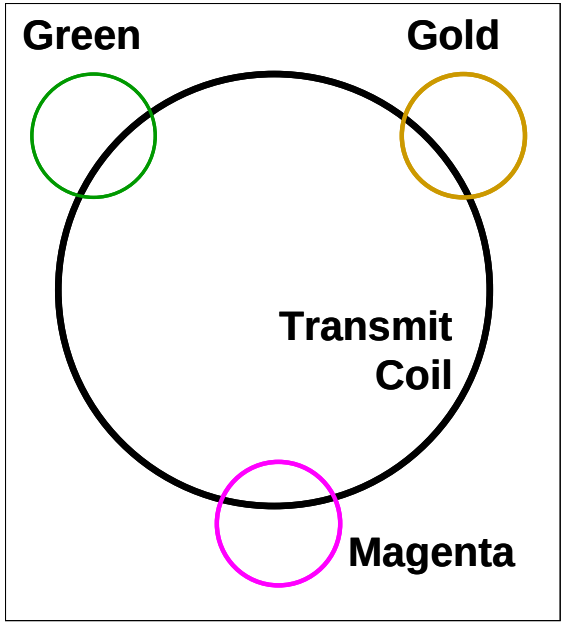

Figure 96. This drawing depicts the arrangement of the three receive coils in the above-ground coil module. The alignment of the coils is in the same heading as Figure 95. The colors of the receive coils match the colors in the data plots. Subsequent figures include this drawing positioned over the grid location where the data set was acquired.

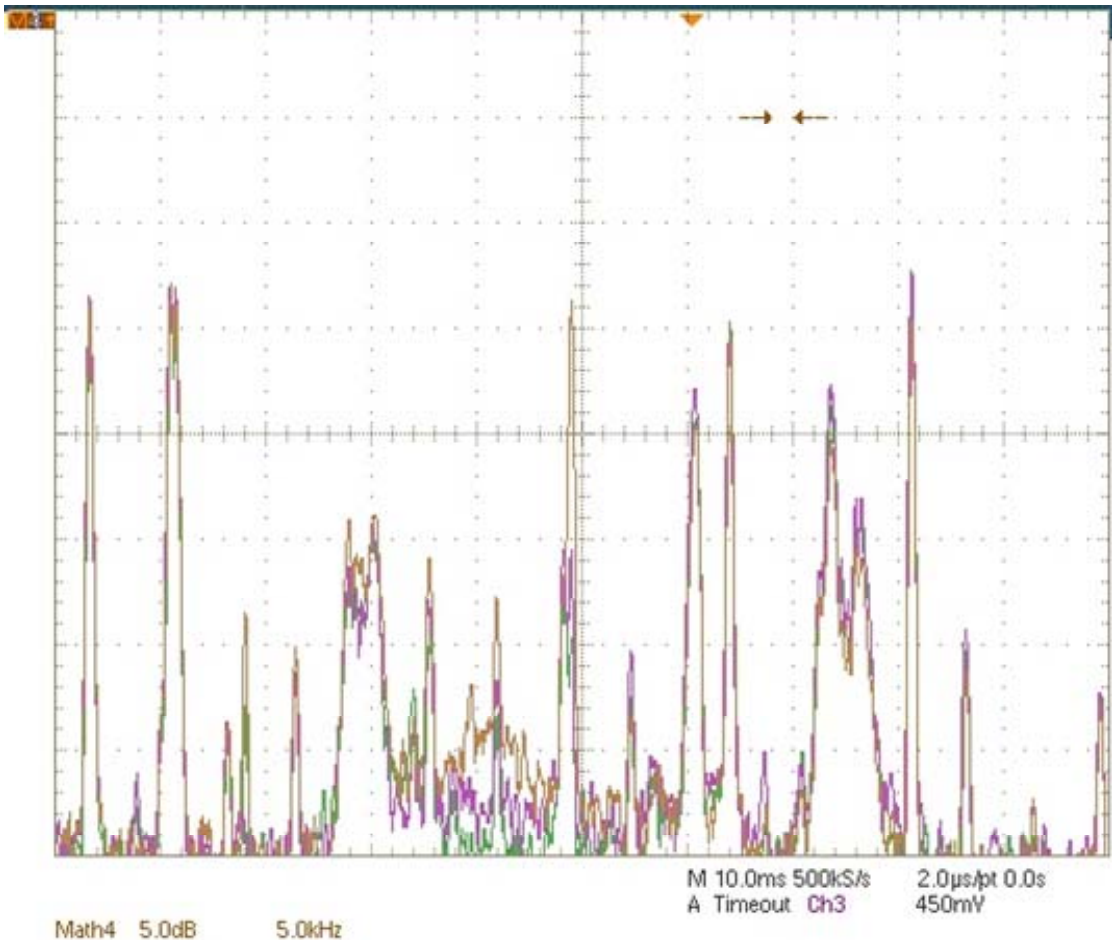

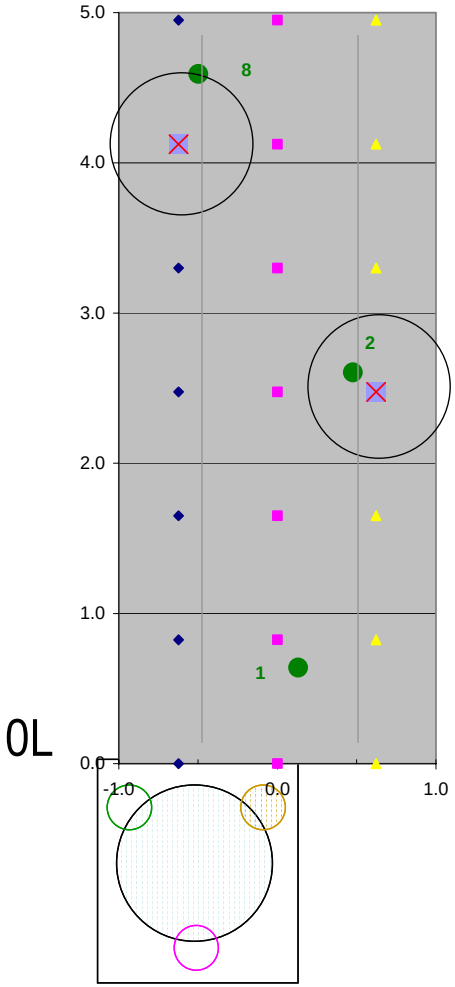

0L

Figure 97. Data taken at position (0, L)

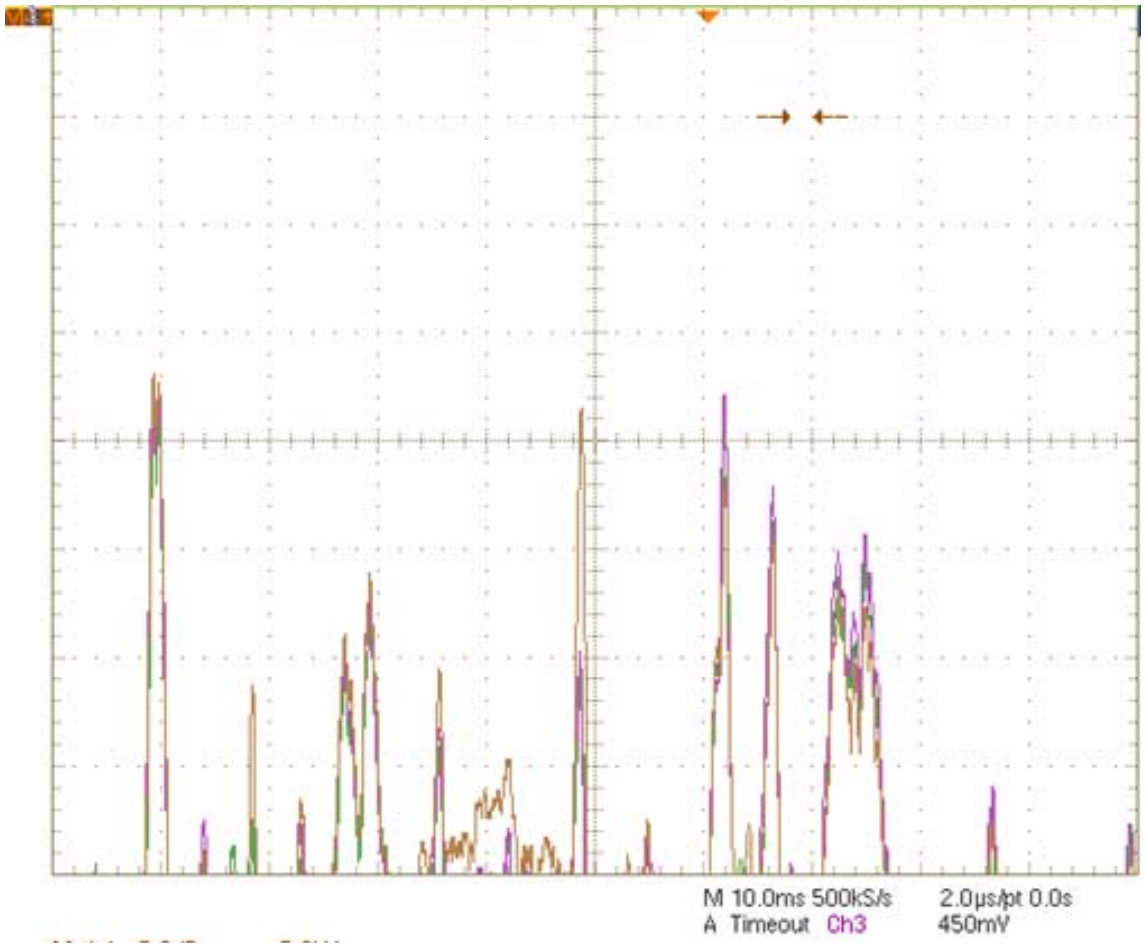

0

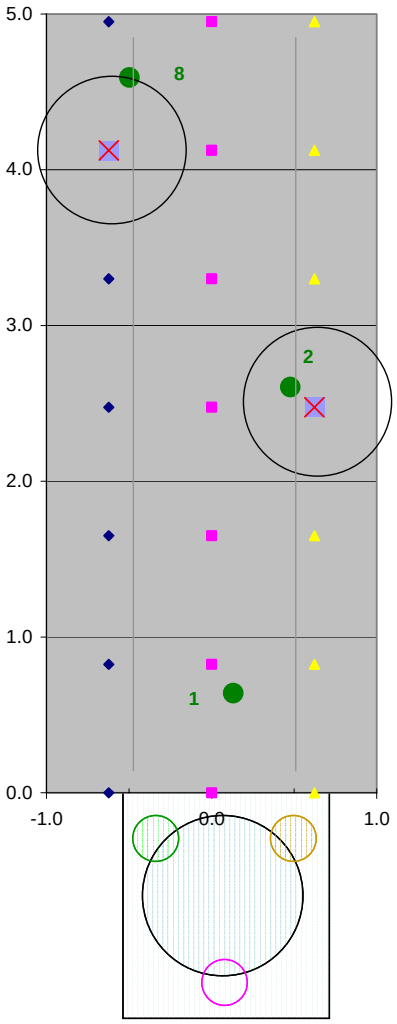

Figure 98. Data taken at position (0, C)

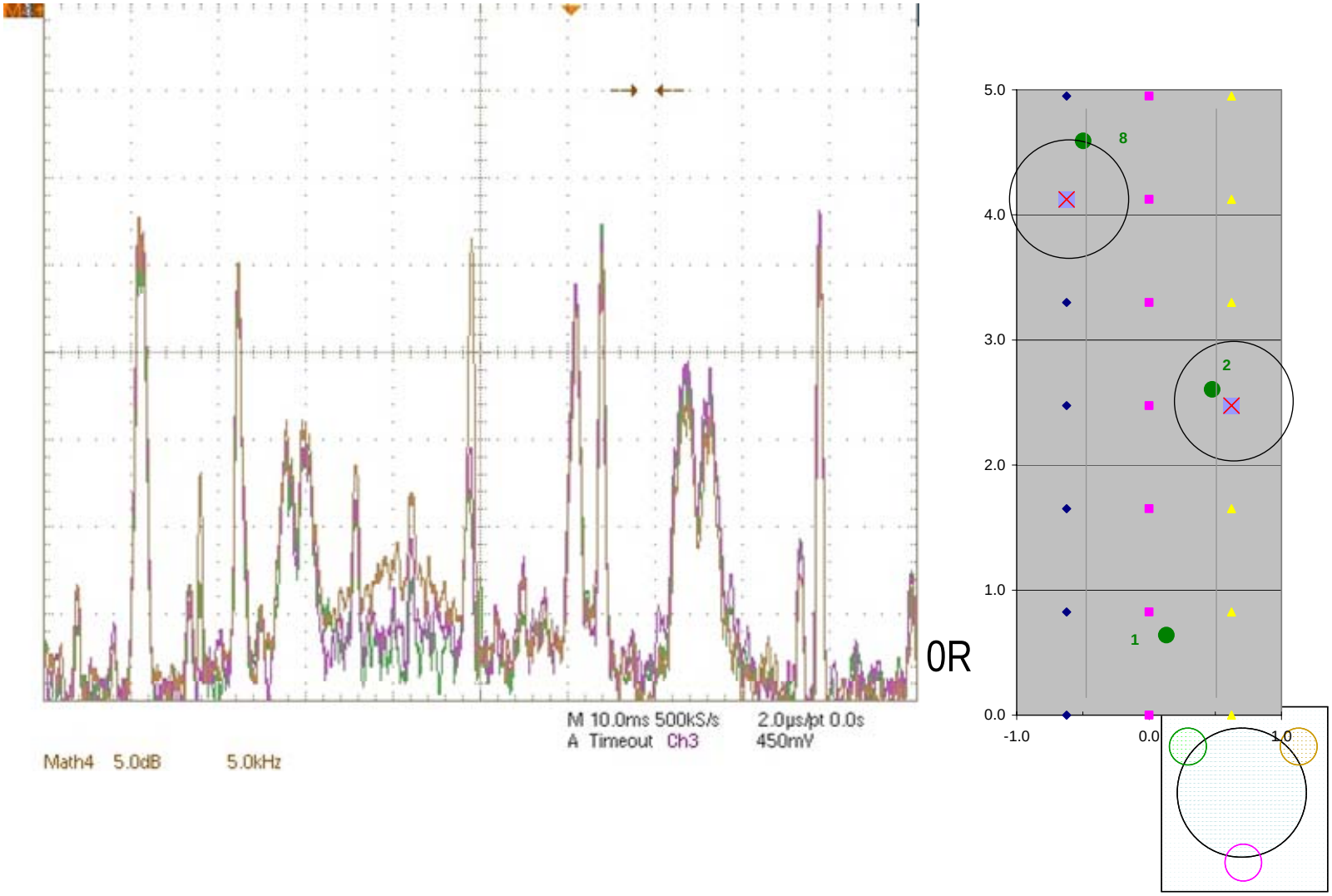

Figure 99. Data taken at position (0, R)

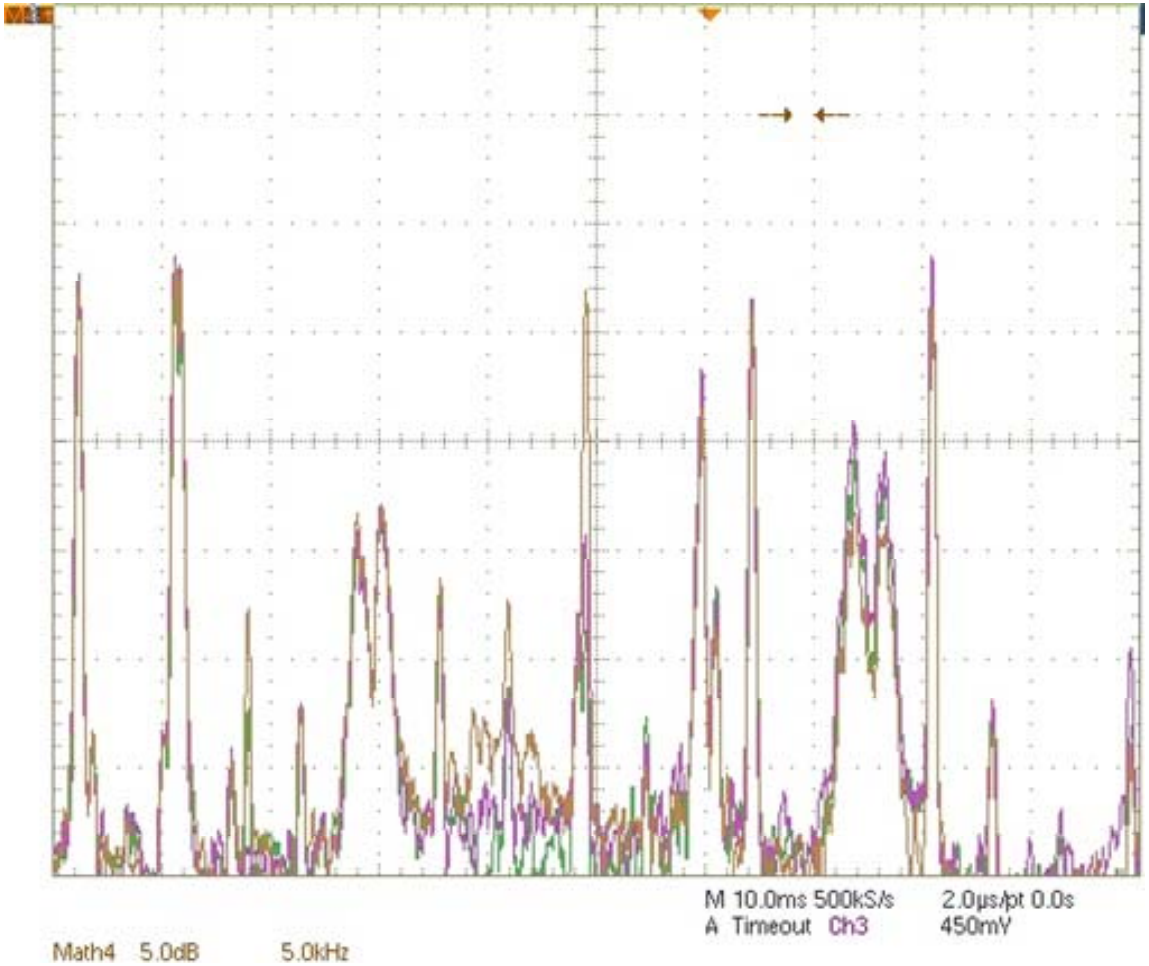

1L

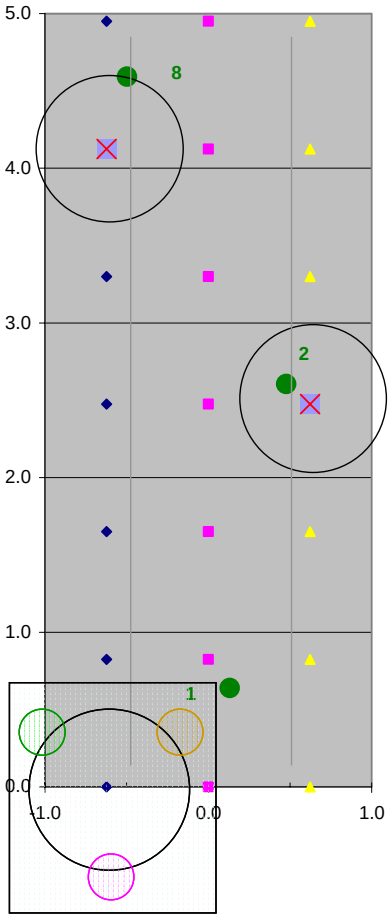

Figure 100. Data taken at position (1, L)

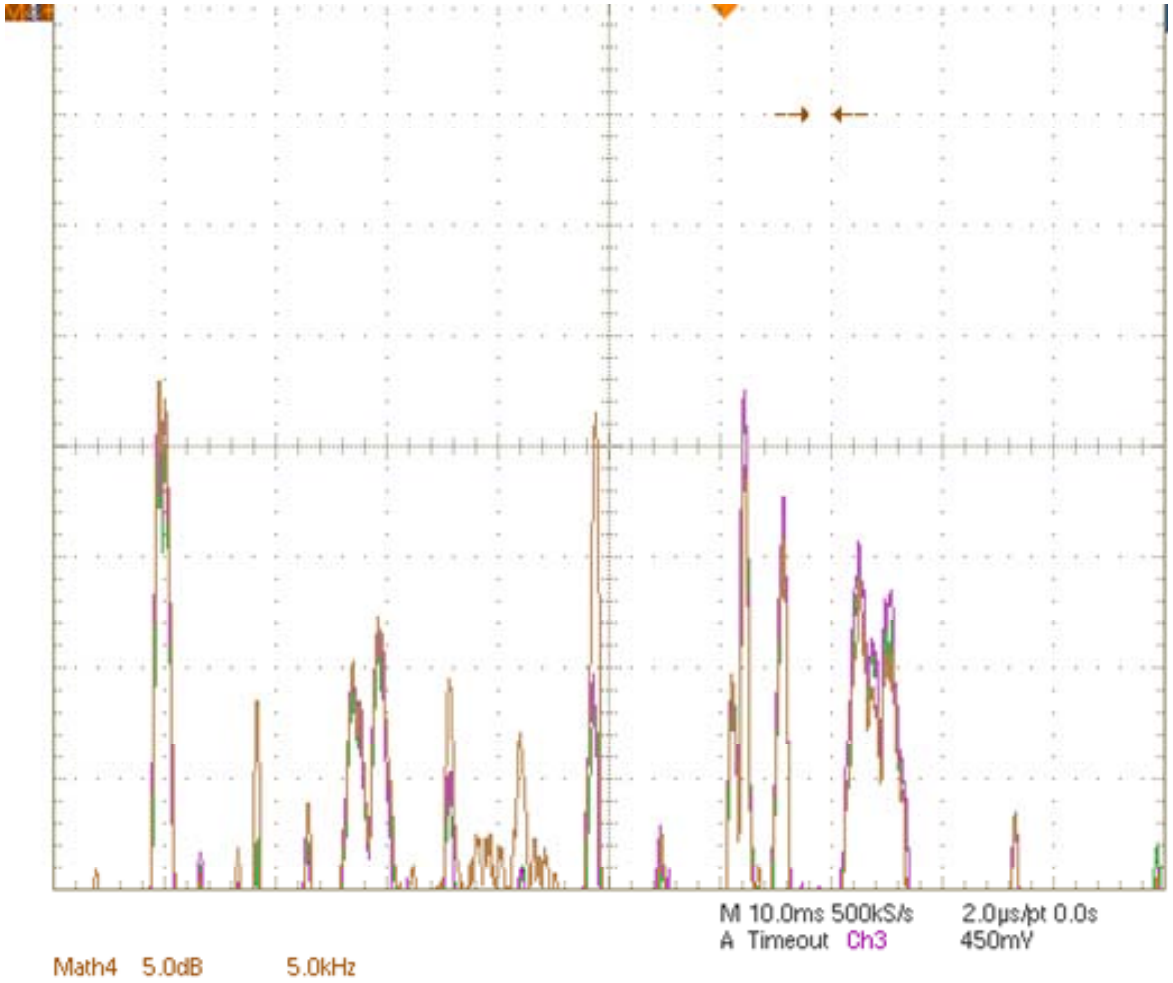

1

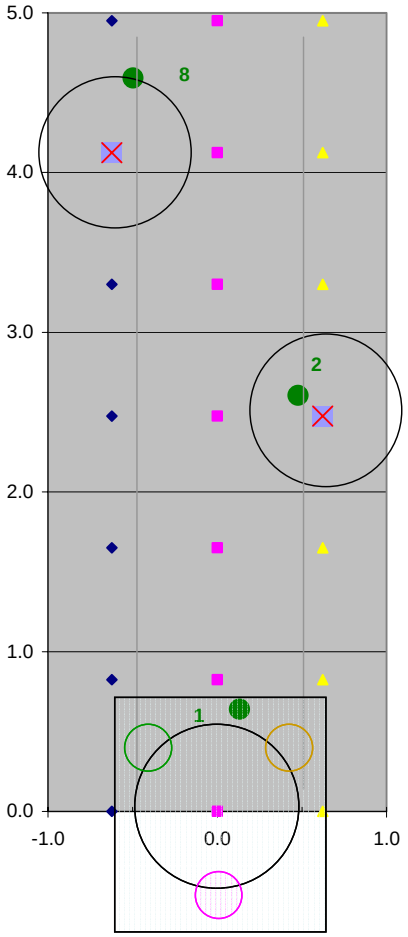

Figure 101. Data taken at position (1, C)

1R

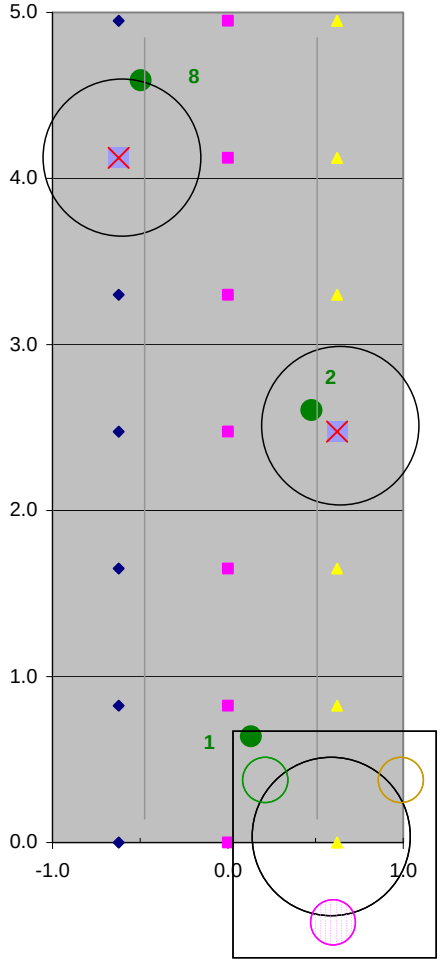

Figure 102. Data taken at position (1, R)

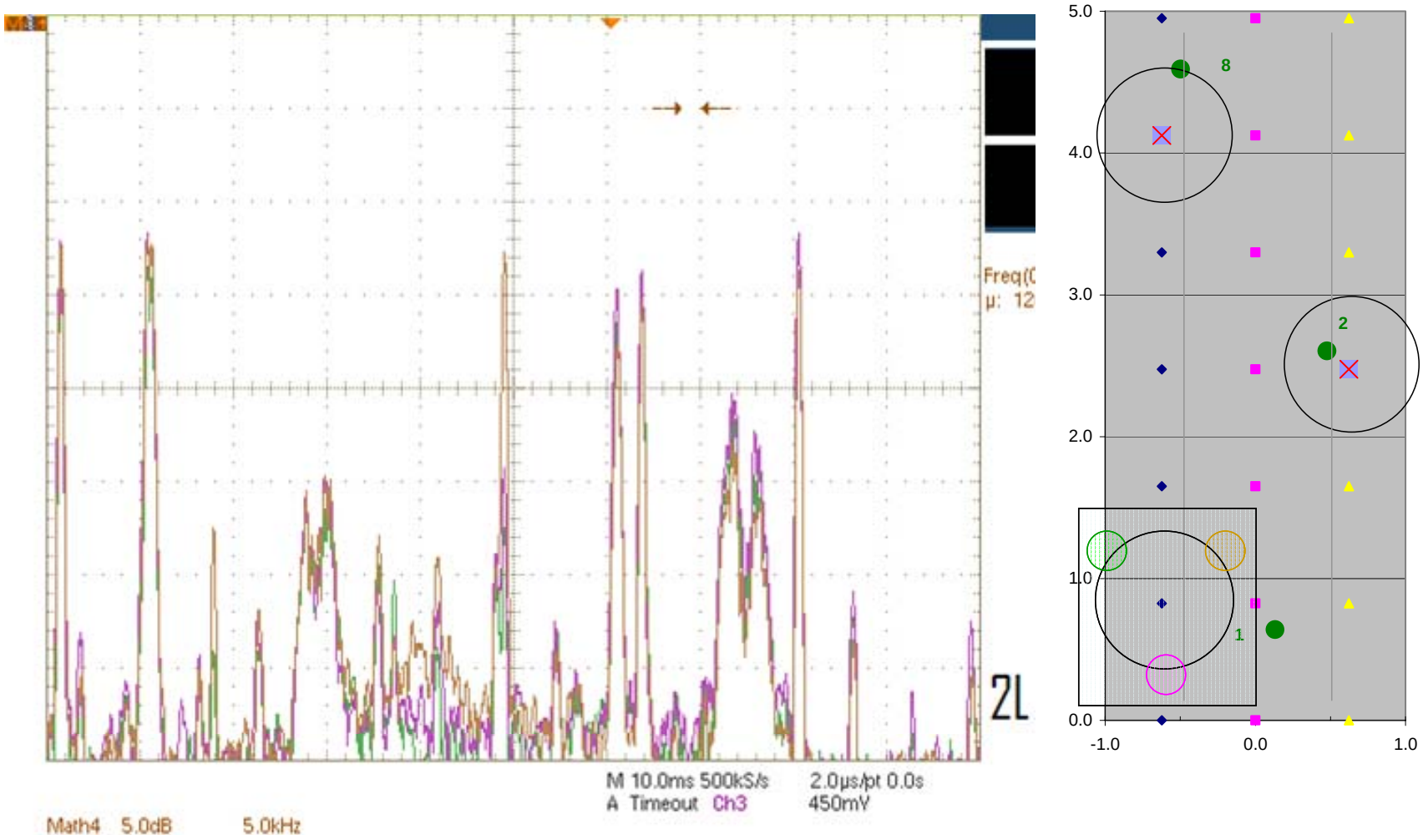

Figure 103. Data taken at position (2, L)

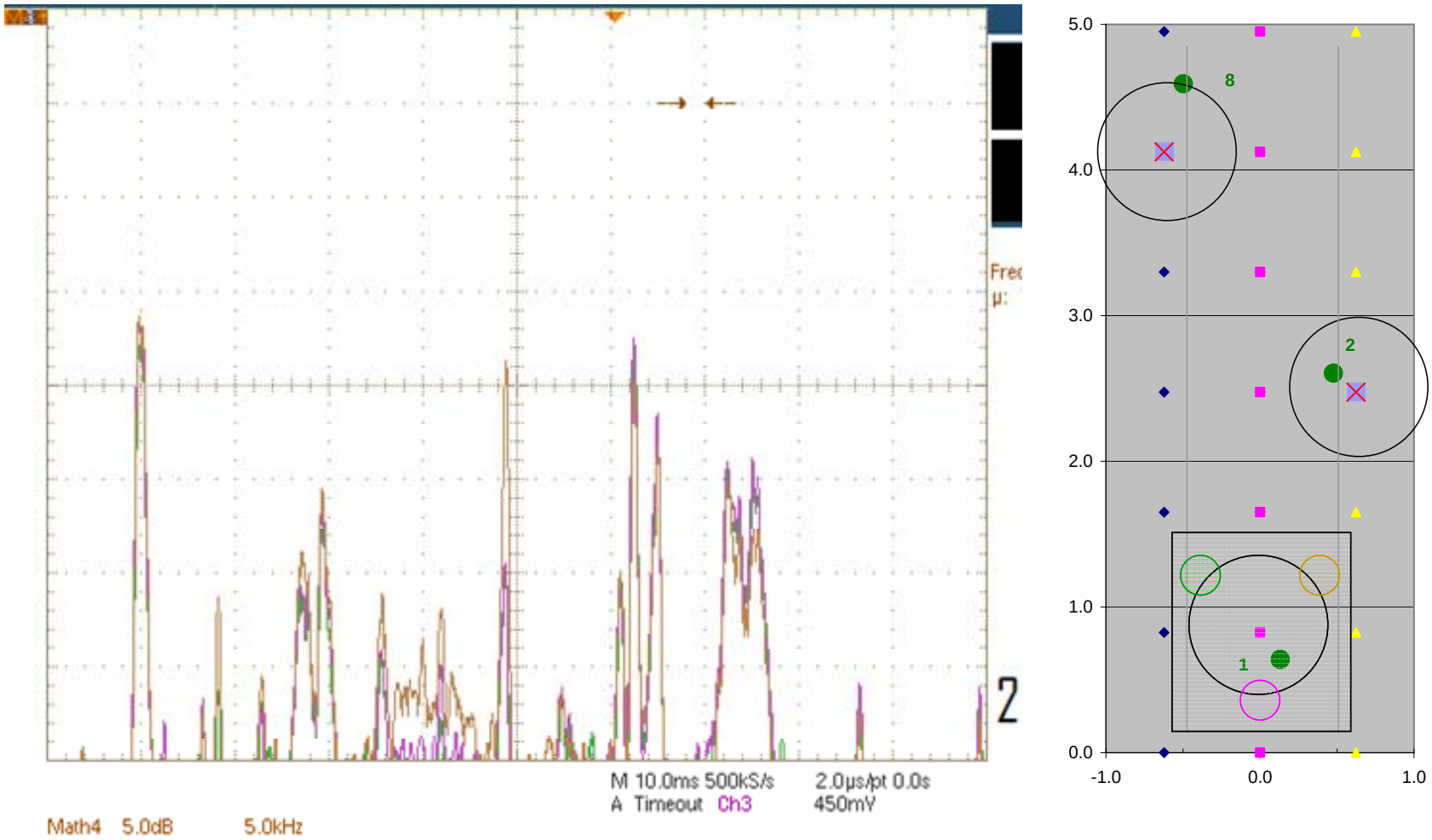

Figure 104. Data taken at position (2, C)

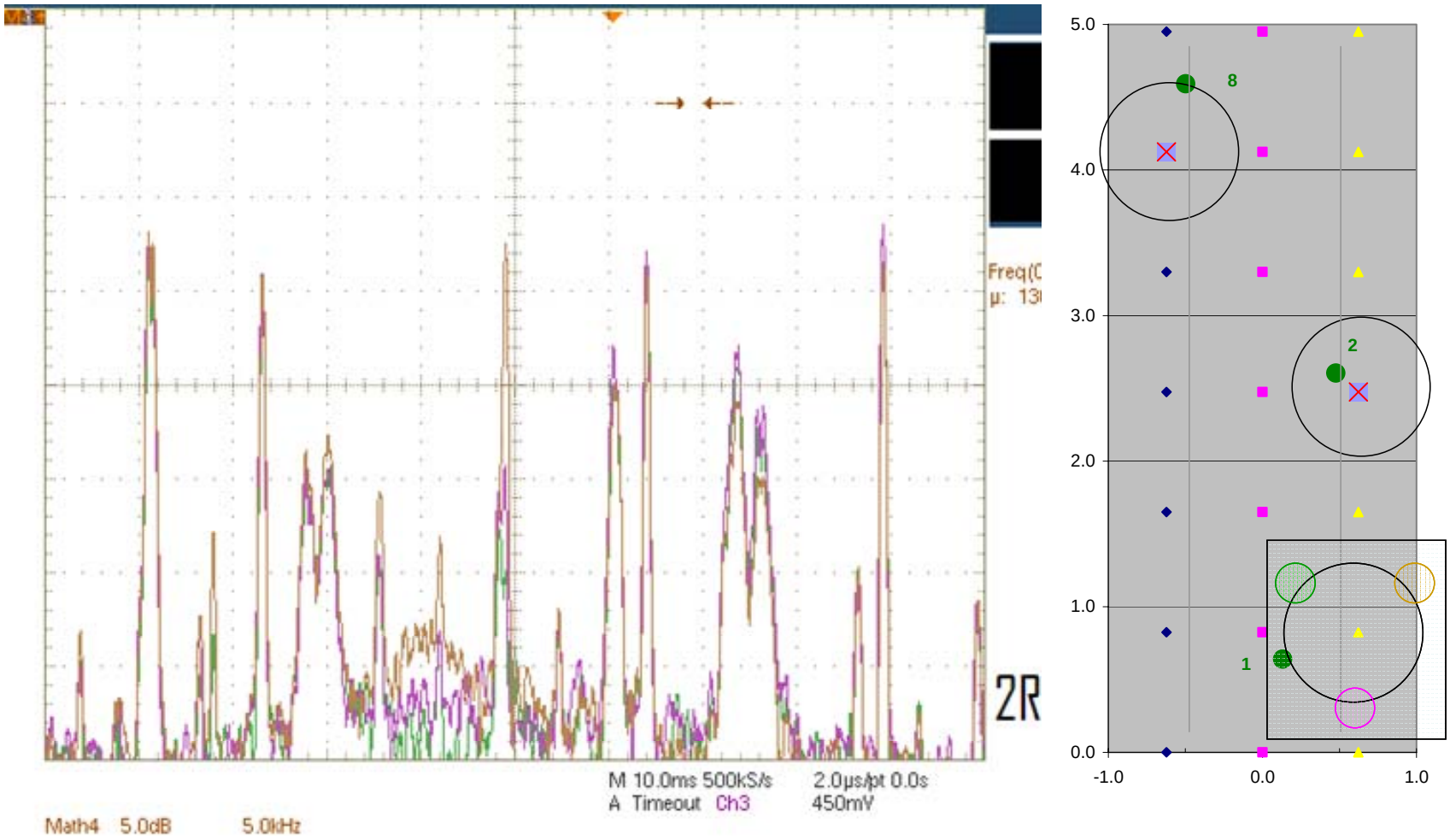

Figure 105. Data taken at position (2, R)

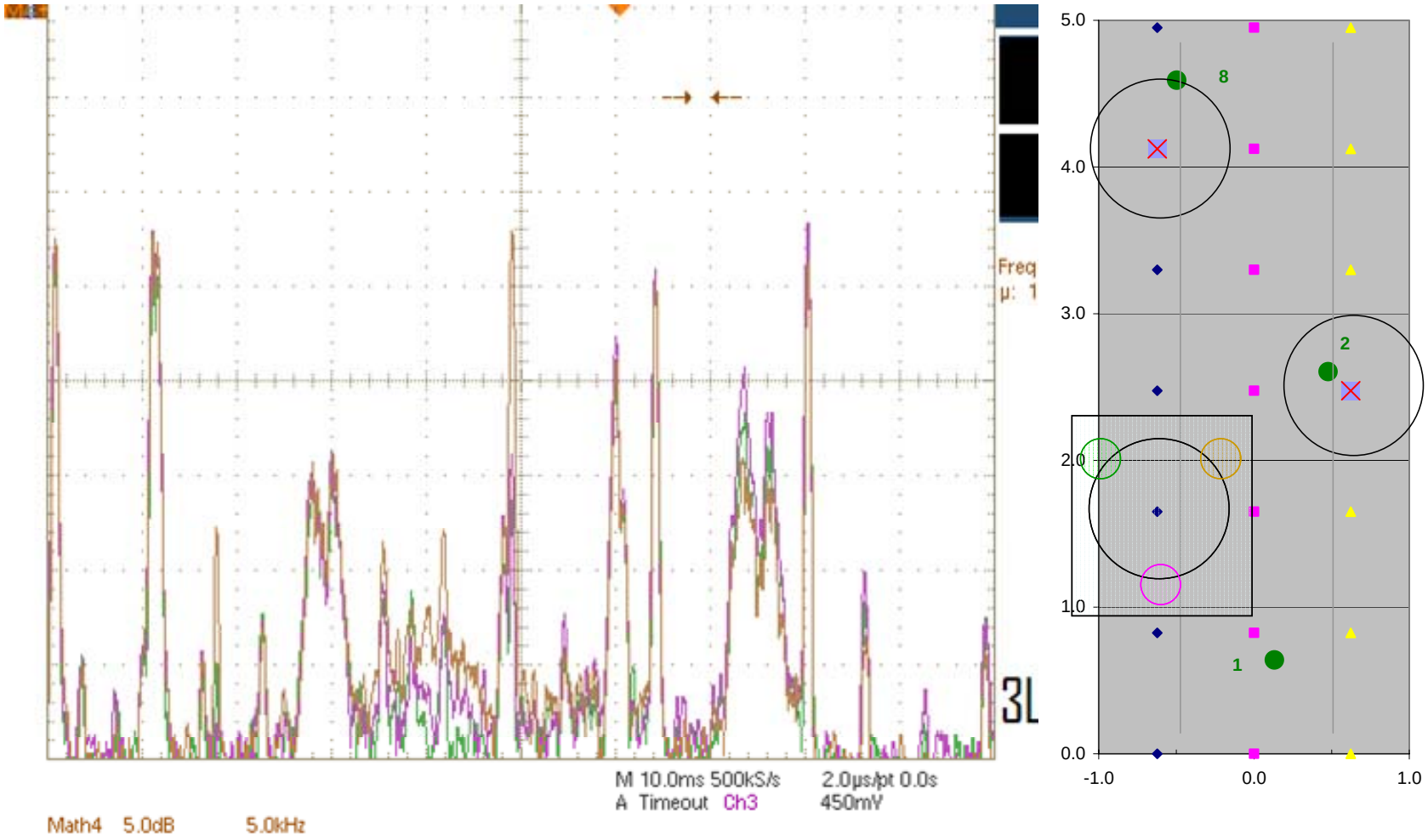

Figure 106. Data taken at position (3, L)

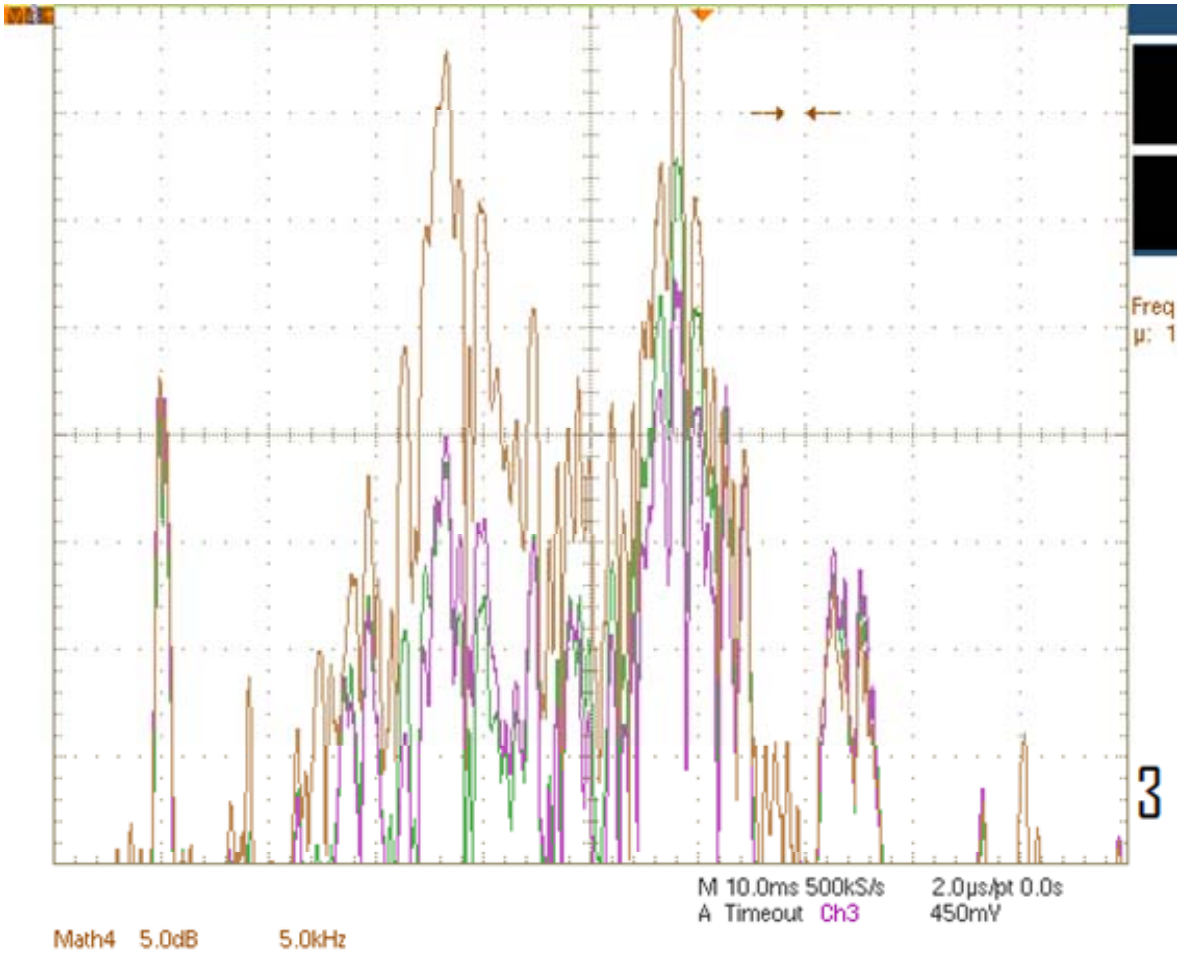

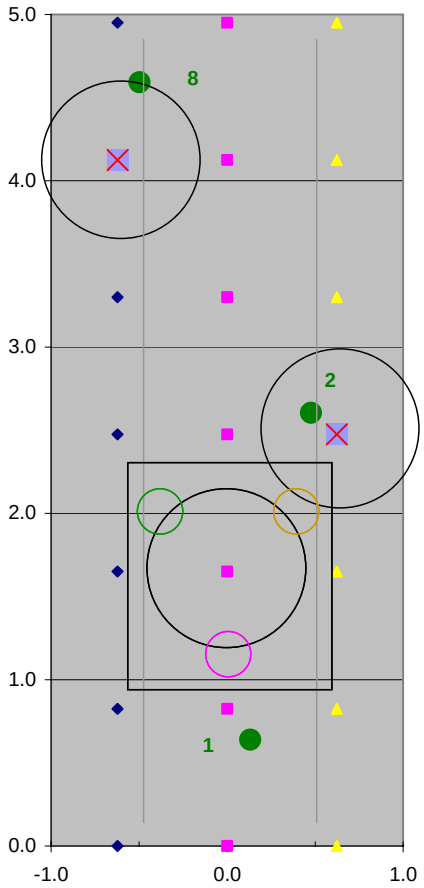

Figure 107. Data taken at position (3, C)

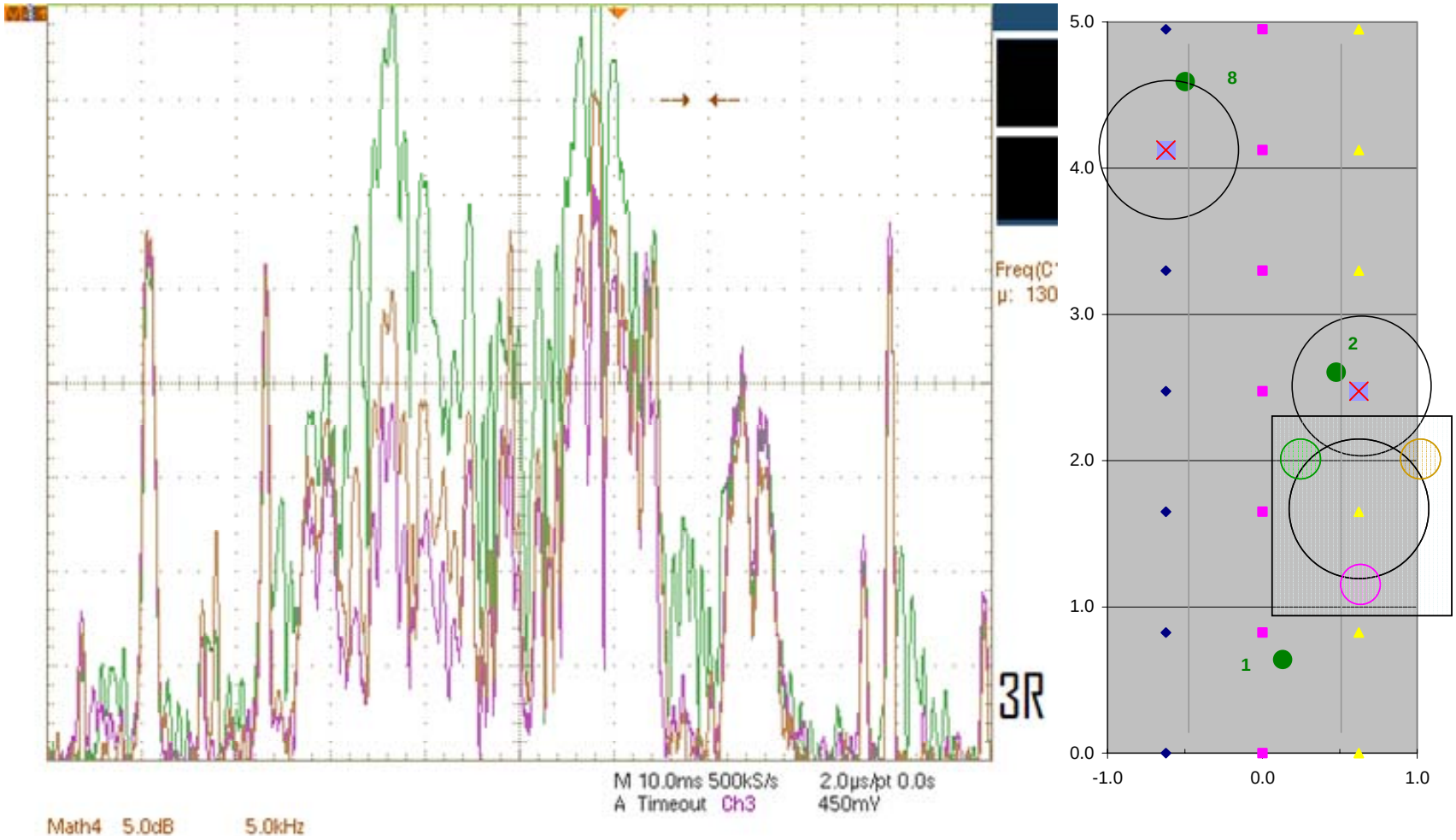

Figure 108. Data taken at position (3, R)

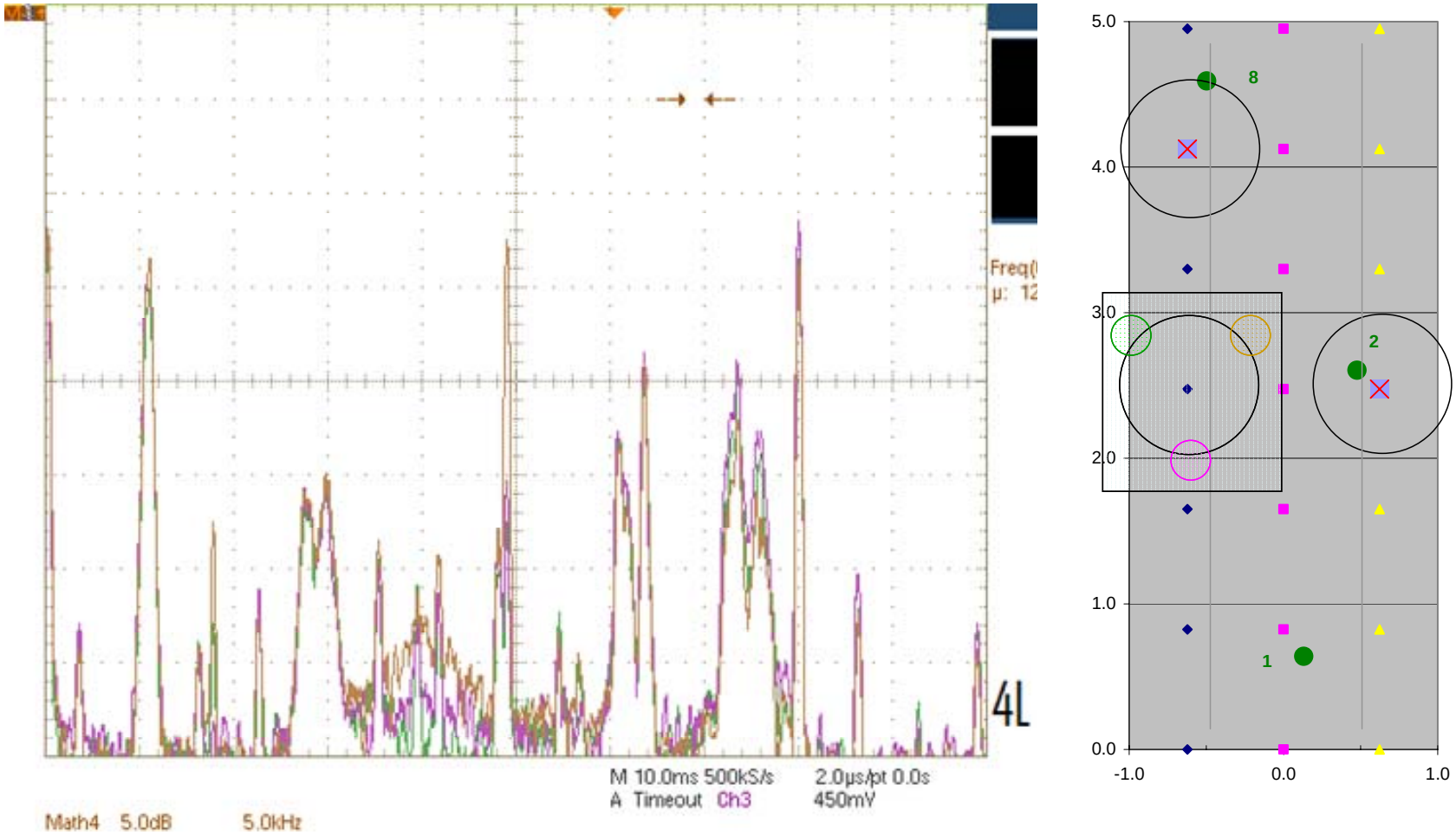

Figure 109. Data taken at position (4, L)

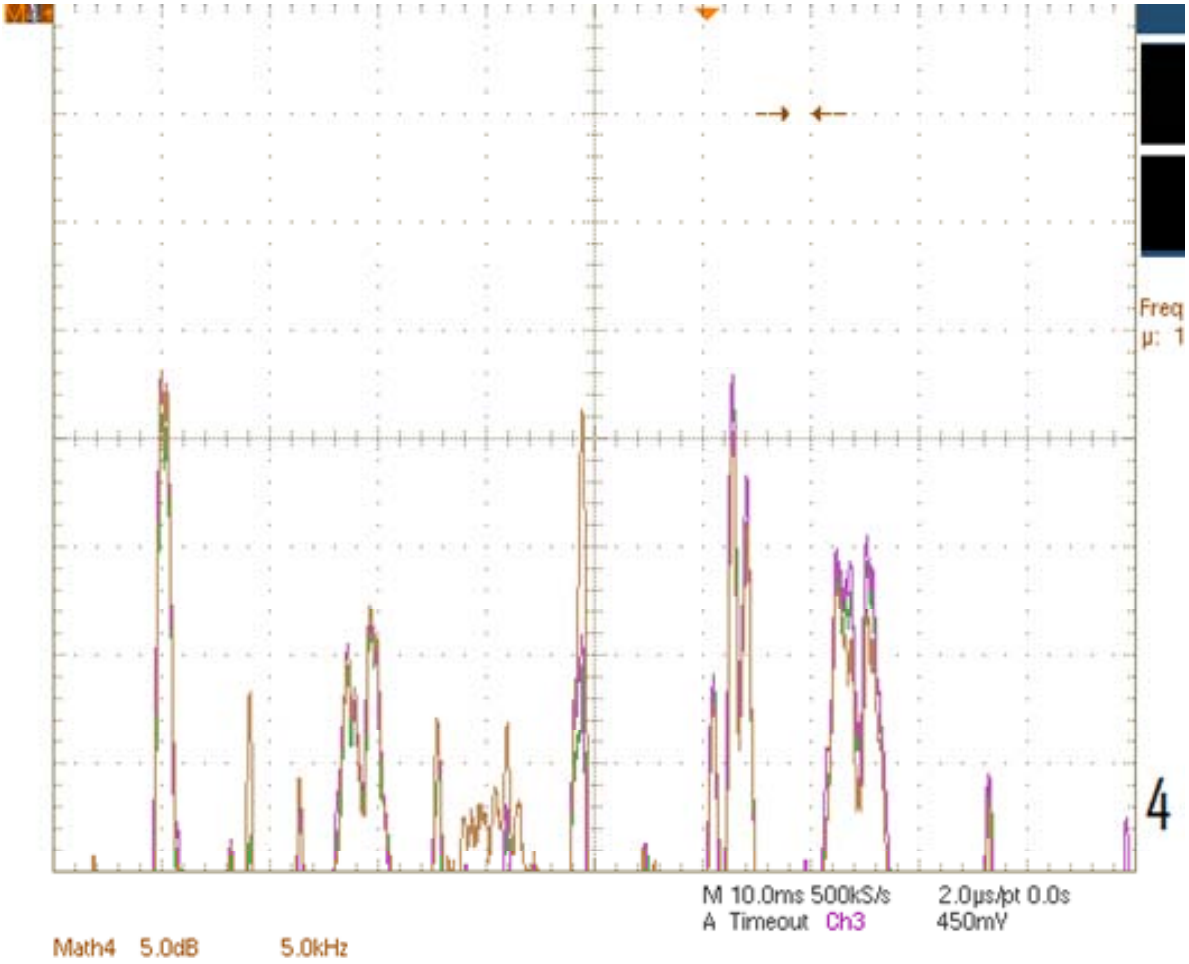

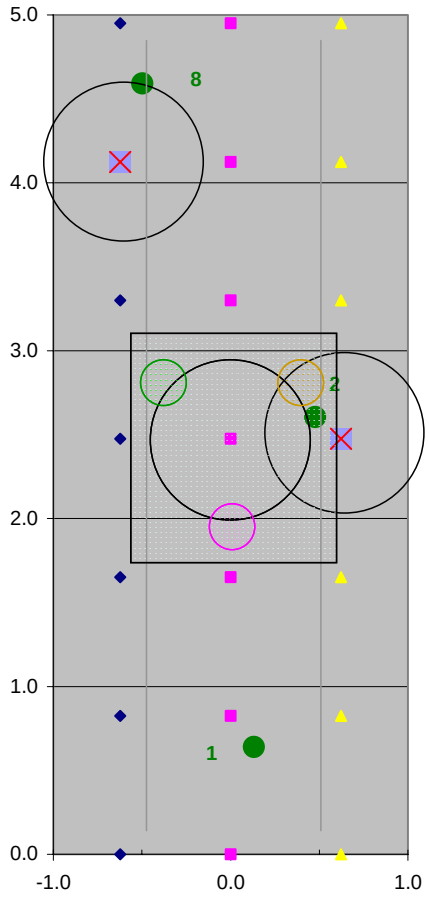

Figure 110. Data taken at position (4, C)

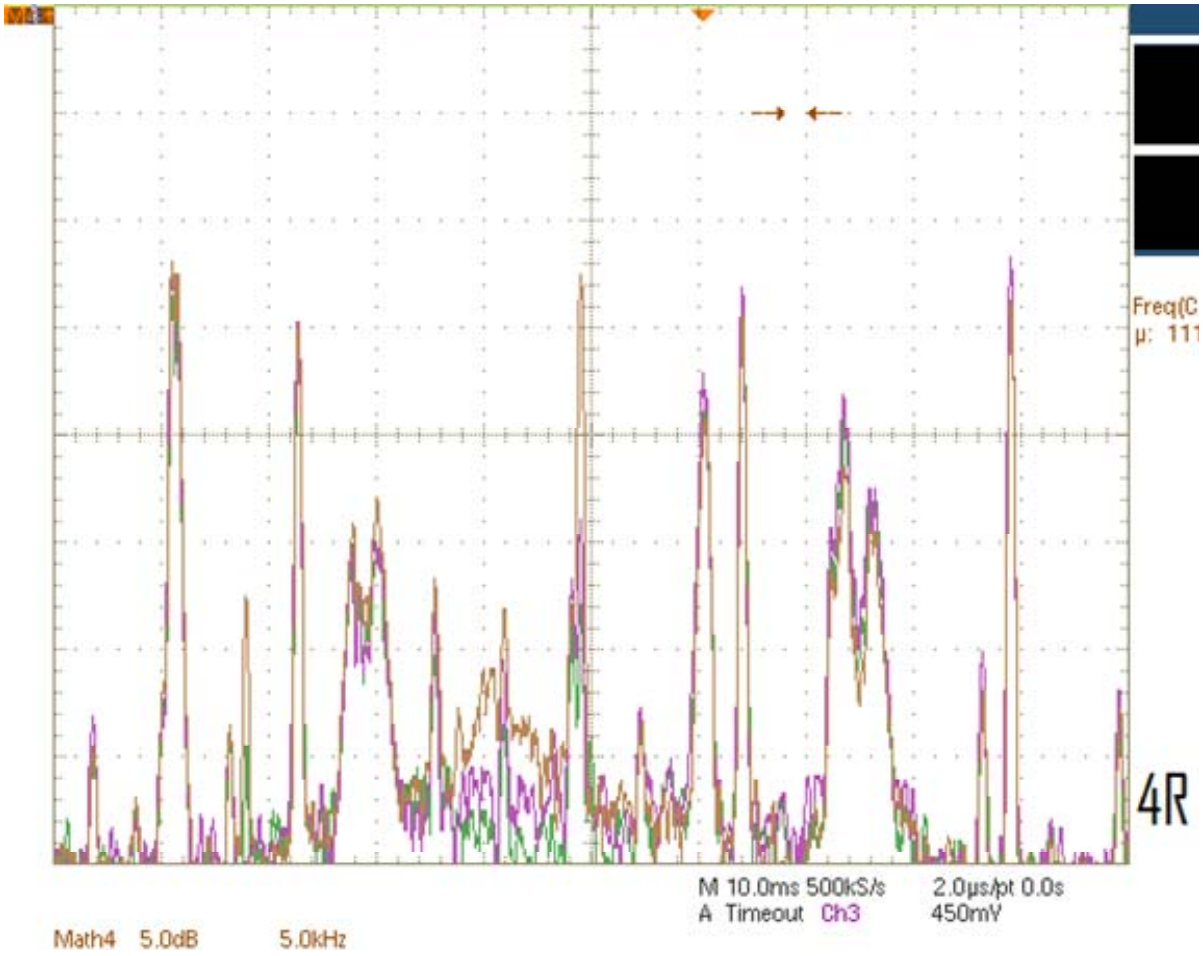

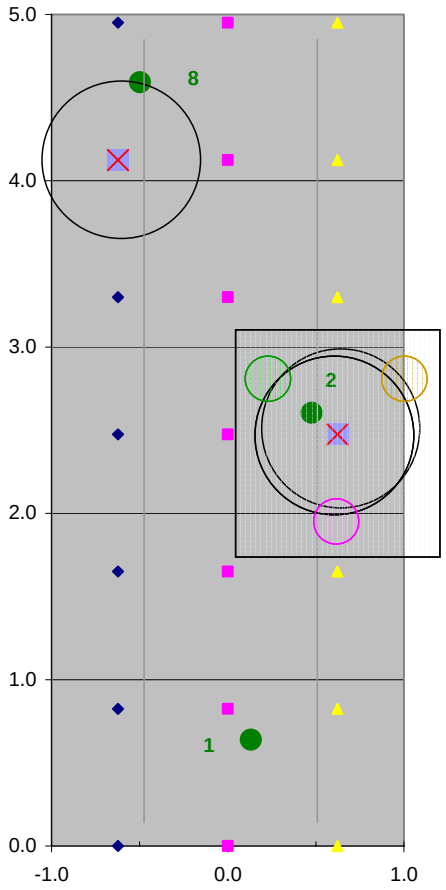

Figure 111. Data taken at position (4, R)

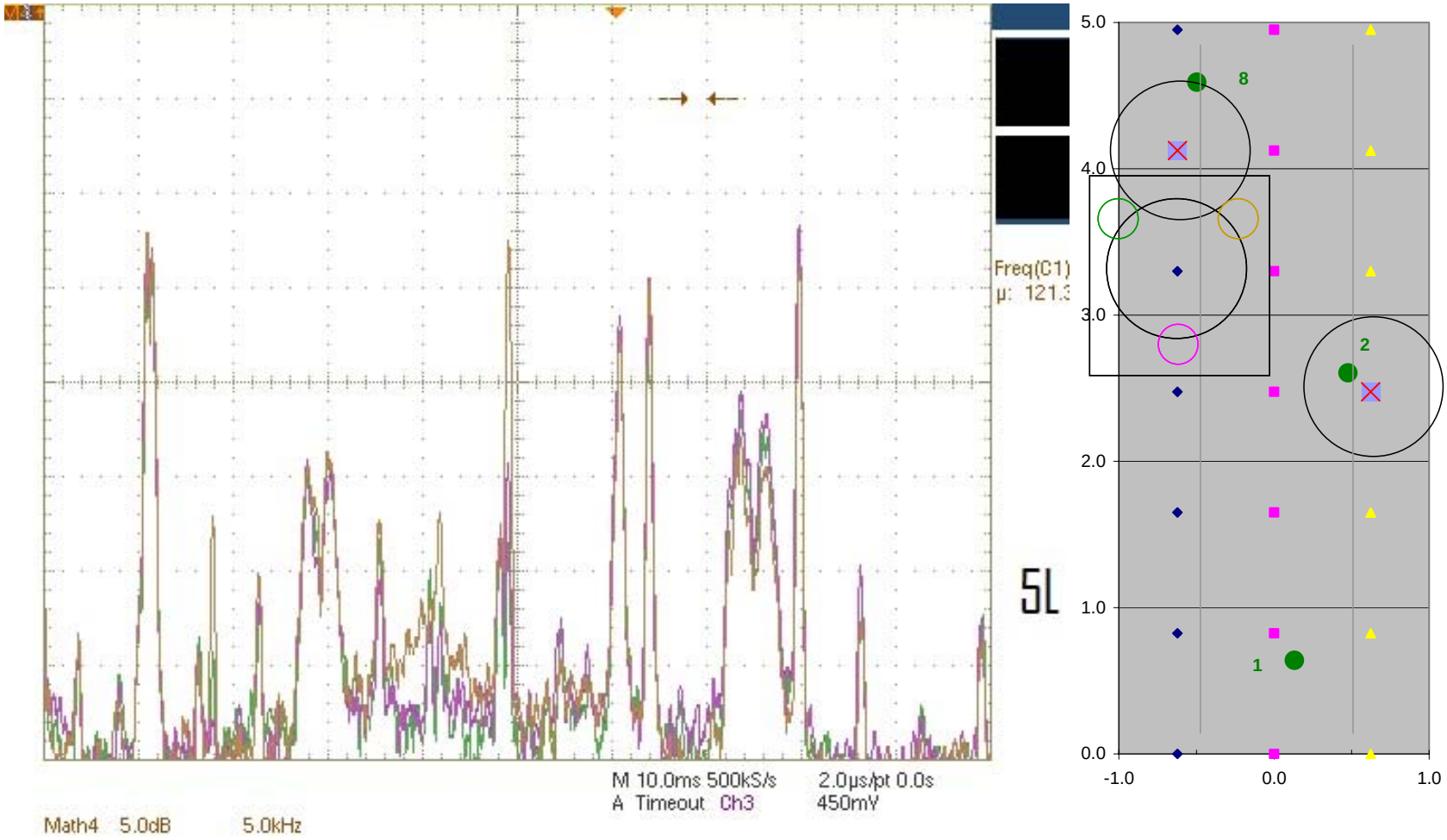

Figure 112. Data taken at position (5, L)

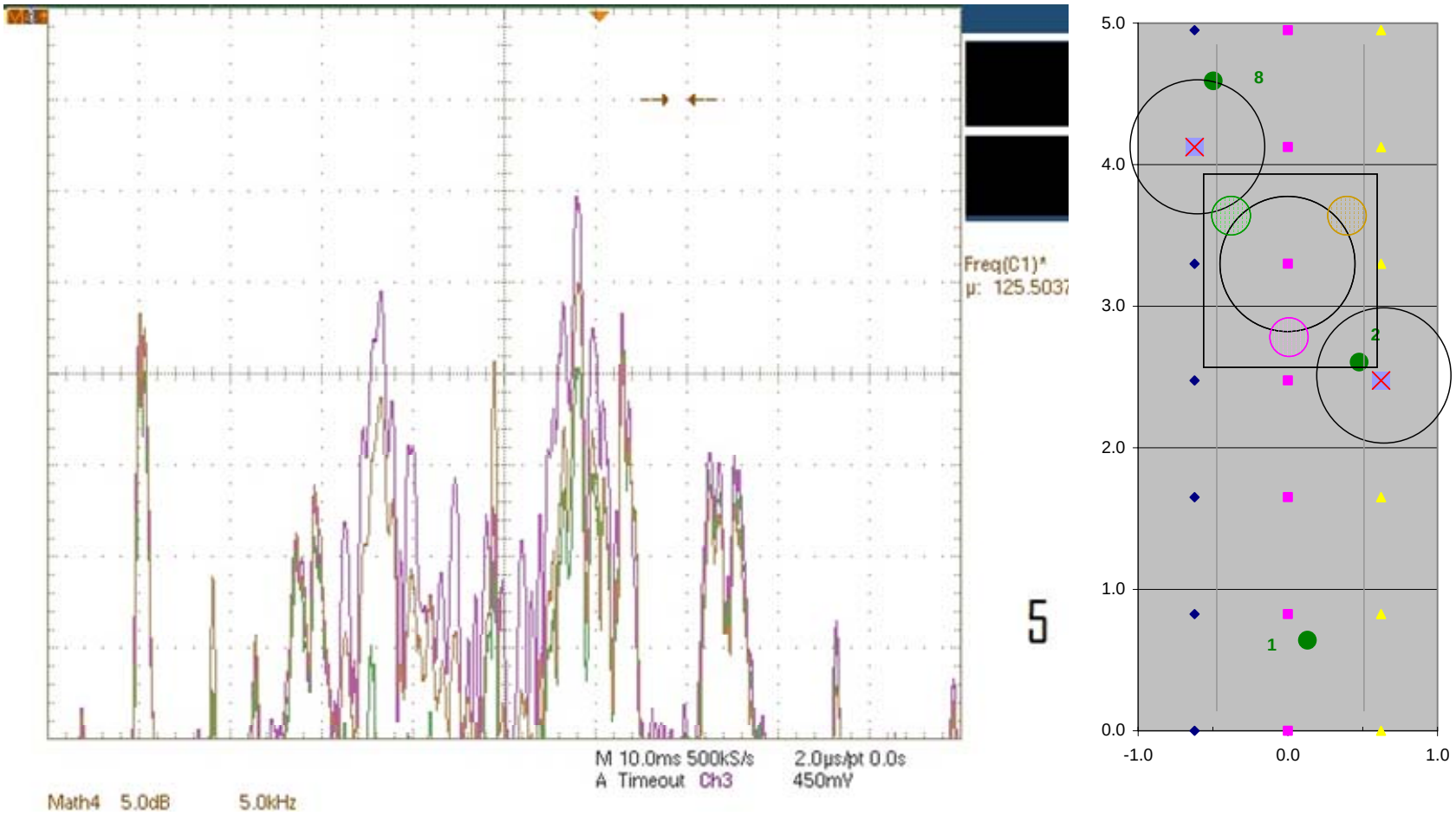

Figure 113. Data taken at position (5, C)

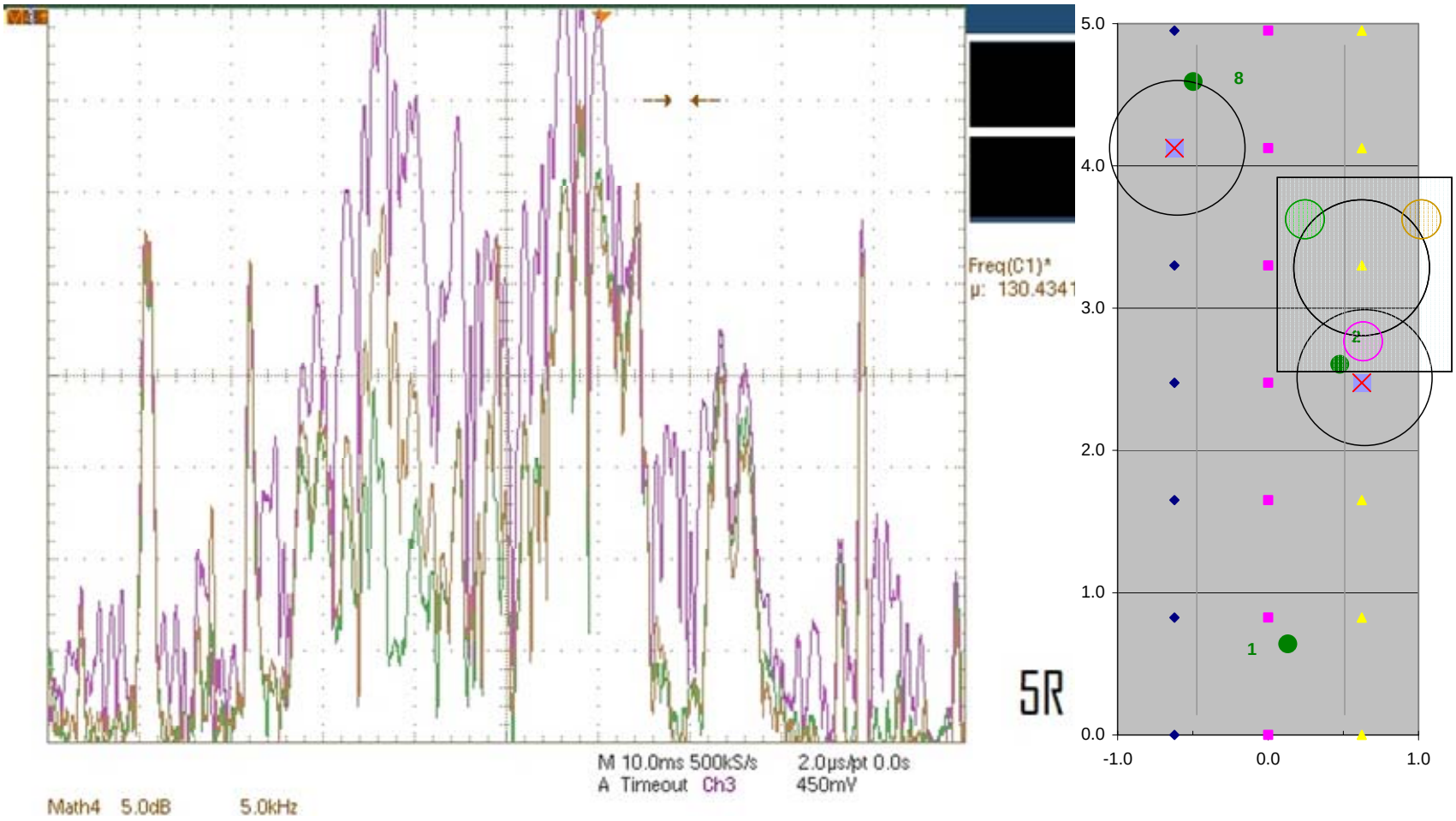

Figure 114. Data taken at position (5, R)

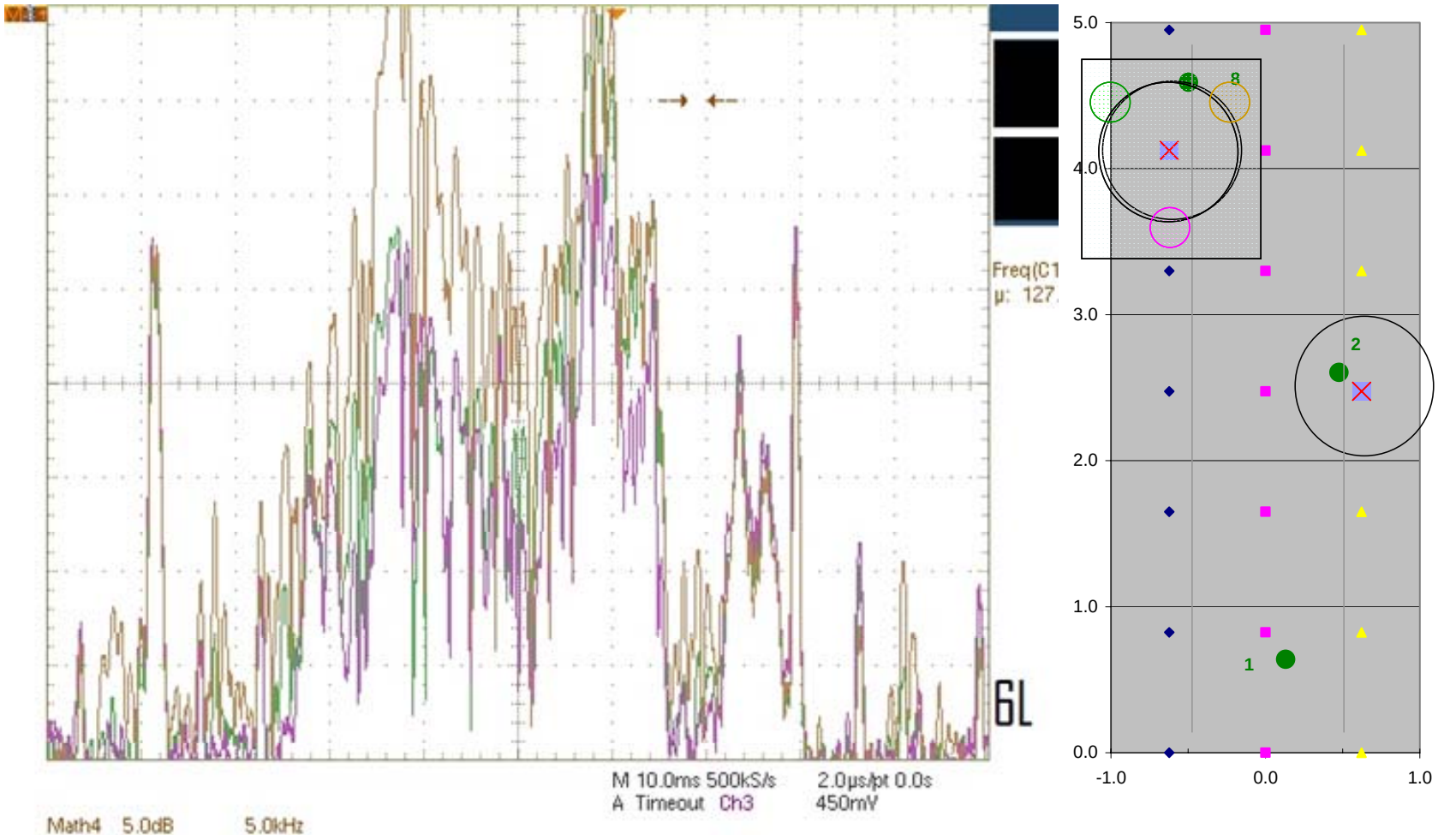

Figure 115. Data taken at position (6, L)

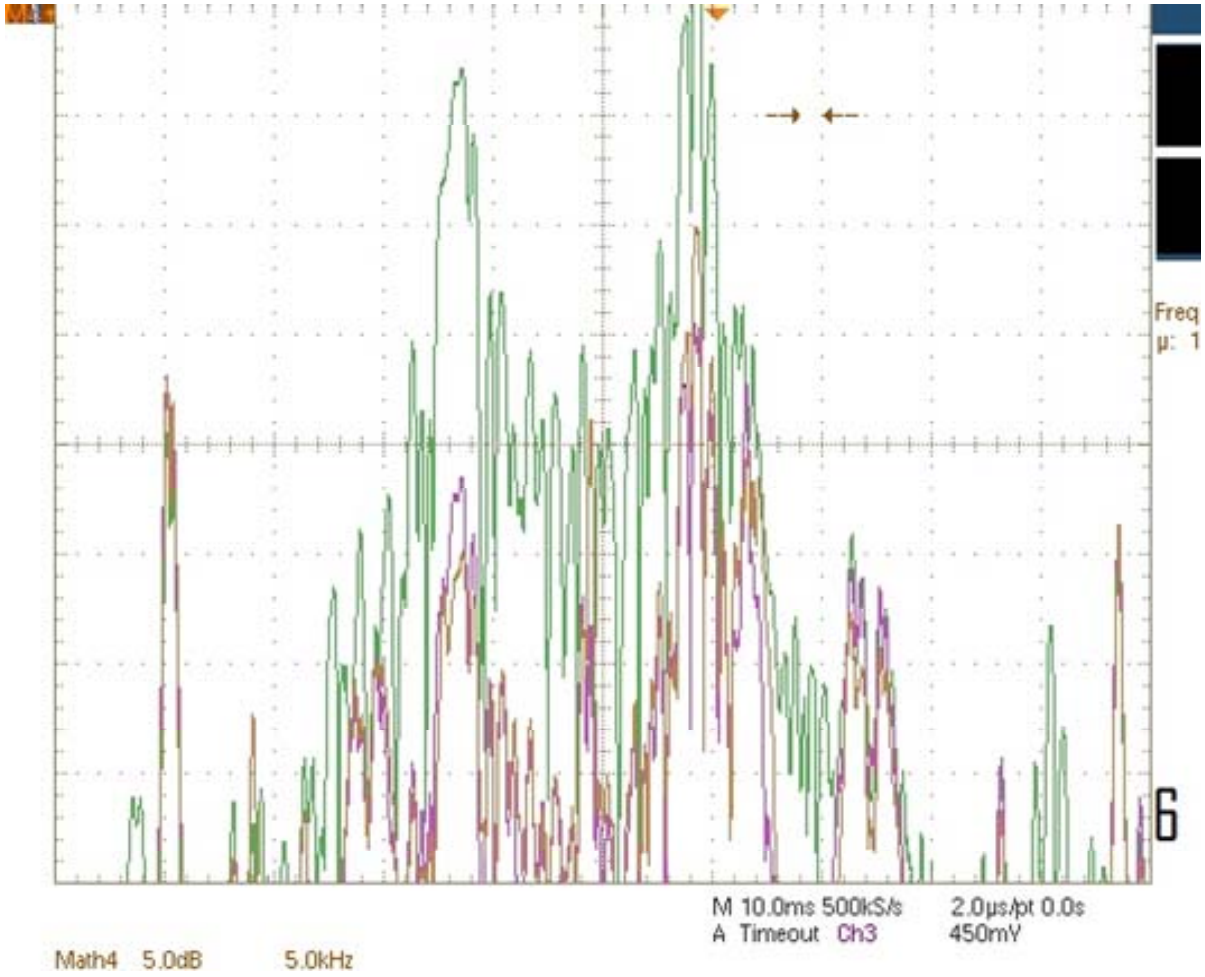

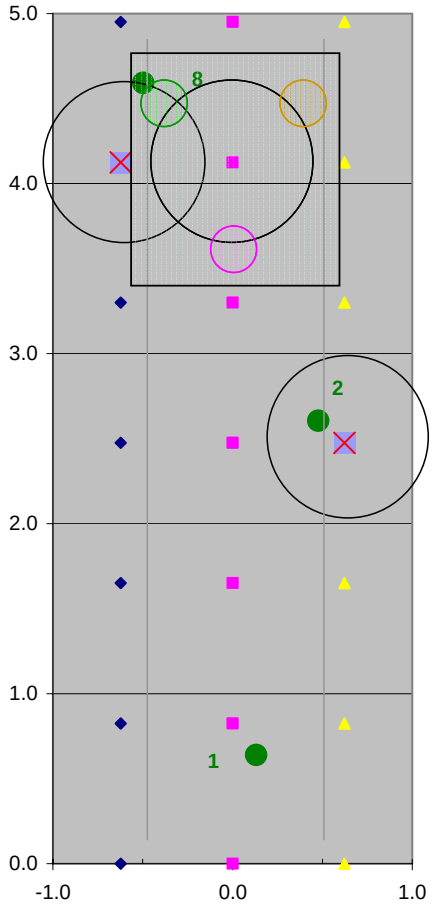

Figure 116. Data taken at position (6, C)

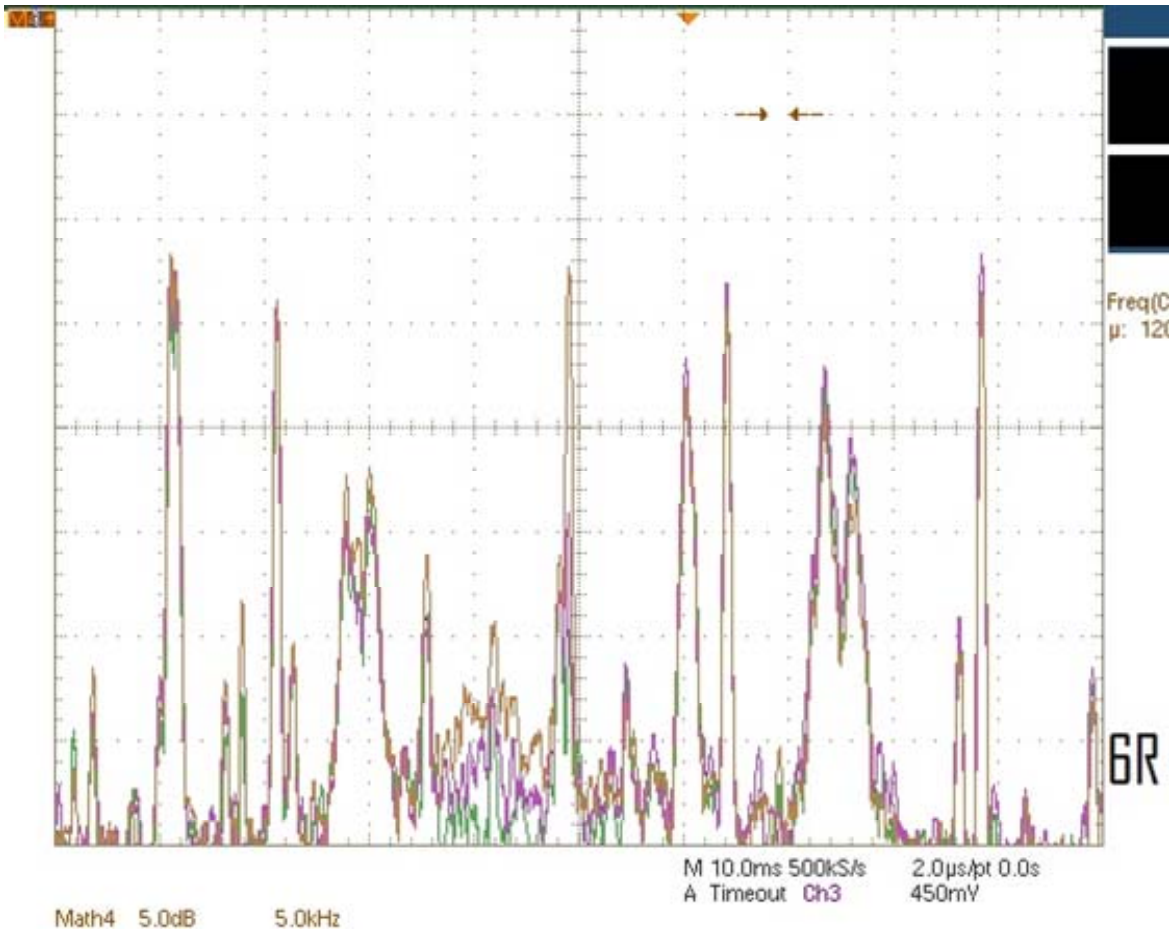

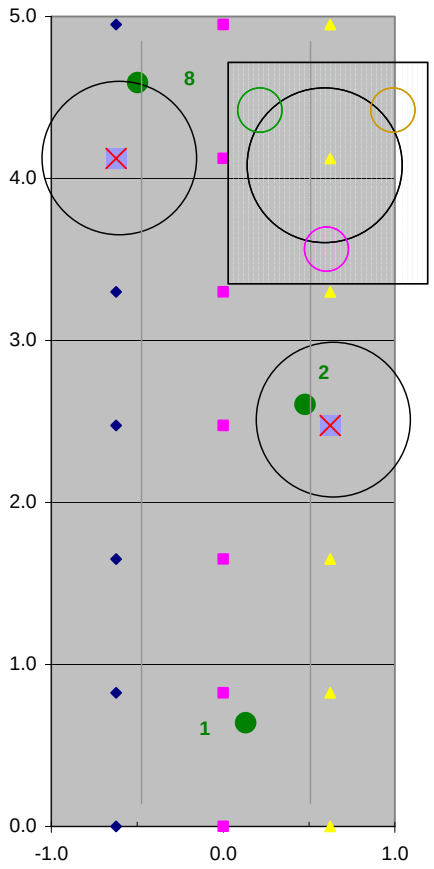

Figure 117. Data taken at position (6, R)

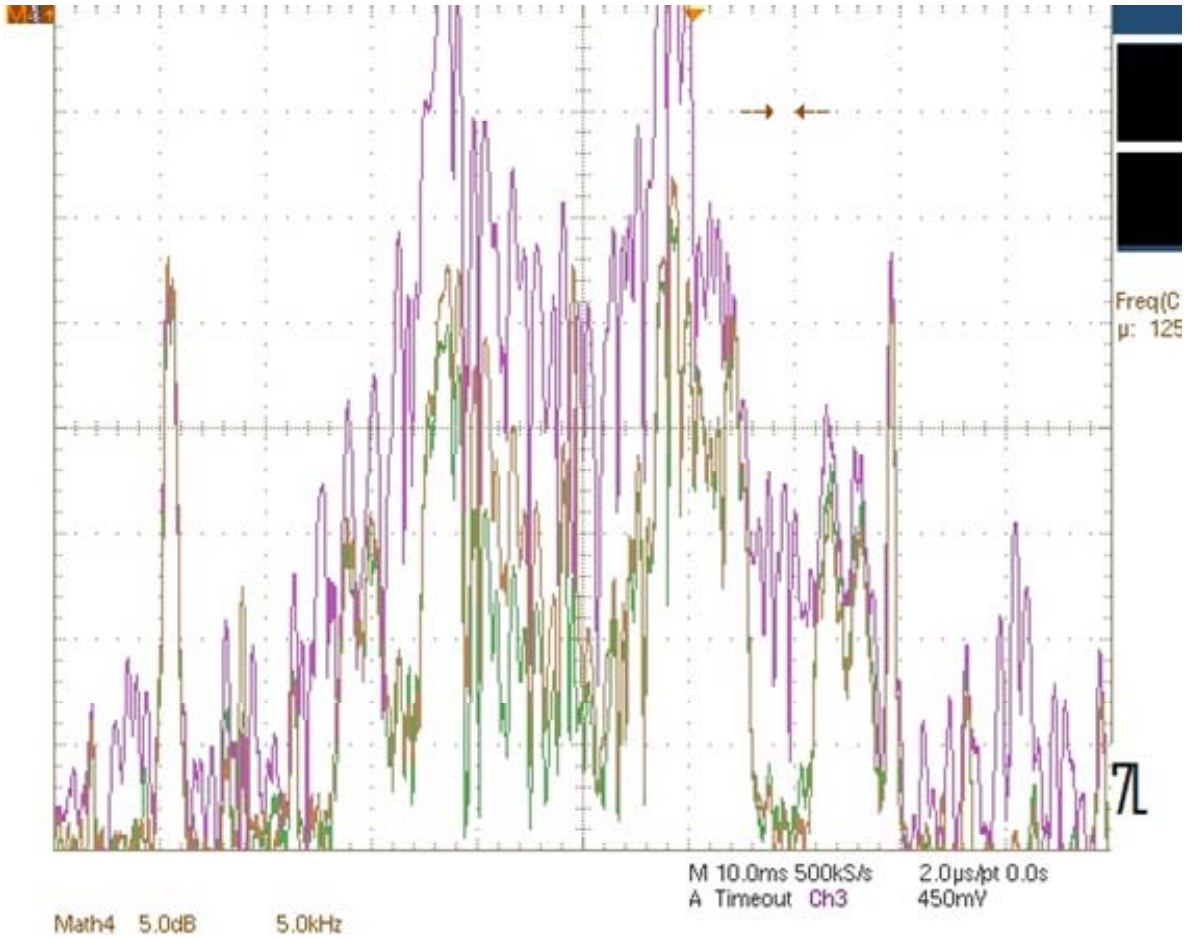

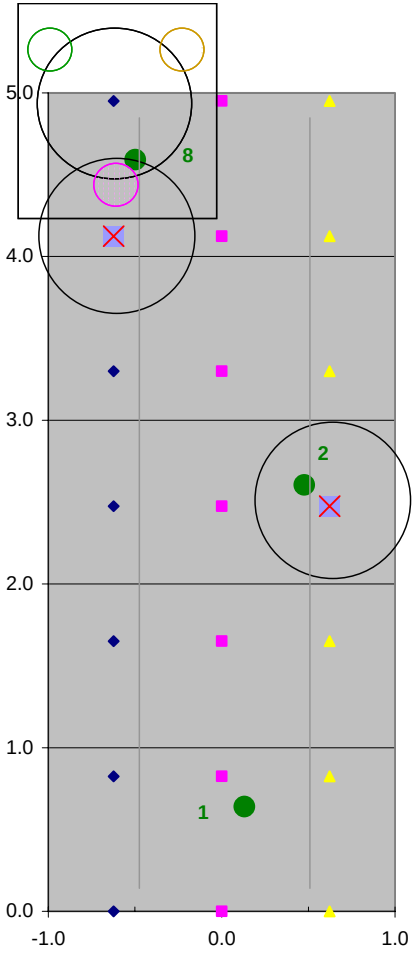

Figure 118. Data taken at position (7, L)

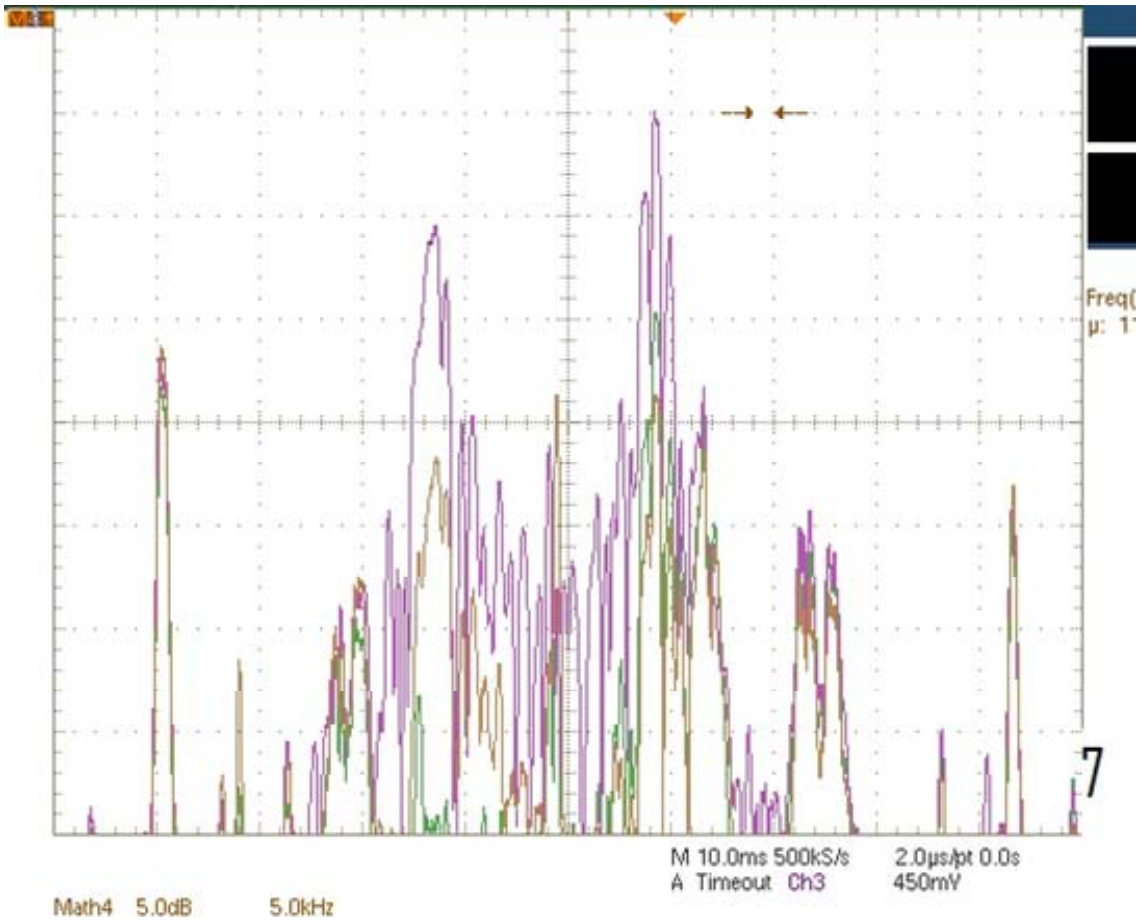

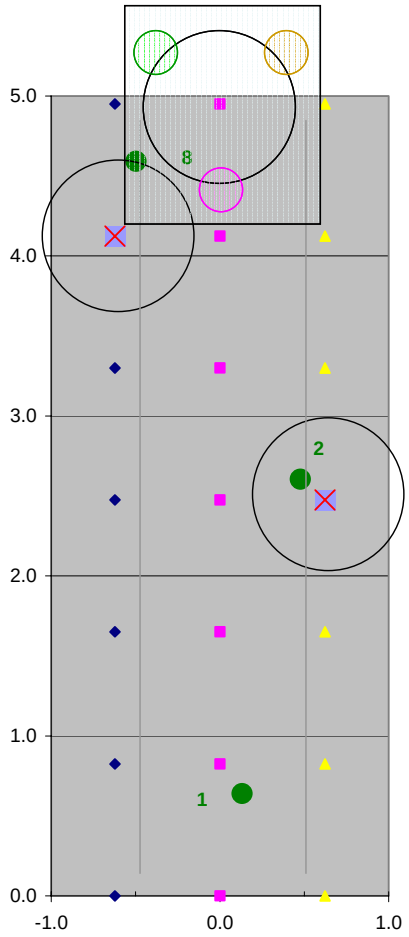

Figure 119. Data taken at position (7, C)

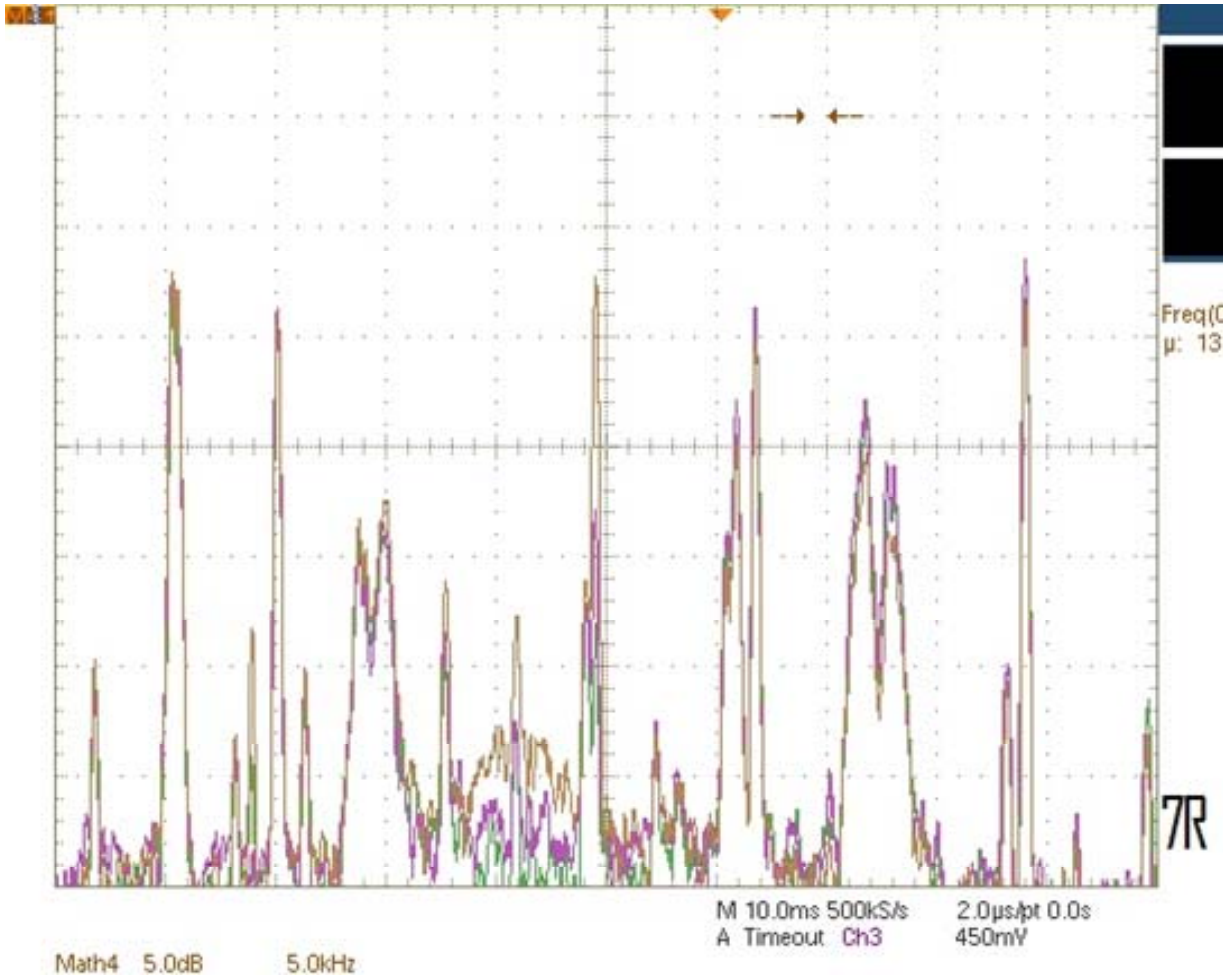

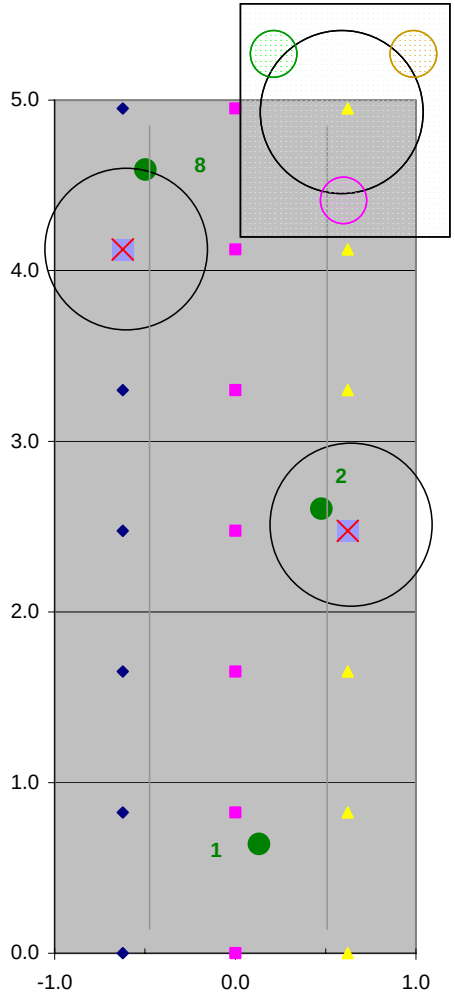

Figure 120. Data taken at position (7, R)

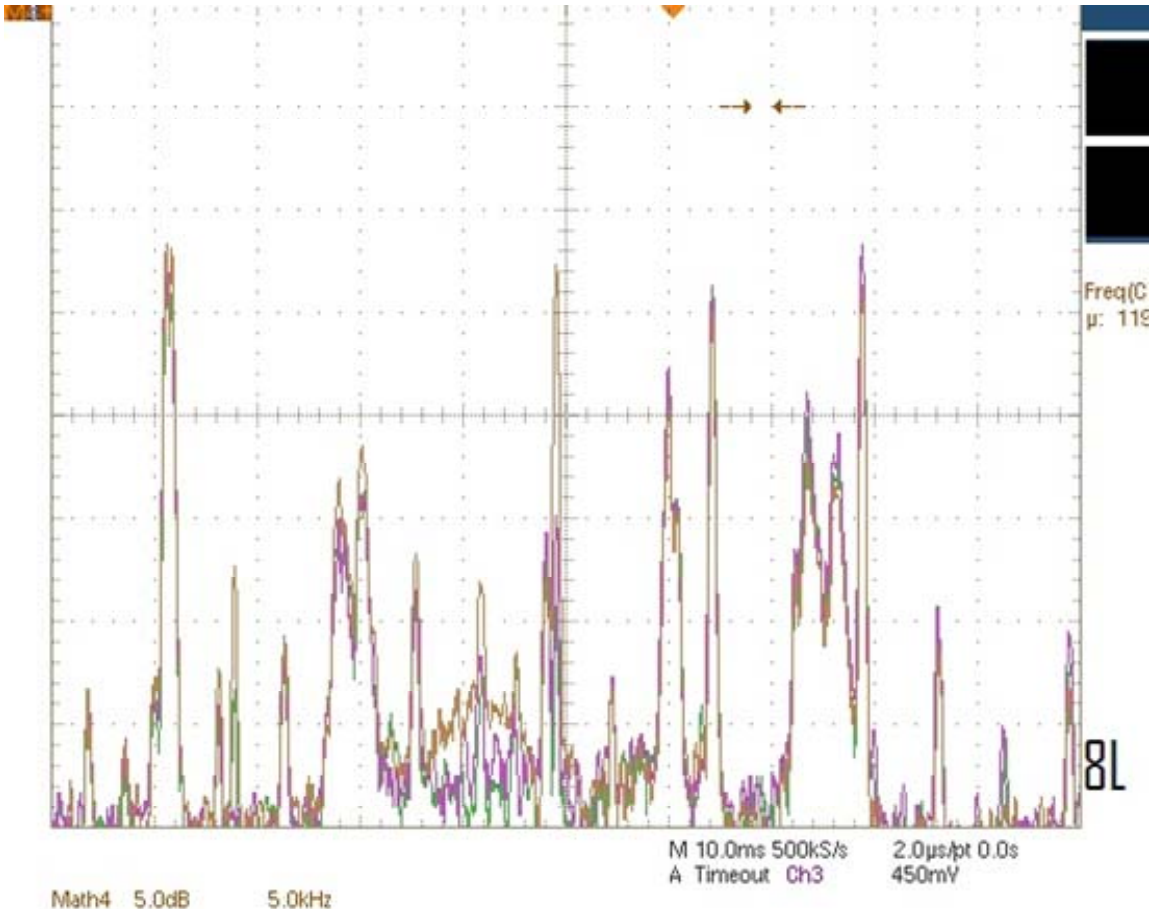

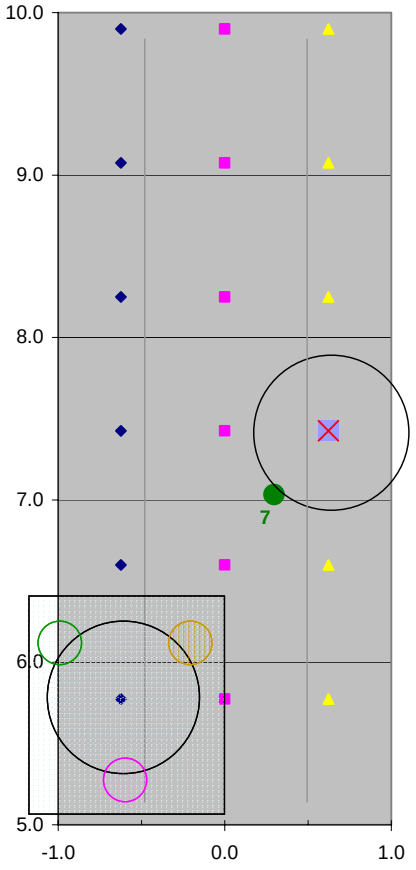

Figure 121. Data taken at position (8, L)

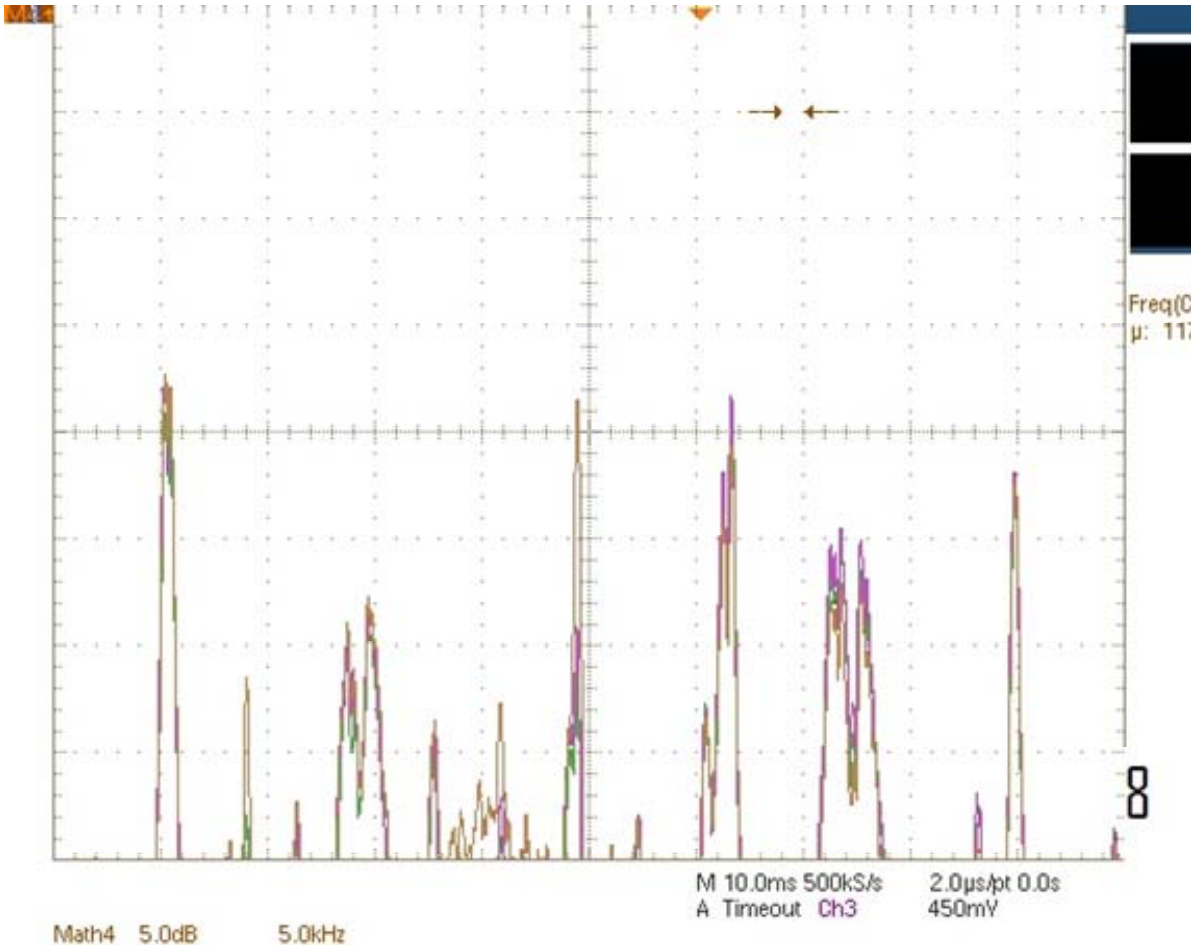

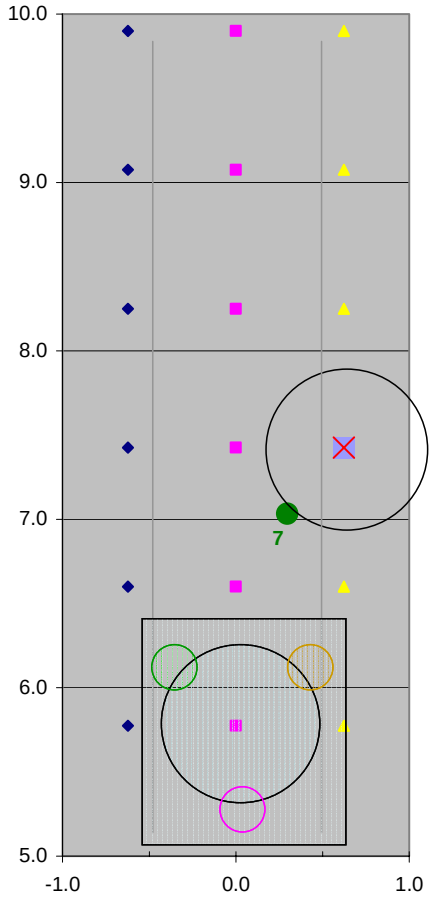

Figure 122. Data taken at position (8, C)

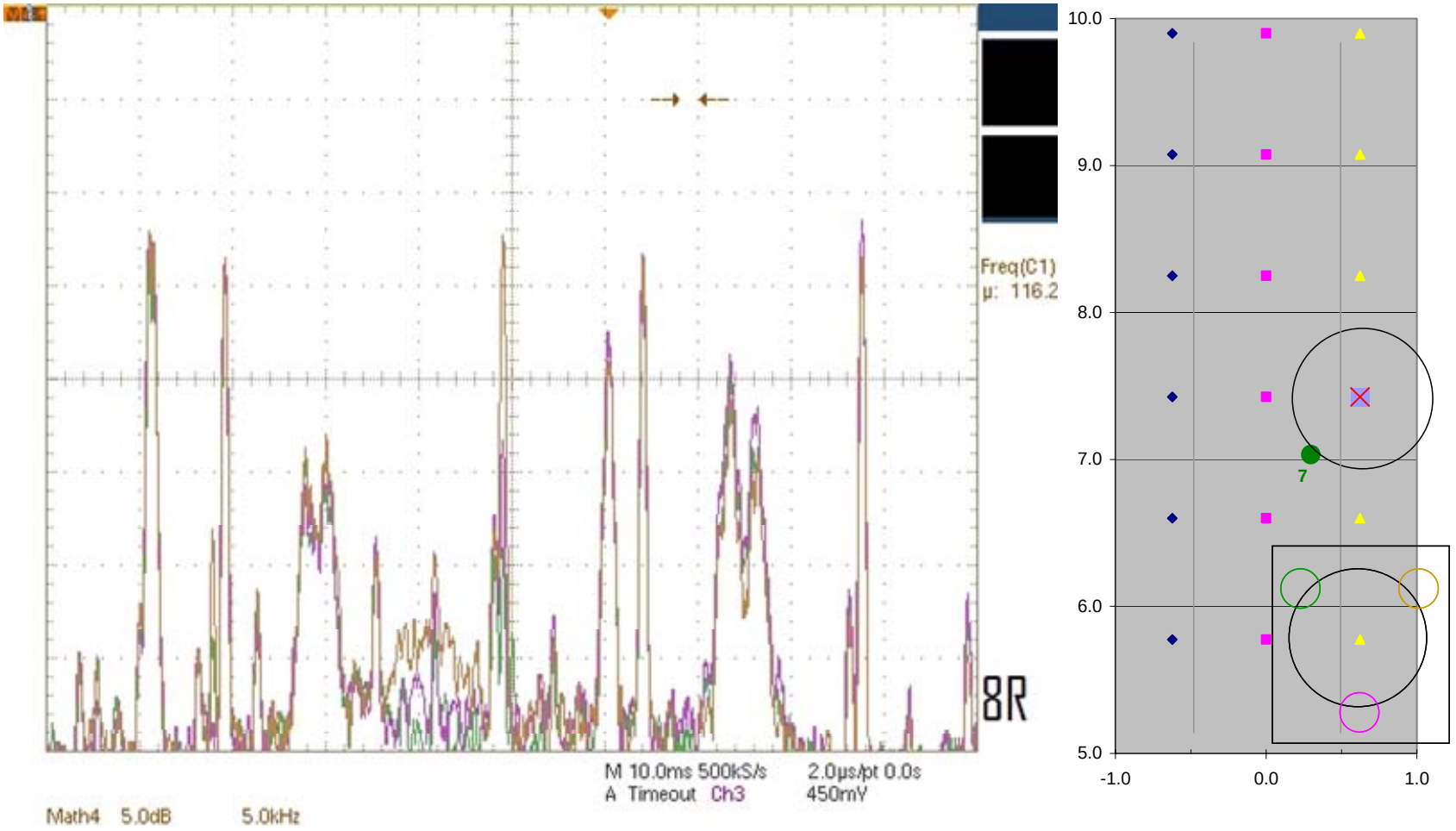

Figure 123. Data taken at position (8, R)

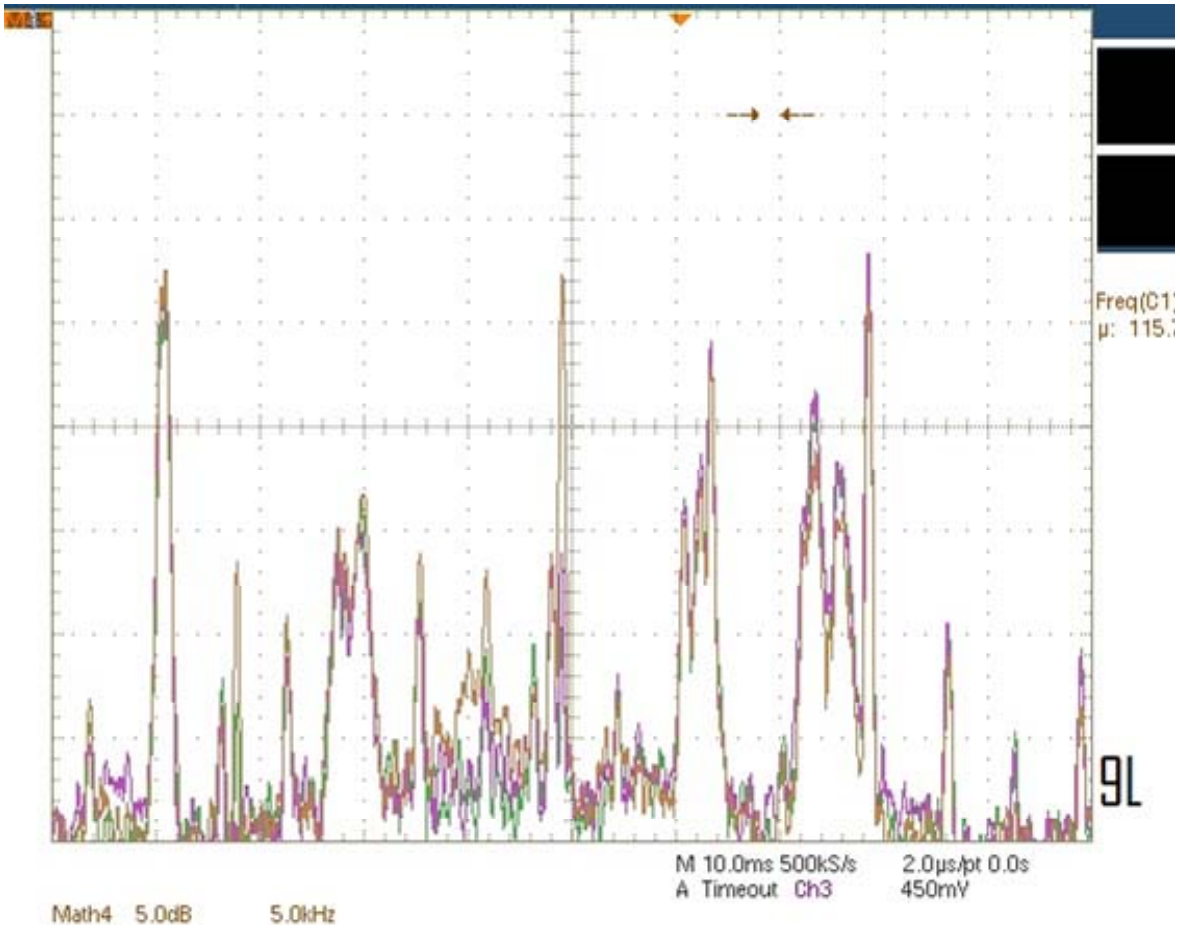

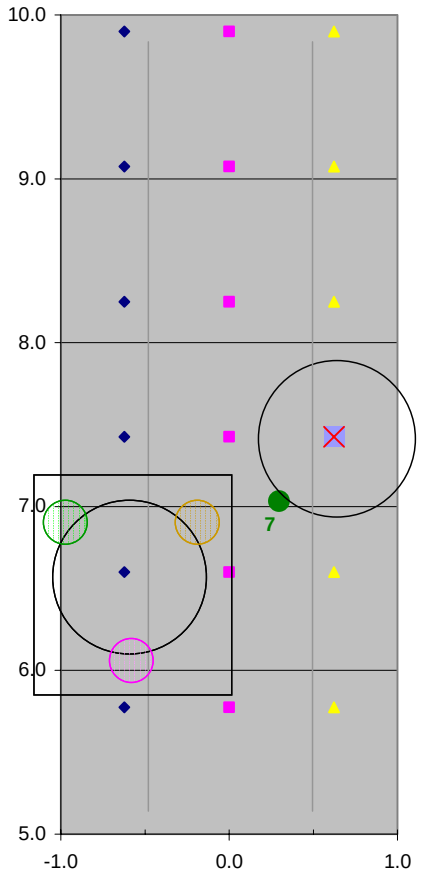

Figure 124. Data taken at position (9, L)

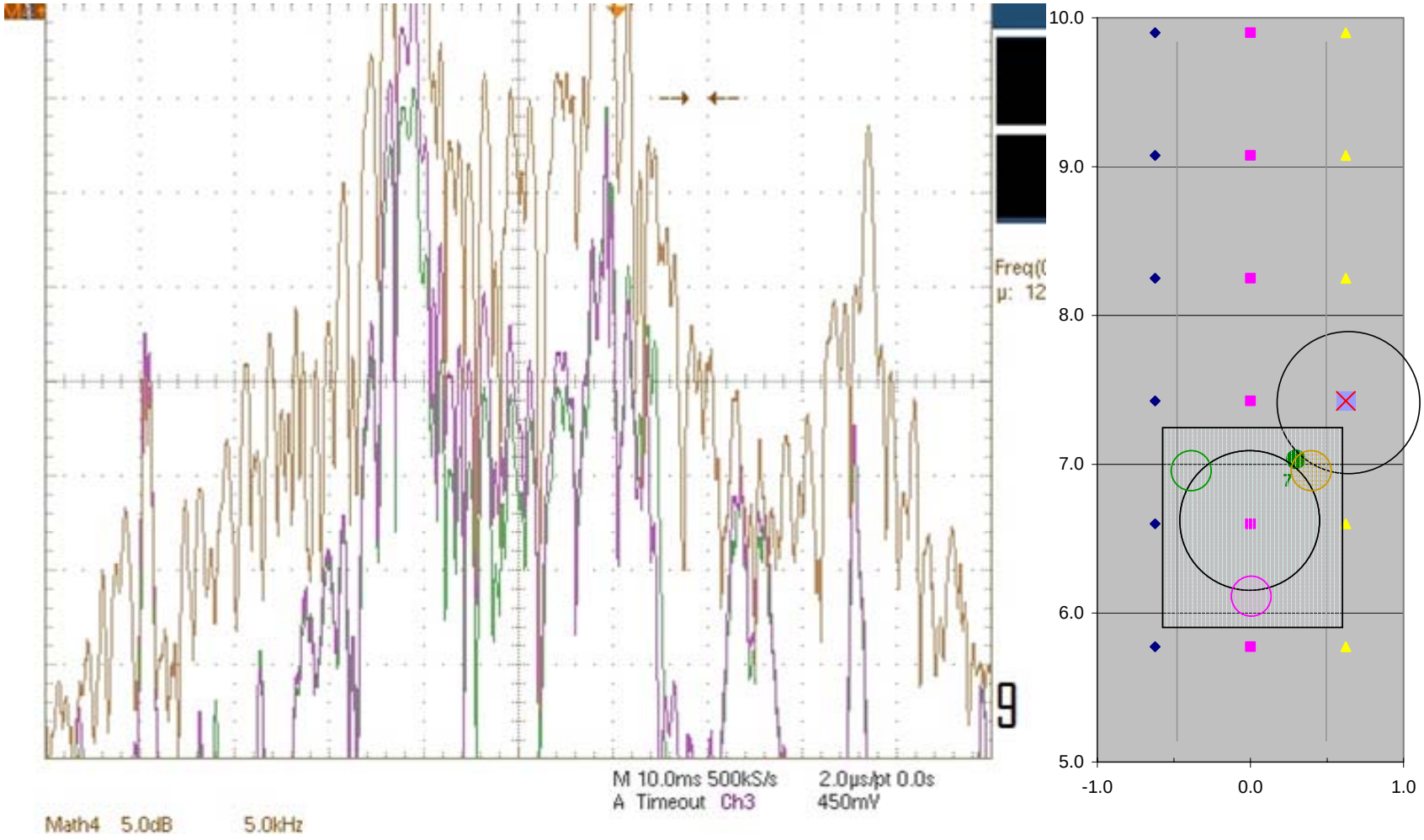

Figure 125. Data taken at position (9, C)

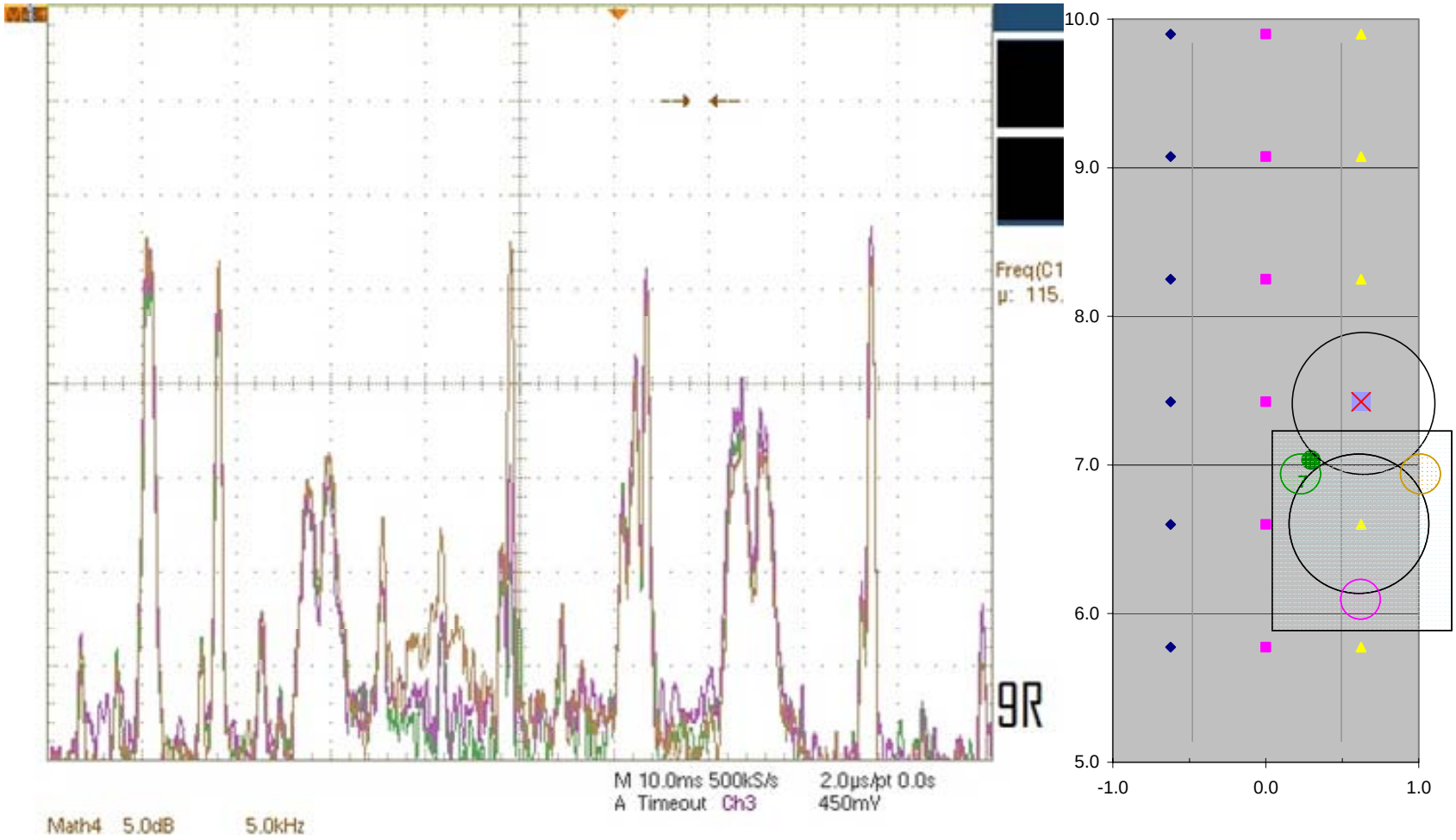

Figure 126. Data taken at position (9, R)

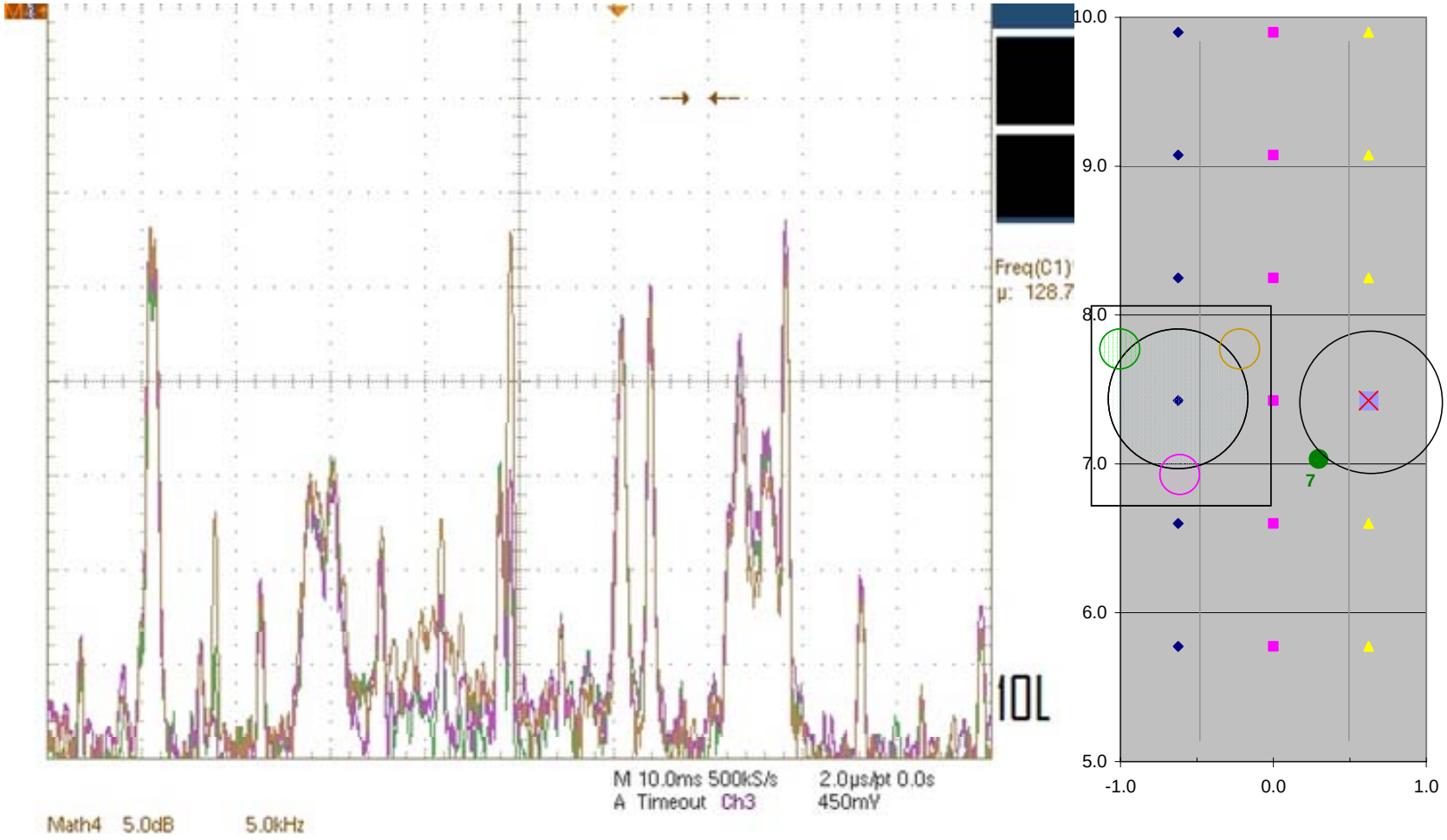

Figure 127. Data taken at position (10, L)

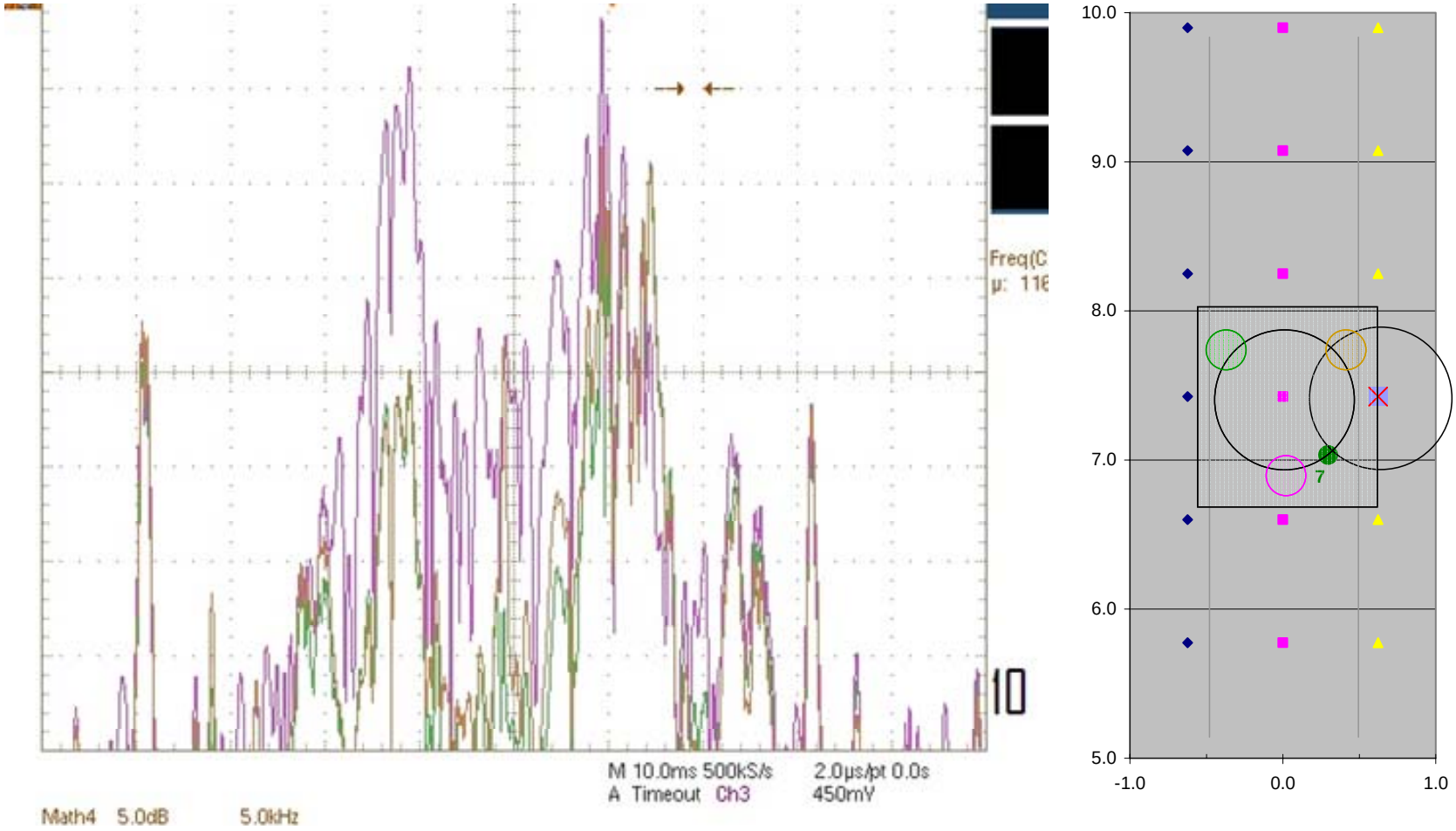

Figure 128. Data taken at position (10, C)

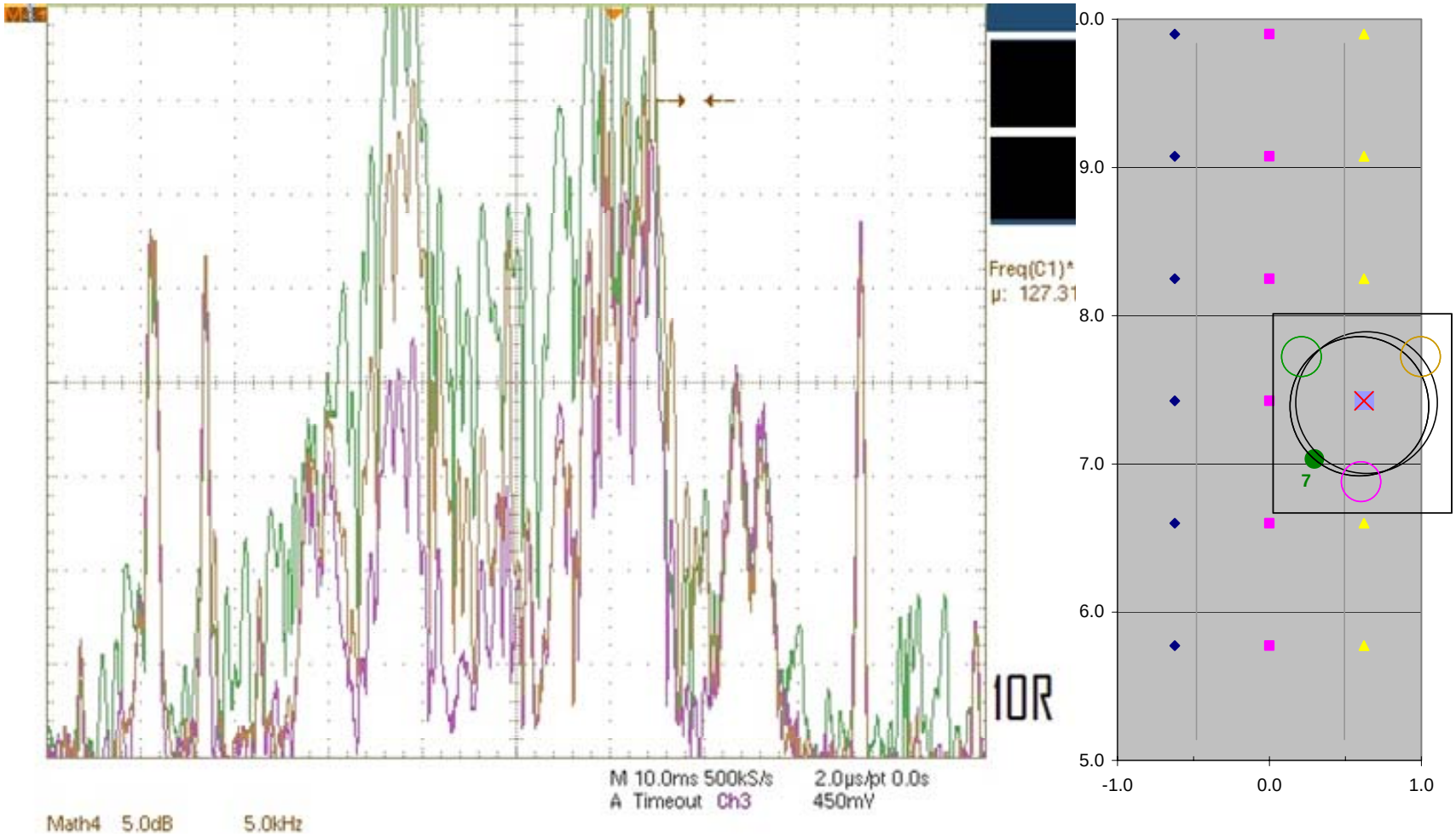

Figure 129. Data taken at position (10, R)

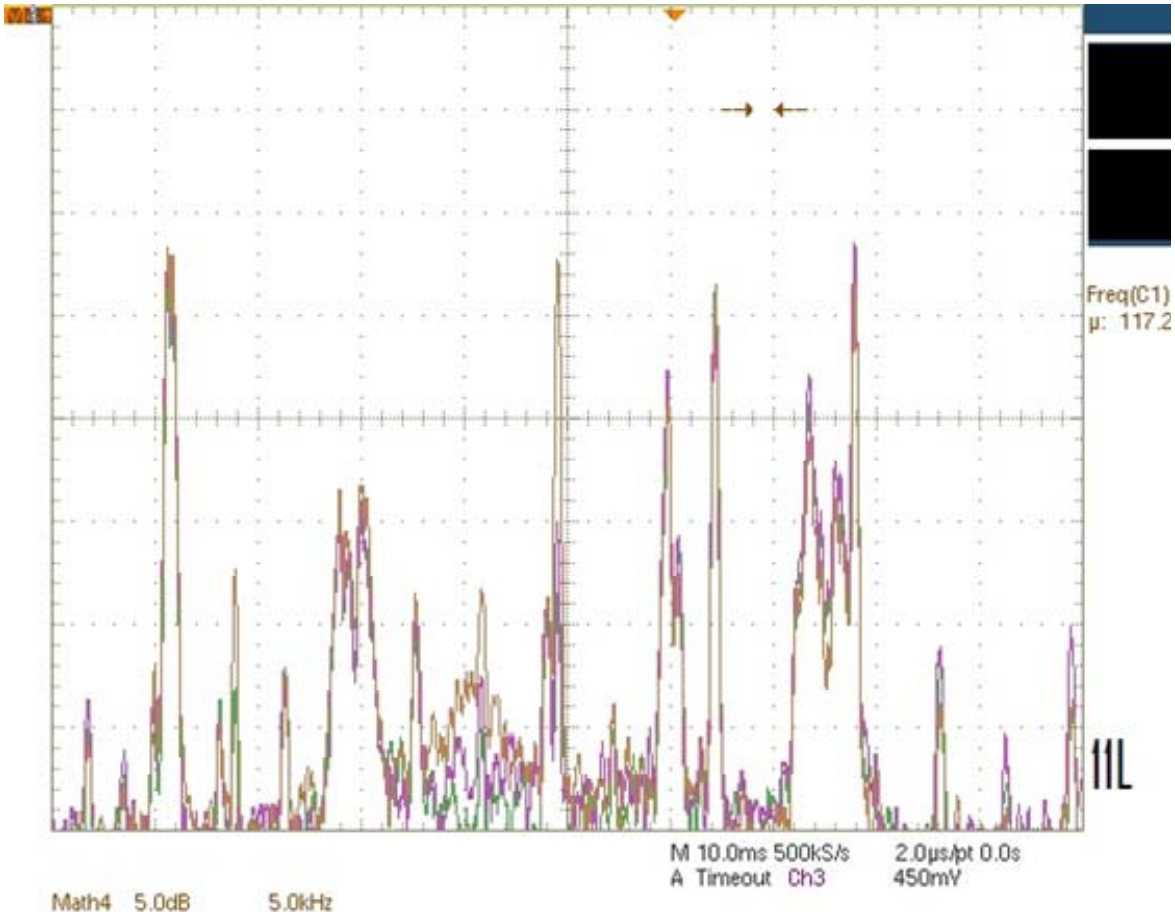

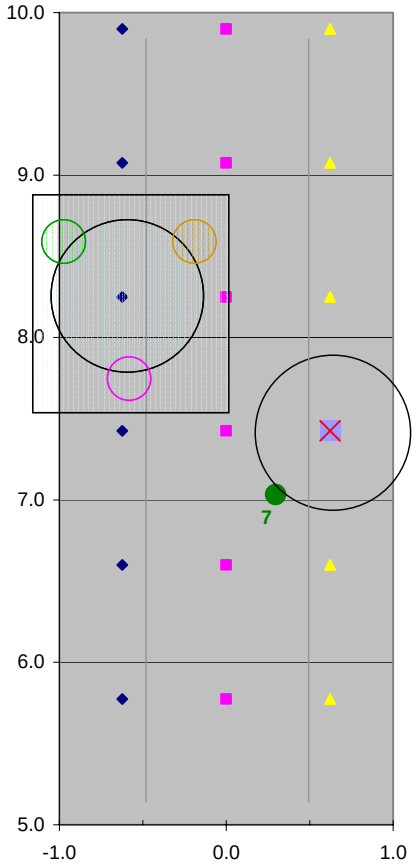

Figure 130. Data taken at position (11, L)

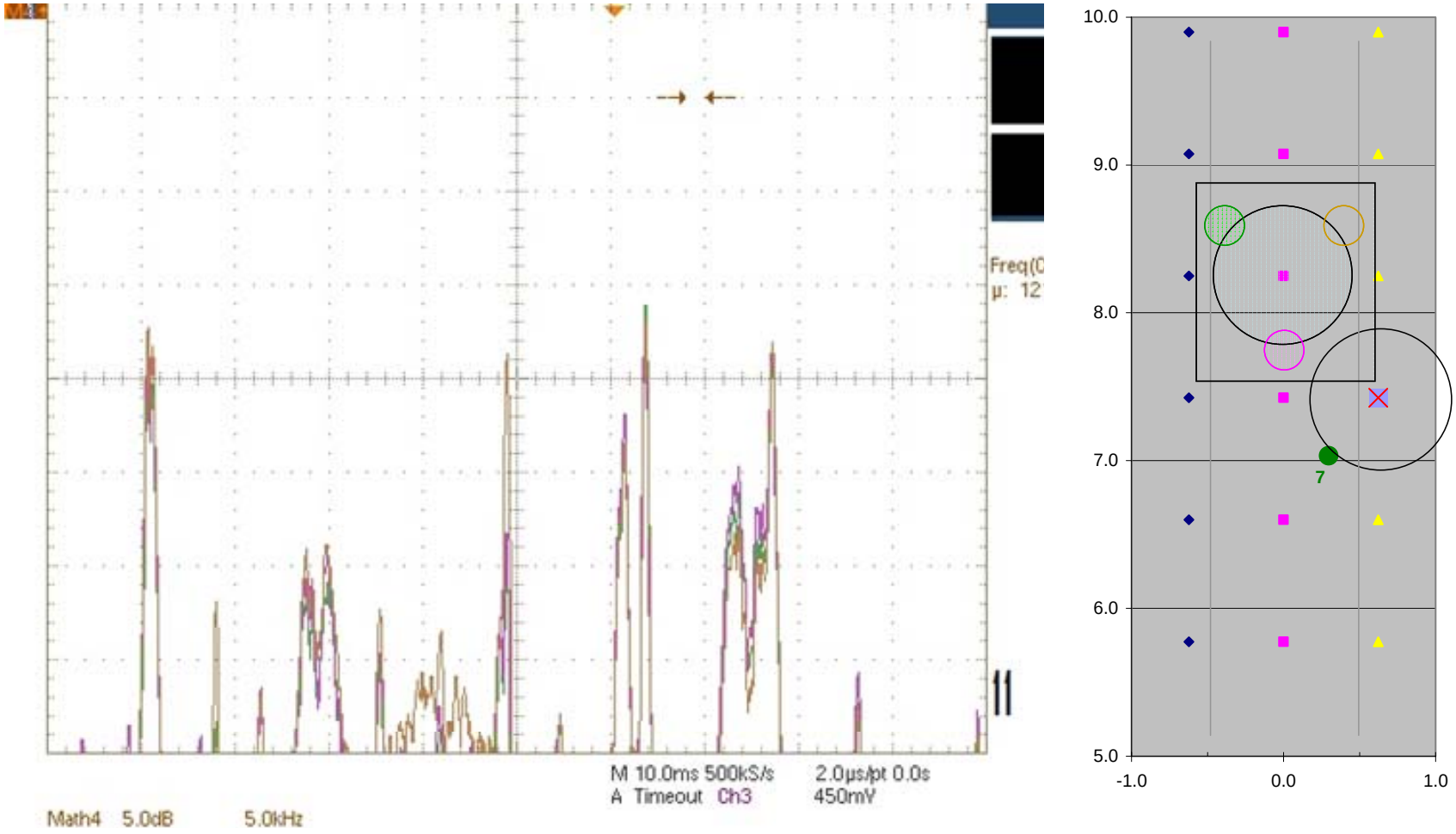

Figure 131. Data taken at position (11, C)

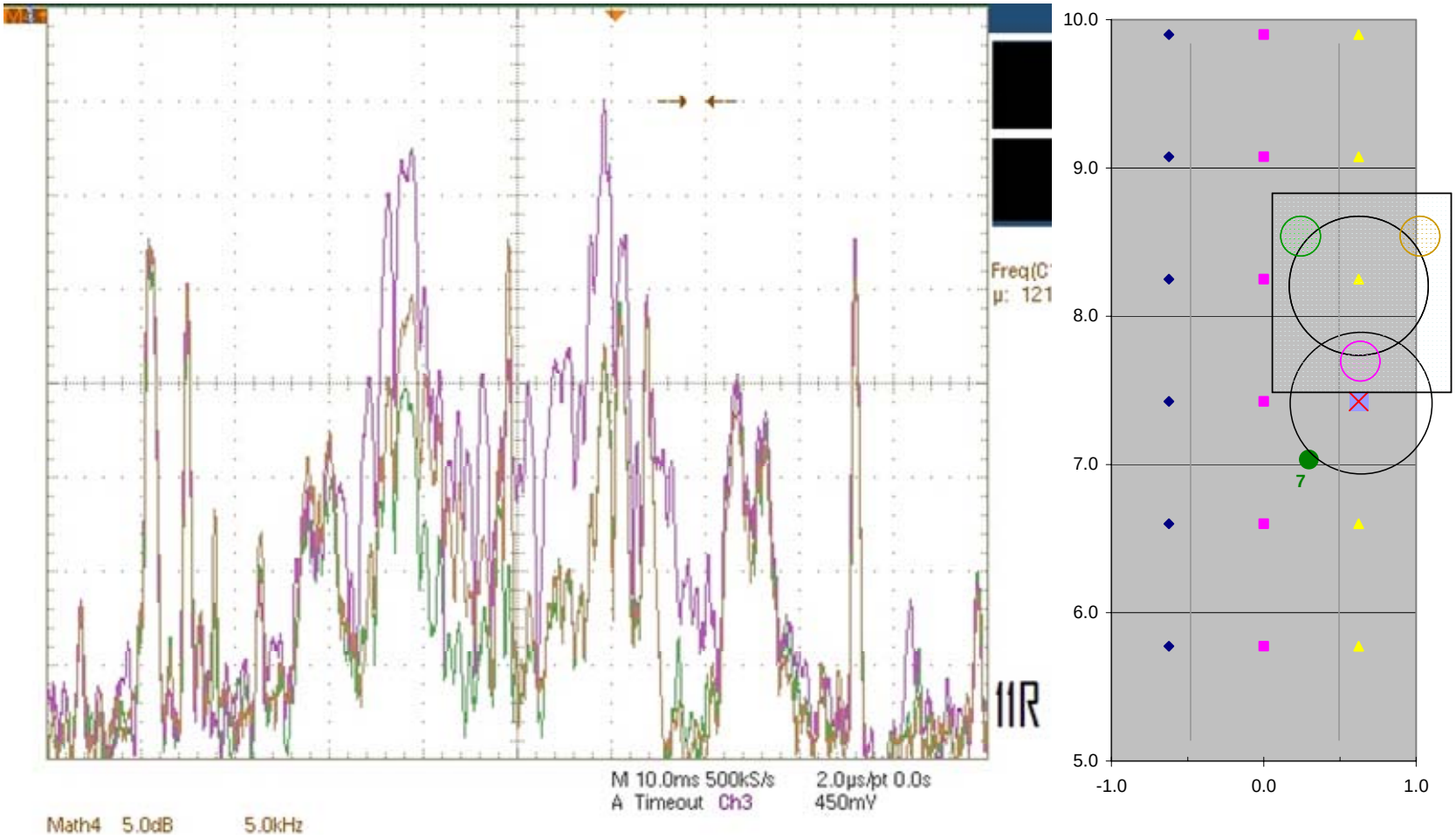

Figure 132. Data taken at position (11, R)

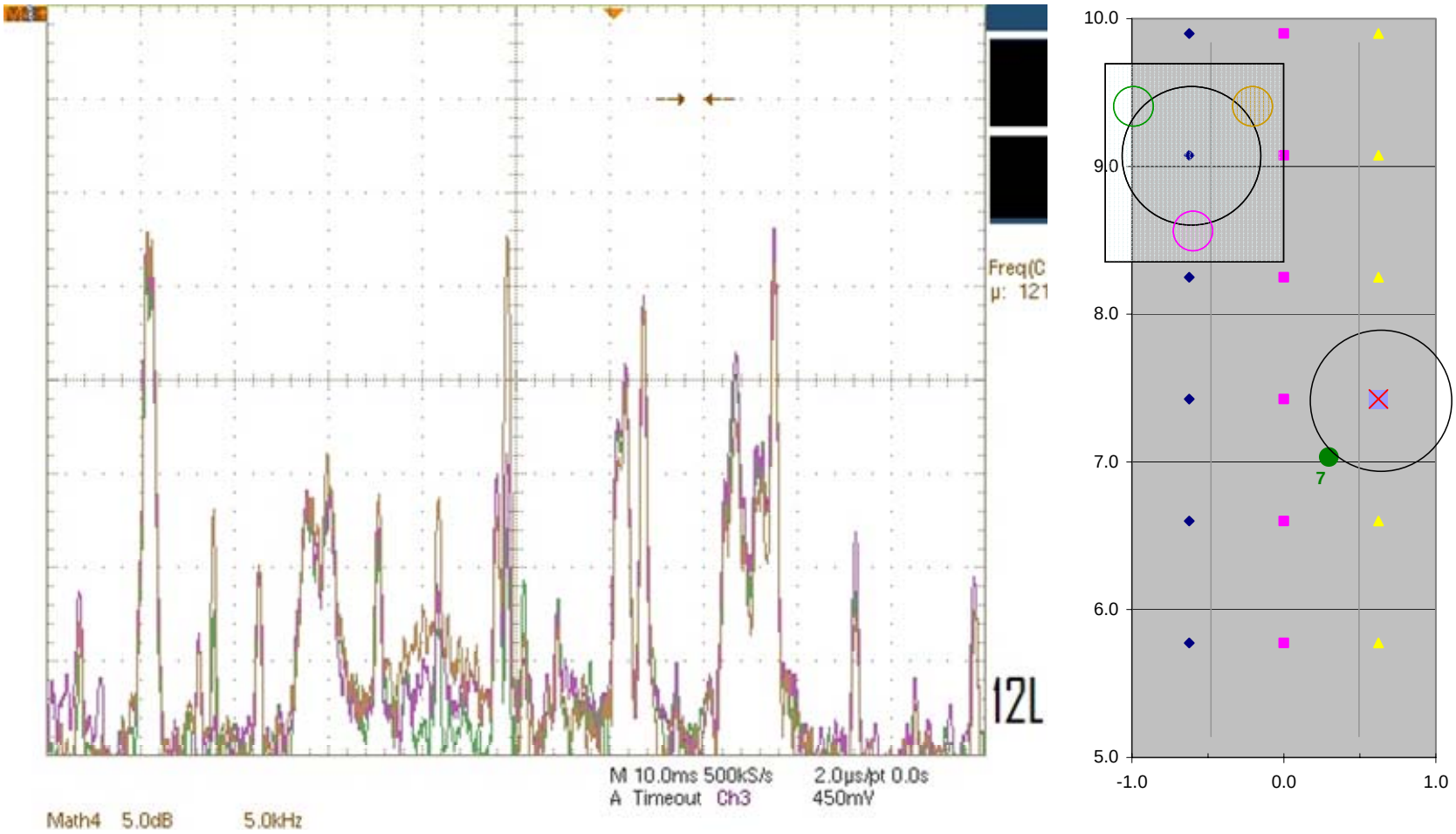

Figure 133. Data taken at position (12, L)

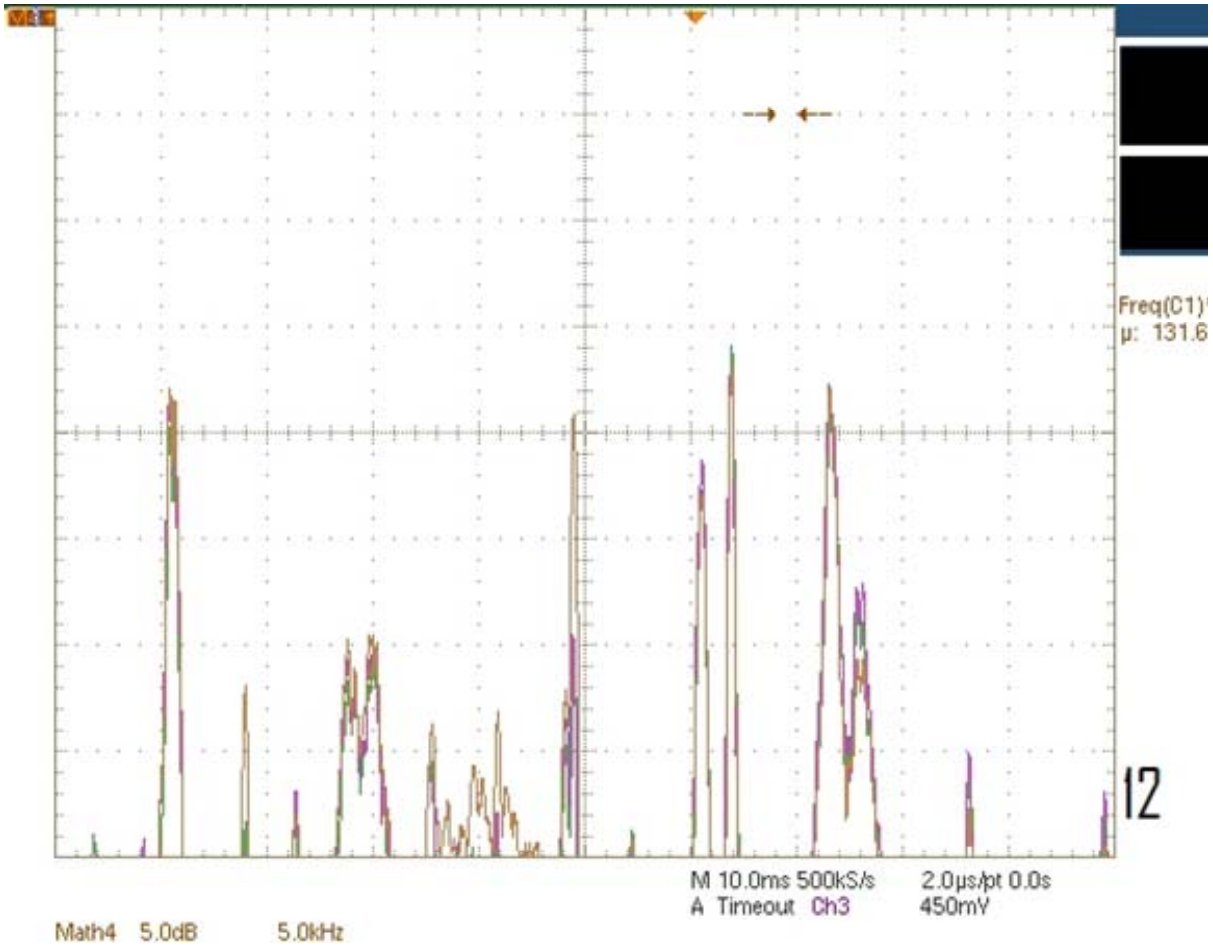

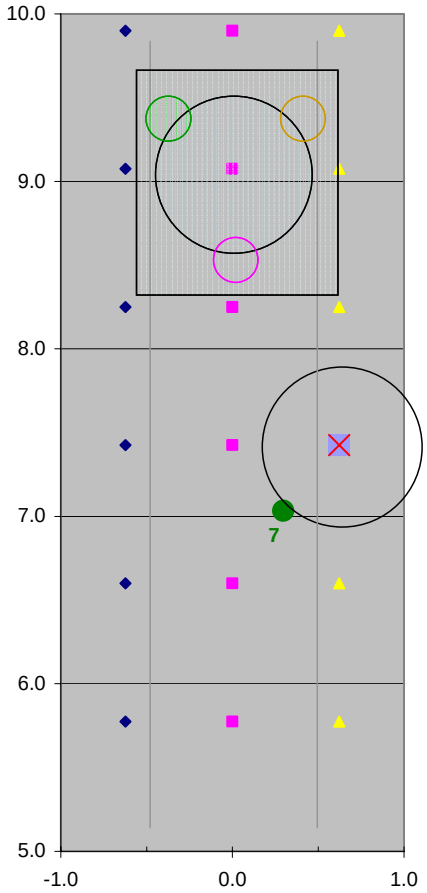

Figure 134. Data taken at position (12, C)

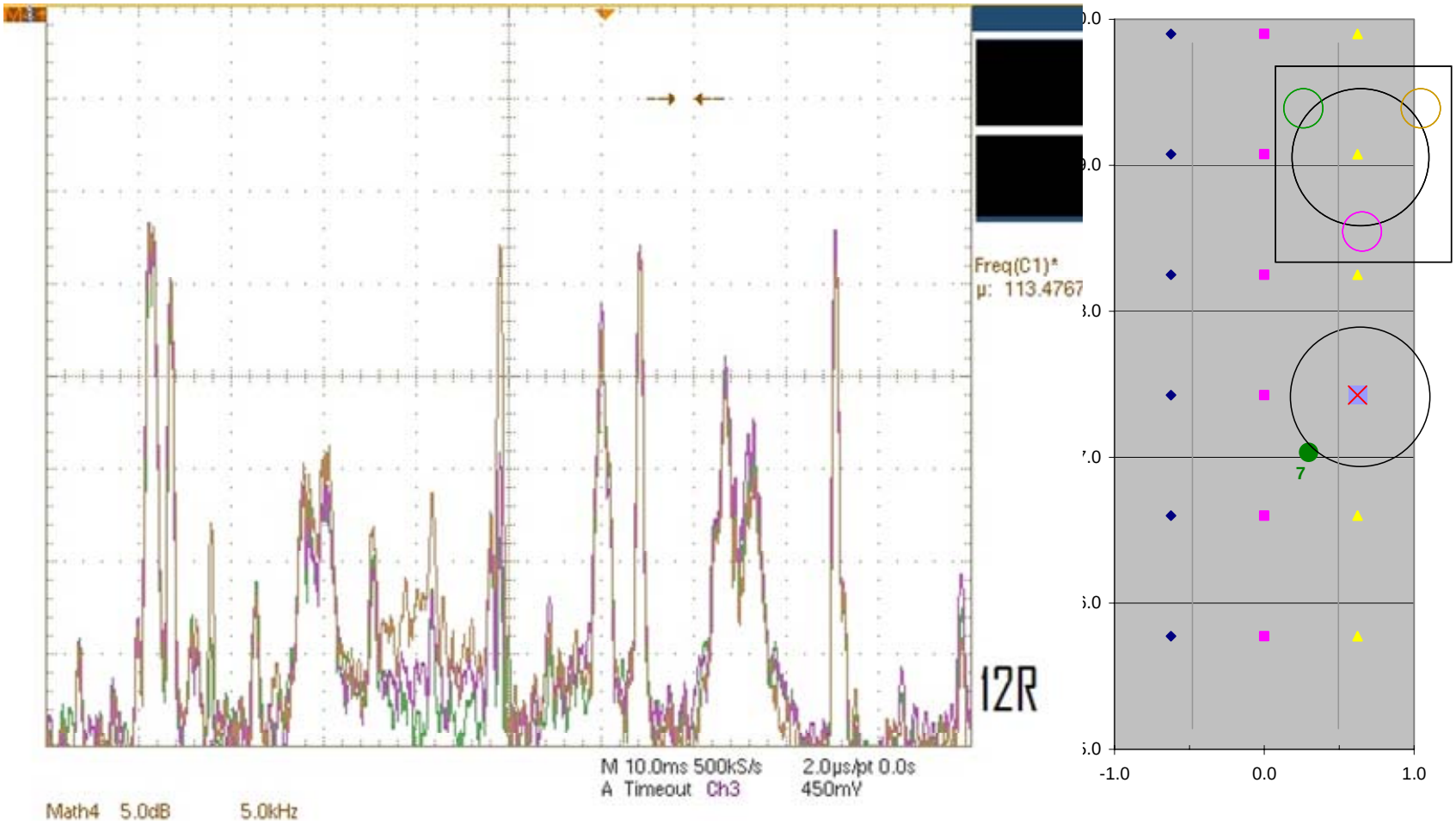

Figure 135. Data taken at position (12, R)

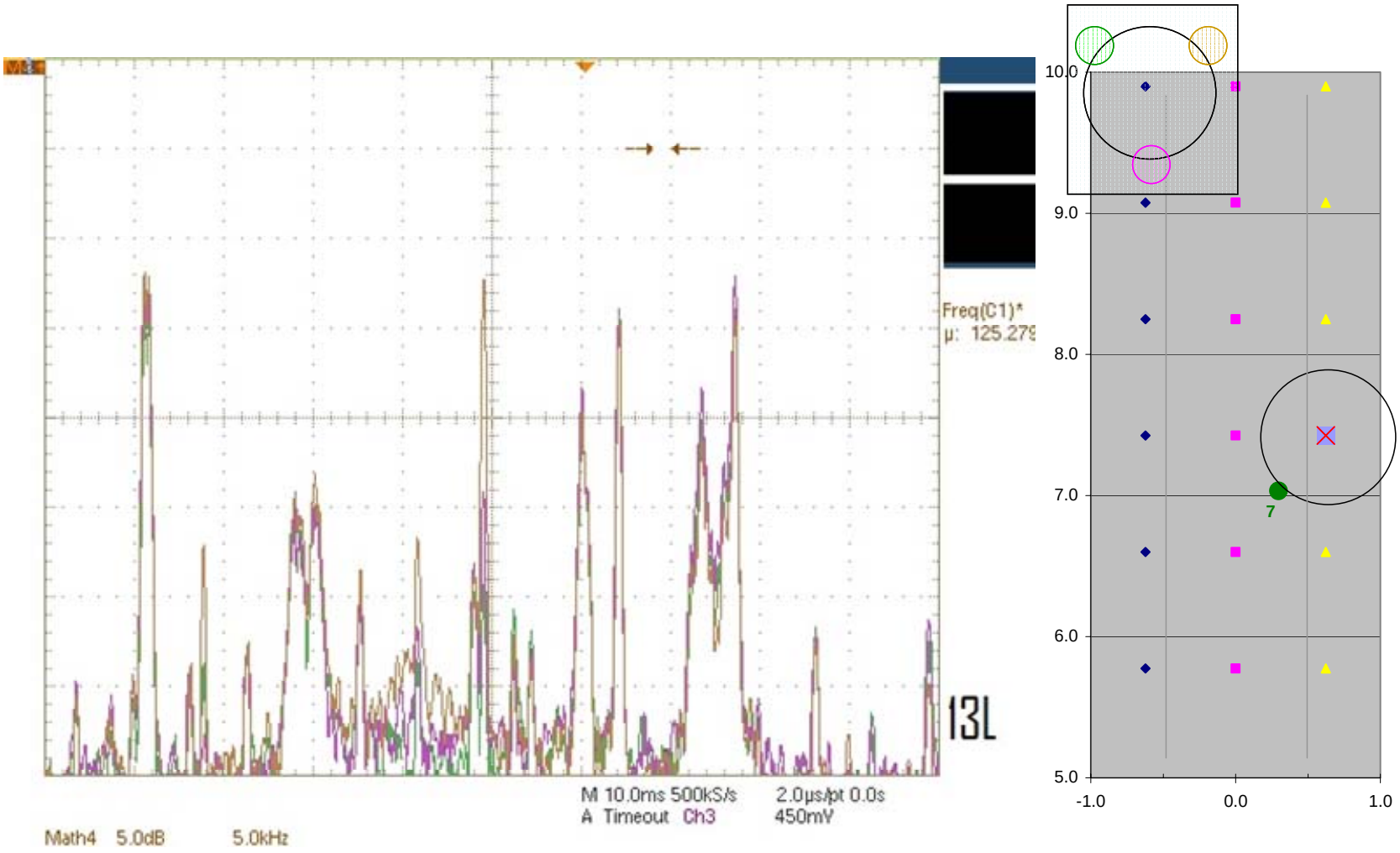

Figure 136. Data taken at position (13, L)

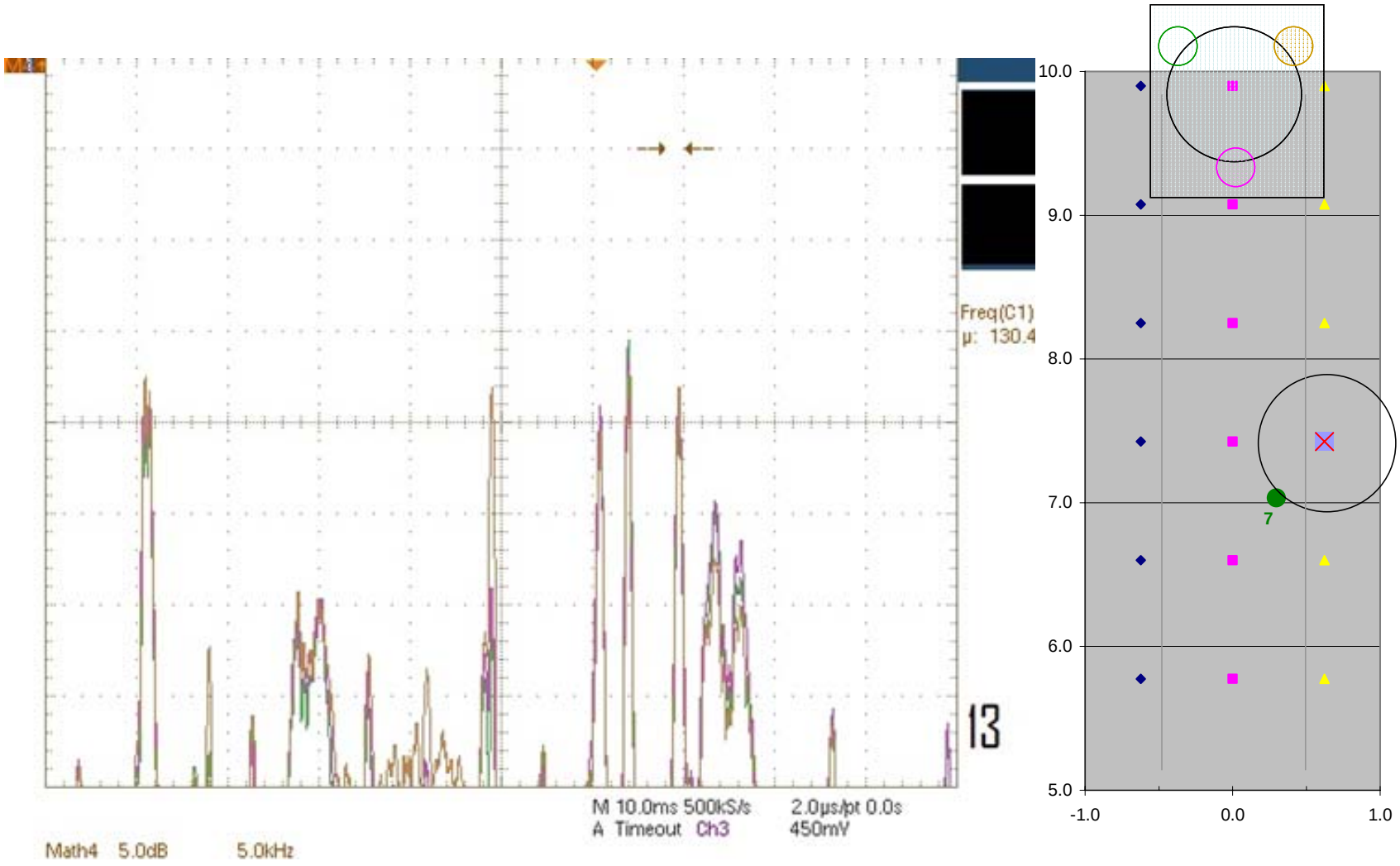

Figure 137. Data taken at position (13, C)

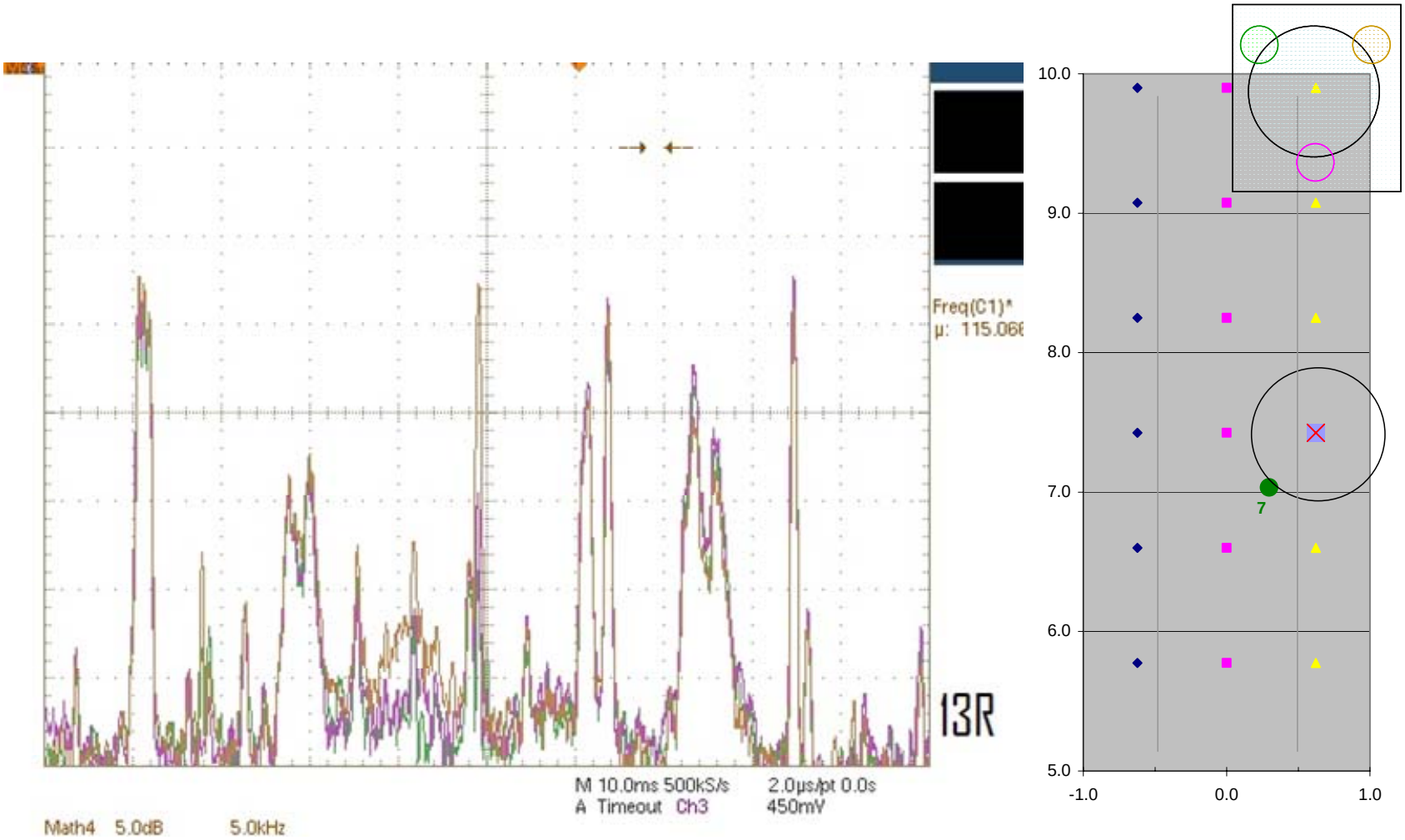

Figure 138. Data taken at position (13, R)

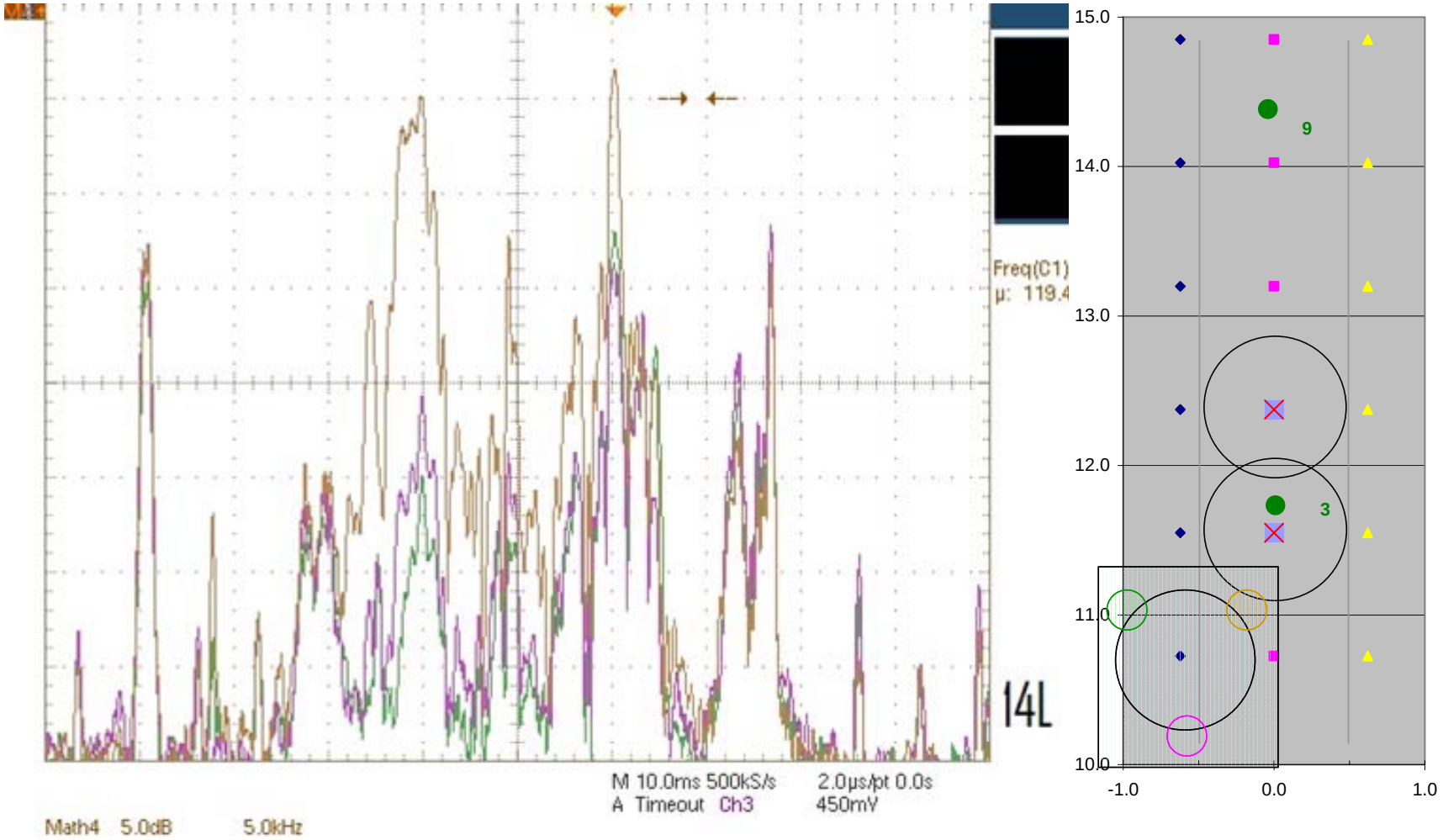

Figure 139. Data taken at position (14, L)

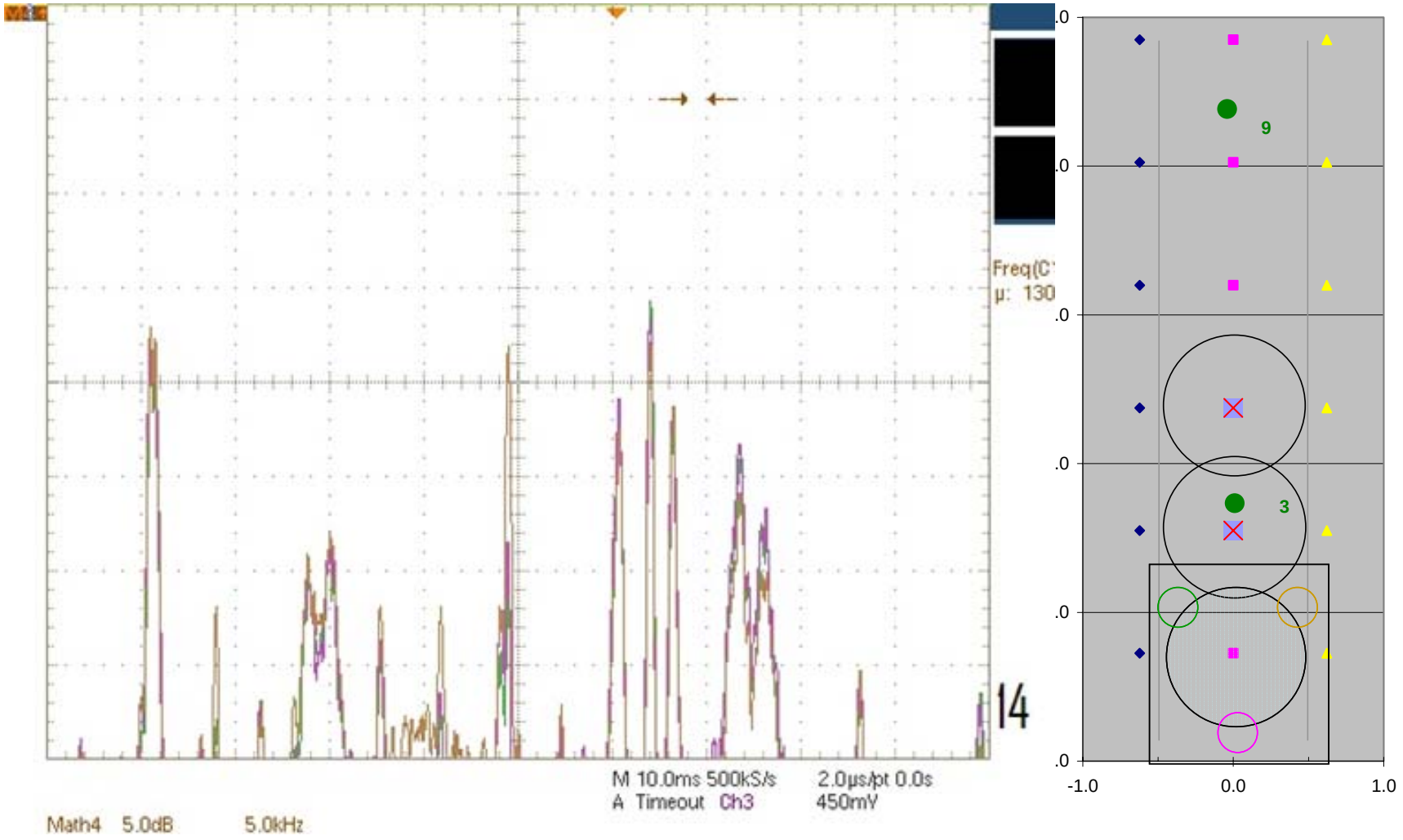

Figure 140. Data taken at position (14, C)

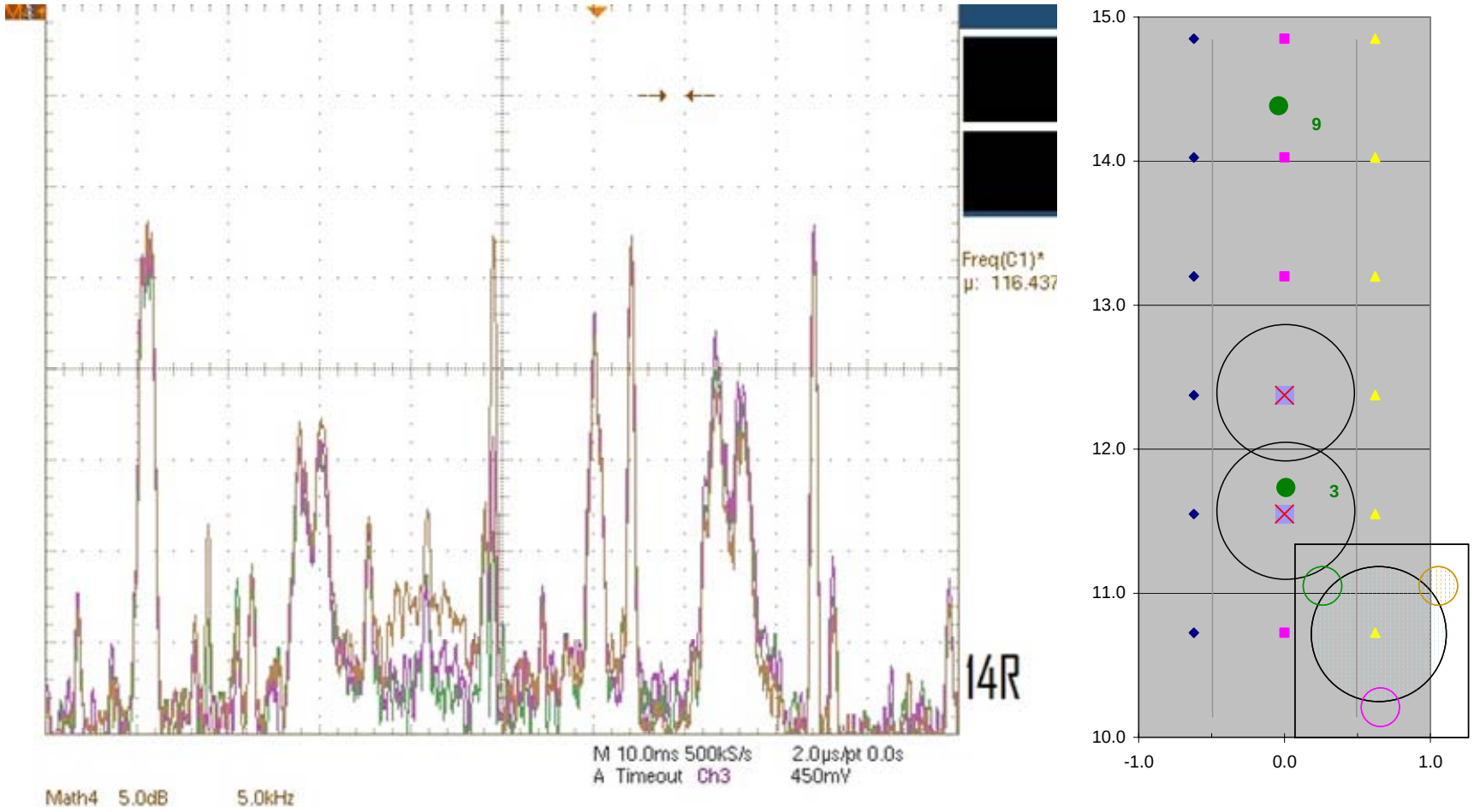

Figure 141. Data taken at position (14, R)

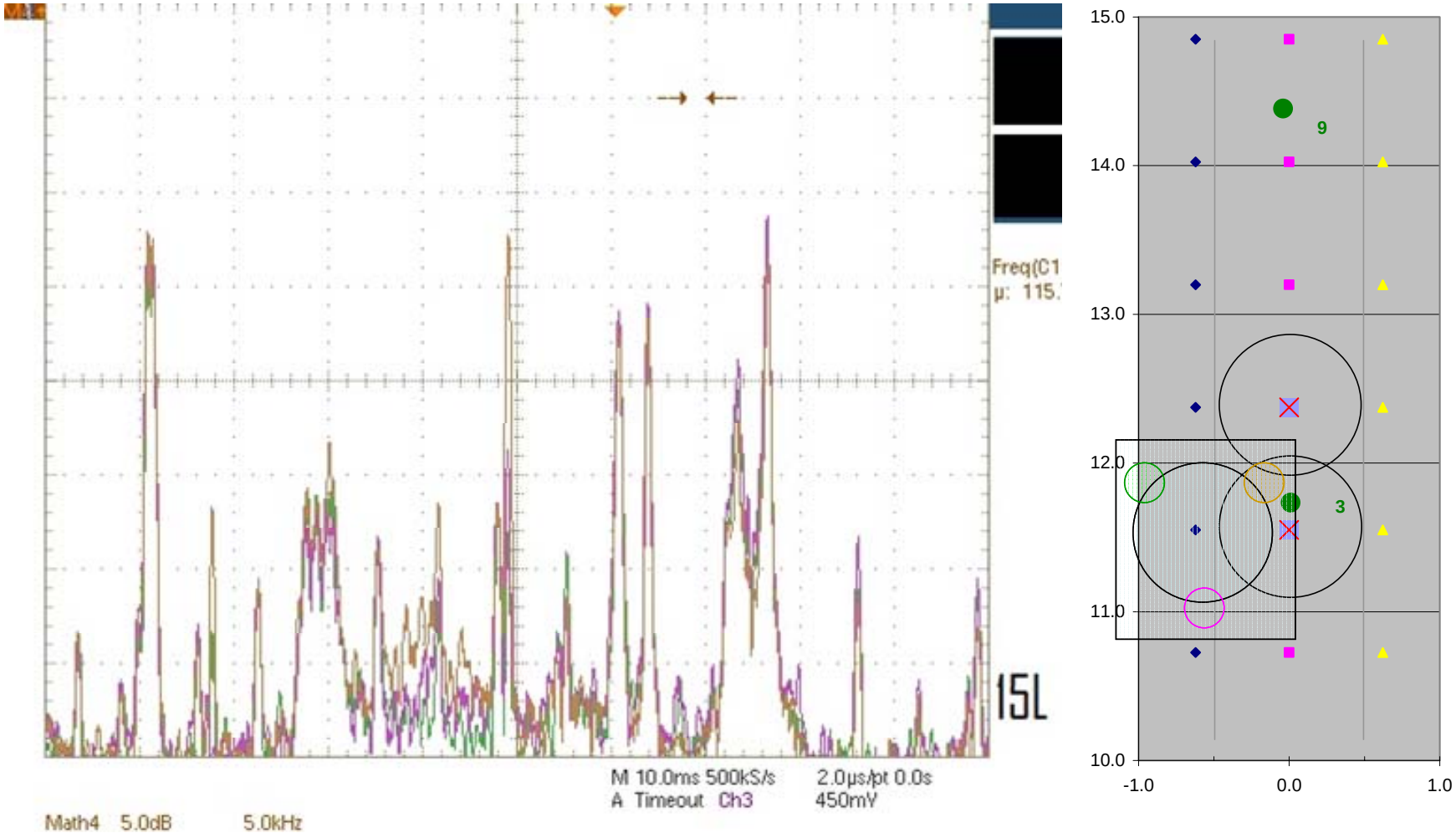

Figure 142. Data taken at position (15, L)

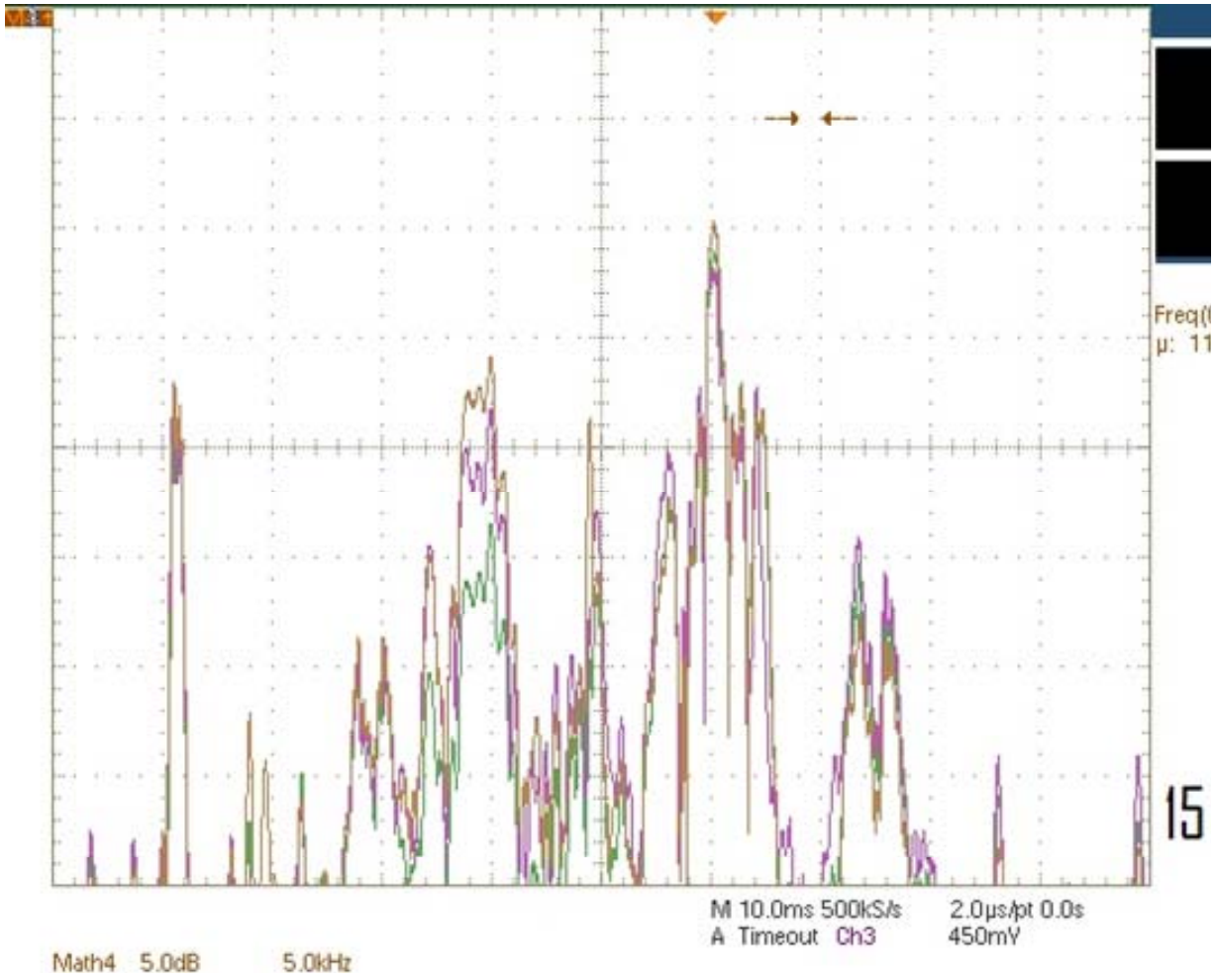

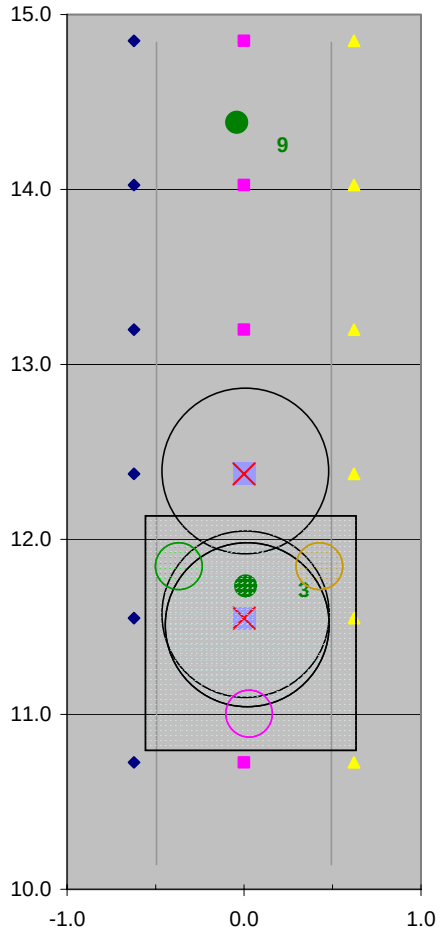

Figure 143. Data taken at position (15, C)

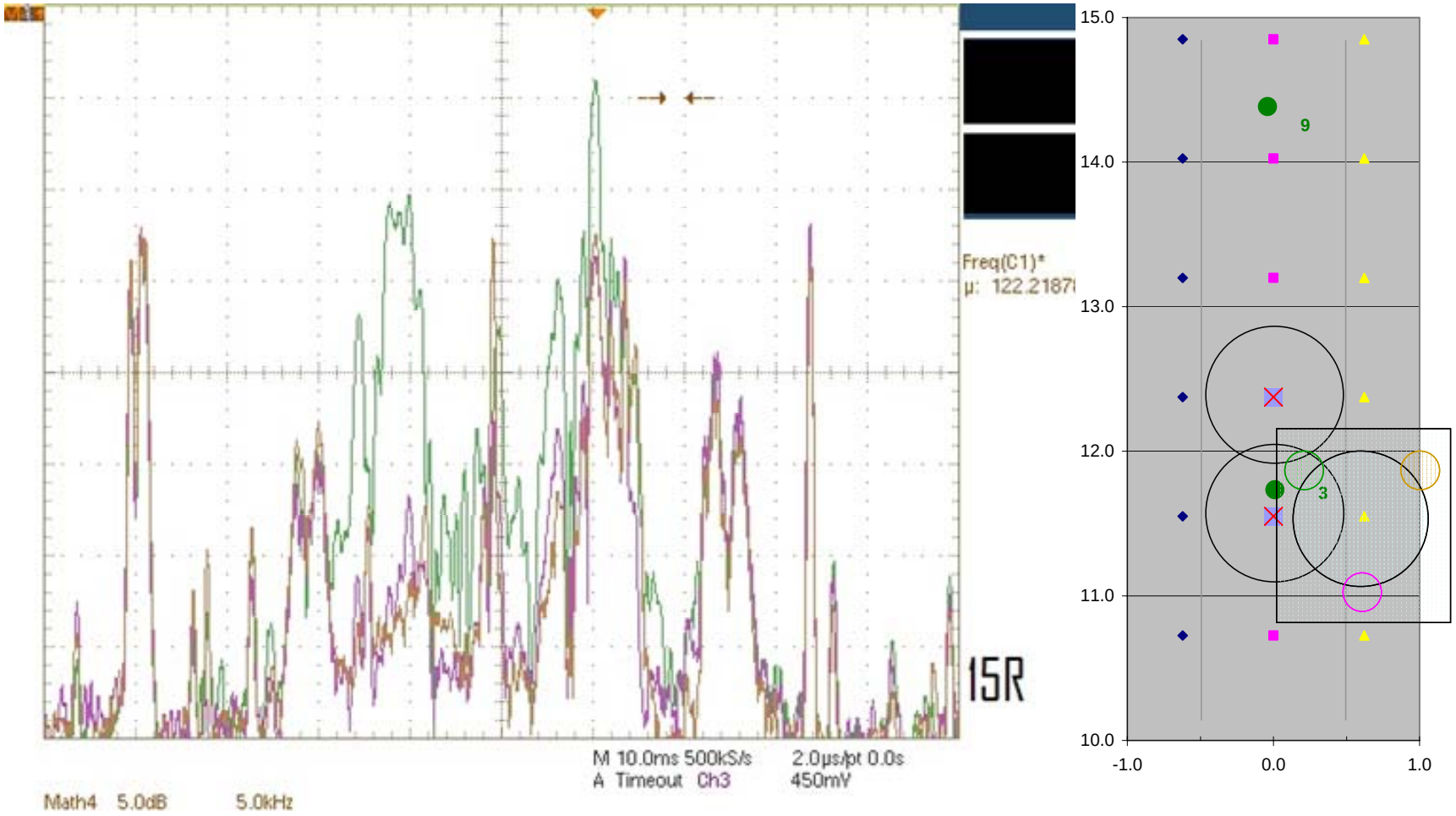

Figure 144. Data taken at position (15, R)

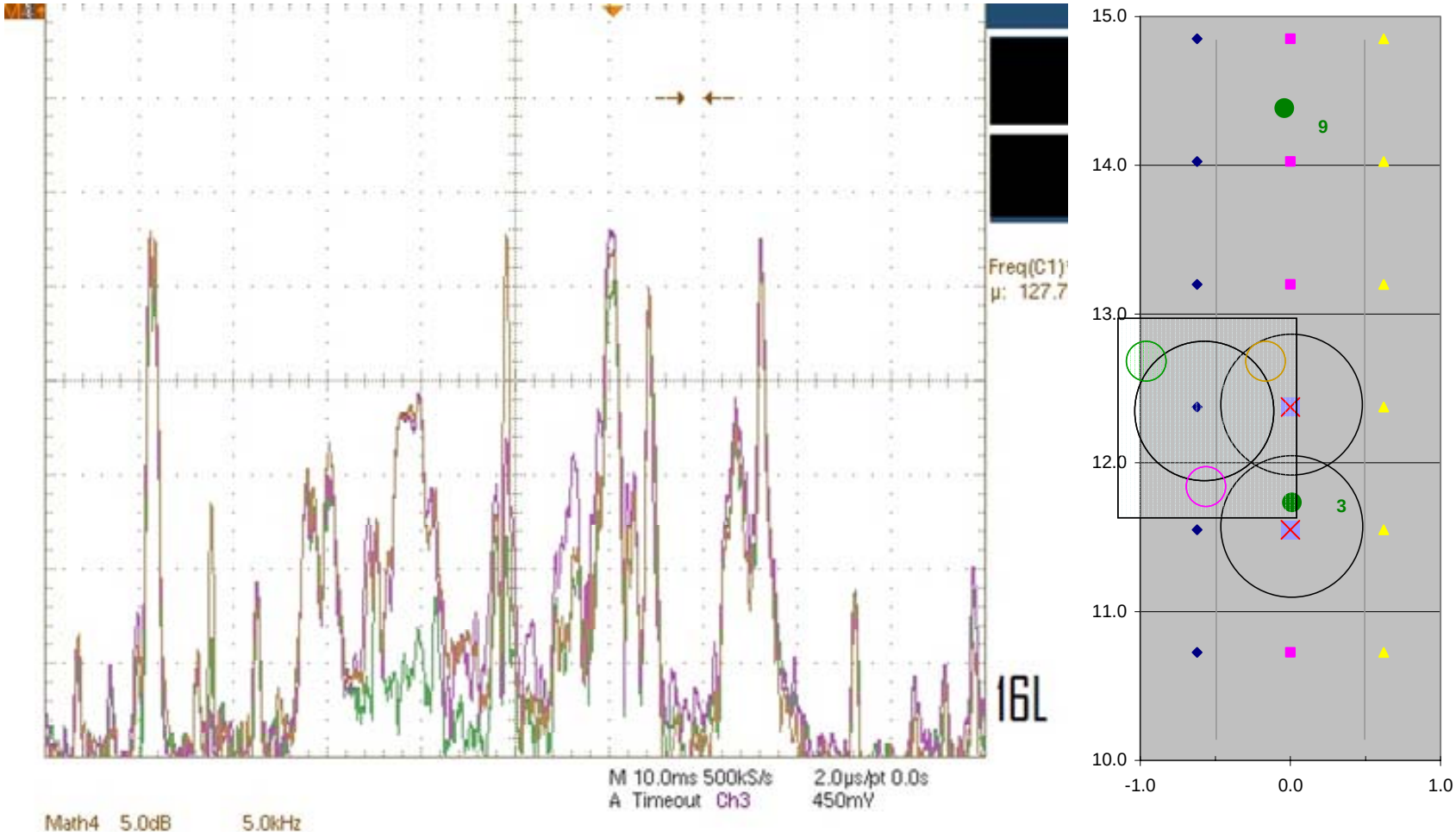

Figure 145. Data taken at position (16, L)

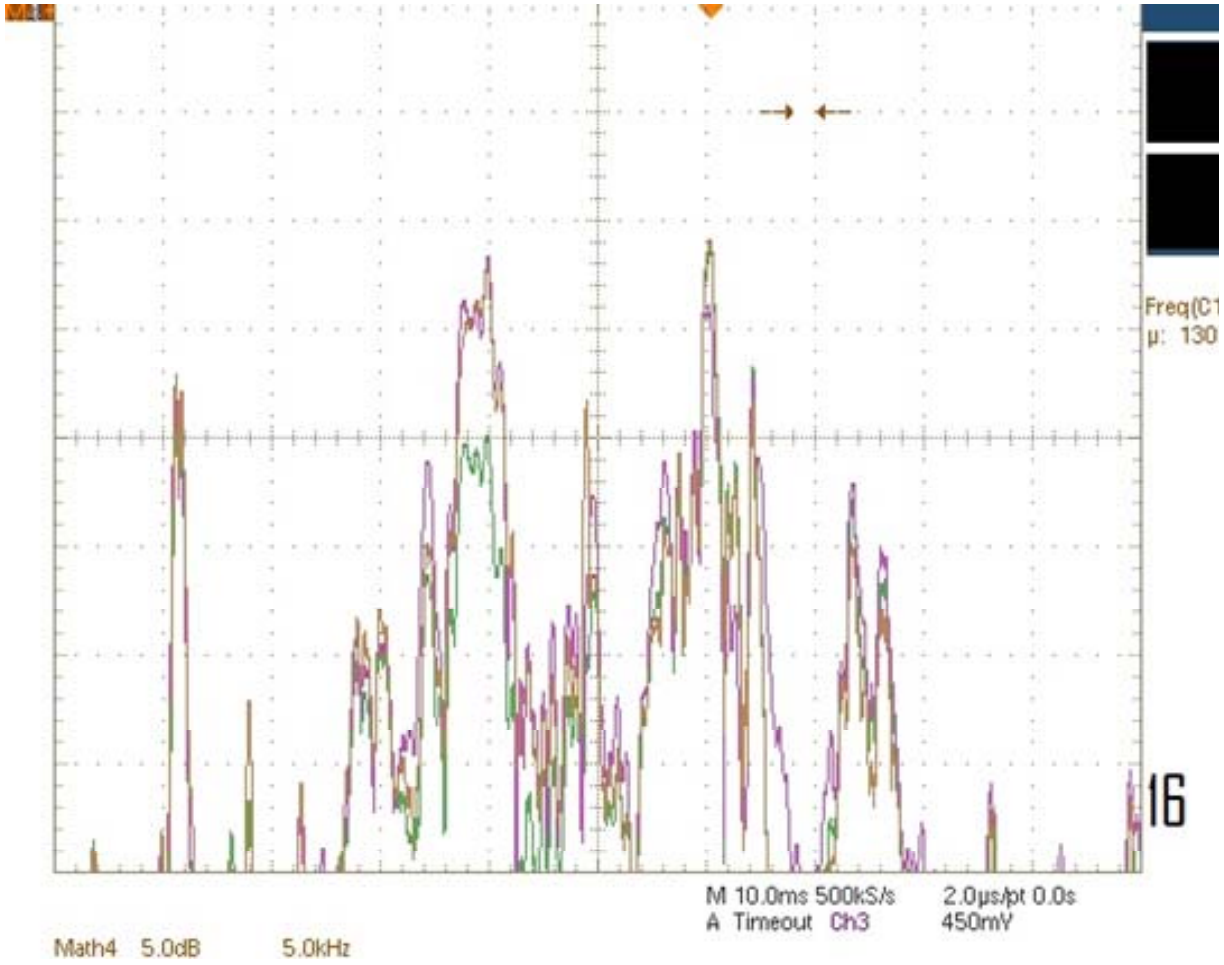

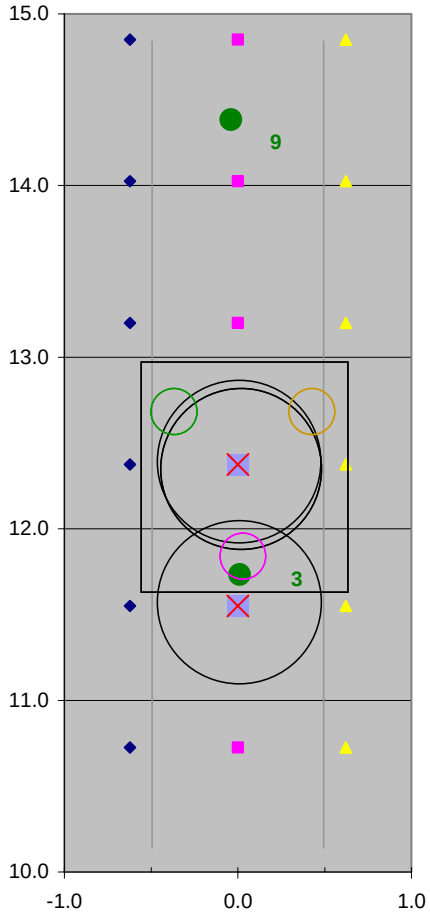

Figure 146. Data taken at position (16, C)

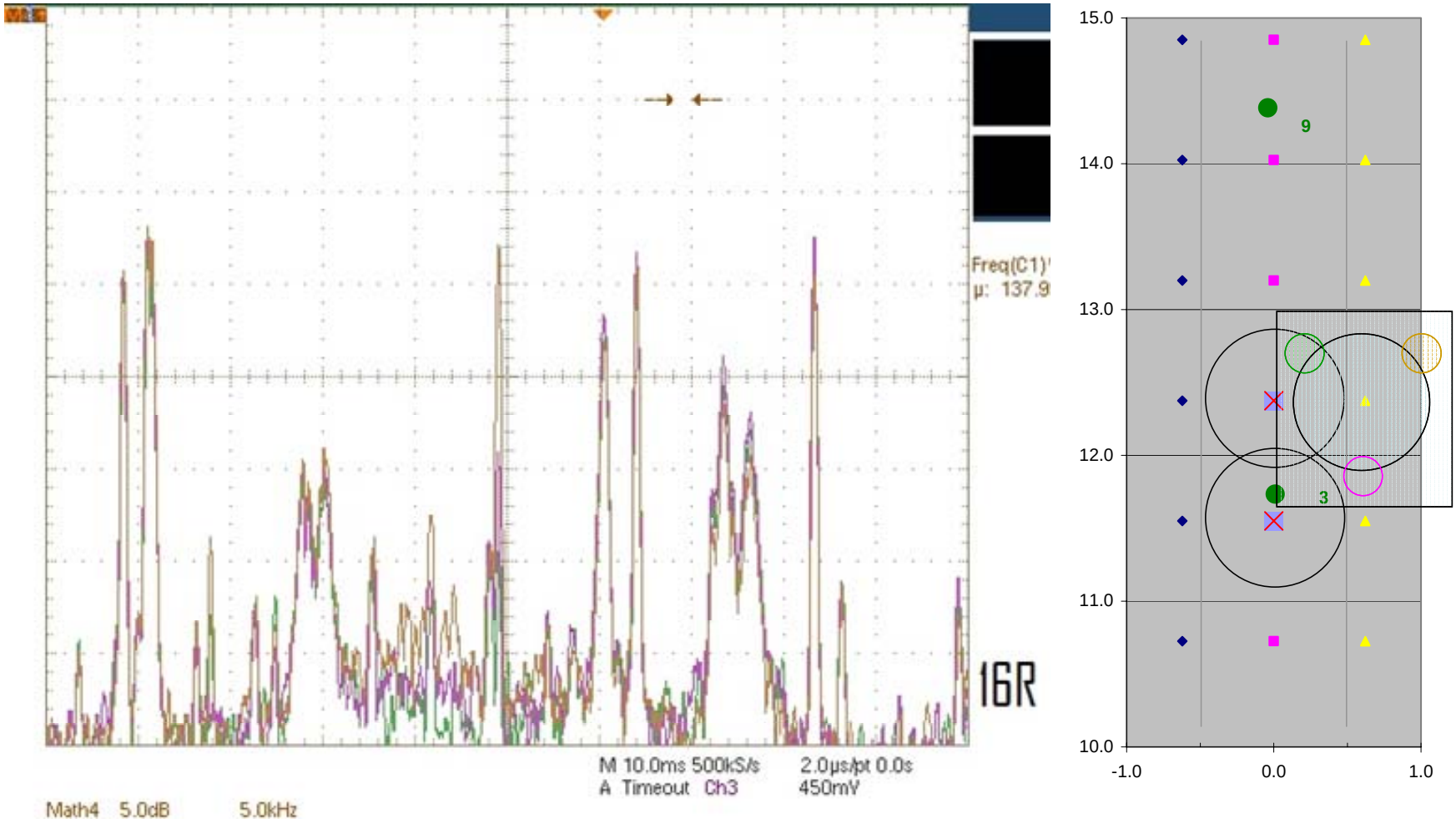

Figure 147. Data taken at position (16, R)

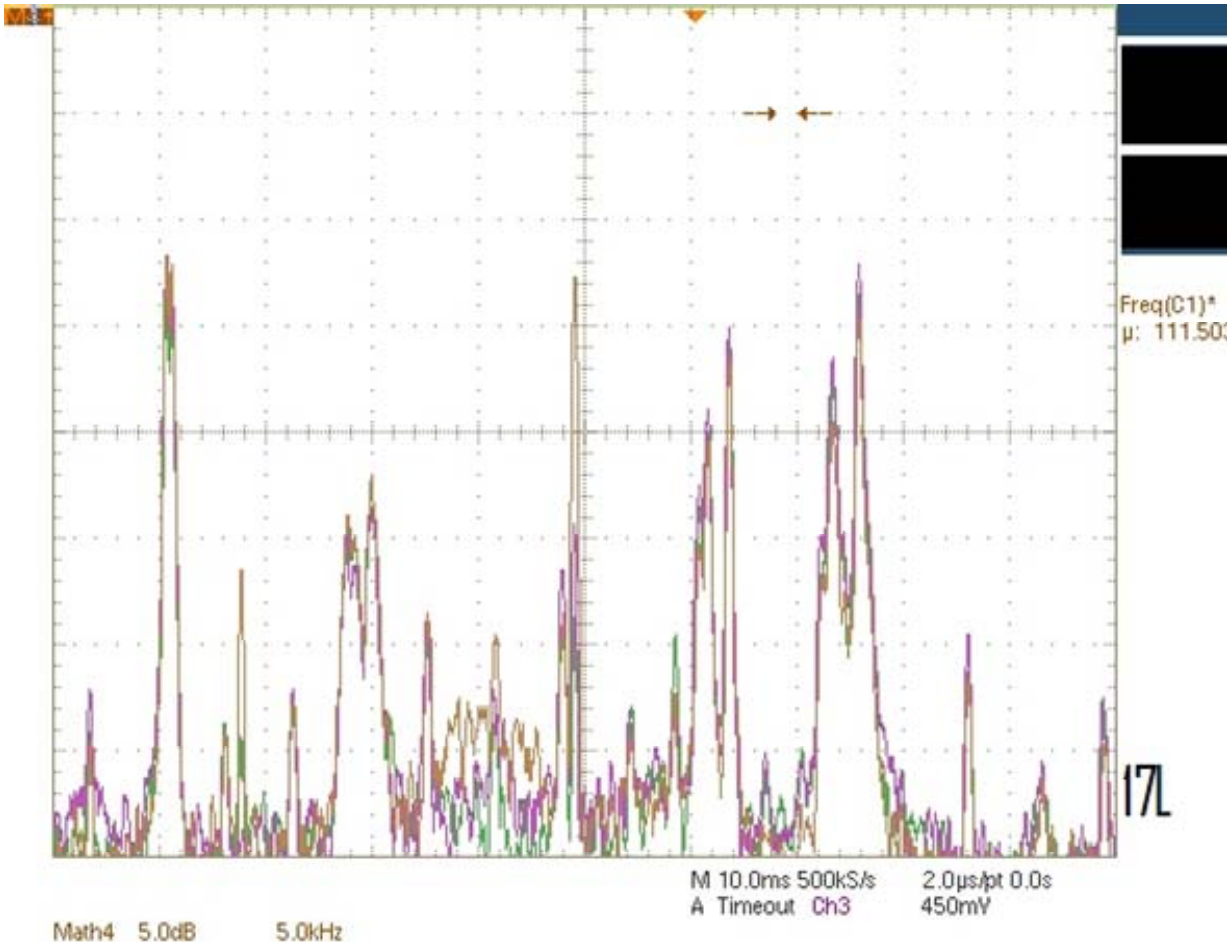

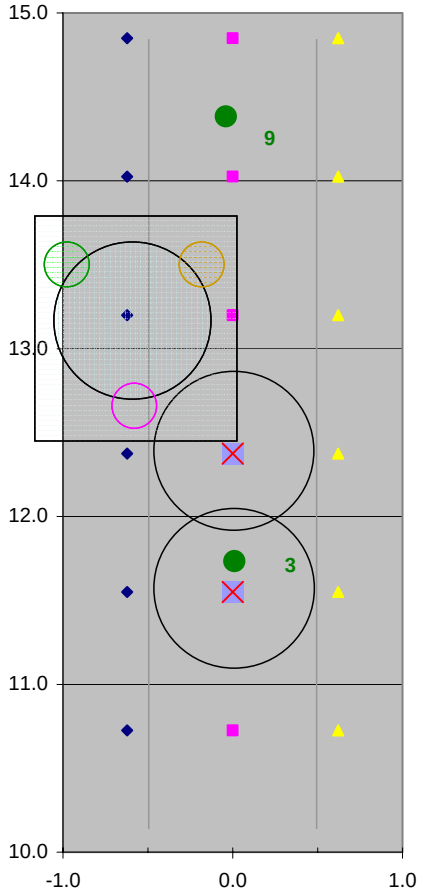

Figure 148. Data taken at position (17, L)

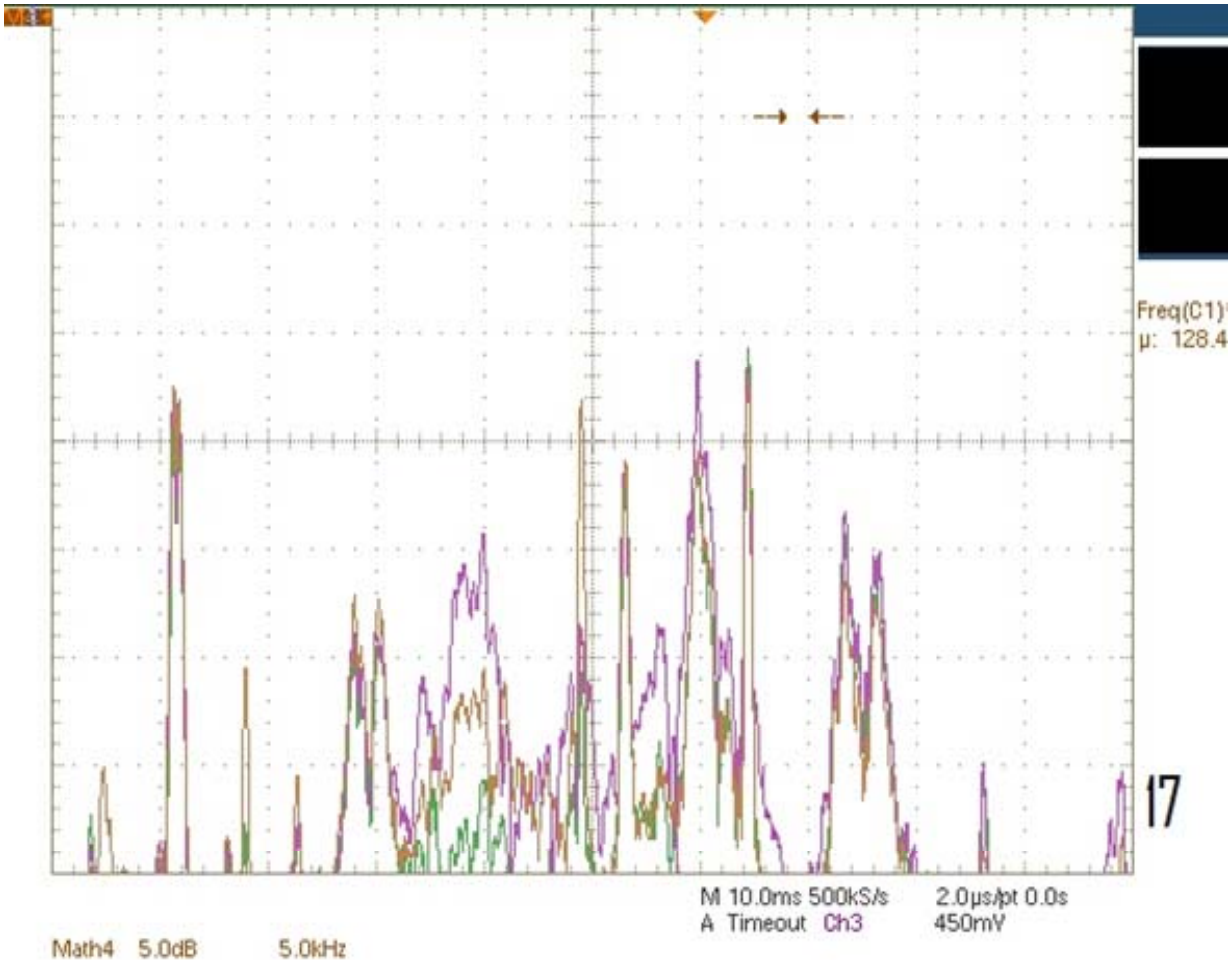

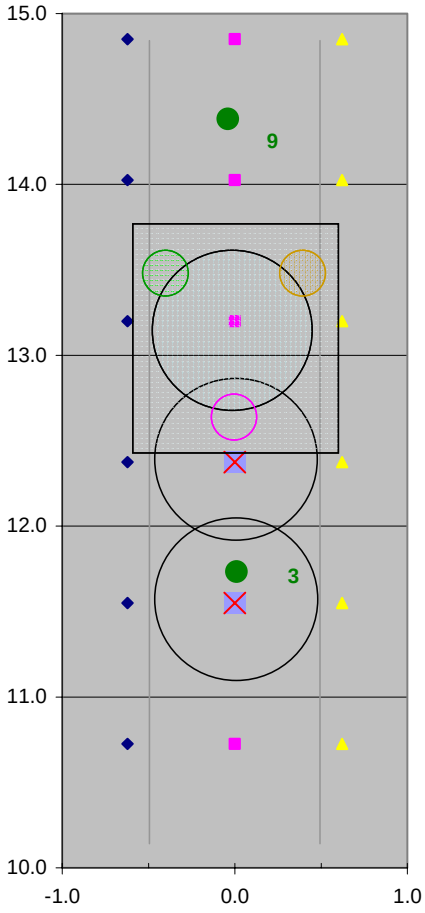

Figure 149. Data taken at position (17, C)

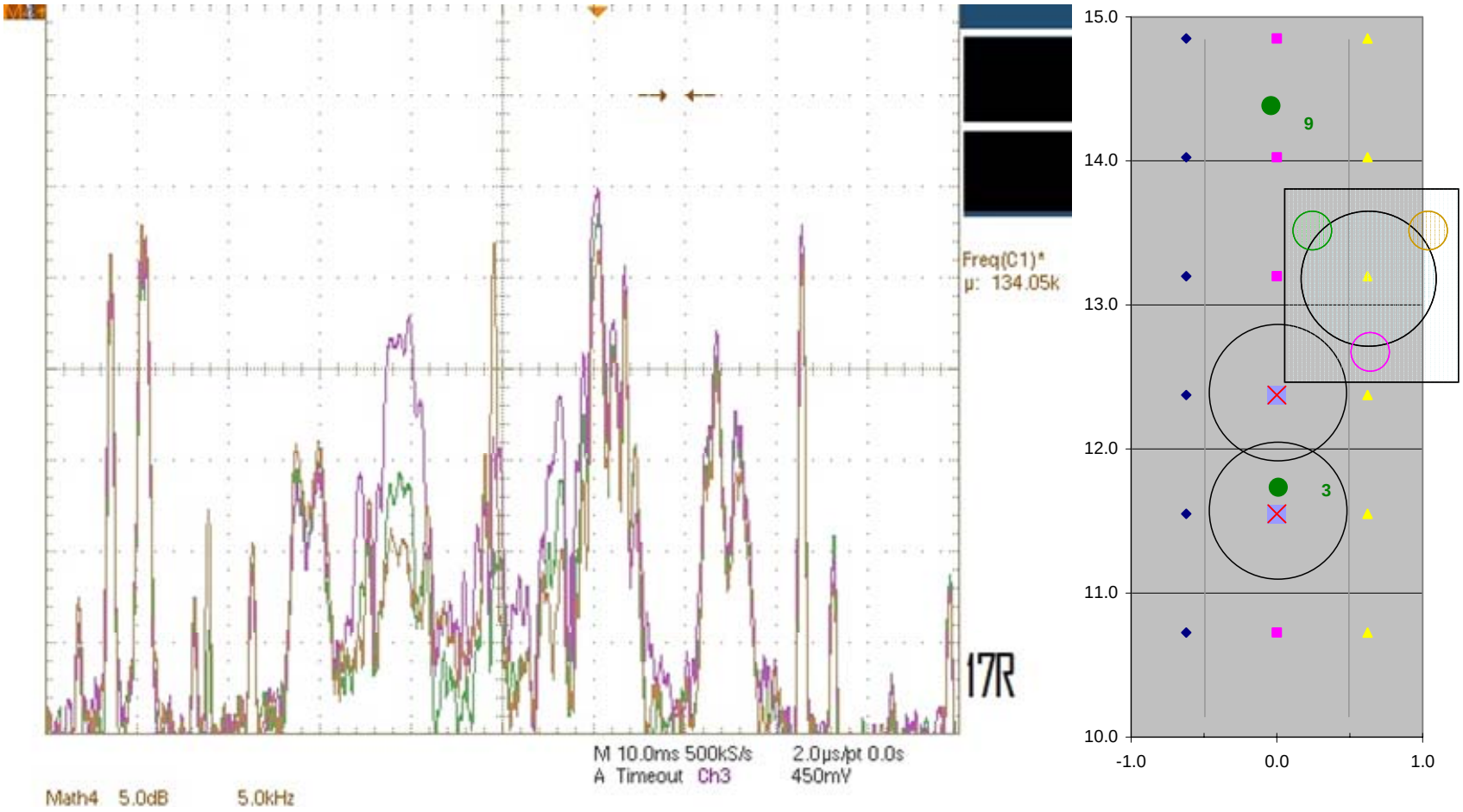

Figure 150. Data taken at position (17, R)

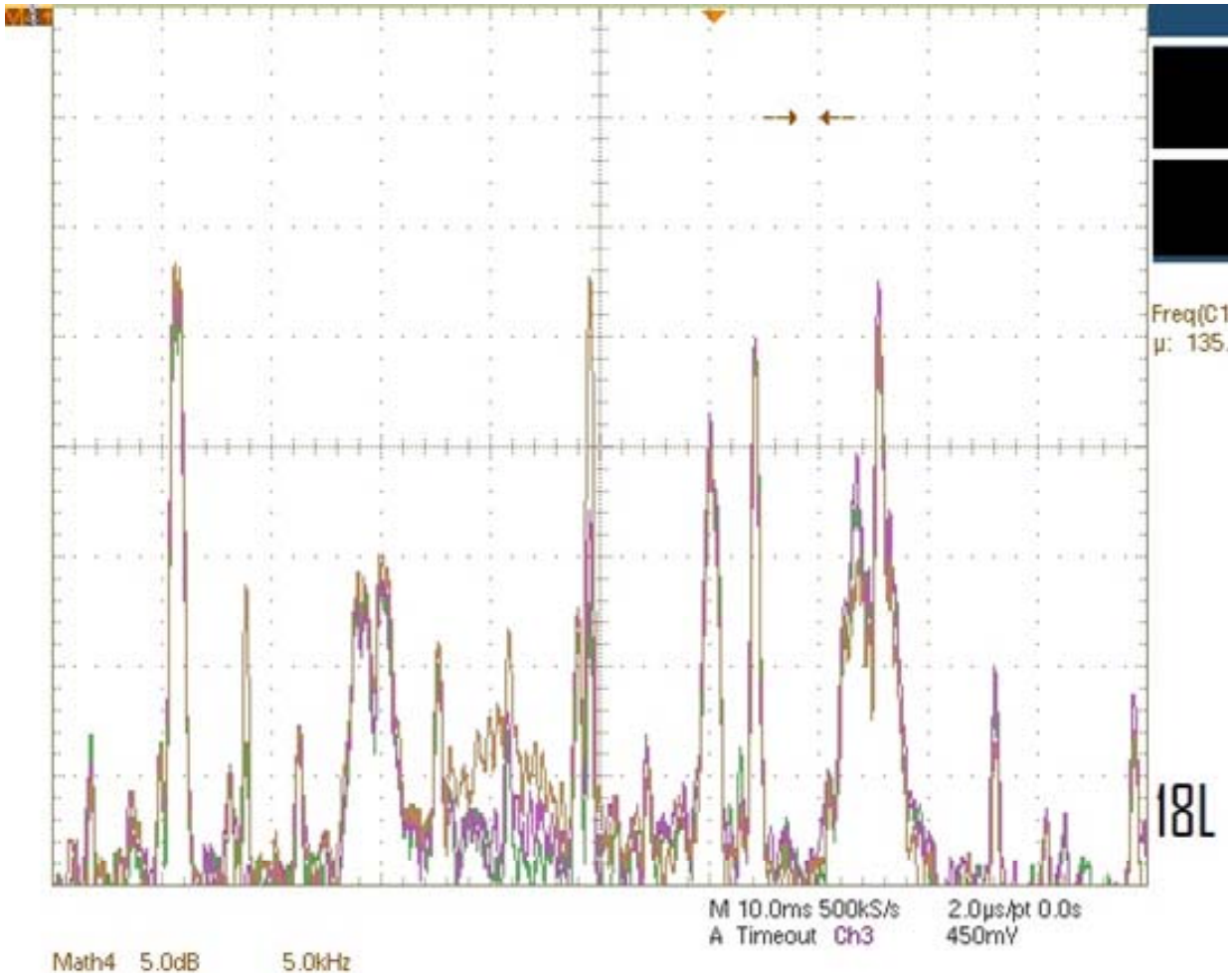

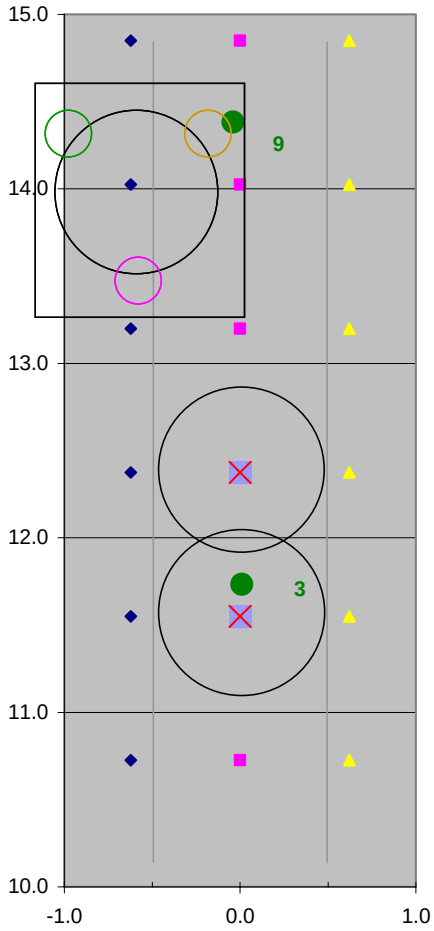

Figure 151. Data taken at position (18, L)

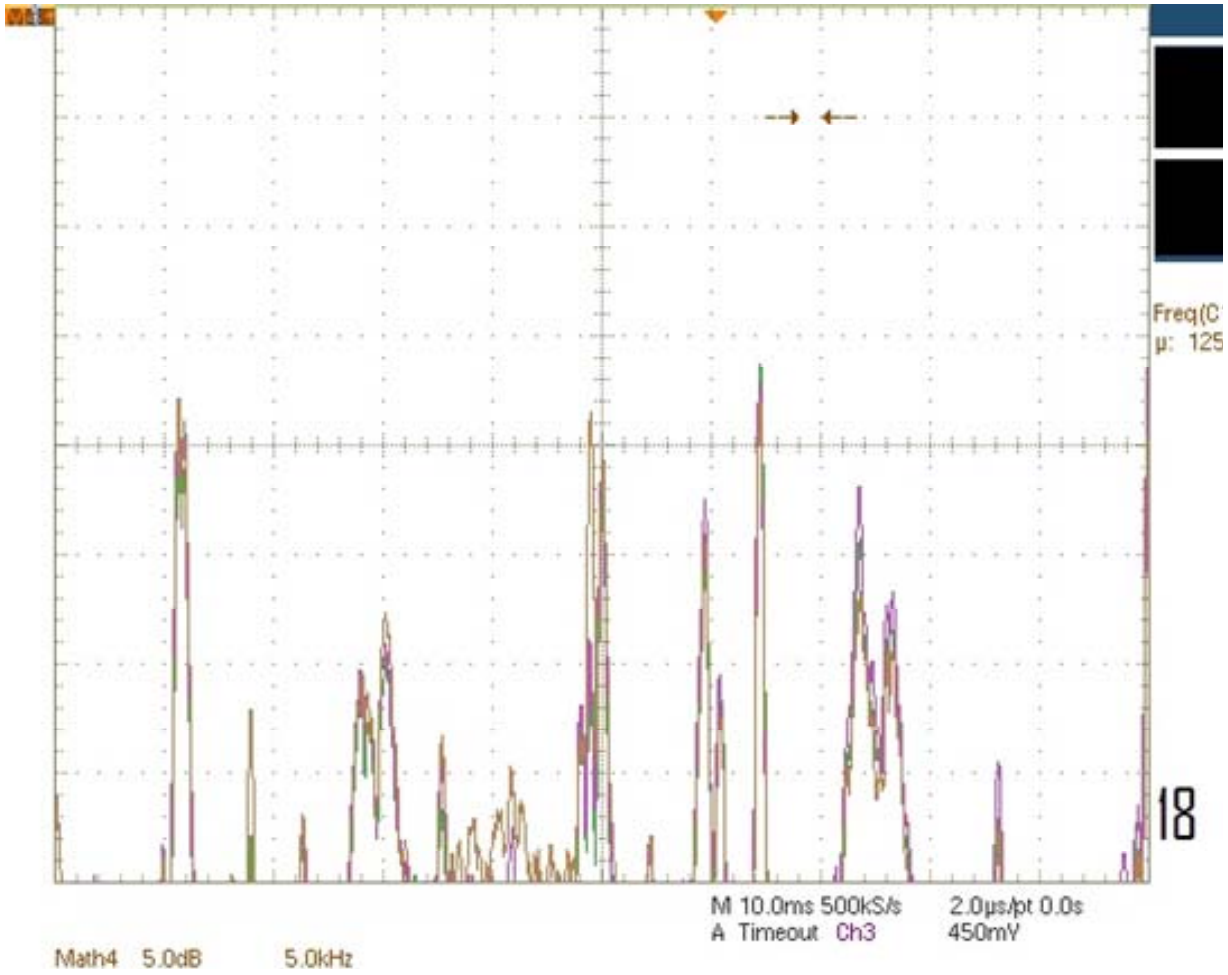

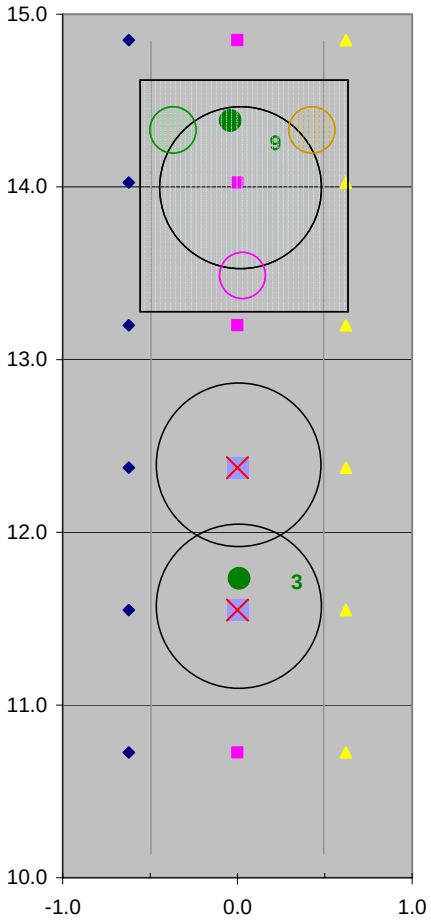

Figure 152. Data taken at position (18, C)

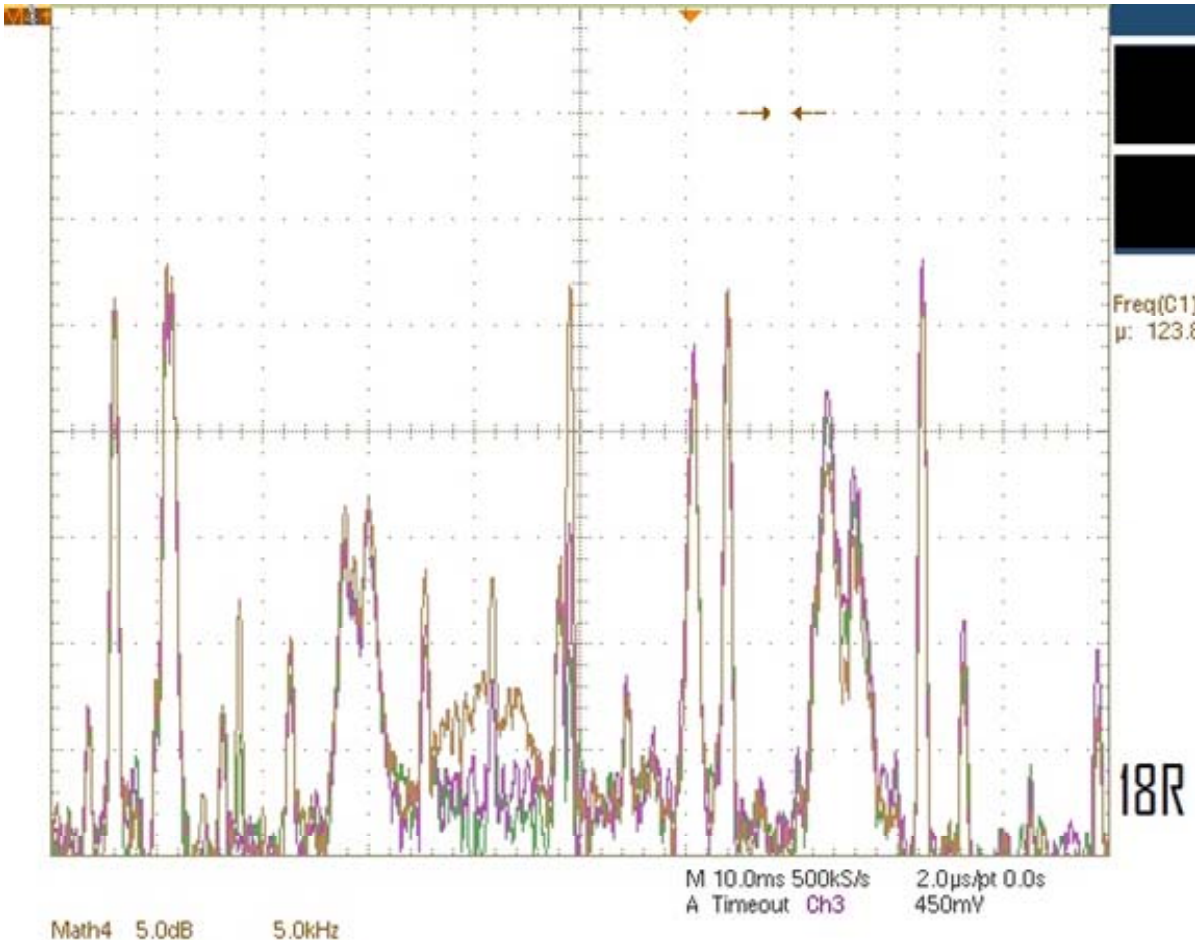

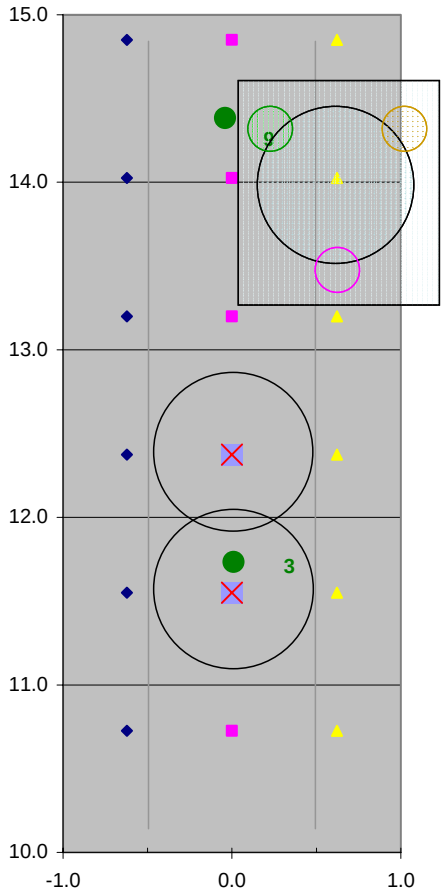

Figure 153. Data taken at position (18, R)

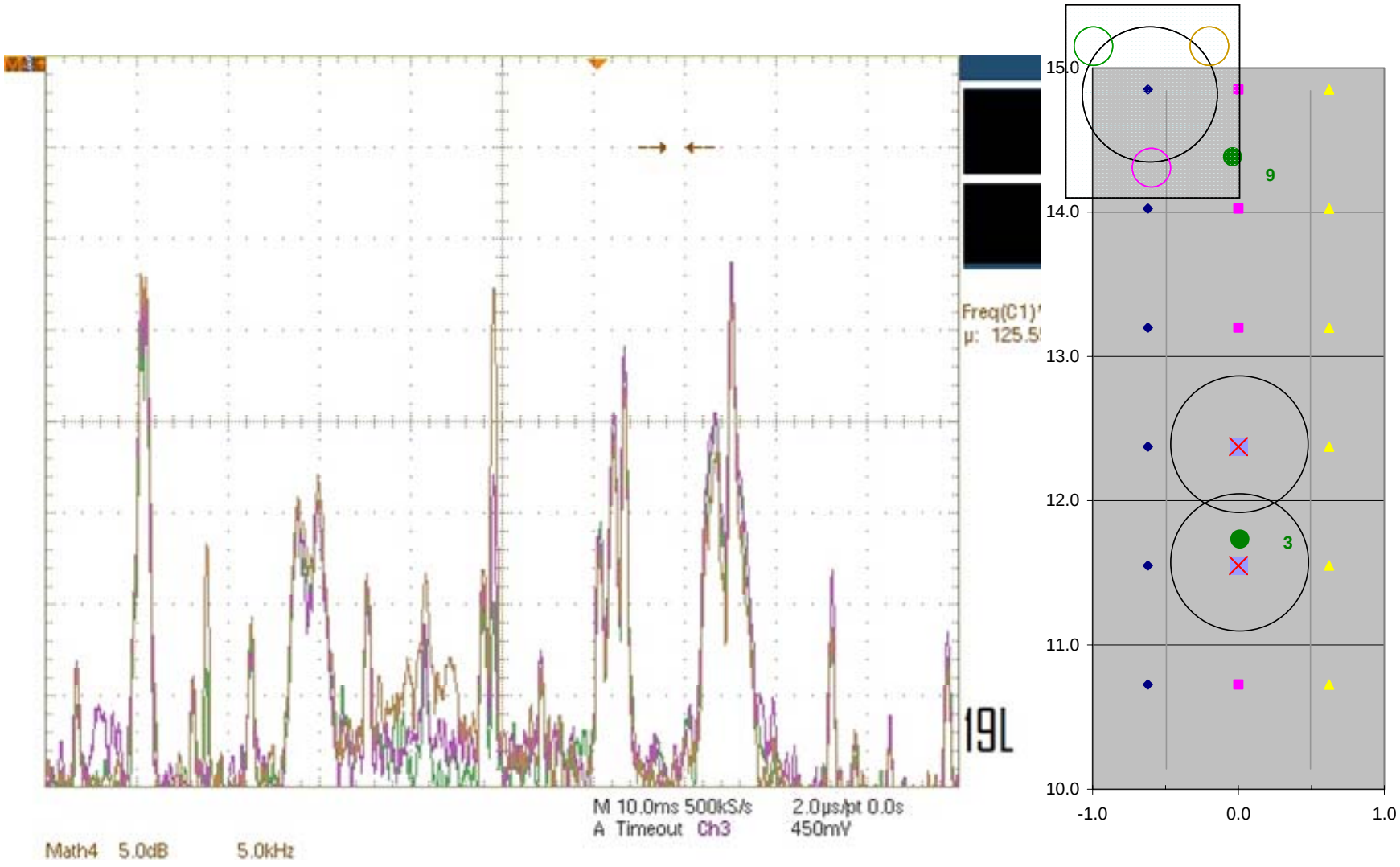

Figure 154. Data taken at position (19, L)

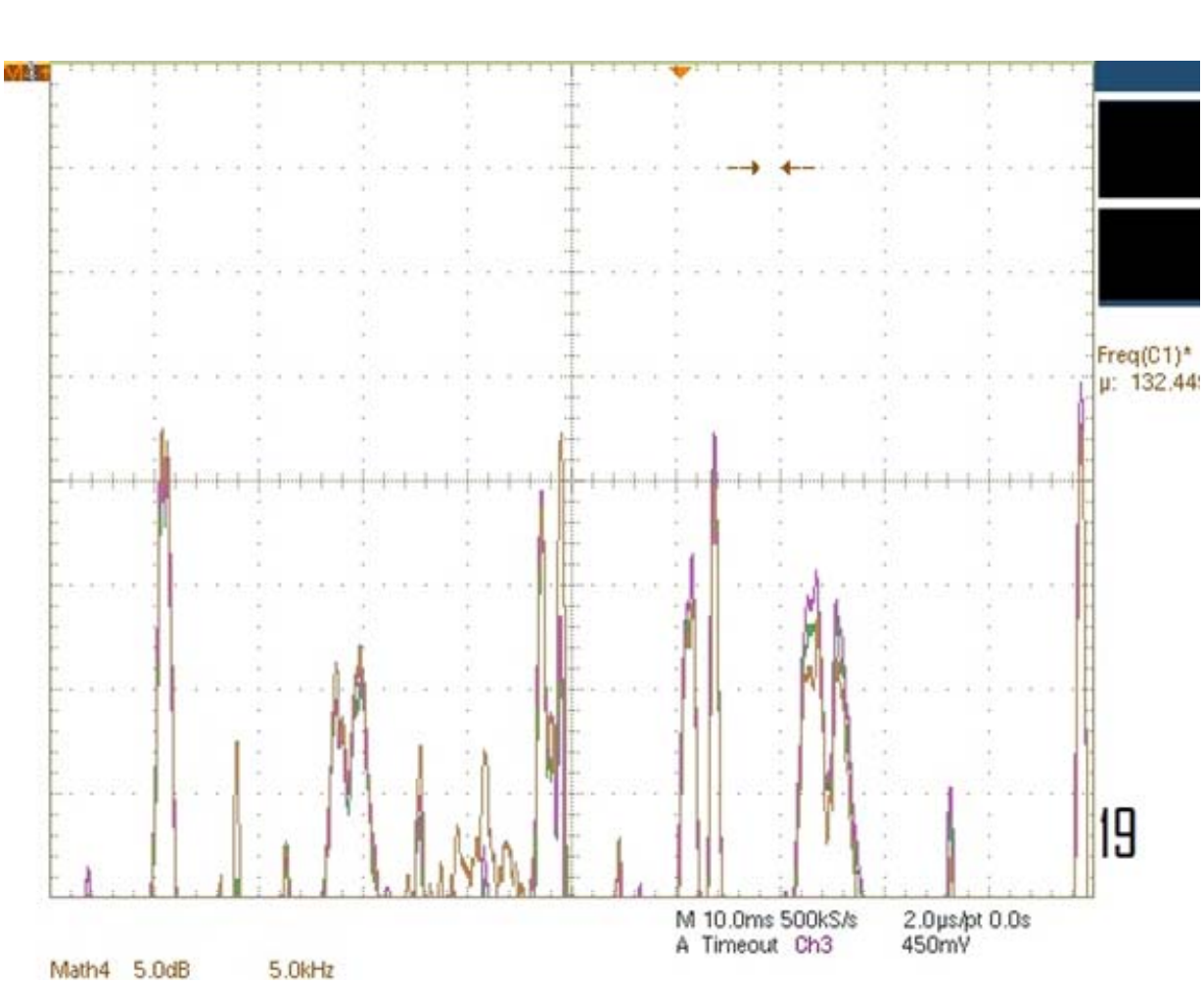

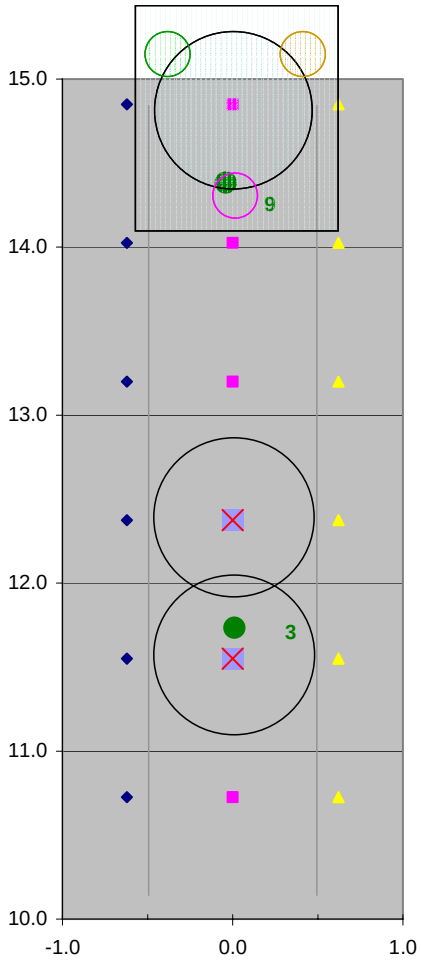

Figure 155. Data taken at position (19, C)

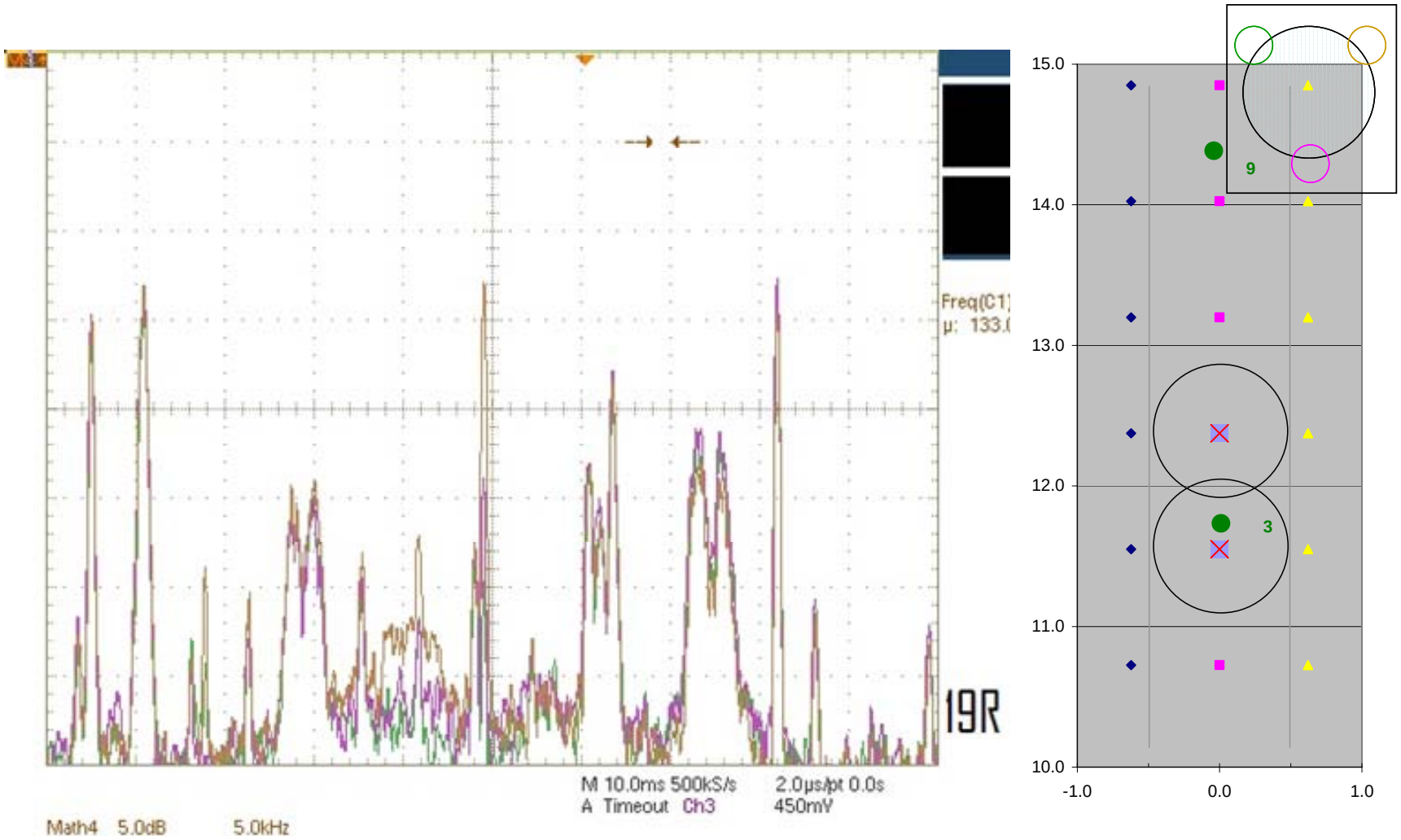

Figure 156. Data taken at position (19, R)

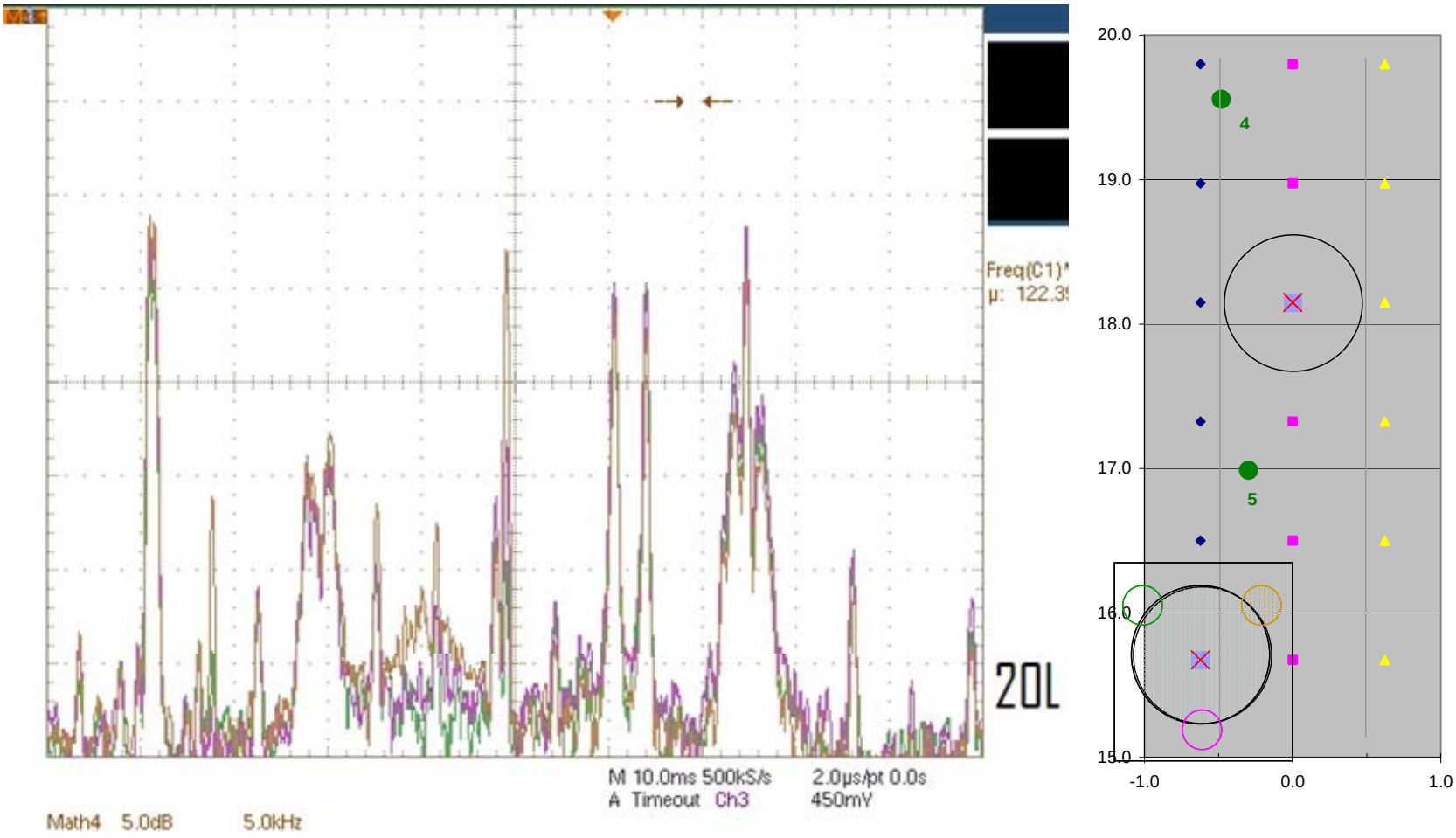

Figure 157. Data taken at position (20, L)

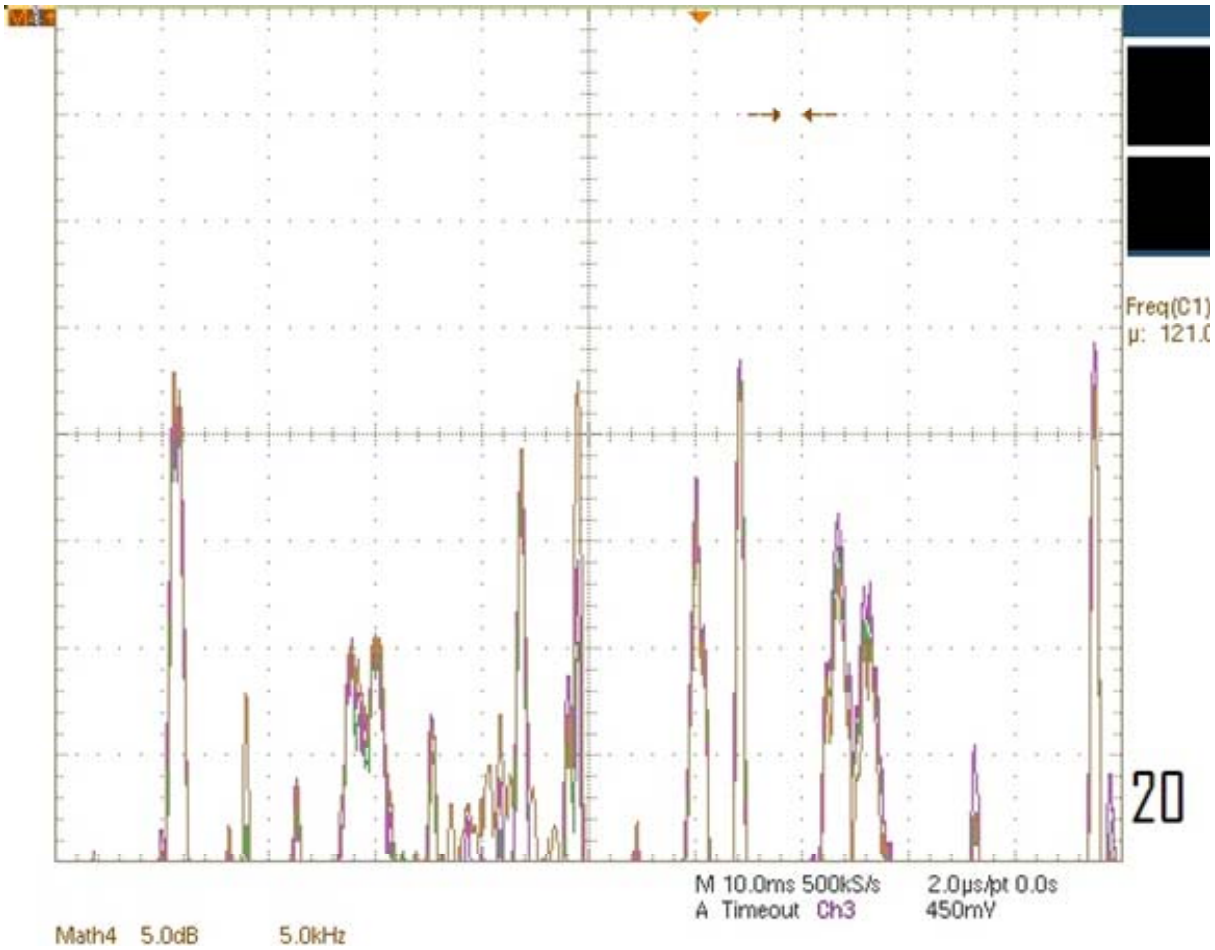

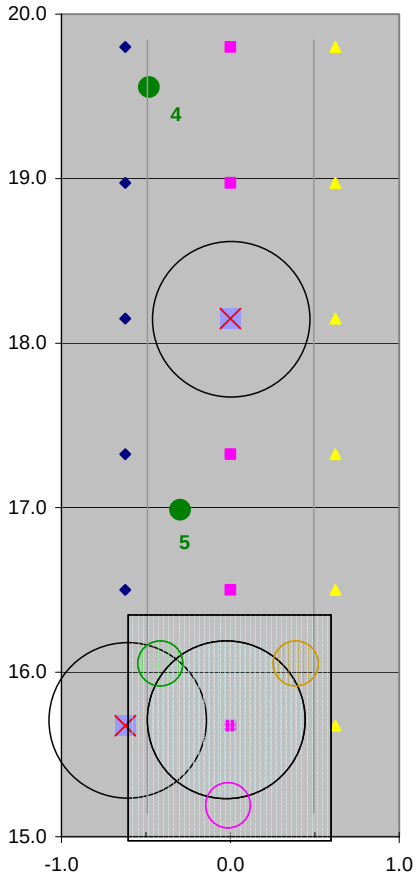

Figure 158. Data taken at position (20, C)

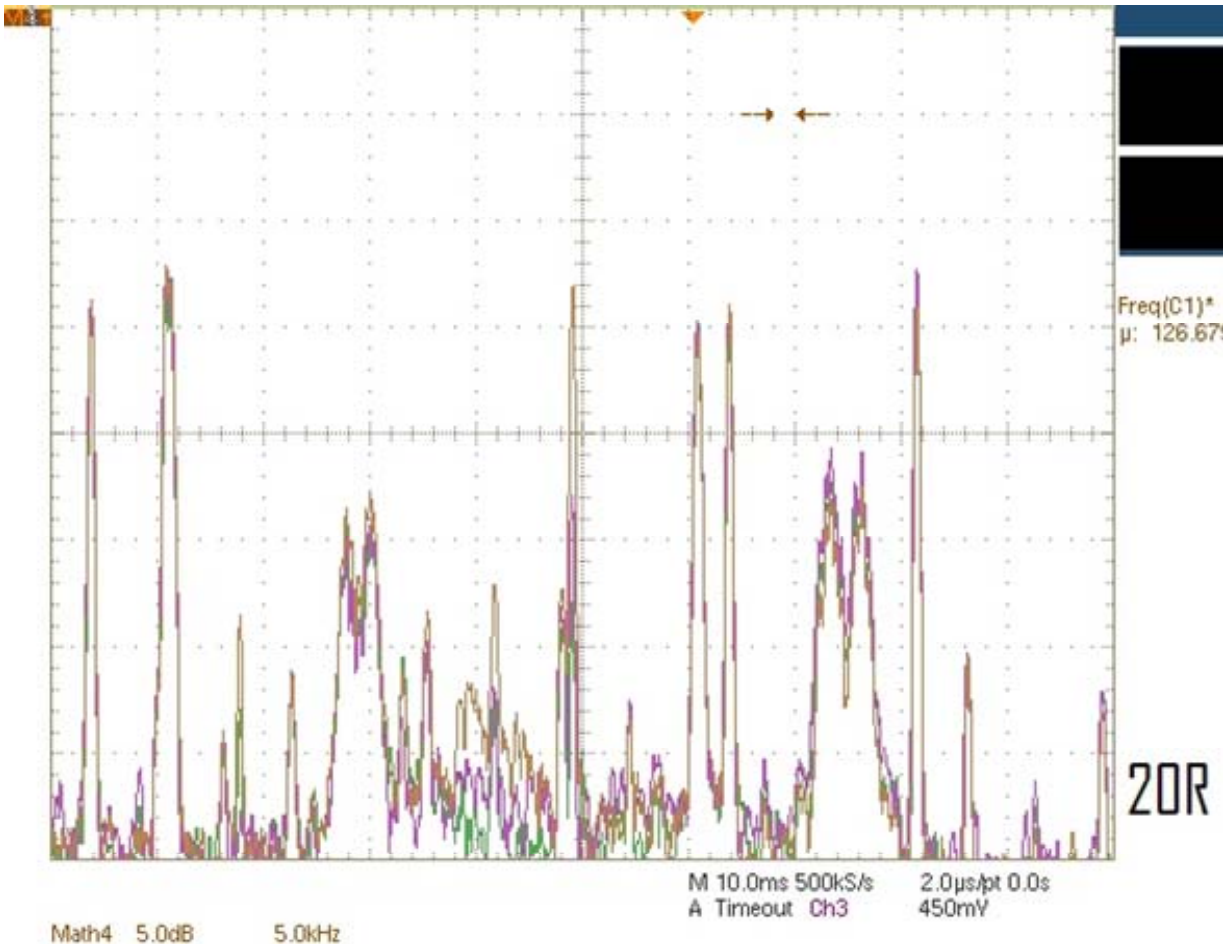

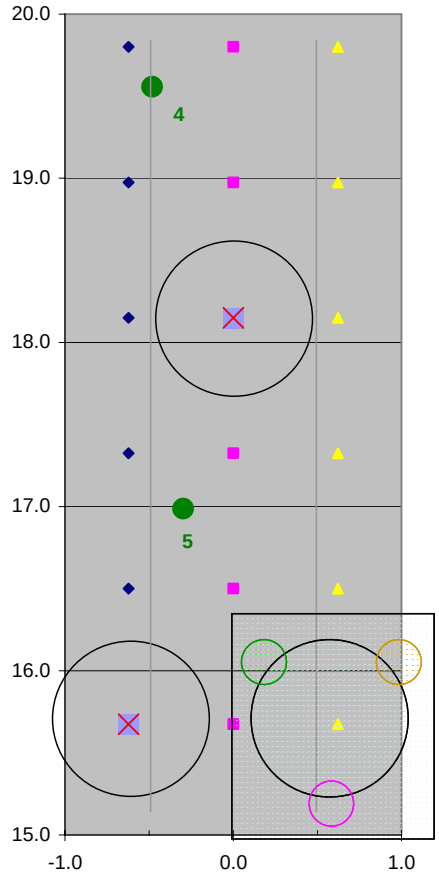

Figure 159. Data taken at position (20, R)

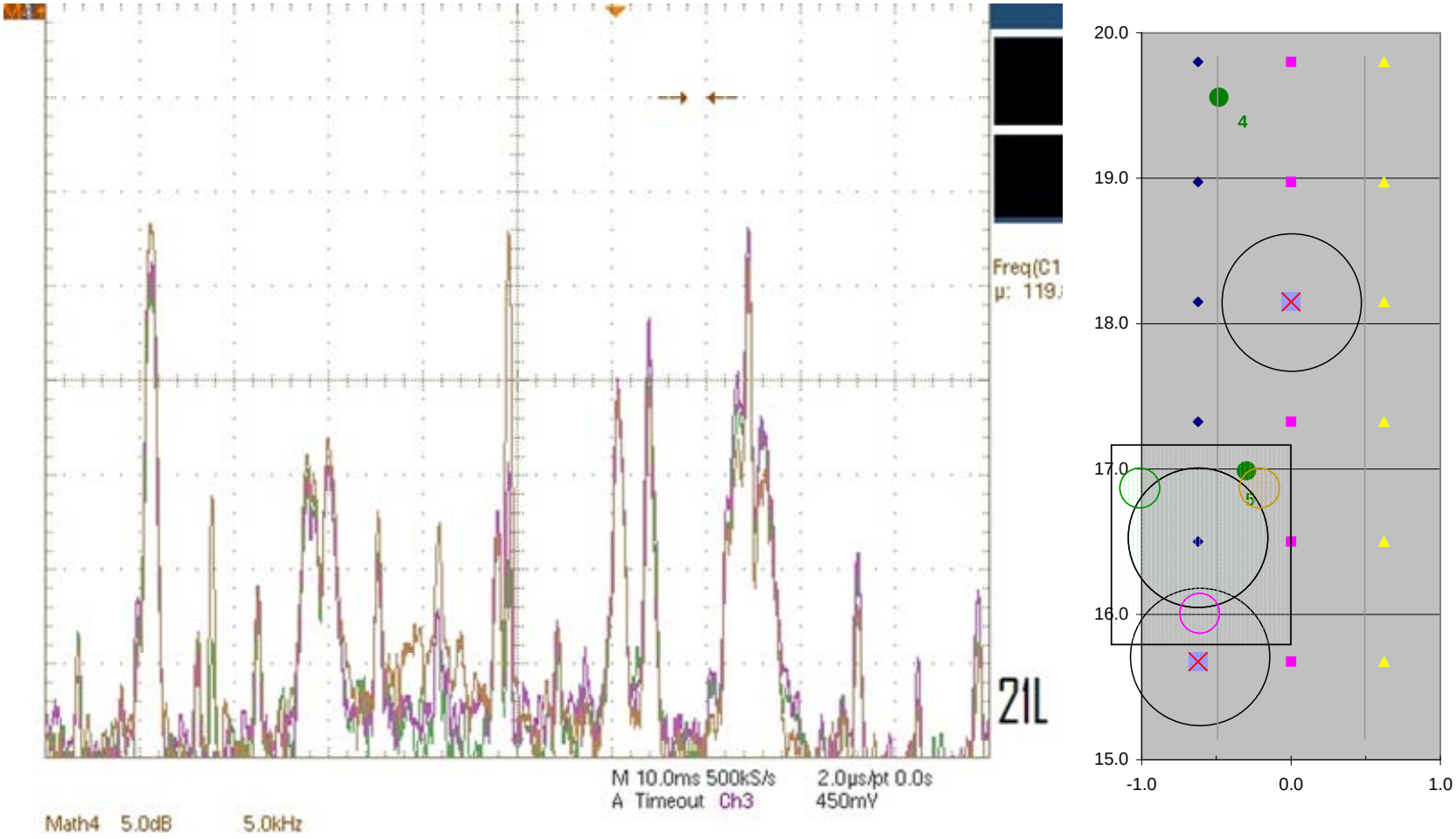

Figure 160. Data taken at position (21, L)

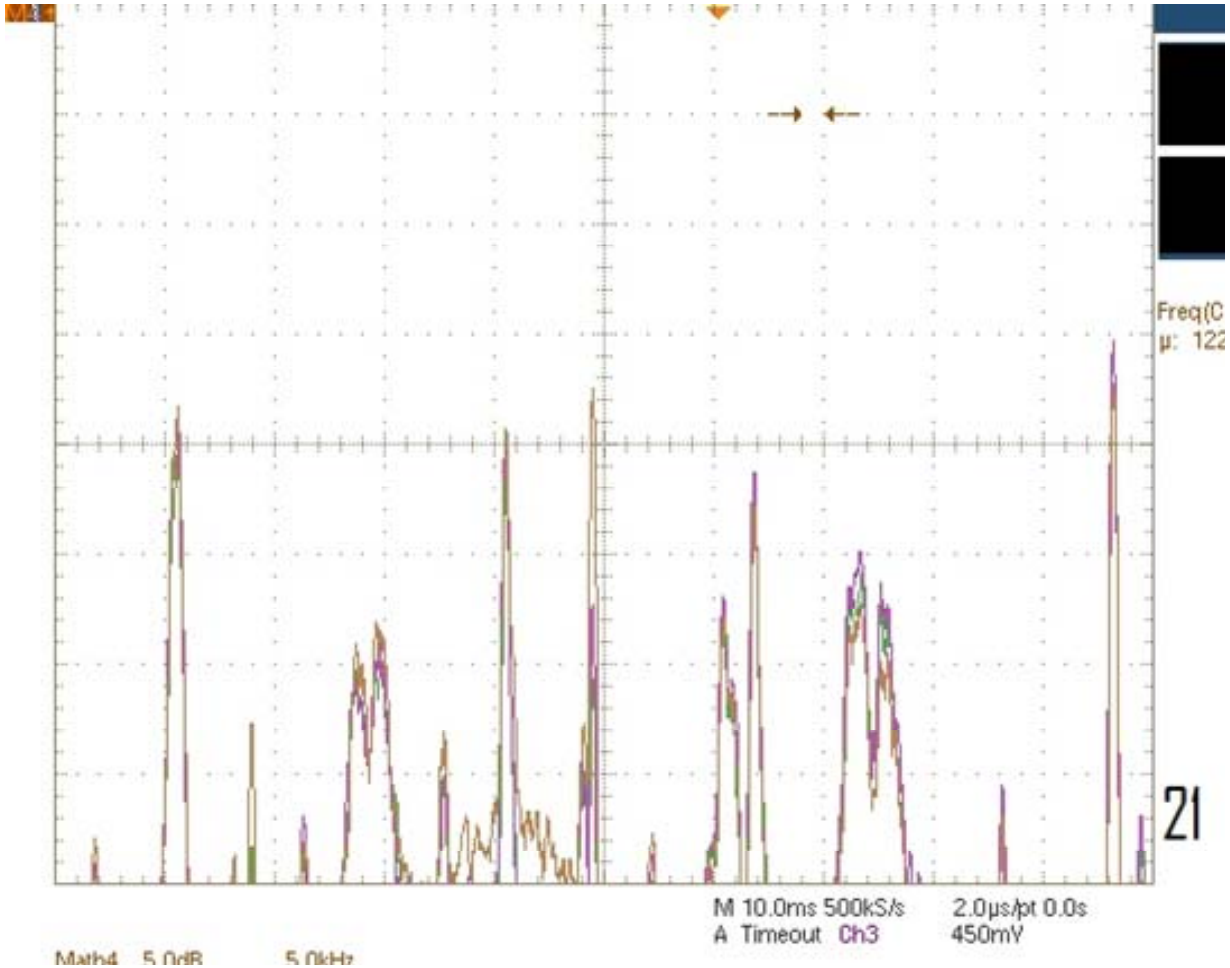

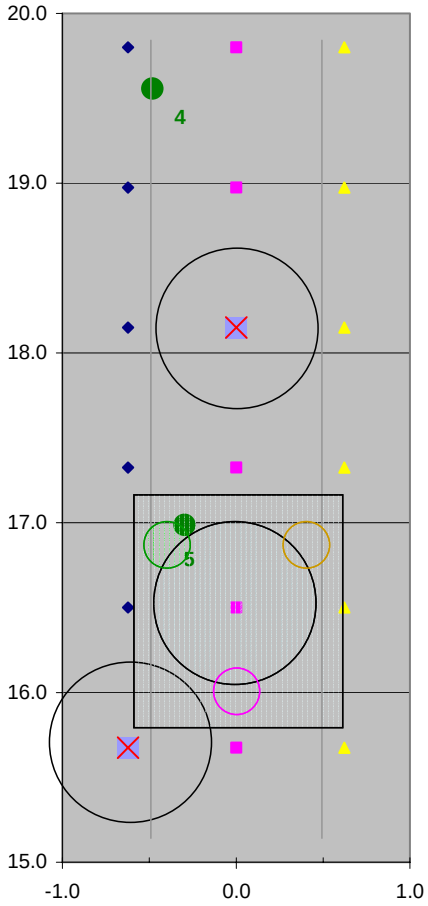

Figure 161. Data taken at position (21, C)

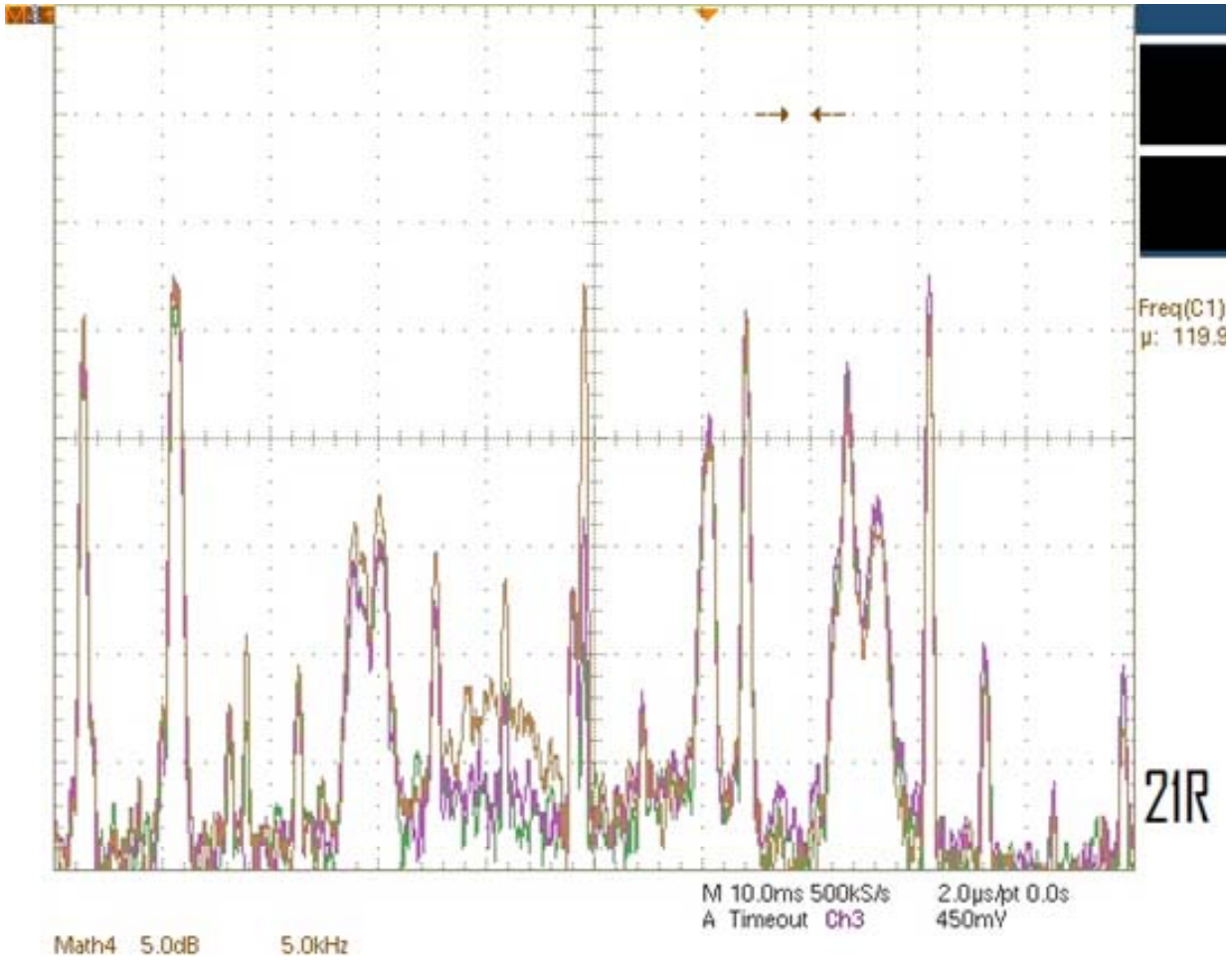

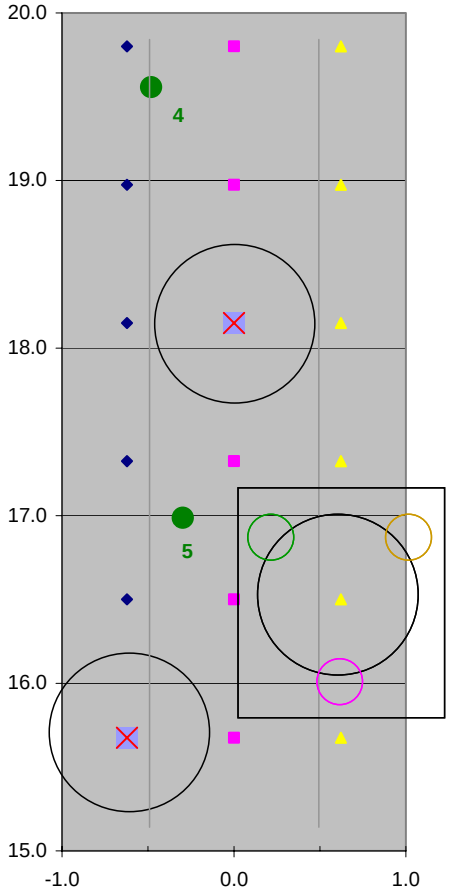

Figure 162. Data taken at position (21, R)

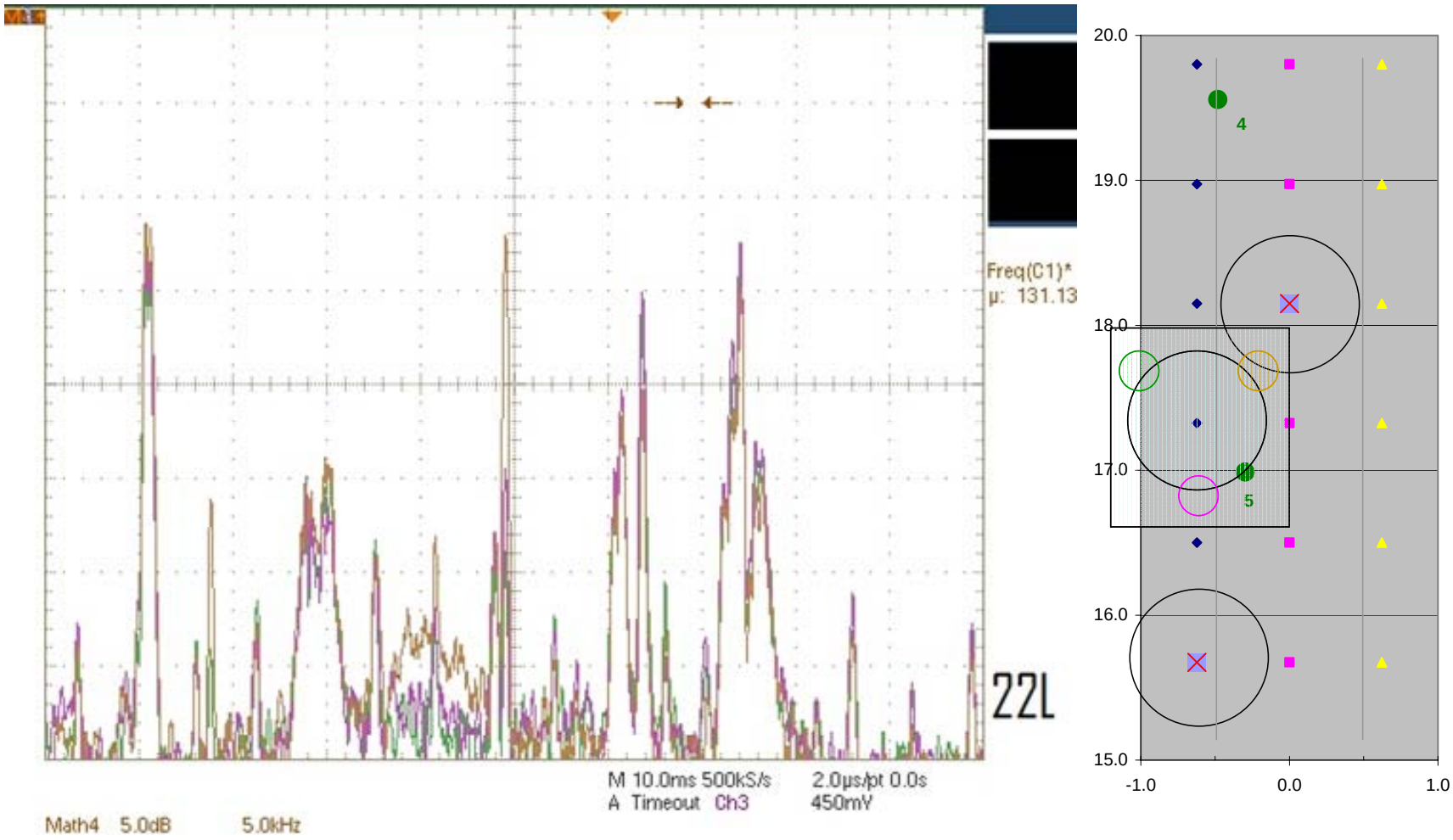

Figure 163. Data taken at position (22, L)

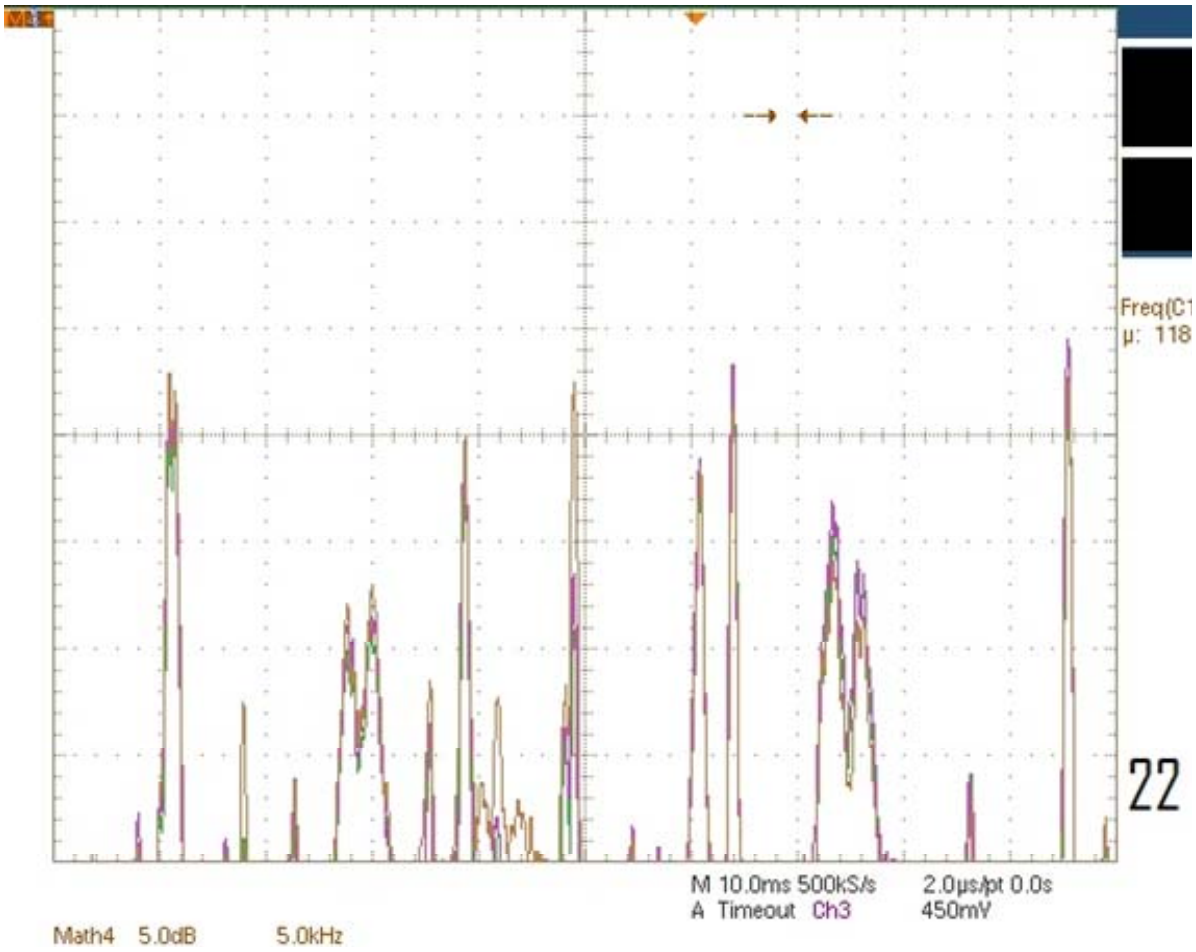

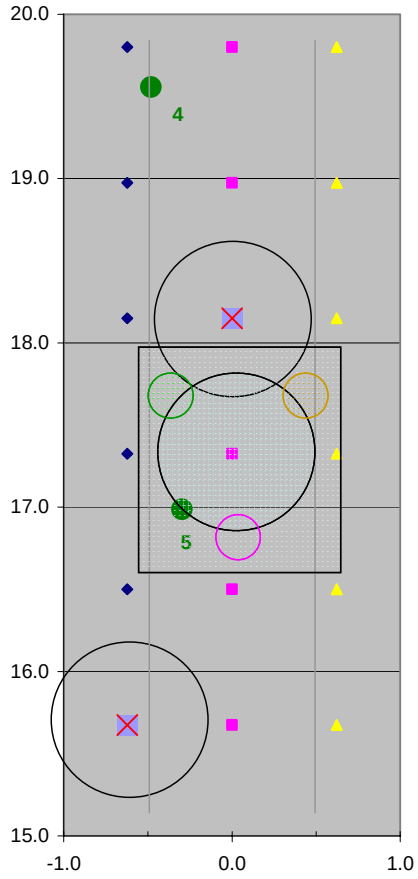

Figure 164. Data taken at position (22, C)

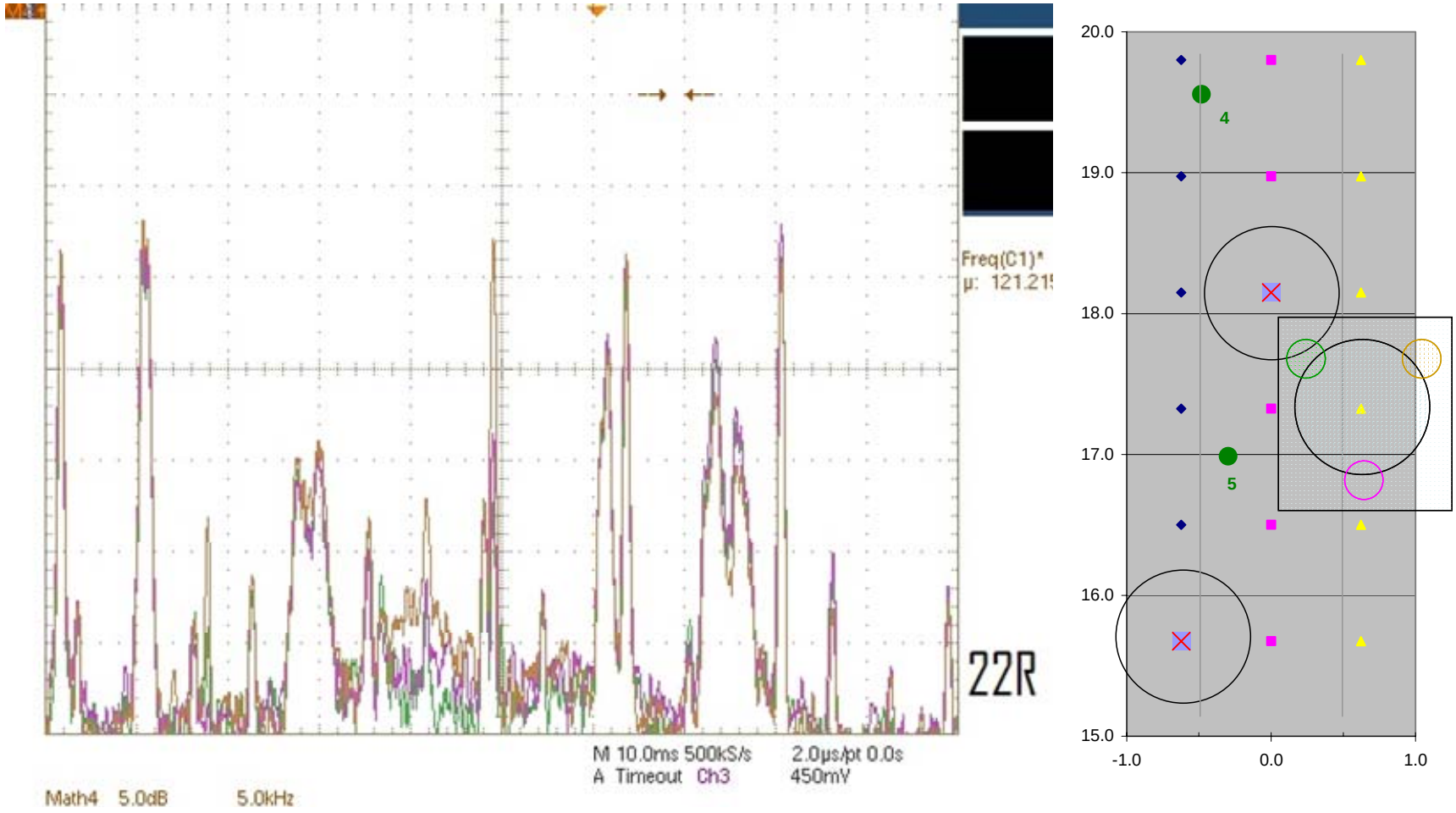

Figure 165. Data taken at position (22, R)

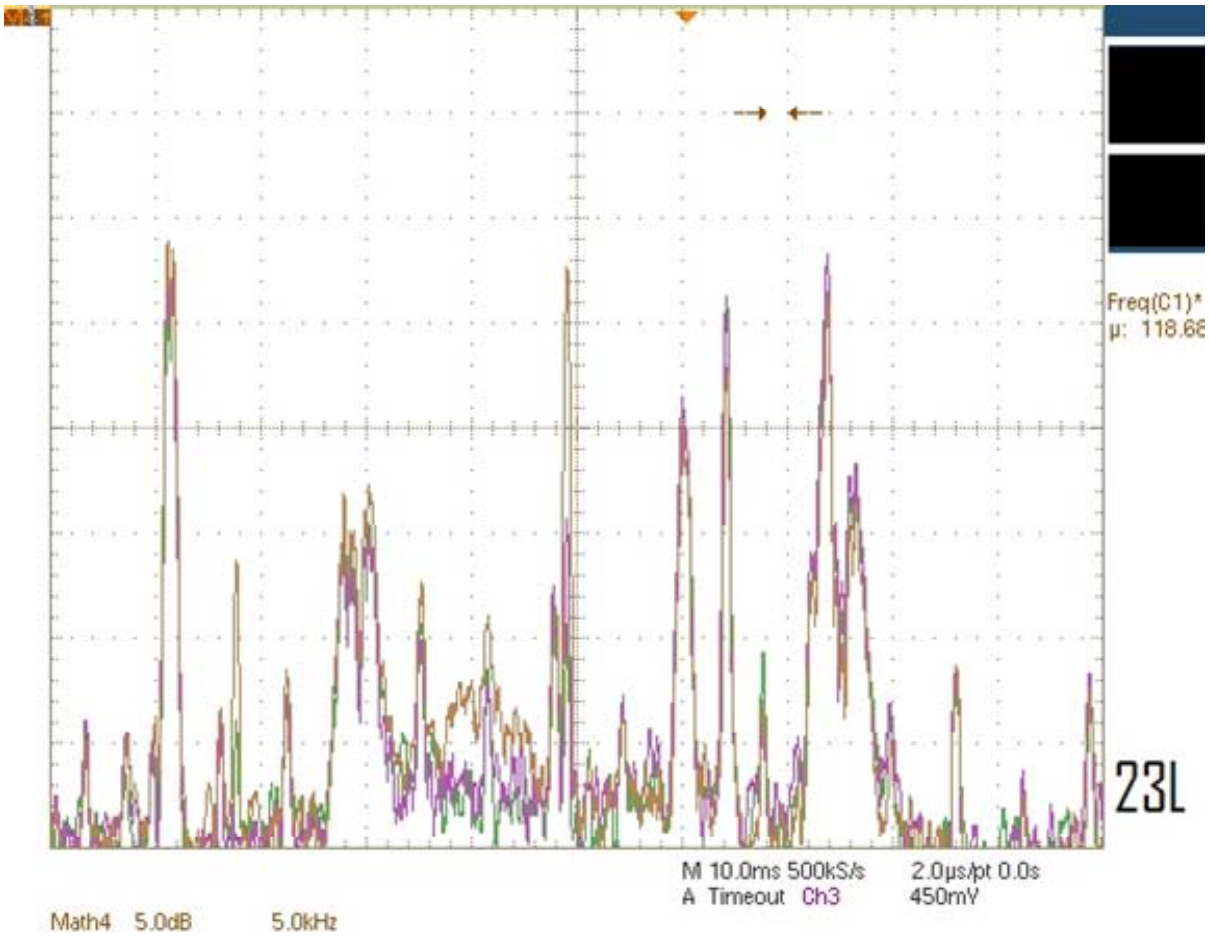

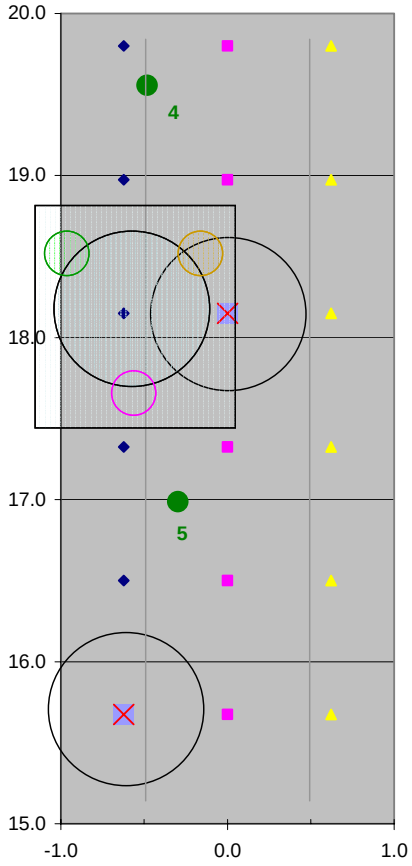

Figure 166. Data taken at position (23, L)

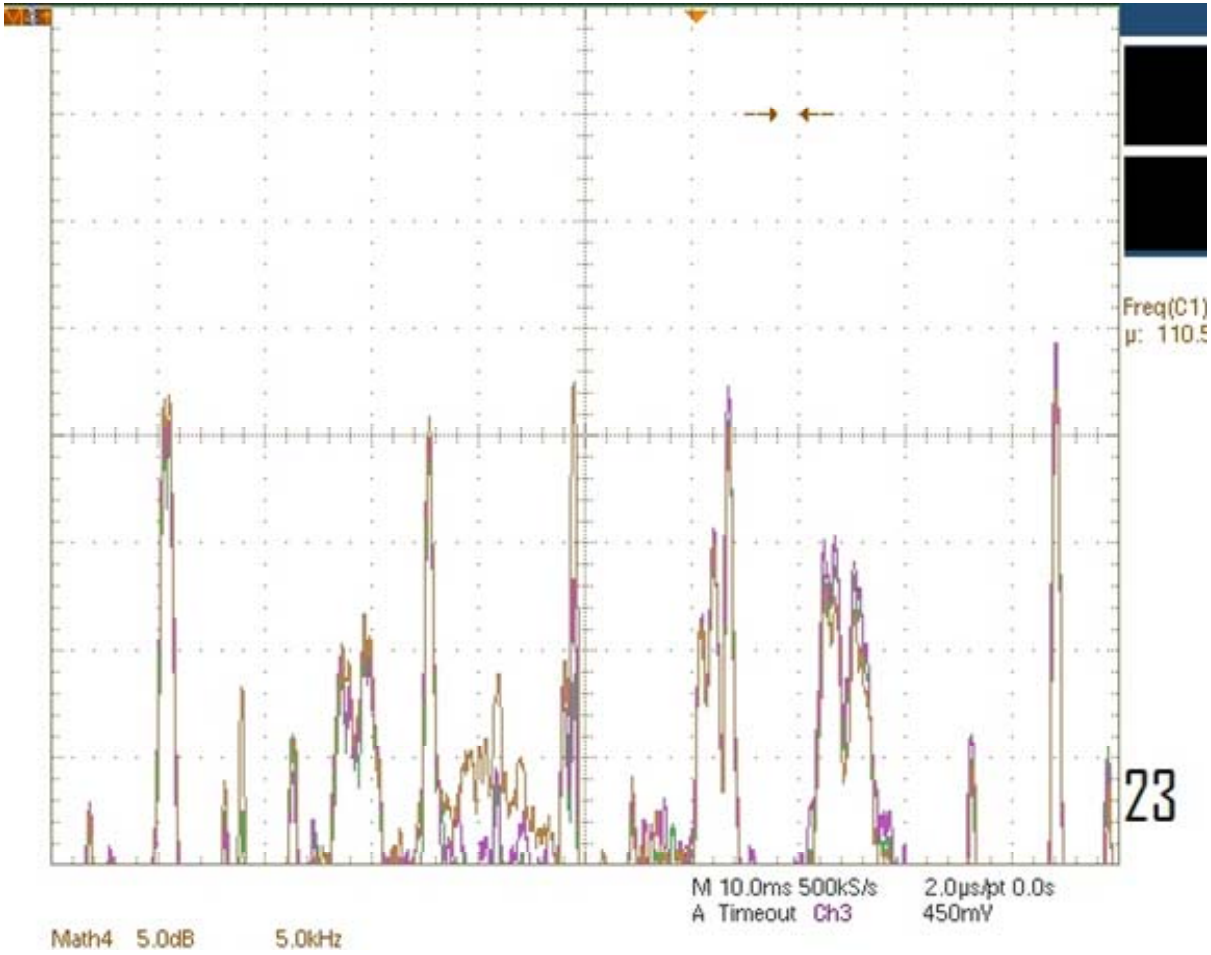

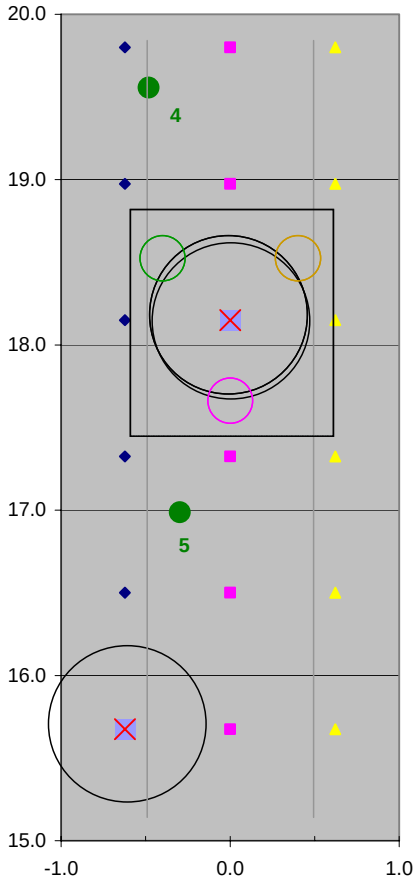

Figure 167. Data taken at position (23, C)

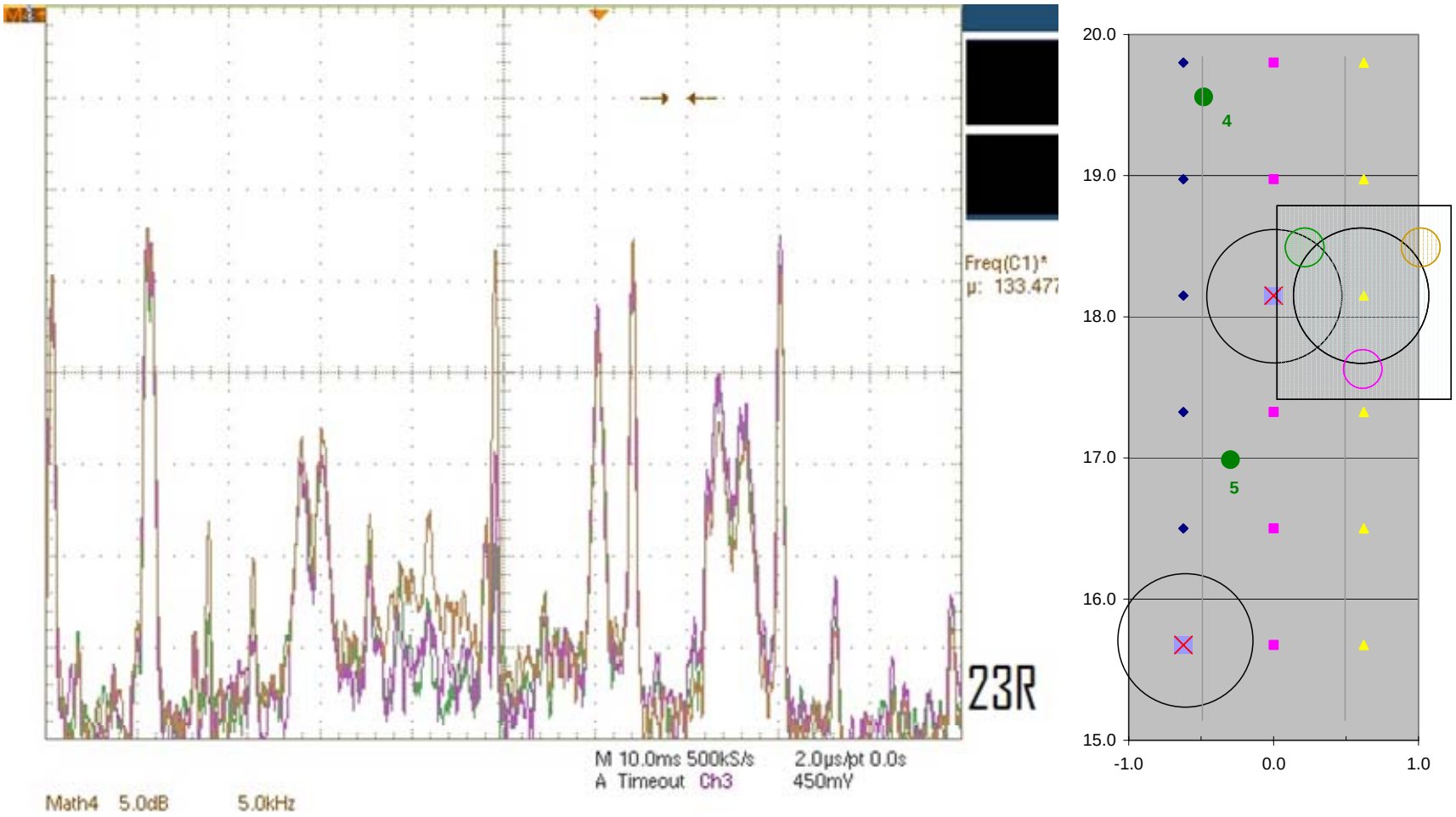

Figure 168. Data taken at position (23, R)

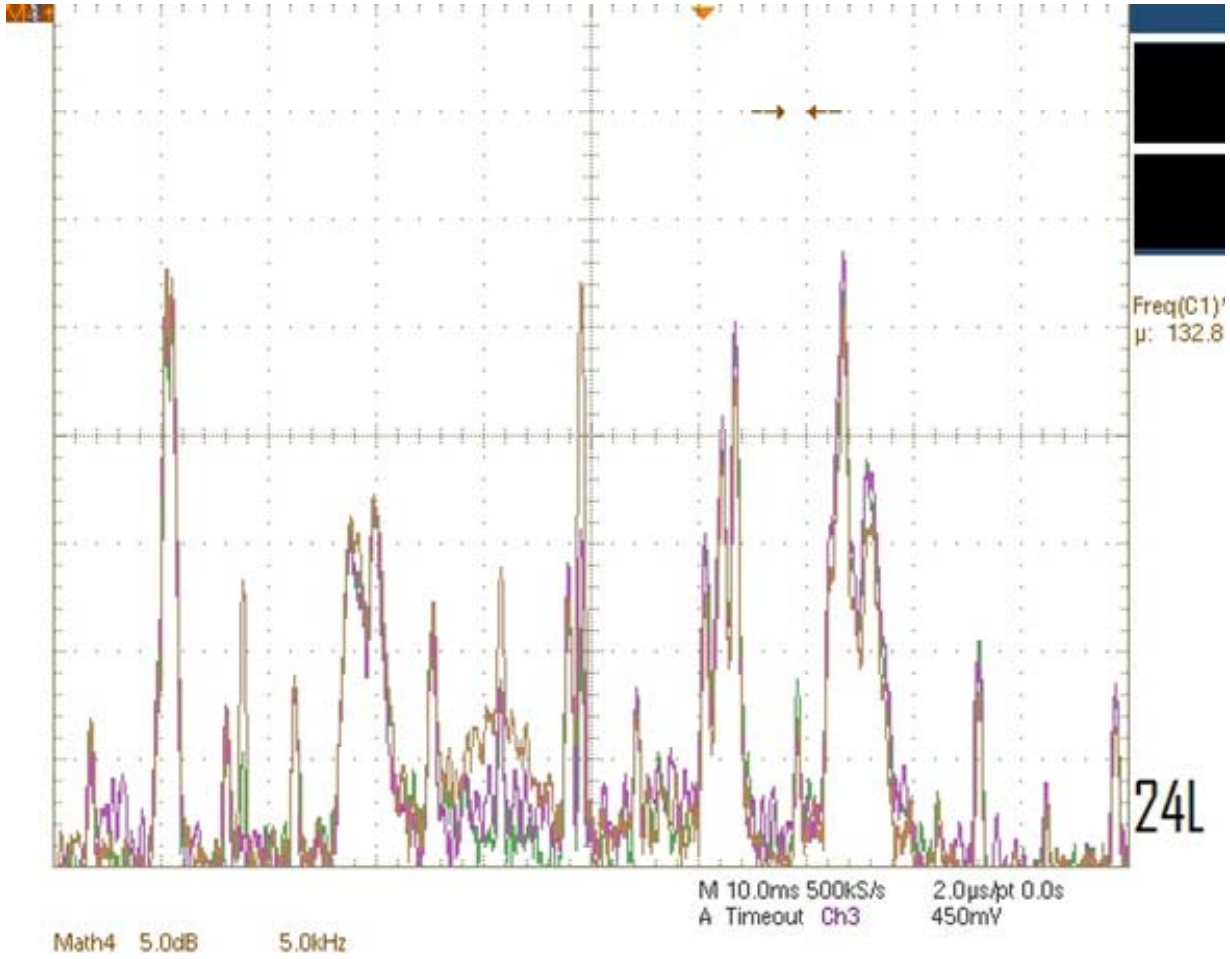

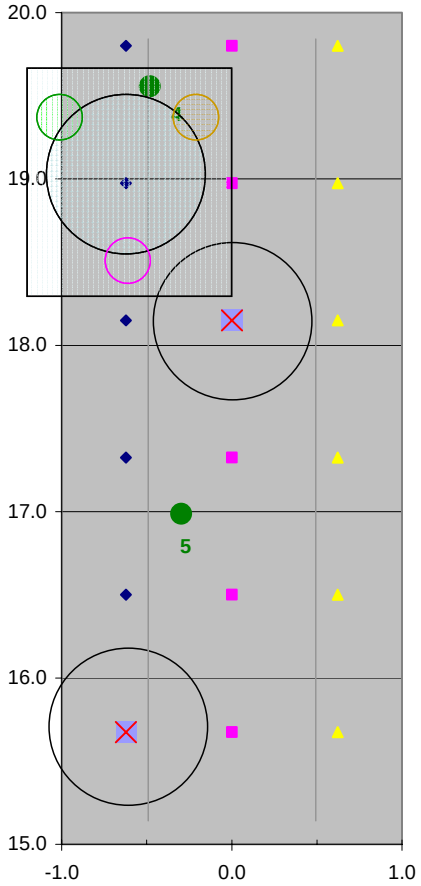

Figure 169. Data taken at position (24, L)

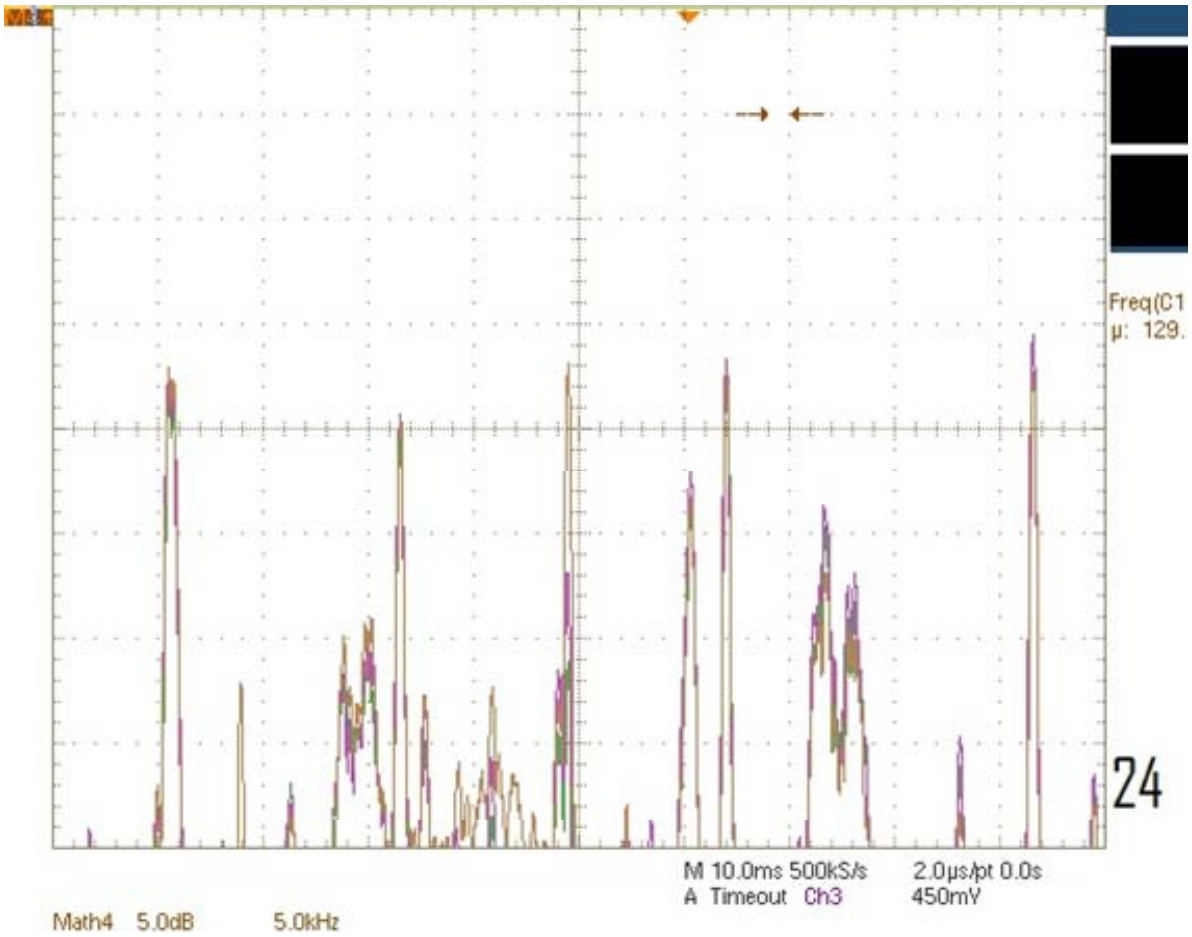

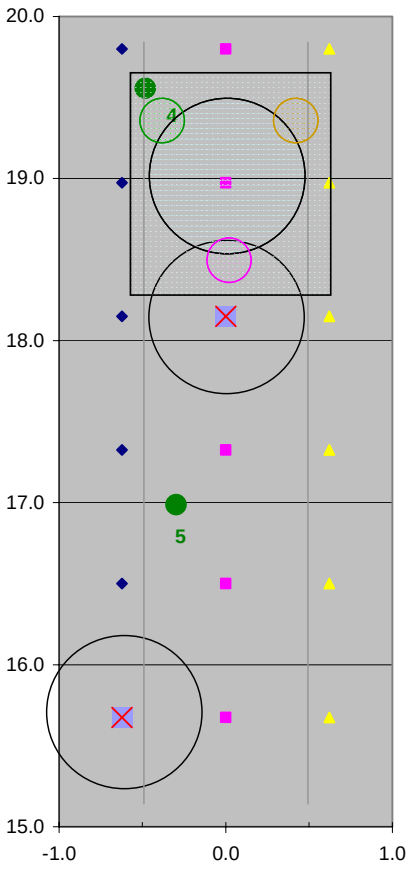

Figure 170. Data taken at position (24, C)

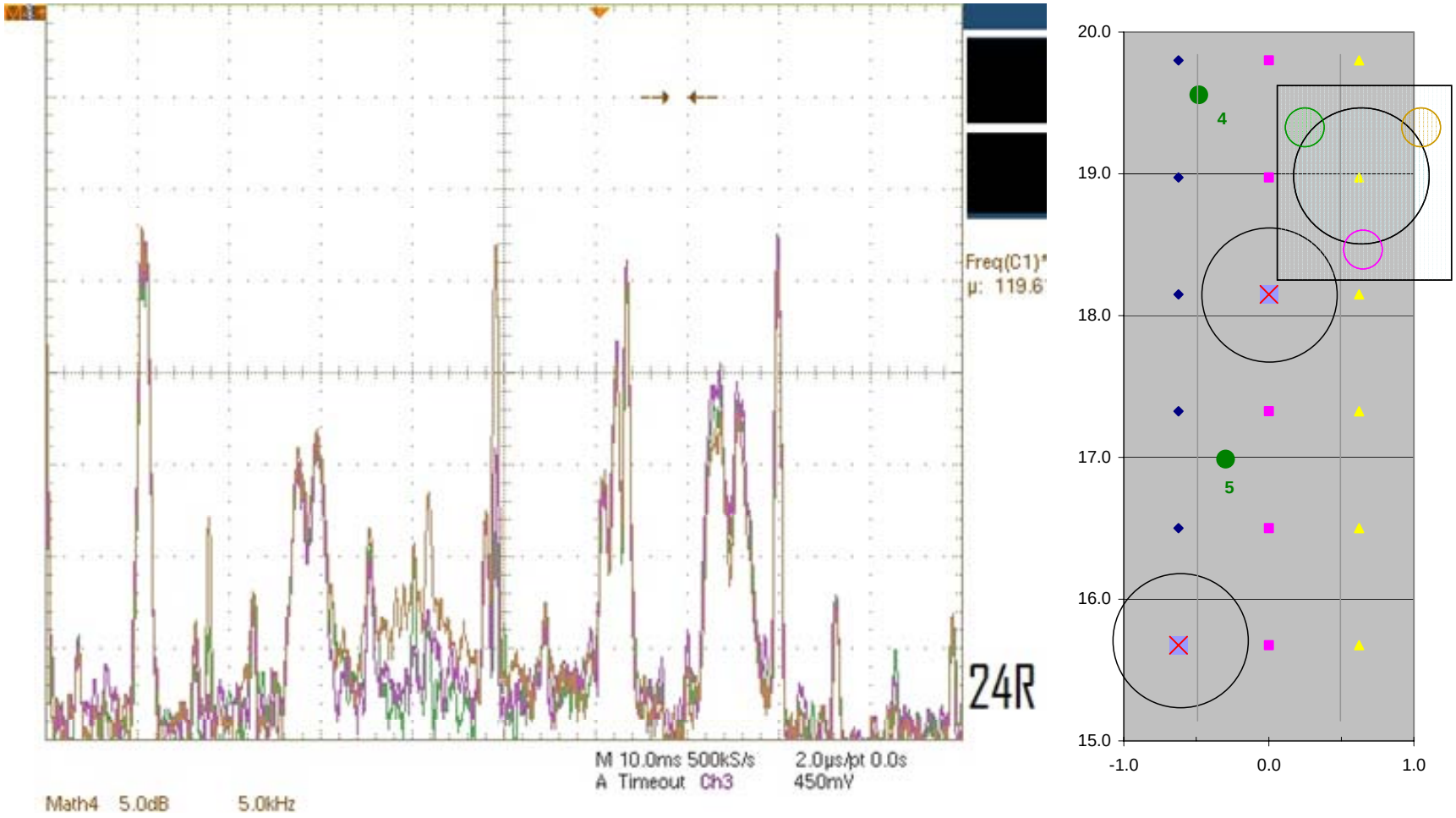

Figure 171. Data taken at position (24, R)

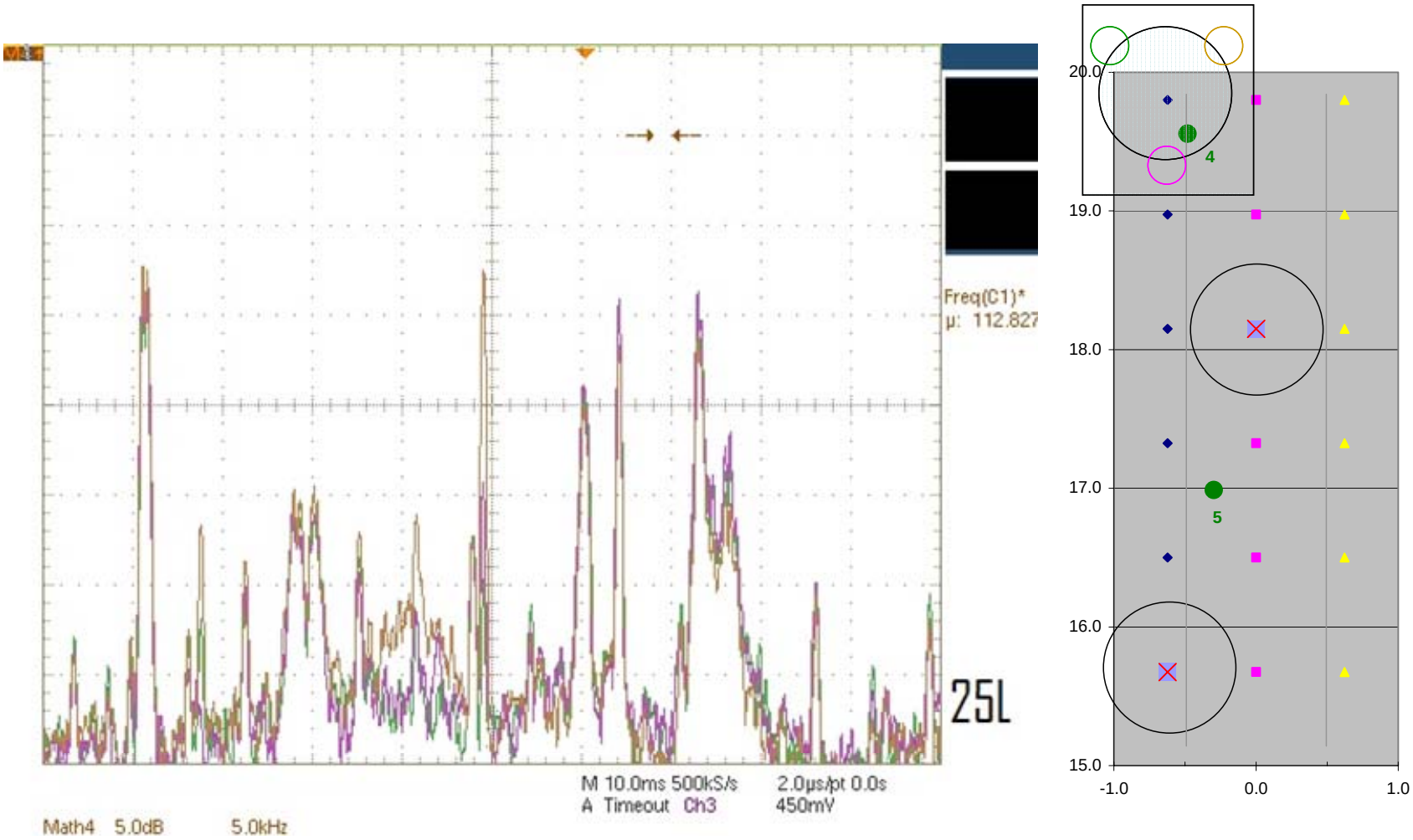

Figure 172. Data taken at position (25, L)

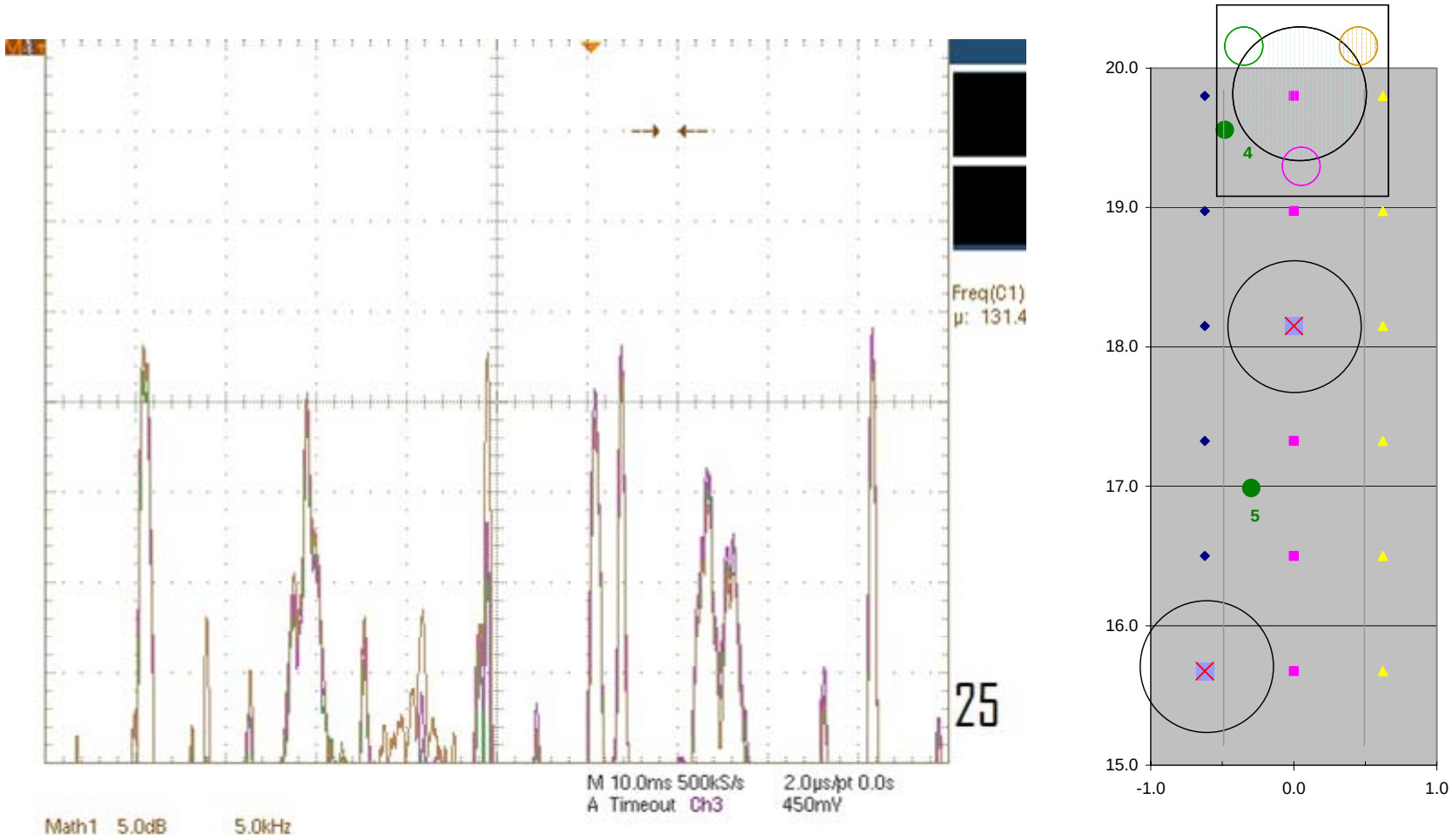

Figure 173. Data taken at position (25, C)

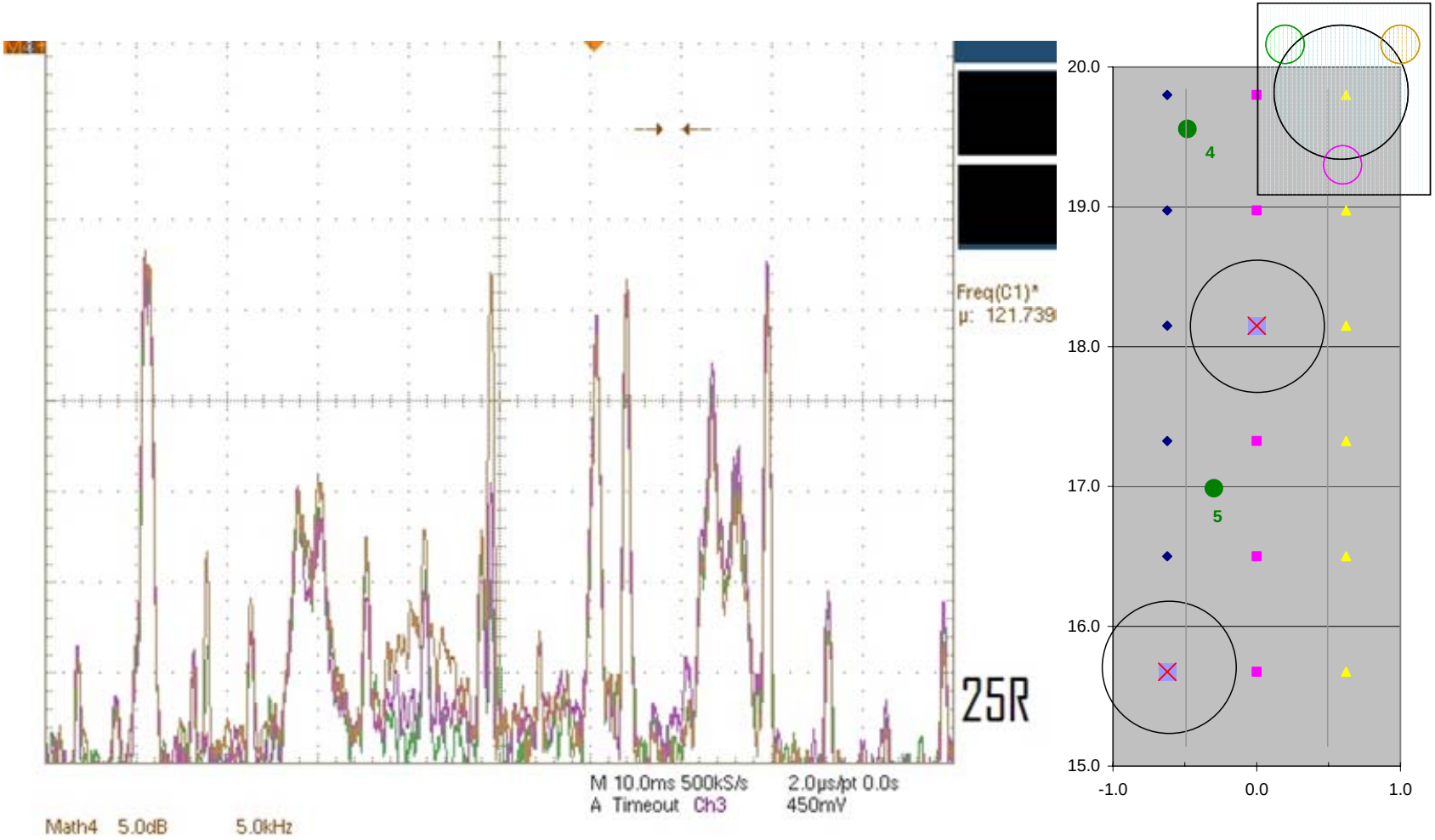

Figure 174. Data taken at position (25, R)

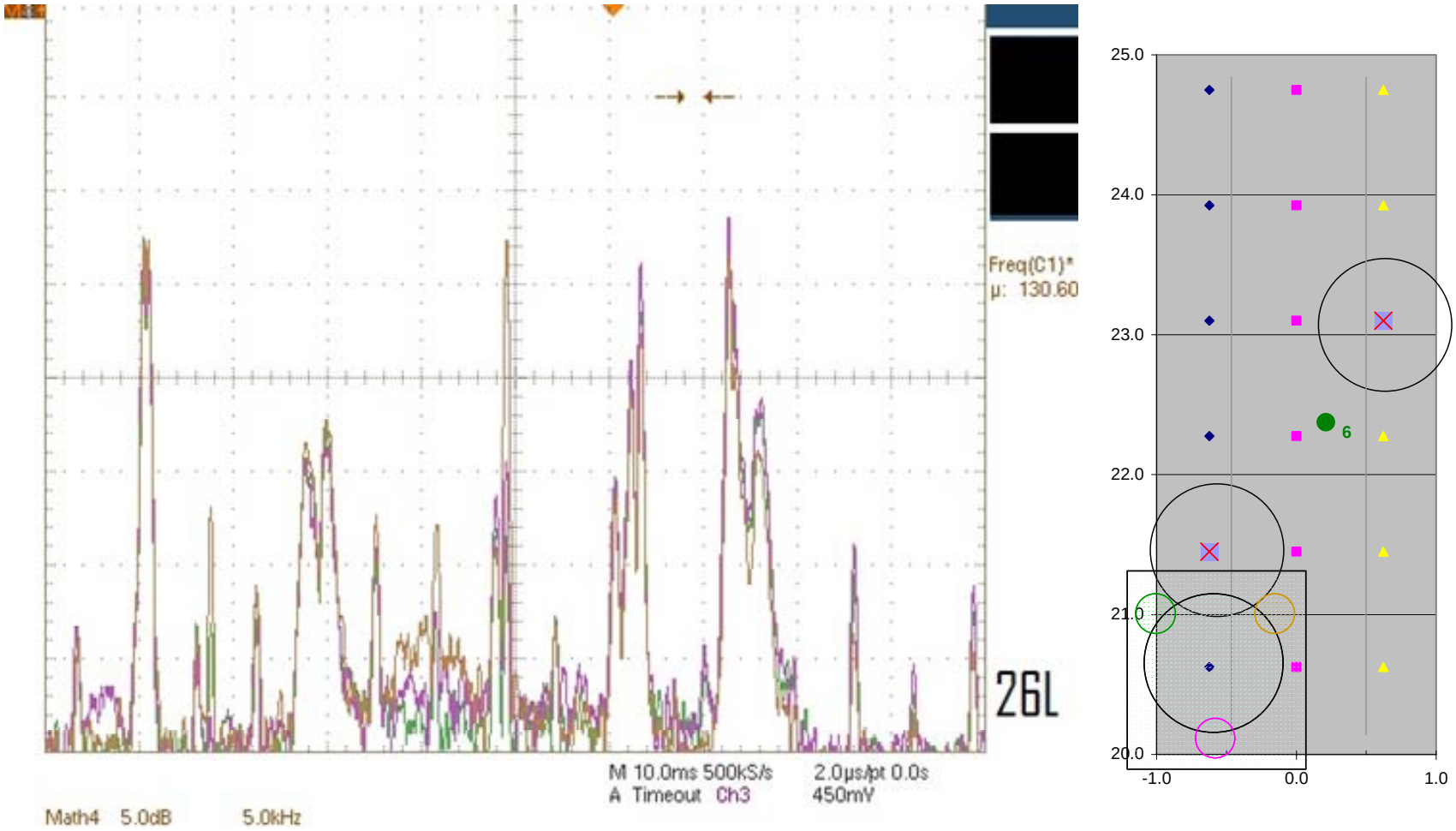

Figure 175. Data taken at position (26, L)

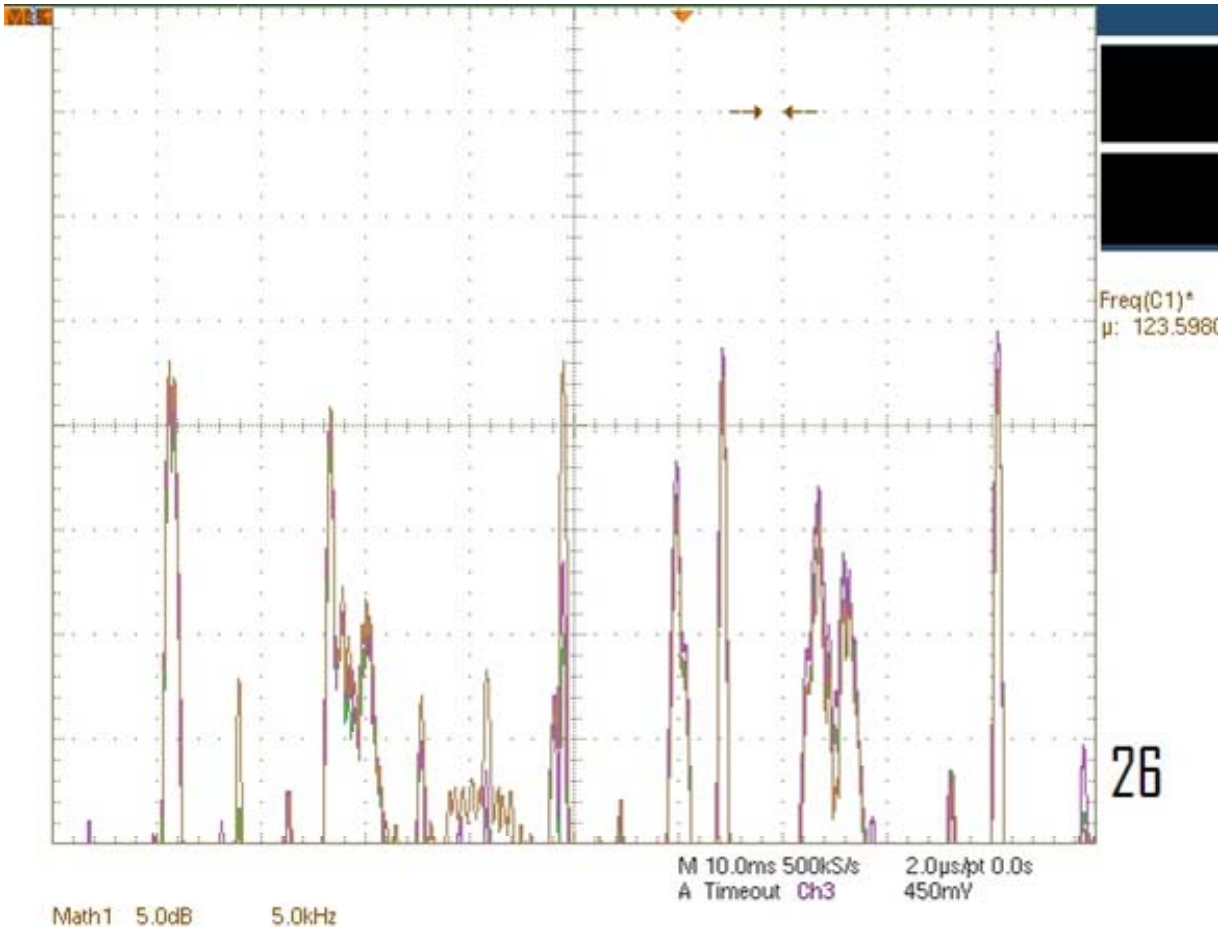

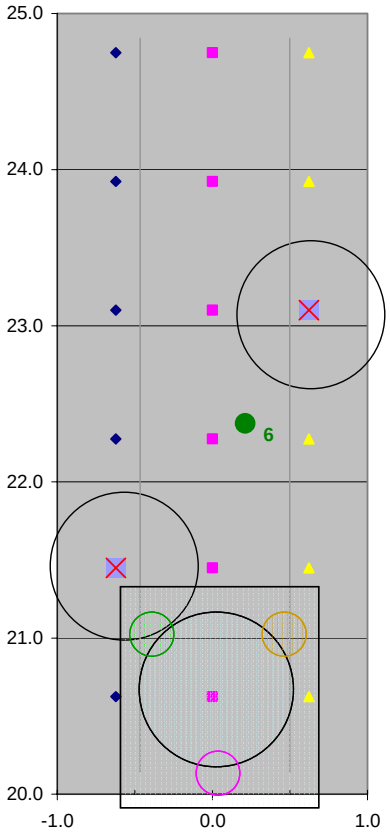

Figure 176. Data taken at position (26, C)

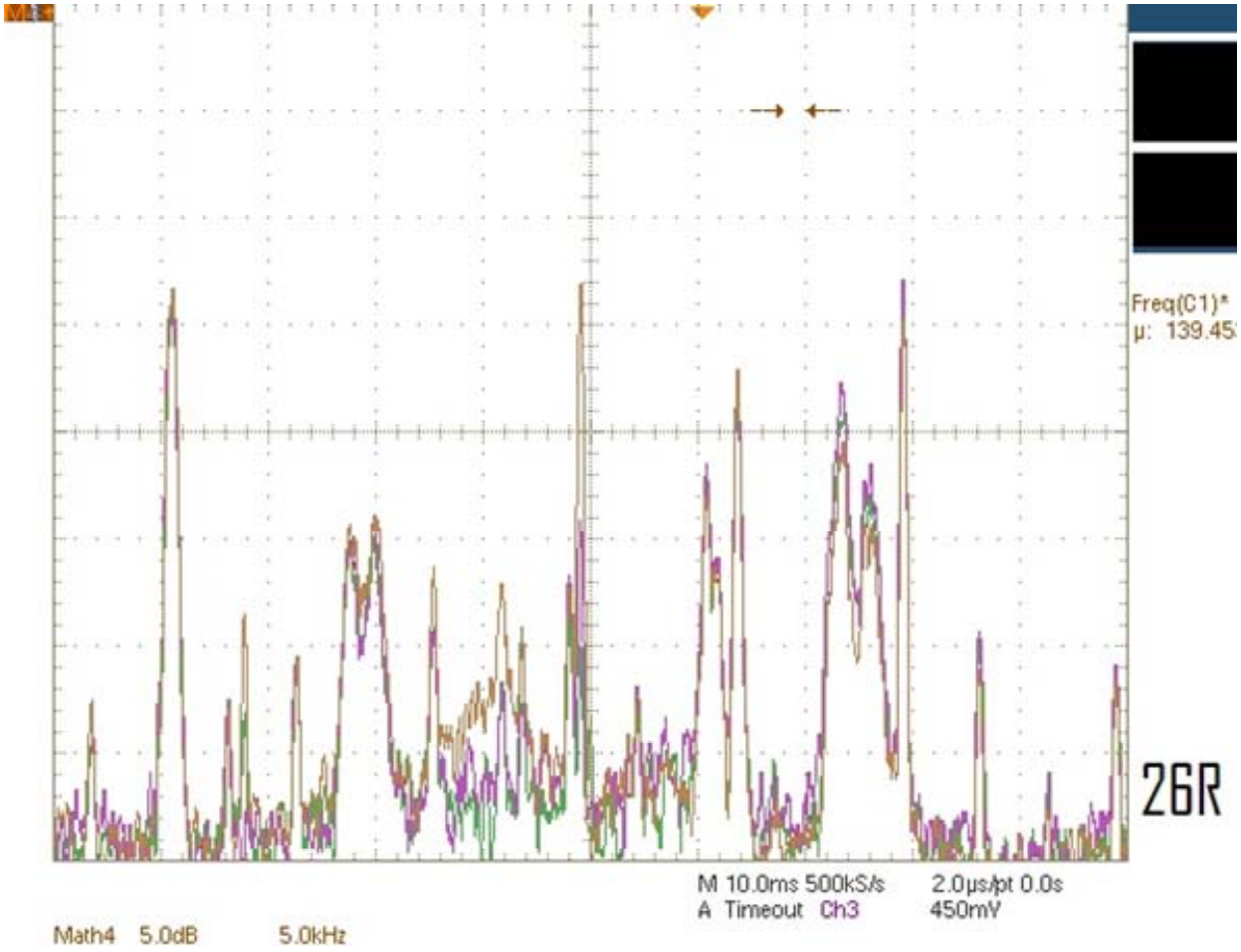

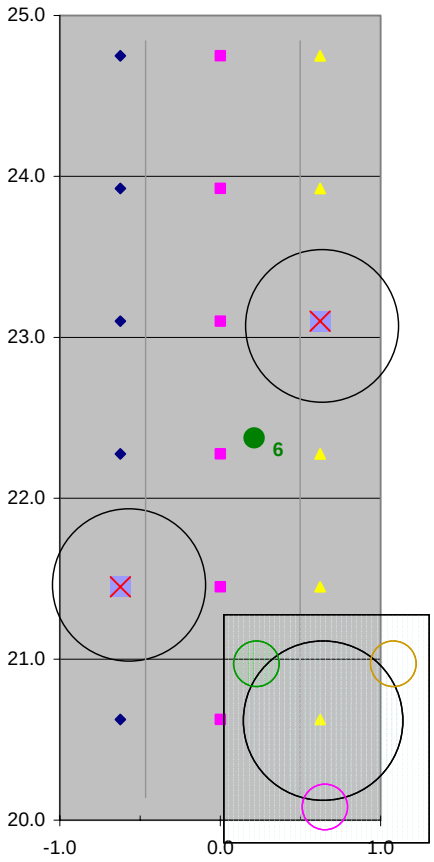

Figure 177. Data taken at position (26, R)

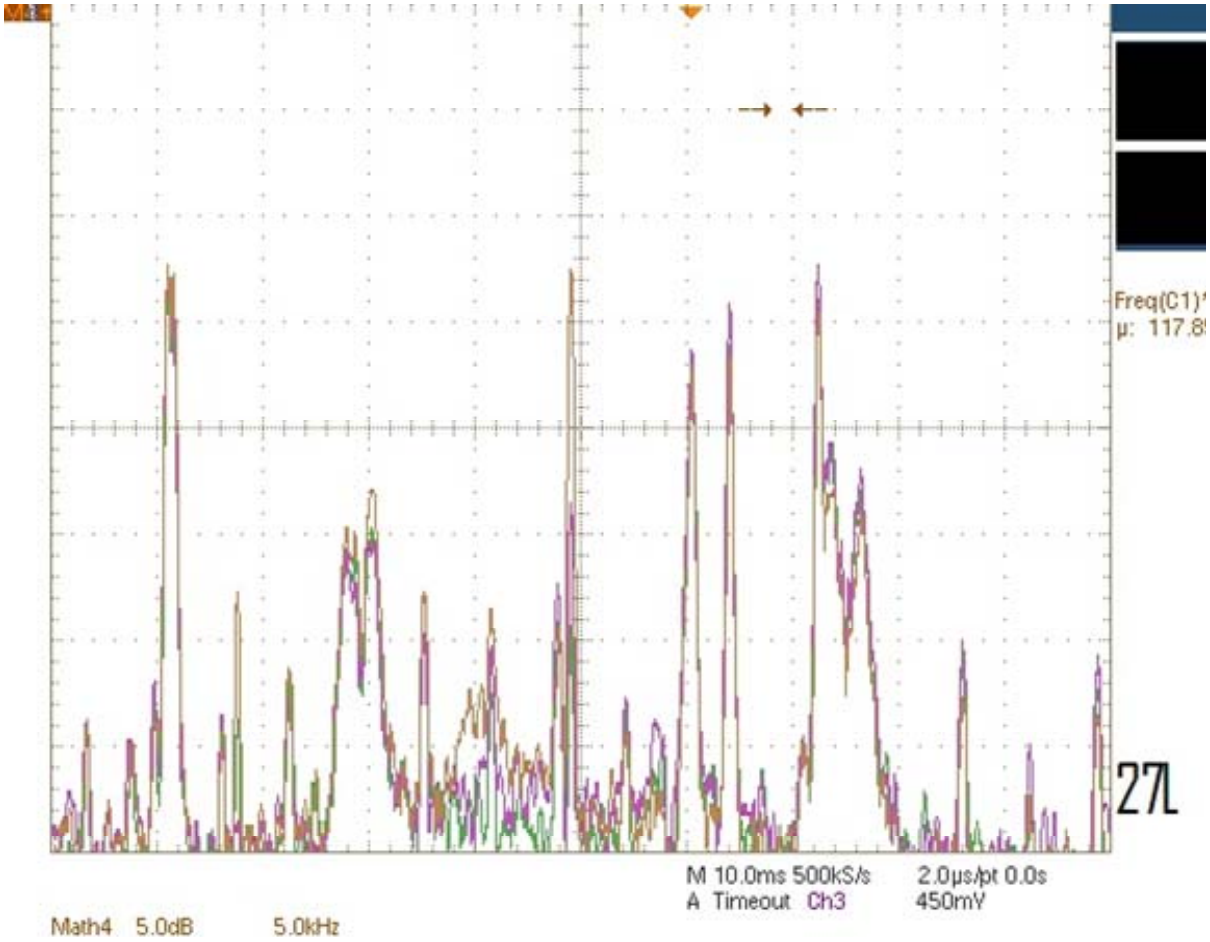

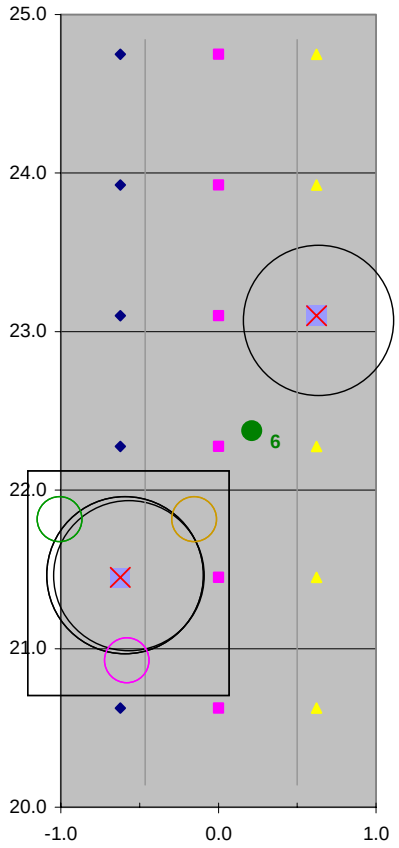

Figure 178. Data taken at position (27, L)

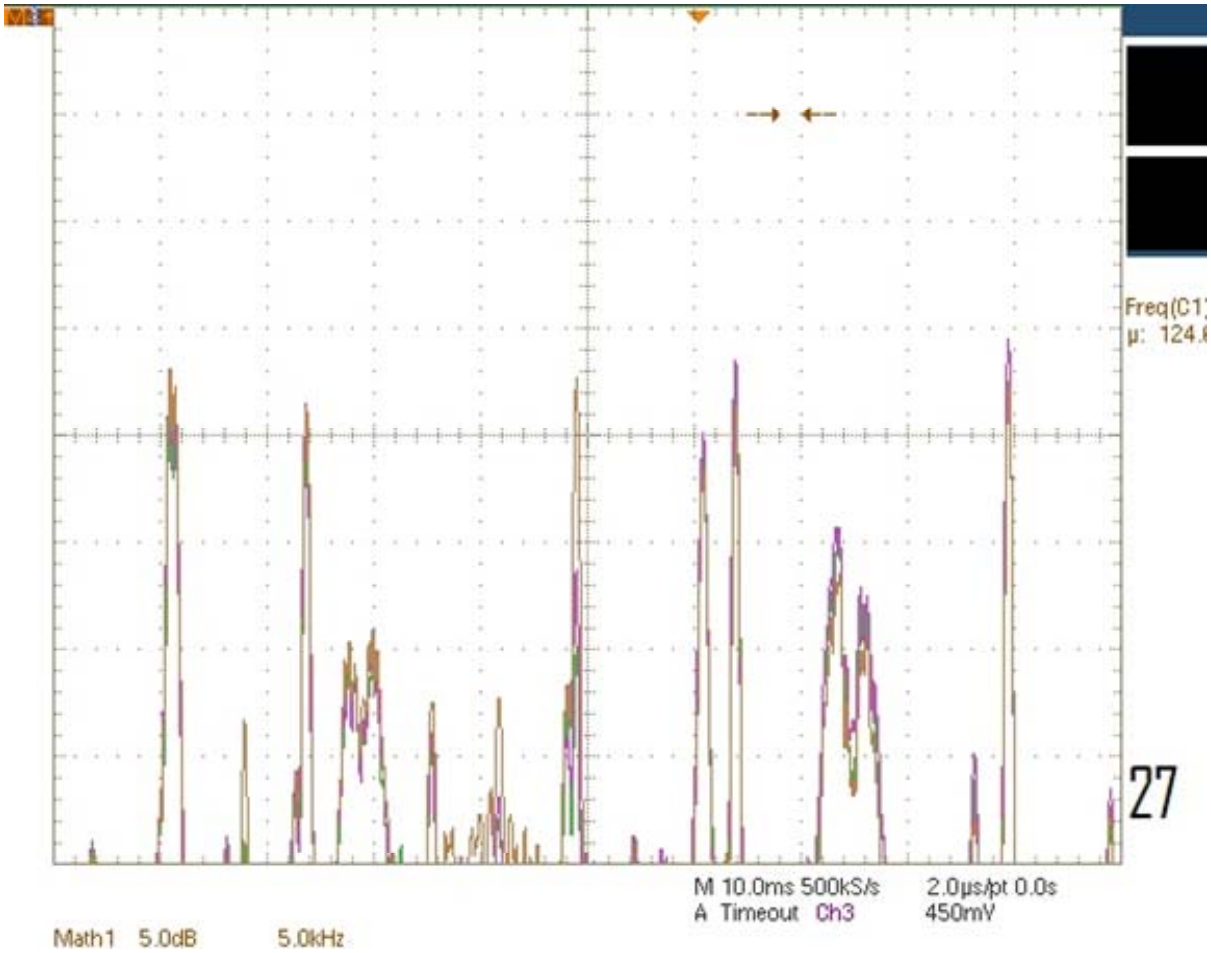

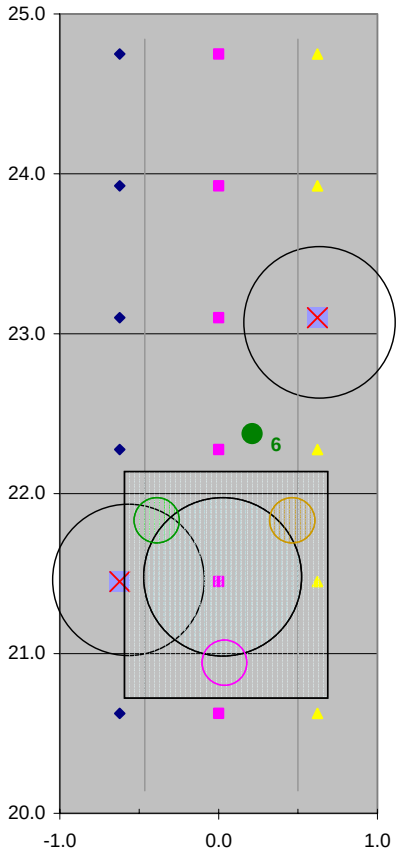

Figure 179. Data taken at position (27, C)

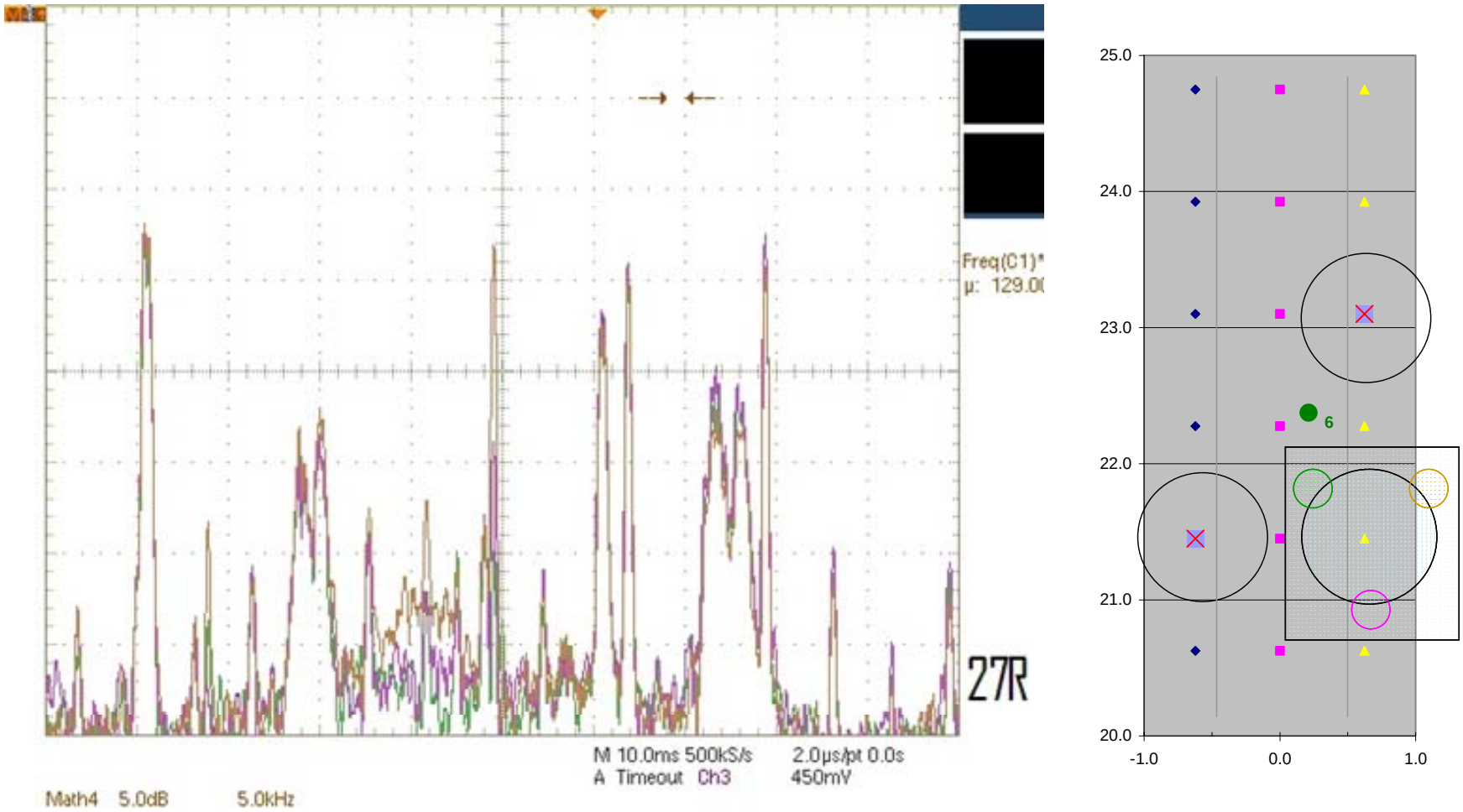

Figure 180. Data taken at position (27, R)

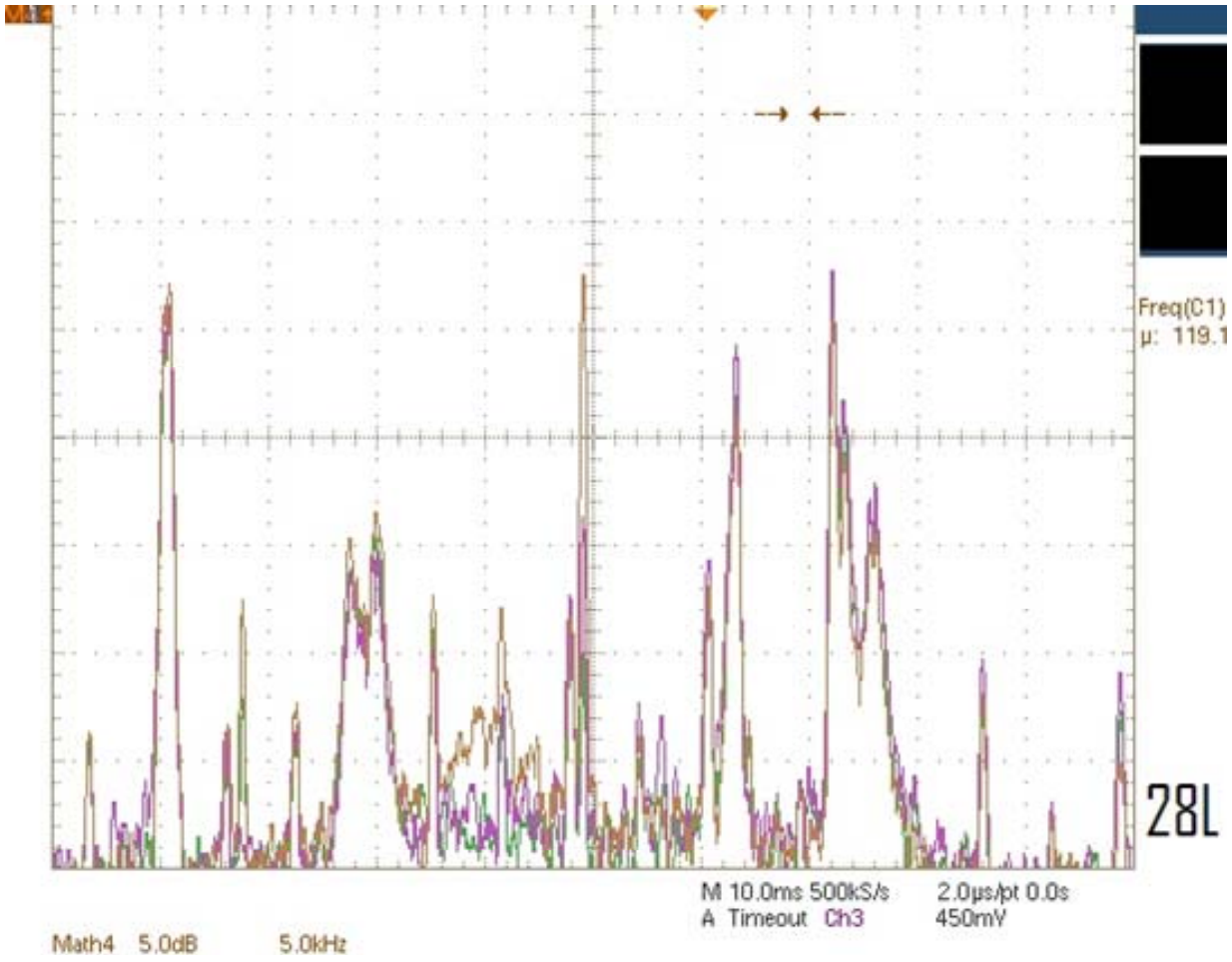

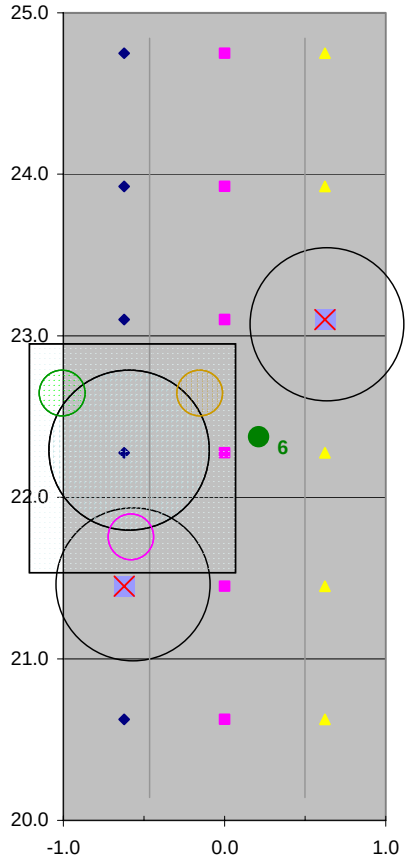

Figure 181. Data taken at position (28, L)

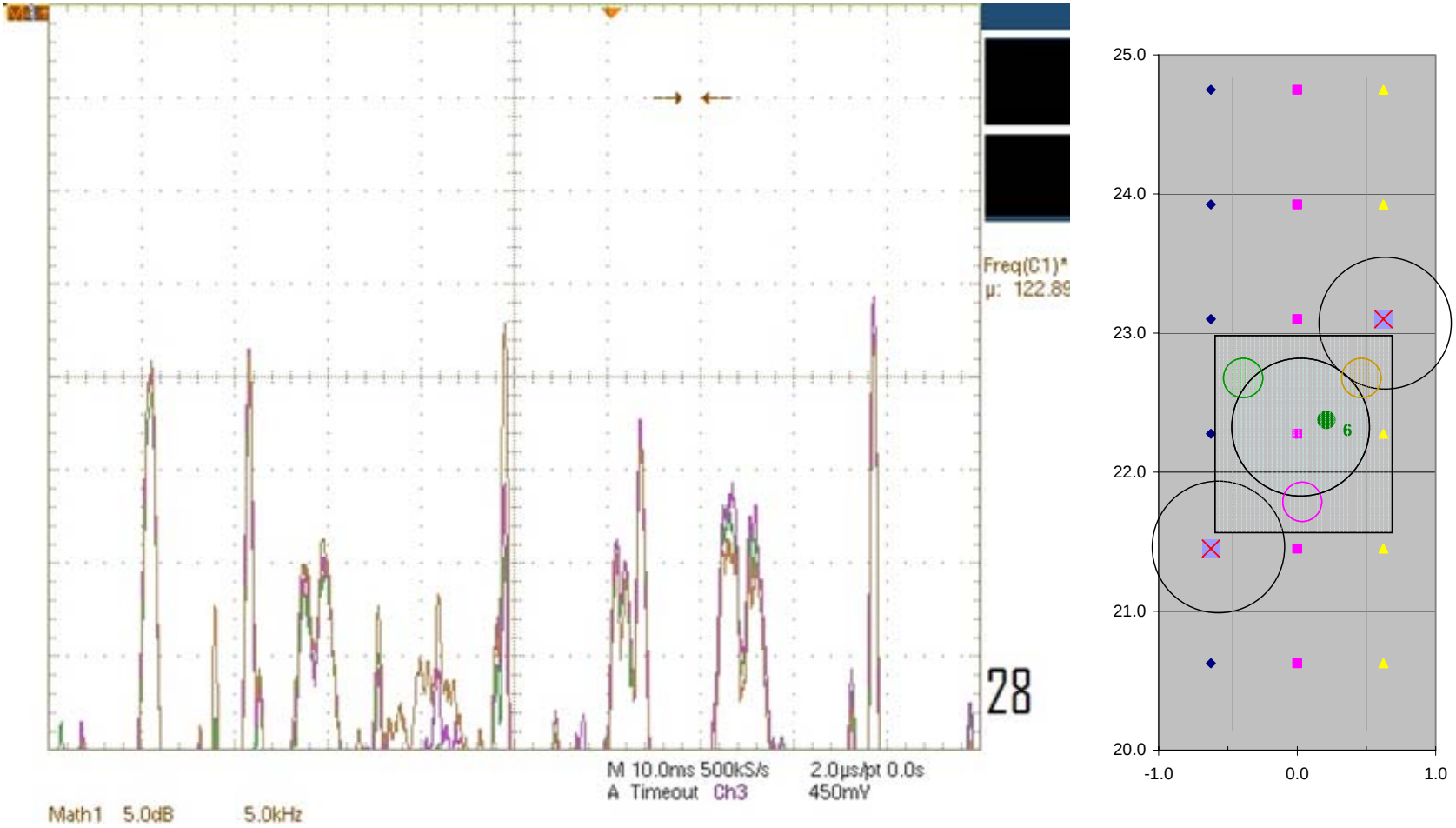

Figure 182. Data taken at position (28, C)

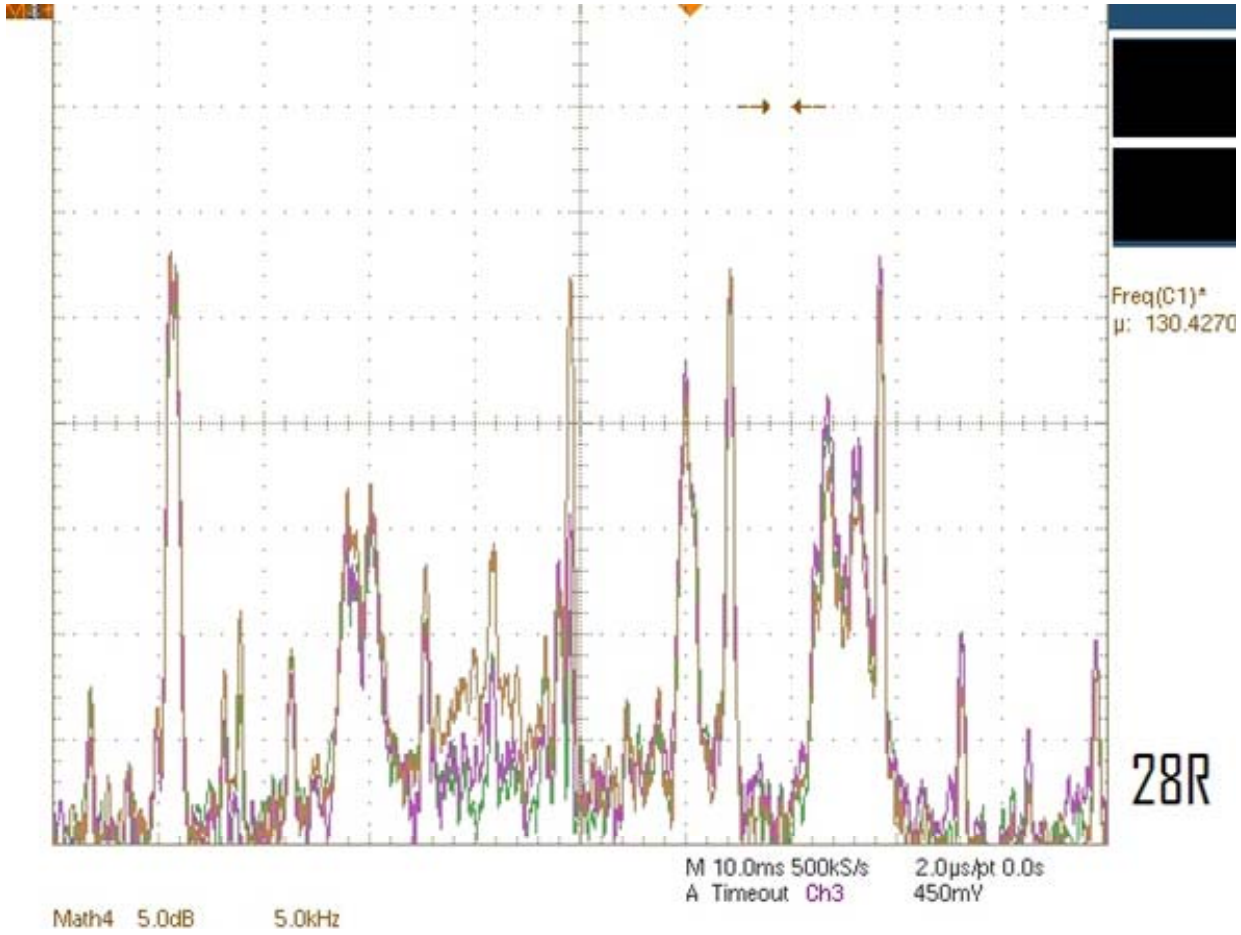

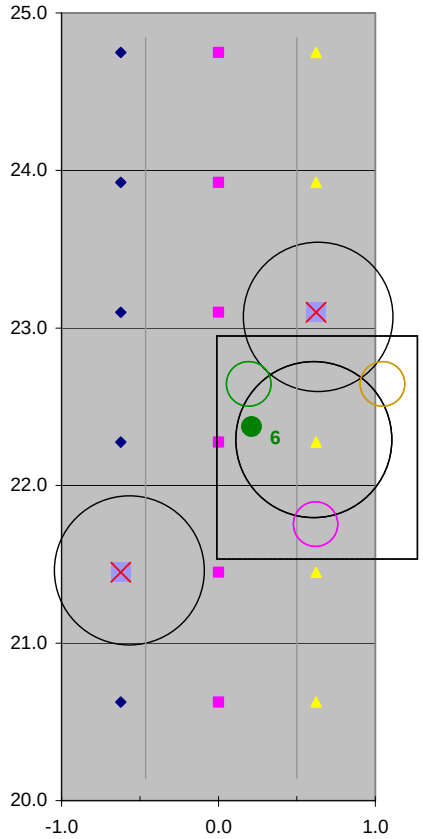

Figure 183. Data taken at position (28, R)

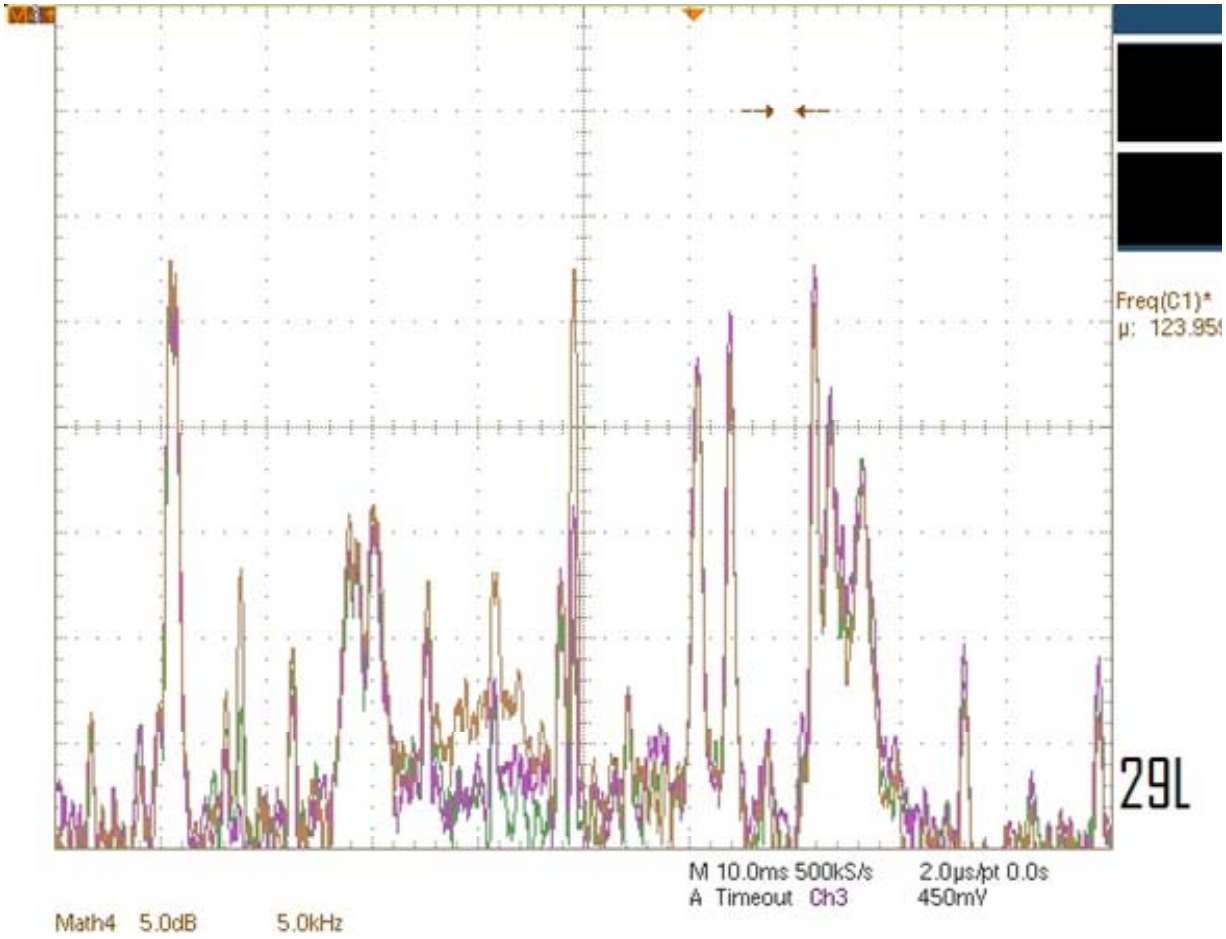

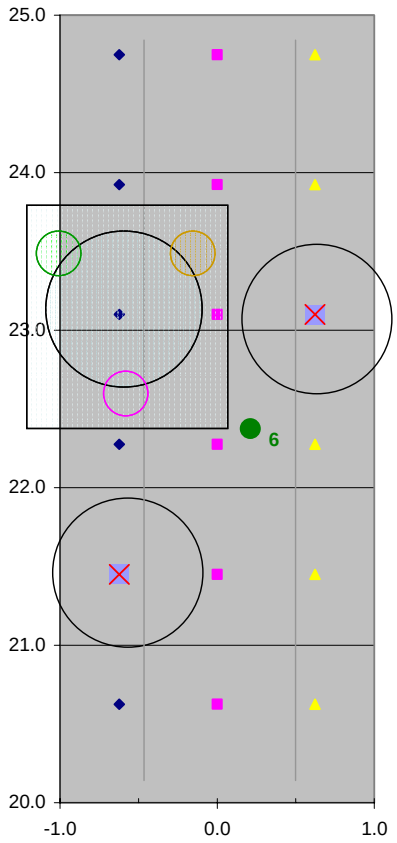

Figure 184. Data taken at position (29, L)

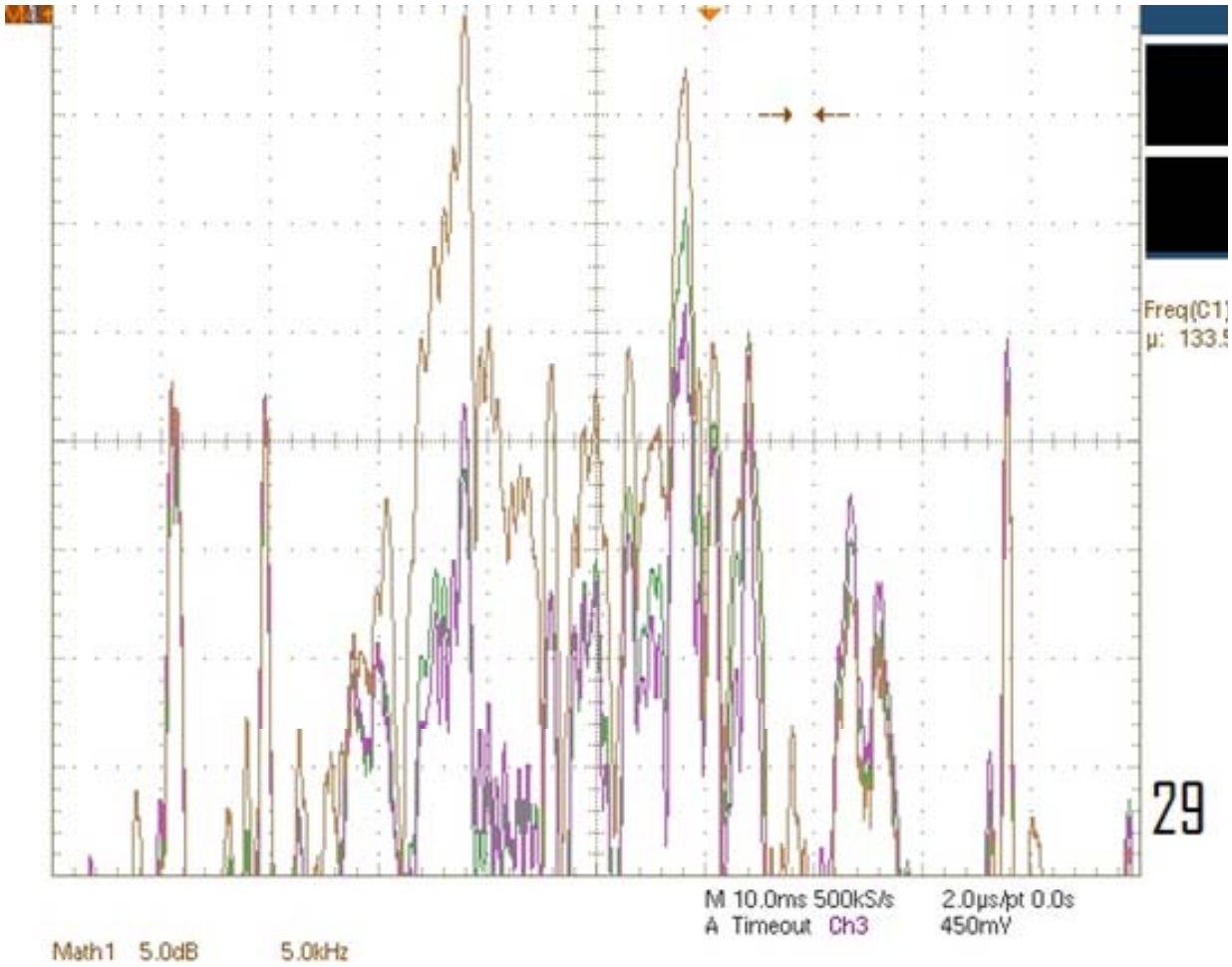

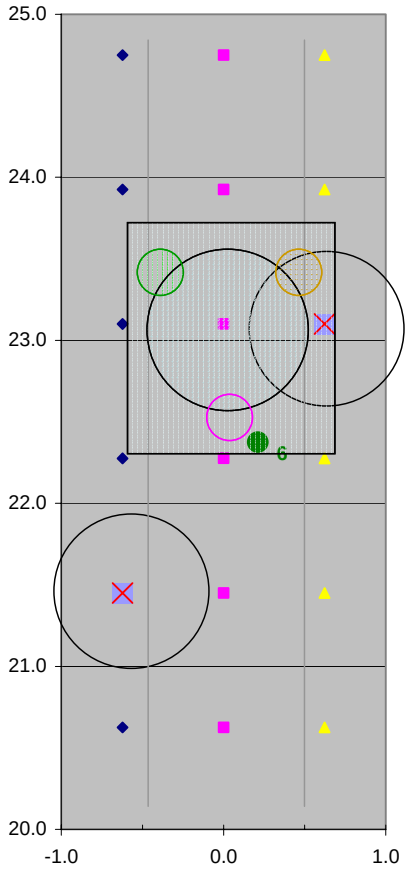

Figure 185. Data taken at position (29, C)

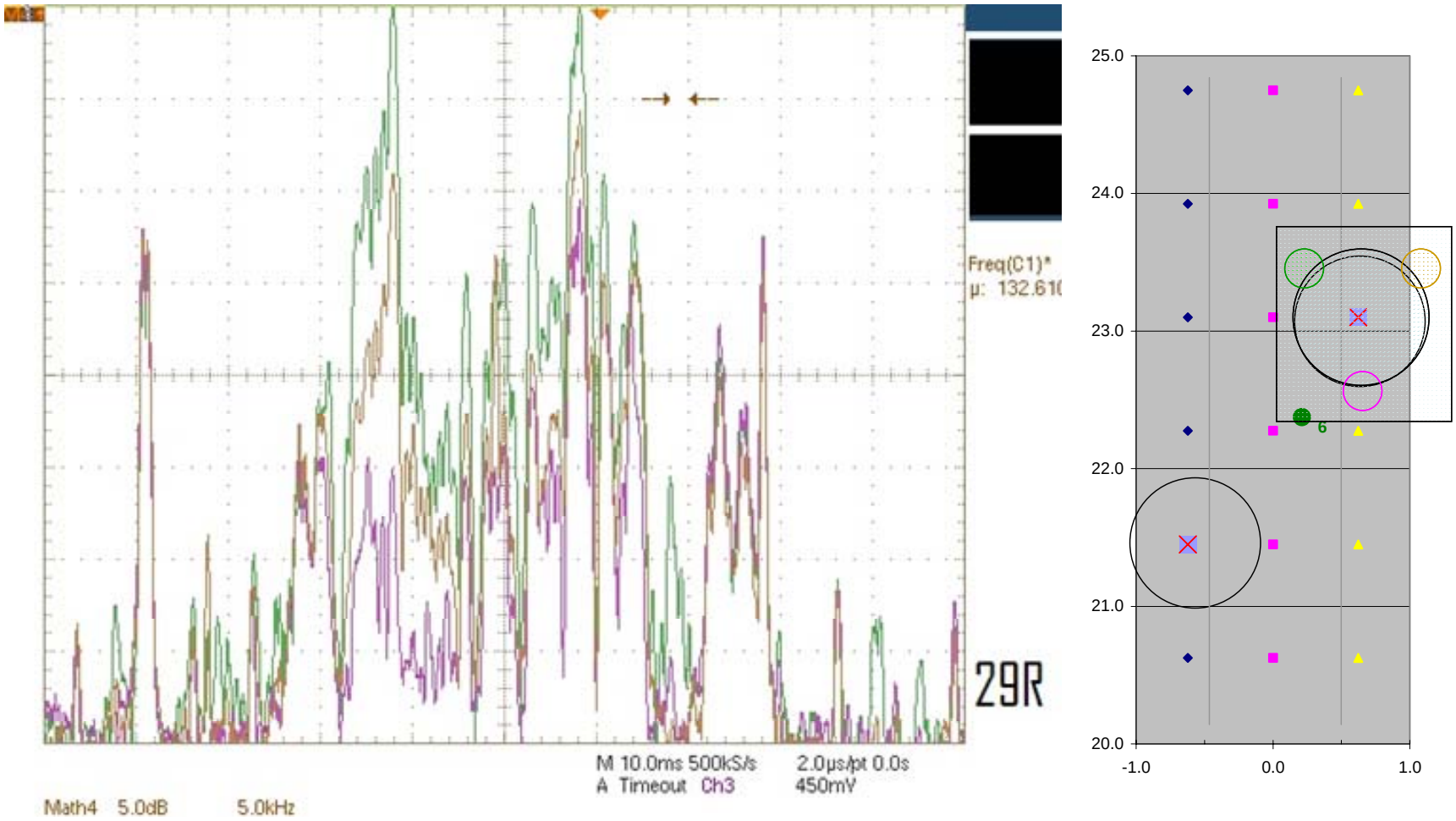

Figure 186. Data taken at position (29, R)

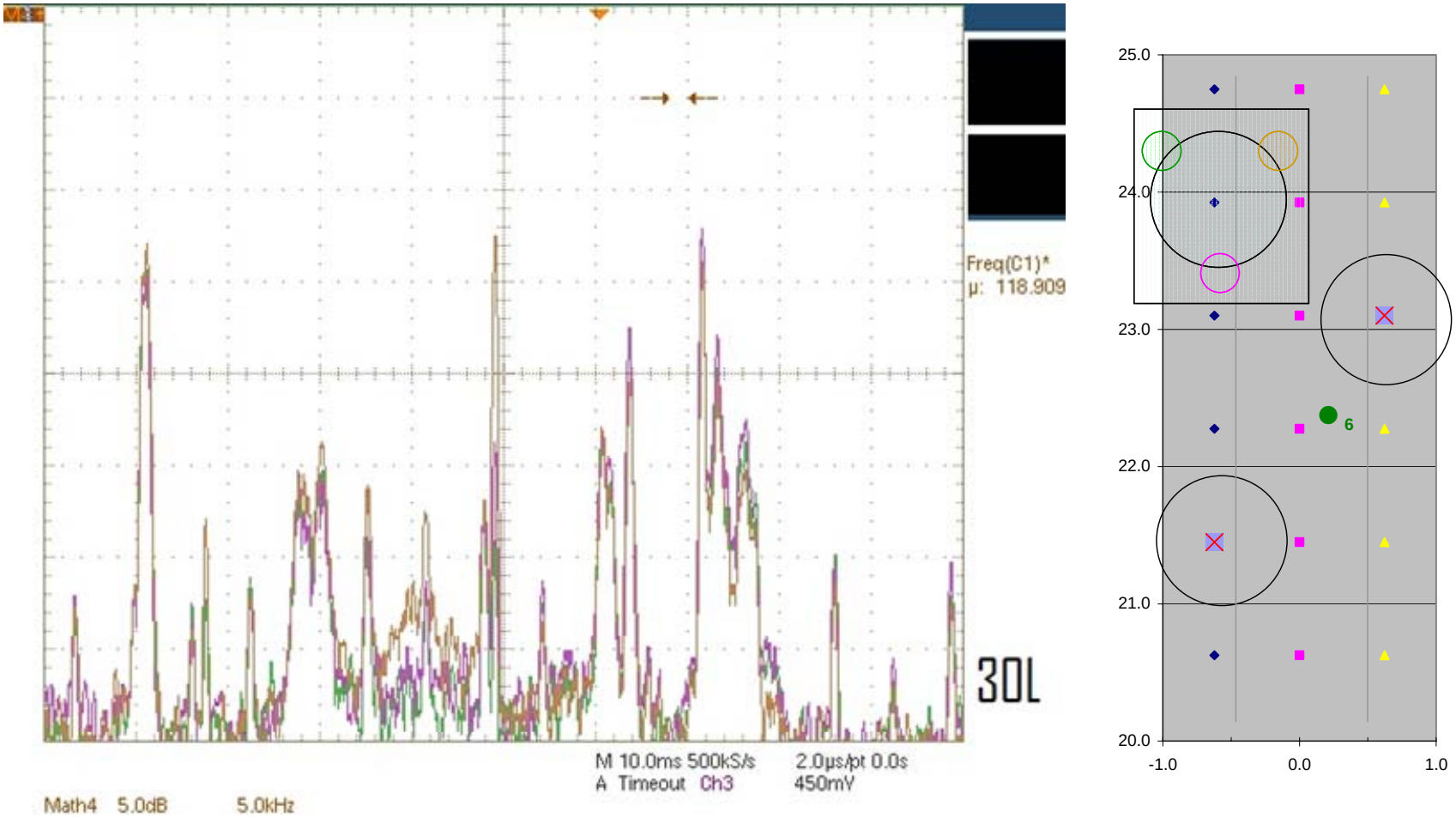

Figure 187. Data taken at position (30, L)

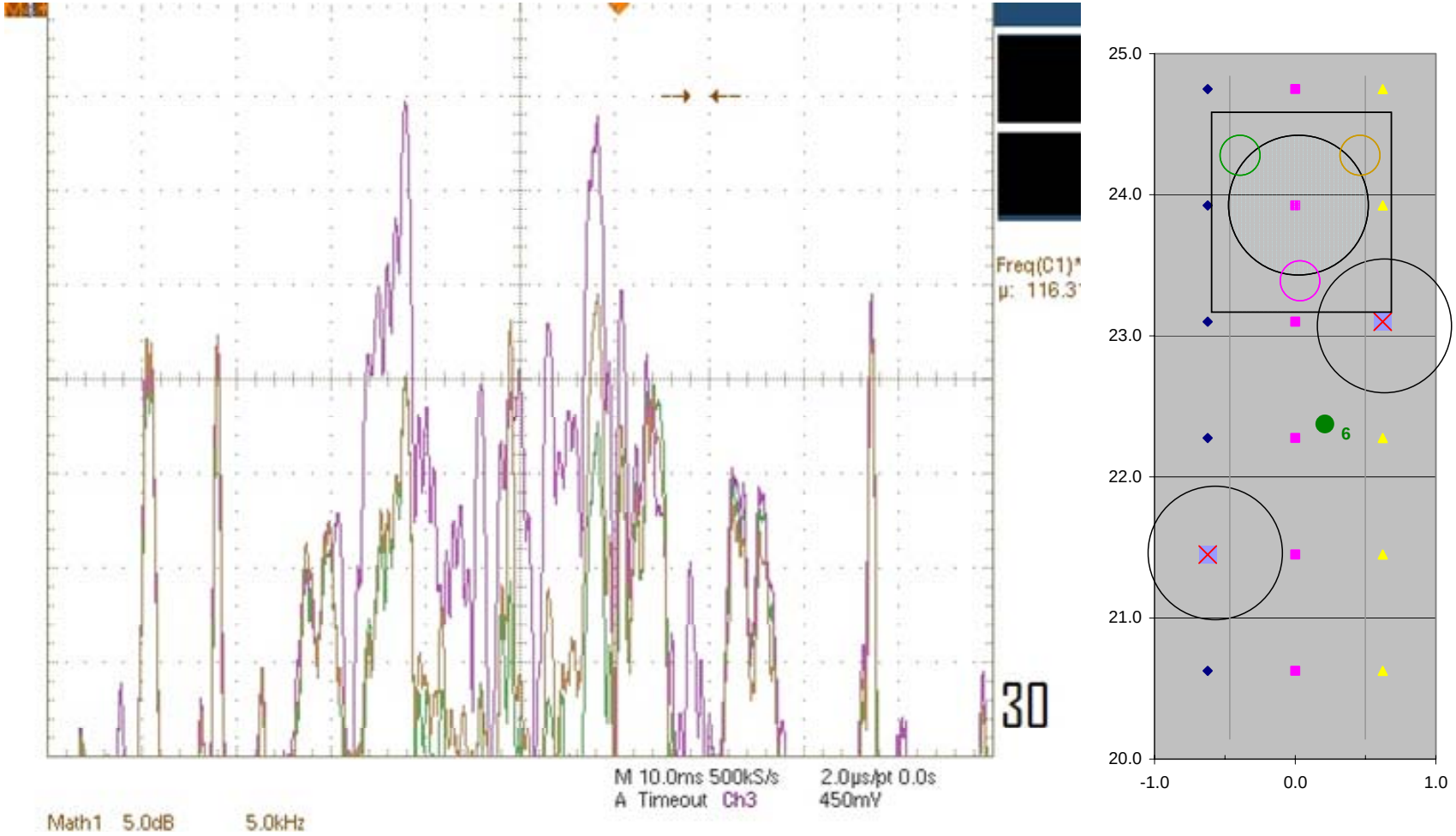

Figure 188. Data taken at position (30, C)

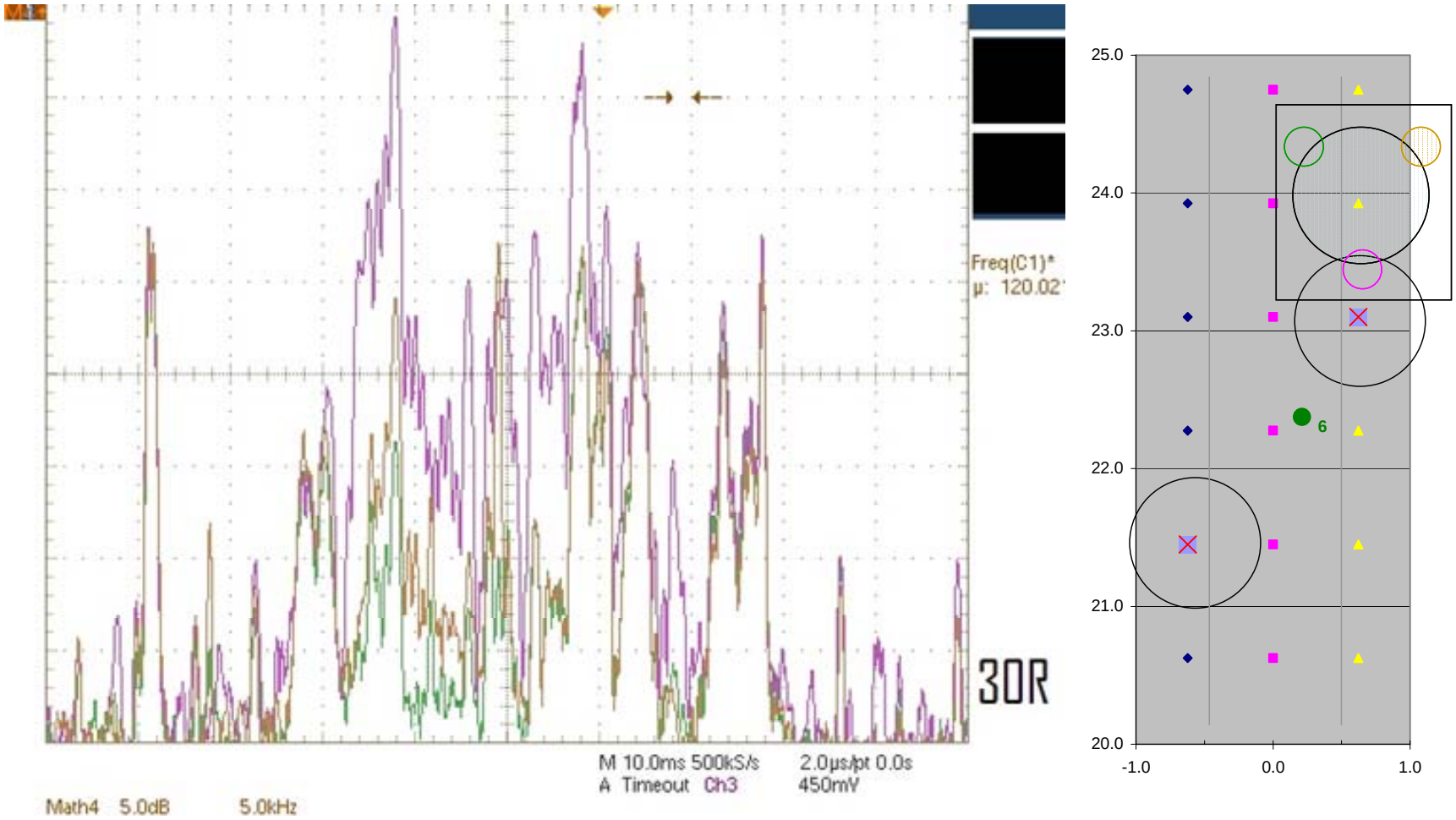

Figure 189. Data taken at position (30, R)

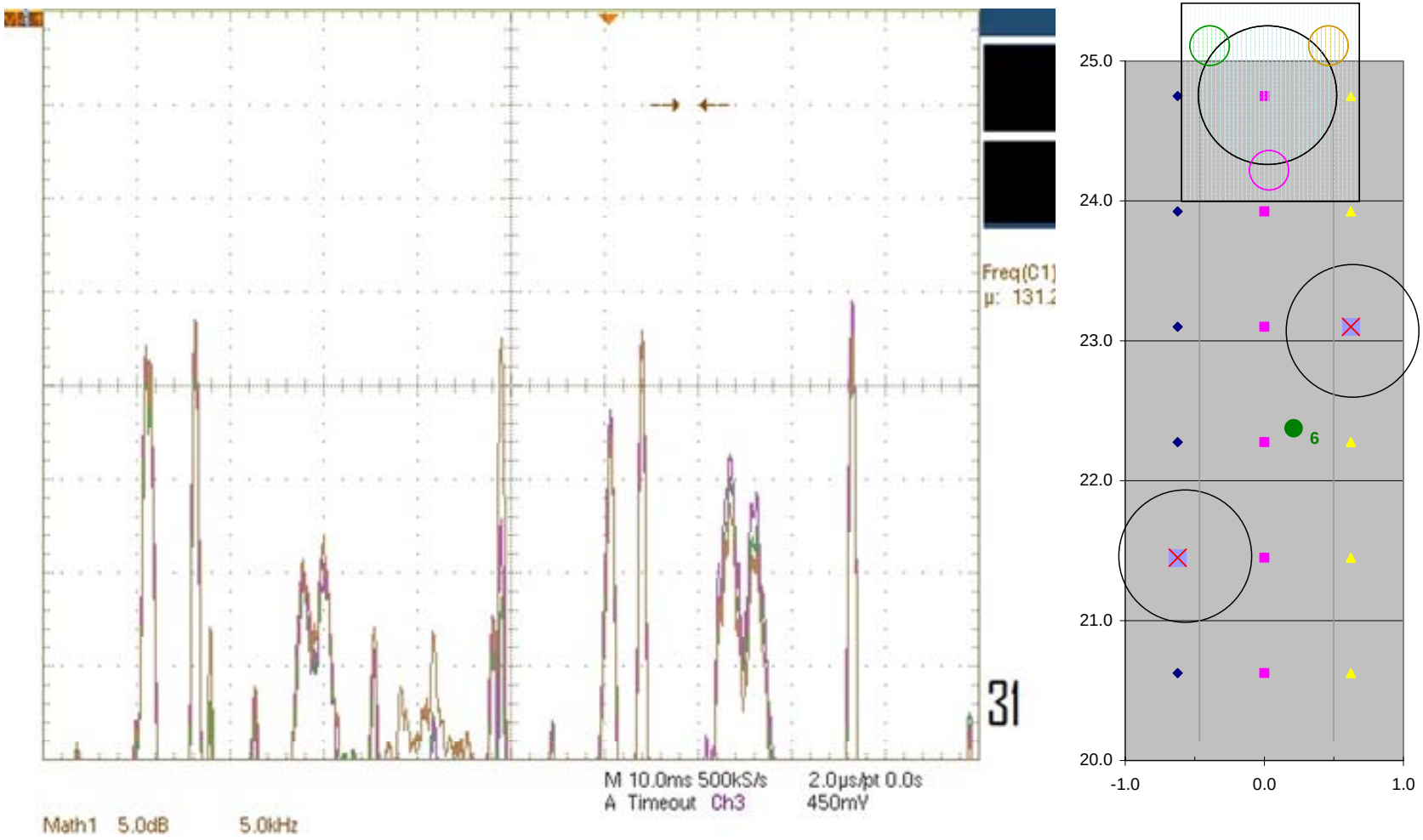

Figure 190. Data taken at position (31, C)

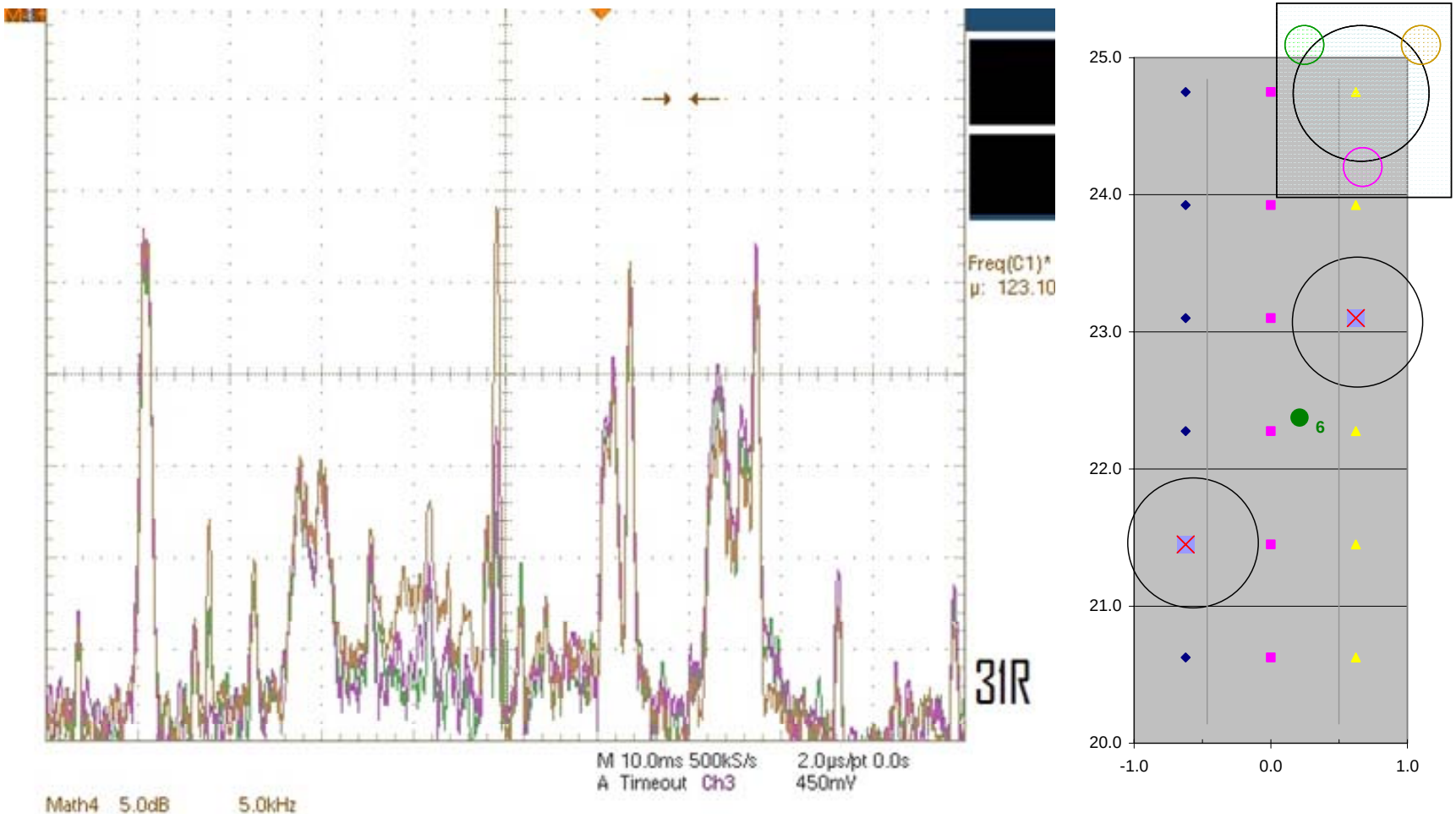

Figure 191. Data taken at position (31, R)